2007

Integrated Modeling of Long-Term Vegetation and Hydrologic Dynamics in Rocky Mountain Watersheds

Robert Steven Ahl
The University of Montana

INTEGRATED MODELING OF LONG-TERM VEGETATION AND HYDROLOGIC DYNAMICS IN ROCKY MOUNTAIN WATERSHEDS

By

Robert Steven Ahl

Master of Science, The University of Montana, Missoula, MT, 1999
Bachelor of Arts, Hartwick College, Oneonta, NY, 1995

Dissertation

presented in partial fulfillment of the requirements
for the degree of

Doctor of Philosophy in Forestry

The University of Montana
Missoula, MT

Spring 2007

Approved by:

Dr. David A. Strobel, Dean
Graduate School

Dr. Hans R. Zuuring, Chair
Department of Forest Management

Dr. Kelsey S. Milner,
Department of Forest Management

Dr. Donald F. Potts,
Department of Forest Management

Dr. Scott S. Woods,
Department of Ecosystem and Conservation Sciences

Dr. William W. Woessner,
Department of Geology

Ahl, Robert, Ph.D., May 2007 Forestry

INTEGRATED MODELING OF LONG-TERM VEGETATION AND HYDROLOGIC DYNAMICS IN ROCKY MOUNTAIN WATERSHEDS

Chairperson: Dr. Hans R. Zuuring

Changes in forest structure resulting from natural disturbances, or managed treatments, can have negative and long lasting impacts on water resources. To facilitate integrated management of forest and water resources, a System for Long-Term Integrated Management Modeling (SLIMM) was developed.

By combining two spatially explicit, continuous time models, vegetation patterns can be simulated forward in time based on management criteria. Output from the SIMPPLLE vegetation simulator are converted into landcover maps at every time-step and used to predict hydrologic watershed responses to time-series landcover change with the SWAT model. Long-term watershed responses to vegetation management scenarios can therefore be evaluated from both terrestrial and hydrologic perspectives.

Watersheds are common landscape analysis units, but vegetation dynamics within them do not function in isolation. Repeated century spanning SIMPPLLE simulations produced succession patterns that were significantly different in 84% of analysis watersheds when each was considered in isolation and within their landscape context. Watersheds with >30% internal forest cover, and <10% barren ground along their perimeters were more connected to landscape processes than those with more barren boundaries, and less forest cover within them.

Calibration of SWAT was based on four years of streamflow and climate data recorded within the Tenderfoot Creek Experimental Forest research watershed. Validation with an additional four years used both traditional and objective regression-based hypothesis testing procedures. Adjustment of snow process, surface runoff lag, and groundwater recession parameters contributed most significantly to model calibration. Results confirm that when calibrated in a forested mountain watershed having snow-dominated hydrology, SWAT can predict annual, monthly and daily streamflow with high levels of accuracy and efficiency.

For demonstration, SLIMM was used to evaluate natural and fire-suppressed forest management alternatives over a 300-year period. Compared to natural development, fire suppression created larger stand sizes, greater levels of aggregation, and increased the likelihood of process propagation across the landscape. Averaged over all simulations, fire suppression reduced annual water yield by up to 3%, streamflow variability by a factor of four, and the magnitude of annual peak flows by 15%. Literature supported results highlight the applicability of SLIMM as a management tool.

PREFACE

The concept of integrated management recognizes that the management of one resource inevitably has impacts on other resources. With an understanding of linkages between resources, it is sometimes possible to develop management alternatives that meet multiple objectives. In the Rocky Mountains, management of forest resources has the potential to impact associated water, wildlife, and other resources of societal value.

In the Rocky Mountain region of western North America, the interactions between forest and water resources have been studied for over 100 years through experimental manipulation, and correlation analysis between patterns observed in historic aerial photographs, vegetation maps and streamflow records. The majority of annual precipitation in this region is delivered in the form of snow, and runoff characteristics from watersheds are in large part determined by seasonal snowmelt. Snow available for melt is affected by patterns of forest canopy composition and configuration. Changes in forest structure therefore have the potential to alter watershed hydrology.

Assessment of projected impacts associated with forest structure due to management alternative requires a modeling perspective because complex interactions and the long time frames involved in forest ecosystem development cannot be directly measured, or extrapolated reliably from limited observations.

In the following work I present a modeling framework to facilitate integrated management of forest and water resources. I demonstrate a linkage between two existing models that are spatially explicit and designed to assess the impact of management over large areas and long time frames. The SIMPPLLE vegetation modeling system is used to project current vegetation patterns forward in time, given stated management objectives. The SWAT model was designed to assess hydrologic impacts of vegetation change at the watershed scale. With the conceptual framework I provide, time-series projections of the vegetation simulation can be interpreted to assess if management practices are achieving desired terrestrial responses, and correspondingly those responses can also be viewed in terms of watershed hydrology.

This interaction between models captures contemporary knowledge of vegetation and hydrologic processes, and provides a relatively efficient method for assessing various

terrestrial and hydrologic implications of forest management over long time frames. I will call this a System for Long-term Integrated Management Modeling (SLIMM). Over the course of four steps, simulations of long-term vegetation change and associated hydrologic watershed responses are increasingly integrated to simplify the modeling process. With a simplified process multiple permutations can be simulated, reducing management uncertainty through efficient evaluation of relative differences between management scenarios.

The conceptual framework for analysis of long-term watershed vegetation and hydrologic dynamics is structured by four chapters that are written in manuscript style. Because each chapter is written as an independent document, there is some overlap.

CHAPTER 1

Chapter 1 addresses the influence of landscape context on vegetation dynamics of individual watersheds. Patterns of vegetation across landscapes are dynamic. The processes that shape observed vegetation mosaics are influenced by climate, topography, and vegetation patterns, and occur over landscape scales, yet the impact of those processes tend to be analyzed at the watershed scale. Watersheds are fundamental analysis units but failure to incorporate interactions with the surrounding landscape can lead to underestimation of the range of variability in areas disturbed by natural processes.

To ensure that the full range of vegetation processes is captured in a watershed over time, simulation of those processes should be conducted within the context of the surrounding landscape. The extent of area beyond the watershed boundary that needs to be considered may vary depending on the topographic and structural vegetation characteristics. To quantify the relationship between biophysical watershed variables and simulated vegetation patterns due to context, a regression equation was developed as an index of landscape connectivity. Watersheds with greater than 30% forest cover, and less than 10% barren ground along a 1 km width spanning their perimeter were affected by landscape processes more strongly than those with larger proportions of barren land along their boundaries, and smaller internal forest components. As a rule of thumb, one layer of watersheds surrounding the watershed of interest should provide sufficient context.

CHAPTER 2

The reliability and usefulness of models depends on how well they are calibrated and subsequently validated. In chapter 2, current vegetation patterns together with onsite measurements of climate and streamflow were used to calibrate the SWAT model for simulation of snowmelt-induced forest hydrology in the mountainous watershed drained by Tenderfoot Creek. This chapter shows that streamflow calibration was strongly affected by the selection of appropriate snow process, groundwater, soil, and landcover parameter values. Of all parameters, snowmelt processes had the greatest influence on model performance. Streamflow predictions were validated over annual, monthly, and daily time-steps, and performance was generally better during the rising, as opposed to the falling limb of the annual hydrograph. This was attributed to misrepresented infiltration during snowmelt periods, and a lack of sophistication in groundwater recession flow algorithms. Overall, measures of performance achieved by the calibrated model were similar to those obtained in other regions where SWAT has been successfully applied. Results indicate that once calibrated, SWAT could be used to assess relative changes in streamflow due to shifting landcover patterns in the Tenderfoot Creek research watershed, and others in the region with similar characteristics.

CHAPTER 3

In chapter 3, the connection between SIMPPLLE and SWAT is made. This chapter uses a long term-assessment of the natural range of variability in landcover patterns to illustrate how vegetation simulations conducted by SIMPPLLE can be used by SWAT to isolate the effect of landcover change on streamflow patterns. A time-series of landcover maps resulting from a 300-year simulation of natural vegetation change conducted by with SIMPPLLE is first examined for composition and structure. Upon quantification of terrestrial patterns, landcover maps are passed through SWAT to evaluate the changes in hydrologic response due to differences in landcover patterns and characteristics. The effect of landcover was isolated by holding all model elements, including topography, soils, watershed configuration, and climate inputs constant. The only element that changed was the landcover maps used to characterize the watershed. In

this way, changes in hydrology could be unambiguously attributed to changes in landcover. While this is somewhat simplistic, it does provide a direct measure of the interactions between vegetative and hydrologic processes at the watershed scale.

CHAPTER 4

Chapter 4 represents the culmination of the previous three chapters. Fire is the dominant natural disturbance agent in Rocky Mountain forests, and the terrestrial and hydrologic patterns associated with two fire management scenarios were evaluated in this chapter. In one scenario a landscape perspective was used to simulate 300 years of fire-suppressed vegetation change, while in the other no fire suppression was assumed. The two sets of time-series landcover maps generated for the same research watershed were first extracted from the landscape extent and analyzed for the terrestrial patterns. Time-series maps were then used to isolate the impact of landcover change on hydrologic responses. Comparison of the two sets of results illustrated how forest management scenarios can be evaluated for multiple objectives.

The final component of this chapter embodies the SLIMM process. After both the vegetation and hydrologic models have been adapted for use in their desired environment, they were calibrated to each other. To relate output of the two independent models to one another, a regression equation was developed to predict the annual water yield estimated by SWAT based on the relative watershed areas occupied by landcover components produced by SIMPPLE. With an established quantitative relationship between outputs of the two models, assessment of forest management alternatives can be streamlined. For example, once vegetation input files have been built for SIMPPLLE, variations of management scenarios can be simulated with relative ease. After each simulation, or set of multiple simulations, an output conversion algorithm can be initiated and landcover time-series landcover maps generated. The spatial pattern of landcover can be assessed, and proportions of relevant landcover types in the watershed can be used to predict patterns of annual water yield associated with each management scenario. With the ability to run a large number of repeated stochastic simulations of vegetation change, uncertainty in management outcomes relating to terrestrial and hydrologic responses can

be reduced by capturing a wide range of variability. This provides an envelope of responses that can be used to characterize each management alternative. Water yield is only one example of how the SLIMM process can be applied.

APPENDIX A

Output from SIMPPLLE cannot be directly analyzed for spatial pattern, or used by the SWAT hydrologic model. The Scaled Multi-Attribute Classification (SMAC) algorithm developed to convert SIMPPLLE output into map-able landcover categories that can be analyzed and used by SWAT is described in Appendix A.

APPENDIX B

Calibration of SWAT was an involved process, and Appendix B gives a detailed account of how values of important parameters were estimated, and how they influenced the performance of the final calibrated model.

APPENDIX C

The effect each landcover category represented by simulations of long-term vegetation change in the research watershed had on hydrologic processes was evaluated in Appendix C.

APPENDIX D

Validation of hydrologic model performance is often a subjective process. A regression-based model invalidation procedure was introduced as an objective validation tool in the SWAT calibration chapter. Appendix D provides an example of how this objective validation method was applied to monthly water yield estimates.

TABLE OF CONTENTS

LIST OF TABLES

CHAPTER 1

CHAPTER 2

CHAPTER 3

CHAPTER 4

APPENDIX A

APPENDIX B

APPENDIX C

APPENDIX D

LIST OF FIGURES

CHAPTER 1

CHAPTER 2

CHAPTER 3

CHAPTER 4

APPENDIX A

APPENDIX B

APPENDIX C

LIST OF ACRONYMS

Acronym	Description
ARS	Agriculture Research Service
ASCE	American Society of Civil Engineers
AVSWAT	ArcView GIS Soil and Water Assessment Tool interface
BRRN	Barren ground landcover type
BRRN_b	Barren ground landcover type measured in a 1 km buffer around the watershed
CI	Circularity Index, compares the dimensions of a watershed to a round circle with the same area
CN	Soil Conservation Service rainfall-runoff curve number
CN2	Soil Conservation Service rainfall-runoff curve number for moisture condition II
CN2B	Soil Conservation Service rainfall-runoff curve number for moisture condition II, soil class B
CONTAG	Contagion Index
DD	Drainage Density, total length of stream features divided by the watershed area
DEM	Digital Elevation Model
DFFR	Douglas fir forest landcover type
DFFR_i	Douglas fir forest landcover type measured in the watershed interior
DIFF	Difference between mean area disturbed per decade of vegetation simulation conducted in the landscape context vs. those conducted in isolation
Dv	Mean deviation hydrologic data comparison statistic
Dv_d	Mean deviation hydrologic data comparison statistic, calculated for daily time-step
Dv_m	Mean deviation hydrologic data comparison statistic, calculated for monthly time-step
ET	Evapotranspiration
FMZ	United States Forest Service designation for Fire Management Zone
FV_i	The sum of all forest landcover types measured in the watershed interior
GLEAMS	Groundwater Loading Effects of Agricultural Management Systems
GLND	Grassland landcover type
GWQ	Groundwater flow
HRU	Hydrologic Response Unit
HUC	Hydrologic Unit Code
LAI	Leaf Area Index, a measure of canopy structure with units of sq. meter per sq. meter
LC	Index of Landscape Connectivity, which is based on an equation designed to predict DIFF
LH-OAT	Latin Hypercube One-At a-Time parameter space sampling method
LND	Vegetation simulation conducted in the context of the surrounding landscape, i.e. the watershed of interest within the landscape context
LPFR	Lodgepole pine forest landcover type
LPFR_i	Lodgepole pine forest landcover type measured in the watershed interior
LPI	Largest Patch Index
LSI	Landscape Shape Index
LTC	Lower Tenderfoot Creek stream discharge measurement flume
LWQ	Lateral water flow
MRPP	Multiple Response Permutation Procedures used for comparison of grouped data
NED	National Elevation Dataset
NHD	National Hydrography Dataset distributed by United States Geological Survey
NRCS	Natural Resource Conservation Service

Table continued

Acronym	Description
NS	Nash-Sutcliffe sum of squares hydrologic data comparison statistic
NS_d	Nash-Sutcliffe sum of squares hydrologic data comparison statistic, daily time-step
NS_m	Nash-Sutcliffe sum of squares hydrologic data comparison statistic, monthly time-step
NWS	National Weather Service
OVN	Manning's index (N) of overland roughness
PCA	Principle Components Analysis - data reduction procedure
PCP	Abbreviation for precipitation
PET	Potential Evapotranspiration
QAFR	Quaking aspen forest landcover type
RE	Relative error metric
REGMOD	Regression model of annual water yield based on landcover proportions
SCE	Shuffled Complex Evolution optimization algorithm
SCS	Soil Conservation Service
SD	Standard deviation
SFFR	Spruce-fir forest landcover type
SILC3	Satellite Image Landcover Classification, version 3
SIMPPLLE	Vegetation simulation model - SIMulating Patterns and Processes at Landscape ScaLEs
SLND	Shrubland landcover type
SMAC	Scaled, Multi-Attribute Classification algorithm for creating landcover maps
SNOTEL	Snow telemetry data collection system
SSQ	Sum of Squares objective function used in optimization algorithm
SSURGO	County levl soil geographic database
STATSGO	State level soil geographic database
STDEV	Standard deviation
STERR	Standard error of estimate
SWAT	Soil and Water Assessment Tool, hydrologic model
SWE	Abbreviation for snow water equivalent
SWQ	Surface water flow
SWRRB	Simulator for Water Resources in Rural Basins
TCEF	Tenderfoot Creek Experimental Forest
TCSWAT	Tenderfoot Creek SWAT model
TM	Thematic Mapper satellite sensor
TMDL	Total Maximum Daily Load
TRI	Terrain Ruggedness Index
TRI3_b	Terrain Ruggedness Index number 3, in a 1 km buffer around watershed boundary
TRNS	Transitional or disturbed forest landcover type
USDA	United States Department of Agriculture
USDI	United States Department of Interior
USFS	United States Forest Service
USGS	United States Geological Survey
VIF	Variance Inflation Factor
WAT	Vegetation simulation conducted in isolation from the surrounding landscape
WATR	Water landcover type

CHAPTER 1

An Index of Landscape Disturbance Connectivity for Vegetation Dynamics in Rocky Mountain Watersheds

ABSTRACT

In natural landscapes forest structure is largely shaped by periodic disturbance processes. The spatial propagation of those processes can be enhanced or restricted by physical and vegetative landscape patterns. When long-term vegetation dynamics in watersheds are assessed, the landscape context may affect the magnitude and distribution of important disturbance processes occurring within individual analysis watersheds. To examine the effect of landscape context on watershed vegetation disturbance processes, SIMPPLLE was used to simulate vegetation change over one hundred years starting from current conditions, across 7.5 million ha of central Montana, USA. Out of 12 defined landscapes, 38 watersheds, bounded by exterior watersheds on all sides (i.e. the surrounding landscape), were selected for analysis, and vegetation dynamics within them were modeled in two distinct ways: 1) in isolation from other watersheds, and 2) in the context of the surrounding landscape. A clear pattern of how individual processes were affected was difficult to establish, but fire of various severities was more prevalent when watersheds were modeled in the landscape context compared to isolated scenarios. When total relative disturbance areas were compared, 84% of watersheds exhibited significantly different patterns due to context. Overall, vegetation simulations conducted in the landscape context resulted in more disturbed areas over time, in contrast with paired simulations conducted in isolation. The difference in mean decadal disturbed areas due to context, interpreted as a measure of landscape connectivity (LC), was modeled as a function of five variables that described the topography, landcover composition and configuration within watersheds, and in a 1 km buffer around their perimeter. Increasing values of LC indicated increasing influence of landscape processes on watershed processes. LC was positively correlated with the proportion of forest cover within watersheds, and negatively associated with the amount of barren ground in the watershed perimeter. Watersheds with > 30% internal forest cover, and < 10% barren ground along the width of their perimeter were affected by landscape processes more strongly than those with larger proportions of barren land along their boundaries, and smaller proportion of forest cover within watersheds.

INTRODUCTION

Interpreting changes in vegetation due to natural or managed processes is a fundamental component of landscape assessment and planning (Barrett, 2001). To measure changes, analysis units must be defined. For analysis of natural processes, zones defined by ecological hierarchies generally provide a more holistic view of landscape units than those defined by administrative boundaries (Klijn and Udo de Haes, 1994). The inherently nested aggregation of drainage basins provides a topographically derived, scaleable approach to sub-division, and for this reason, watersheds are a fundamental land unit in ecosystem analysis and management (Lundquist et al., 2001). Although the watershed approach to holistic land management is a good one, a primary law of geography states that 'all things are connected, but near objects are more related than distant objects' (Forman, 1995). Relating spatial theories to landscape assessment suggests that watersheds should not be analyzed in isolation due to likely connections to the surrounding landscape.

The context within which a watershed is nested in some landscapes may be as or more important than its content. The surrounding mosaic can have a greater effect on vegetation community function and change than the present characteristics of a stand within it (Forman, 1995). If, for instance, a fire starts in one stand and wind is blowing in the direction of an adjacent unaffected stand, it will likely burn as well, regardless of its current condition. The same principle may be applied to watersheds. In watersheds of North America's Rocky Mountains, fire and destructive insect infestations are among the major agents of change in the forest matrix (Arno and Fiedler, 2005). Fires may originate outside of an analysis watershed, but if conditions are favorable they could overcome topographic divides and affect internal vegetation dynamics. Overlooking the influence of adjacent disturbance processes on internal watershed vegetation dynamics can result in an underestimate of the full range of possible conditions in the unit over time. If canopy altering processes are not accounted for, associated resource interpretations may be flawed. From a hydrologic perspective, changes in the chemical composition, sediment load, and water yield from Rocky Mountain watersheds are often related to the removal or thinning of the forest cover. Underestimating the affect of landscape level disturbances

on internal watershed function can therefore lead to erroneous predictions of the hydrologic response due to disturbance-induced changes in vegetation structure.

The level of connection between landscape and watershed vegetation processes may be enhanced or retarded by patterns of terrain and landcover heterogeneity (Turner, 1989). Within landscapes and watersheds, both landcover and terrain features may be either susceptible or resistant to disturbance processes. The proportion and arrangement of features in a watershed will either help or restrict the movement of disturbances across its area. Hard boundaries such as rock ridgelines or water bodies may act as barriers to spread, while continuous connected patches of susceptible landcover, or gentle terrain may facilitate the spread of disturbances. Considering fire or insect infestation, decadent stands of lodgepole pine may be considered susceptible to disturbance, while adjacent stands of quaking aspen may be less likely to act as a vector for the propagation of the same disturbance.

In the Boundary Waters Canoe Area of northern Minnesota, for example, large fires tend to follow prevailing winds and burn from west to east; large lakes with north-south orientation interrupt the spread of fires (Heinselman, 1973). Examination of forest fire histories in Quebec and Labrador were indicative of similar phenomenon. While the average size of fires was around 10,000 ha, fires that burned in areas dissected by lakes and rivers were generally less than 1,000 ha (Hunter, 1993). Likewise, fire regimes on islands in boreal forest lakes differ from that of the mainland. On the mainland, a fire started from a single ignition can spread across large areas of forest. Islands isolated from fire spread, burn far less (Bergeron and Brisson 1990). The spread of disturbances may also be related to continuity in fuel loads. Mature forest stands tend to have a greater accumulation of dry and dead wood, yielding more fuel than young, regenerating stands. Thus, the arrangement of young and mature forest stands is likely related to fire spread potential (Turner and Romme, 1994).

Although hydrologic divides are invariant, processes that affect the internal terrestrial and aquatic function of watersheds may overcome and spread across these boundaries. When watersheds are analyzed in isolation the occurrence of significant disturbance events may not be considered, rendering planning efforts less effective. In forested environments where significant, mosaic altering events are not likely to occur

often, a long-term perspective is invaluable for an assessment of natural processes. Understanding the possible range of variability in vegetative states for particular landscapes helps place current patterns in a context of possible conditions. Documenting past vegetation change is helpful, but limited by available information. Predicting how vegetation will change in the future requires the use of some type of modeling process to incorporate knowledge of ecological and biophysical interactions. Estimating future changes based on current or planned actions makes it possible to evaluate the possible outcomes of those plans.

The goal of this research is to evaluate the influence of landscape context on internal watershed processes when vegetation dynamics are simulated over long time periods. In other words, the main question being asked is "how connected are the natural vegetation dynamics in a watershed to those occurring around it". To address this fundamental issue of context, experimental simulations were conducted to answer three basic questions:

- *Does the landscape context in which vegetation dynamics are simulated affect the distribution of processes that occur in an analysis watershed over time?*
- *Is the amount of disturbed areas occurring in analysis watersheds affected by the context in which they are simulated?*
- *What are the factors that contribute to or diminish the relationship between watershed and landscape processes?*

Predicting landscape level changes in vegetation over time is valuable for solving many natural resource management issues, and a wide variety of modeling systems have been developed for this purpose (Barrett, 2001; Lee et al., 2003). The SIMPPLE model which was originally developed for the U.S. Department of Agriculture, Forest Service (USDA-FS) to simulate vegetation changes in Rocky Mountain landscapes (Chew et al., 2002), was utilized in this study.

Thirty eight watersheds, distributed across all of the major mountain ranges of central Montana, USA, were selected for analysis. Each analysis watershed was

surrounded by landscapes that maintained at least one additional layer of neighboring watersheds on all exterior sides of the analysis unit (i.e. the surrounding landscape). Vegetation dynamics for each watershed were simulated 100 years forward in time from current conditions, at a decadal time-step. SIMPPLLE is a stochastic model, and in order to create an ensemble of responses for each time-step, simulations were repeated 100 times. To assess the impact of context on long-term vegetation patterns in each watershed, two sets of simulations were generated for each watershed. The first set represented watershed-based vegetation dynamics that were modeled in isolation from their surrounding landscapes. This set was referred to as WAT, for isolated watershed simulation. The second set of simulations modeled vegetation change across the entire landscape each watershed was nested within, but kept track of the internal watershed processes. These simulations were called LND, indicating that each watershed was simulated in its landscape context. Processes simulated by SIMPPLLE can be divided into disturbances and succession. Disturbances can include planned treatments but only the occurrence of natural agents like fire, insect and disease were simulated for this analysis. In the absence of disturbance processes, vegetation communities are advanced through their estimated developmental pathways. For either disturbance or succession, respective watersheds areas affected by each process are reported by the model at every time-step. To facilitate comparisons across watersheds, interpretations were based on relative areas.

Results from both simulation sets were then compared to determine if differences in processes distributions, and pattern of disturbance could be detected between scenarios. Differences between context simulations were interpreted as an indication that context influenced internal watershed dynamics. Large differences suggests strong connections between landscape and watershed processes, while small differences indicated that processes in a watershed tend not to be connected to those of the surrounding landscape.

Multiple regression procedures were then used to relate watershed characteristics to differences in the simulated disturbances due to context. In essence, this predictive equation could be interpreted as an index of landscape connectivity, where larger values suggest greater levels of connectivity between landscape and watershed processes.

METHODS

STUDY AREA DESCRIPTION

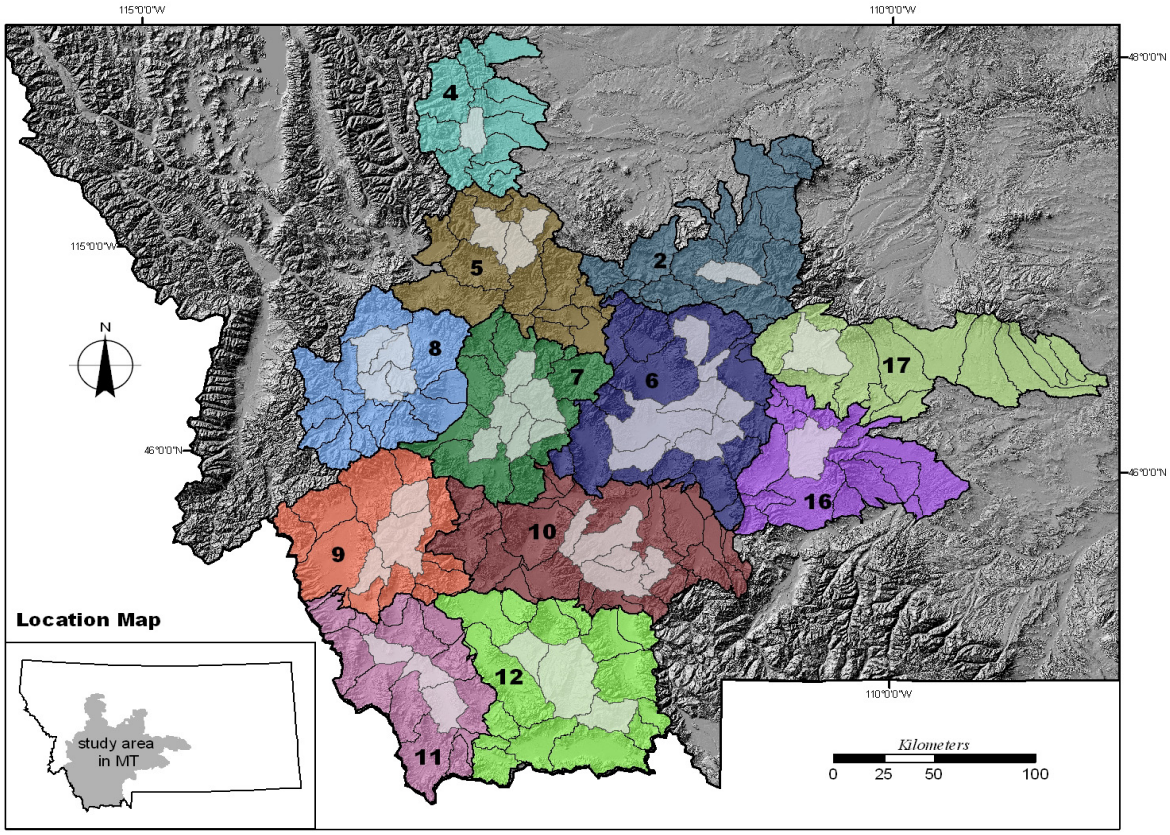

Figure 1. *Landscape context study area in Montana, USA. Landscapes are subdivided by hydrologic divides, and those watersheds completely on the interior of each landscape were analyzed in this study. Analysis watersheds are highlighted in gray.*

The geographic extent of this study spanned 12 landscapes representing the diversity of mountain ranges across central Montana, USA (Figure 1). Each landscape is an aggregation of land units (watersheds) that encompassed ecologically similar conditions and together cover roughly 7.5 million hectares of land.

When landscapes must be divided into analysis units, delineation based on a watershed approach is desirable for the investigation of ecological processes. In Montana, landscape delineation based on hydrologic divides can be stratified by three levels of resolution, consisting of 1) river basins, 2) watersheds, and 3) sub-watersheds. Delineated basins are identified by hierarchical hydrologic unit codes (HUCs), based on the levels of

classification in the hydrologic unit system (Seaber et al., 1987). Statewide, there are about 100 HUC4 river basins with an average size of 365,000 ha. At the next level of resolution subdivision, HUC5 delineations represent watersheds approximately 40,500 ha in size, and there are there are roughly 900 such units in the state of Montana. The finest level of spatial resolution is the sub-watershed. These drainages range from 4,050 to 16,000 ha, and are called HUC6 delineations. To characterize the natural flow of energy and matter across the landscape, HUC5 watersheds were selected as sampling units.

SITE SELECTION

The 12 previously mentioned landscapes were composed of an aggregation of HUC5 watersheds. Within each landscape, only watersheds that were completely surrounded by other watersheds on all sides were selected as analysis units (Figure 2).

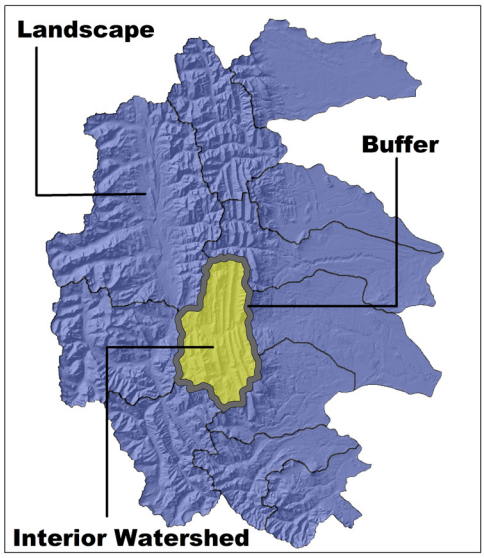

Figure 2. *Landscape context site selection and characterization components. Landscapes represent groupings of watersheds, whereas interior watersheds are wholly surrounded by other watersheds on all sides. Biophysical variables were summarized within analysis watersheds and within a 1 km buffer around the analysis watershed boundaries to describe ridgeline attributes. Analysis unit 4_1, referring to watershed 1, within landscape 4 is shown in this schematic.*

In total, 38 watersheds covering 1.5 million ha were studied in this analysis of vegetation dynamics. Analysis watersheds ranged in size from roughly 12,500 to 95,000 hectares, and averaged approximately 35,000 ha. The 12 landscapes that contained the analysis watersheds varied from 375,000 and 850,000 ha, with an average size of 625,000 ha (Table 1).

Table 1. *Landscape and watershed spatial characteristics.*

Landscape	Landscape Area (ha)	Watershed	Watershed Area (ha)
2	376,450	2_1	28,121
4	584,173	4_1	23,671
5	556,937	5_1	34,106
5		5_2	29,870
5		5_3	17,516
6	566,851	6_1	31,341
6		6_2	12,441
6		6_3	31,554
6		6_4	21,805
6		6_5	90,412
6		6_6	42,851
6		6_7	32,159
7	850,976	7_1	25,899
7		7_2	37,534
7		7_3	29,026
7		7_4	20,568
7		7_5	15,630
7		7_6	21,934
8	673,613	8_1	29,141
8		8_2	28,487
8		8_3	26,953
8		8_4	19,470
9	547,857	9_1	27,210
9		9_2	66,396
9		9_3	23,896
10	534,581	10_1	21,676
10		10_2	49,975
10		10_3	18,642
10		10_4	44,261
10		10_5	21,543
11	576,635	11_1	24,736
11		11_2	25,134
11		11_3	38,454
12	825,004	12_1	32,553
12		12_2	95,678
12		12_3	38,071
16	553,622	16_1	58,546
17	827,582	17_1	66,383
Total Area	**7,474,281**		**1,303,642**
min	376,450		12,441
mean	622,857		34,306
max	850,976		95,678

MODEL DESCRIPTION

A computer program that predicts the type and amount of future vegetation for a particular landscape is a model. A computer program that has been designed so that it can be modified and applied to a number of different landscapes is a modeling system (Barrett, 2001). Predicting landscape level changes in vegetation over time is valuable for many natural resource management concerns, and a wide variety of modeling systems have been developed for this purpose (Barrett, 2001; Lee et al., 2003). The SIMPPLE model was originally developed for the USDA-FS to simulate vegetation changes in the presence of natural and human disturbance processes in Rocky Mountain landscapes (Chew et al., 2002), and was therefore selected for use in this study.

SIMPPLLE is an acronym for SIMulating Patterns and Processes at Landscape Scales (Chew et al., 2002). SIMPPLLE was developed as a management tool to help provide an understanding of how processes and vegetation interact to affect landscape change. Specifically, this modeling system was designed to:

- Simulate future vegetation changes caused by disturbance processes
- Simulate ranges of plant community conditions
- Simulate how changes in vegetation patterns influence disturbance processes
- Help identify high priority treatment areas, given specific resource objectives
- Simulate impacts over time on a variety of resources objectives
- Help identify the probability of disturbance processes and vegetation conditions

To meet its objectives, SIMPPLLE was developed with an object-oriented design. This type of architecture captures knowledge obtained from both research and expert opinion, and incorporates many useful features. First, the model is spatially explicit. Each vegetation unit, defined as a polygon-based stand, is unique and carries attributes that identify its adjacent stands. Rather than model the development of individual trees, SIMPPLLE projects stand-based interaction between disturbances processes and the vegetative pattern of a landscape. SIMPPLLE simulates succession and 12 major natural disturbance processes, including wildfire, bark beetles, and root diseases (Table 2). A fairly sophisticated fire spread algorithm is used, that integrates topographic effects,

wind, and stand history. If required, management treatments can also be scheduled to stands over time.

Existing vegetation is represented by discrete states, described by dominant species, size-class, and a measure of canopy coverage for density. Ecological groupings of potential natural overstory and understory vegetation, based on site characteristics, are know as habitat types (Pfister et al., 1977) and are used to stratify states (Chew et al., 2002). State advancement as a result of a process is stored in a collection of all possible states for a dominant species in an ecological grouping. These collections of potential states are referred to as pathways.

At each state of a stand's development there is a probability it will either advance to a future state, or be altered by a disturbance process. The assignment of process probabilities is stochastic, rather than based on a transition matrix approach. The probability of a process originating in or spreading out of a stand is determined by attributes describing stand condition, what exists around it, and what processes have occurred in the past.

SIMPPLLE is not designed to predict exactly when and where processes will occur. Rather, it is intended to provide an understanding of general trends and ranges. The model is continuous, and can be run with annual or decadal time steps for up to 500 years into the future starting from current conditions. For every time-step, the aerial extent over which individual processes occur on the landscape is summarized. Just as output is summarized for the whole landscape, model results can also be tracked for individual stands, or collections of stands. Furthermore, single or multiple simulations can be initiated. Because the assignment of processes is probabilistic, repeated or multiple simulations can provide a range of possible process distributions for a specific landscape. Single simulations can be used as an example of one possible outcome for a given landscape over time. Individual simulations can also be extracted from a set of multiple simulations to represent minimum, maximum, mean, or most likely scenarios.

Table 2. *Succession and natural disturbances modeled by SIMPPLLE.*

Disturbance Process Code	Description
SB	*spruce bark beetle (Dendroctonus rufipennis)*
DFB	*Douglas fir beetle* (*Dendroctonus pseudotsugae*)
WBP MPB	*Whitebark pine mountain pine beetle* (*Dendroctonus ponderosae*)
PP MPB	*Ponderosa pine mountain pine beetle* (*Dendroctonus ponderosae*)
S LP MPB	*severe lodgepole pine mountain pine beetle* (*Dendroctonus ponderosae*)
L LP MPB	*light lodgepole pine mountain pine beetle* (*Dendroctonus ponderosae*)
S WSBW	*severe western spruce budworm (Choristoneura occidentalis Freeman)*
L WSBW	*light western spruce bud worm (Choristoneura occidentalis Freeman)*
RD	*root disease (Armillaria ostoyae, and Heterobasidion annosum)*
LSF	*light severity fire*
MSF	*mixed severity fire*
SRF	*stand replacing fire*
SUCC	*succession (lack of disturbance)*

SIMPPLLE is publicly supported software and is available for download at:
www.fs.fed/rm/missoula/4151/SIMPPPLLE/index.htm

MODEL DATA

The data required to model natural vegetation change over time included information about topography, estimates of potential natural vegetation, description of current vegetation composition, structure, and configuration, multiple levels of analysis unit boundaries, fire start and spread probabilities, and stream network features (Table 3). A raster-based digital elevation model (DEM) that spanned the study area with 30 m pixel resolution was extracted from the National Elevation Dataset (NED) (Gesch et al., 2002). From this map layer, landscapes, watersheds, and stands were characterized with various levels of detail. With the original elevation data, slope, aspect, curvature, and terrain ruggedness index (TRI) attributes were calculated for every pixel. While all topographic attributes were associated with the landscape and watershed analysis units, individual stands were only attributed with elevation, slope, and aspect characteristics. The relative slope position of stands was also determined from these data, indicating aspect directions, and whether stands were above or below one another. Estimates of potential natural vegetation were modeled independently by USDA-FS scientists (Jones, 2002), and used to ecologically stratify the landscape, based on biophysical site

characteristics. From these characteristics plant community habitat types (Pfister et al., 1977) were assigned, and groupings of types defined basic elements of stand potential.

Existing vegetation was mapped and described by the Satellite Image Landcover Classification dataset for Montana, version 3 (SILC3). The original satellite data were collected across the study area in 1996 with 30 m resolution Thematic Mapper (TM) sensors, and processed by the Wildlife Spatial Analysis Laboratory {Redmond, et al., 2001) for the USDA-FS. Final vegetation data consisted of classified raster-based maps of dominant species or species combinations, size-class, and canopy coverage density classes. Together with topographic and ecological assignments, these data were used to create the vegetation input data necessary to establish current state definitions for all plant communities of the study area.

Fire is a dominant disturbance agent in Montana forests, and the likelihood of ignition is closely related to stand conditions and the occurrence of lightning strikes. Fire start and spread probabilities have been recorded and projected across the study area. Using these data, regions of similar burn potential were defined and stored in a polygon-based fire management zone map layer (FMZ). This data layer was used to weight the burn potential of stands, given their ecological grouping, condition, and surroundings when process probabilities are assigned to plant communities.

Linear elements representing perennial stream channels were extracted from the National Hydrography Dataset (NHD), and used to characterize the drainage patterns of the study area watersheds.

Table 3. *Model input data types, names, sources, and spatial dimensions.*

Information Type	Dataset	Source	Resolution / Units
Raster / Topography	NED	USDI-GS	30 m
Raster / Potential Vegetation	PVT	USDA-FS	30 m
Raster / Observed Vegetation	MTSILC3	USDA-FS	30 m
Polygon / Landscape Boundaries	AMS Zones	USDA-FS	1:100,000
Polygon / Watershed Boundaries	HUC5	USDI-GS	1:100,000
Polygon / Fire Mgt. Zones	FMZ	USDA-FS	1:100,000
Arc / Streams	NHD	USDI-GS	1:100,000

VEGETATION CHARACTERIZATION

Vegetation communities, or stands, derived from satellite imagery were attributed with species, size-class, canopy coverage density classes and habitat type group designations. The minimum area defining a stand was 2 hectares. Mapped stands were attributed with habitat type group designations derived from an intersection with raster-based potential natural vegetation data (Jones, 2002). Mean elevation, slope, aspect, and stand adjacency were additionally associated with each vegetation community. Together these characteristics provided the information needed to parameterize SIMPPLLE for vegetative state advancement (Chew et al., 2002). Natural vegetation dynamics were the focus of this study, and to represent the current landscape in unaltered terms, attributes of stands classified as agricultural were converted to those of native grassland.

Multiple attributes associated with each stand make it impossible to display a map that depicts cover and structural elements of the land and vegetative surface simultaneously. For instance, young stands of lodgepole pine exhibit a different structure than mature stands, and simply mapping the distribution of this species fails to account for differences in size and density components. Using the stand attributes mentioned earlier, a scaled, multi-attribute classification (SMAC) algorithm was developed to produce a set of landcover categories that resemble those of the Anderson Level II (1976) classification used by many federal agencies in the USA. The main difference between the SMAC and Level II cover types is a greater resolution in forest cover diversity. The Level II system only accounts for deciduous, evergreen and mixed forest whereas SMAC forests include riparian, quaking aspen, ponderosa pine, Douglas fir, lodgepole pine, and spruce-cover types.

The SMAC algorithm uses habitat type group stratification to assign forest or non-forest vegetation community status. Species combinations are then reclassified into more general categories representing barren ground, natural grassland, pasture, agricultural land, shrubland, riparian, and multiple forest types. Following that, size-class and density distributions are used to assign non-forest, disturbed forest, or mature forest structural designations. A full description of the classification procedure, output, cover type characteristics and associations, and automation is provided in Appendix A.

Based on results from the SMAC algorithm new landcover maps, representing the current condition of the entire study area, were created. These raster maps contain up to 15 landcover categories represented by 30 m grid cells. As part of the watershed characterization, the distribution of the current landcover condition was tabulated for each of the 38 analysis watersheds. The fractional area of cover types in each watershed was summarized to examine the central tendency of landcover across the study area watersheds. The spatial pattern of landcover was also computed, and represented by a suite of landscape metrics (McGarigal and Marks, 1995) that measured patch dimension (Largest Patch Index), configuration (Landscape Shape Index), and distribution (Contagion Index) within watersheds and surrounding areas.

SIMULATION STRATEGY

Although SIMPPLLE can simulate planned treatments, only natural stand development and disturbance processes were modeled in this analysis. To account for natural propagation of disturbance and regeneration processes, artificial boundaries were avoided. Only watersheds wholly on the interior of the study area landscapes were considered because they are entirely connected to their surrounding landscapes (Figures 1 and 2). Watersheds sharing a border with the periphery of the landscapes were excluded from the analysis because they have an artificial boundary. No data exist on the other side of their exterior perimeter and therefore processes cannot occur or propagate out from there, and this misrepresents the true landscape dynamic.

Vegetation dynamics of 38 analysis watersheds bounded by exterior watersheds on all sides (i.e. the surrounding landscape) were simulated in two ways: 1) within their landscape context and 2) in isolation from the surrounding landscape. In the landscape context scenario, vegetation change was simulated across the entire landscape, while processes occurring within the selected watersheds were tracked. For isolated watershed simulation, the selected watersheds were extracted from the landscape and simulated by themselves. Upon completion, process results of the two different simulations were compared.

For each scenario, SIMPPLLE was initiated to simulate natural vegetation change for a period of 100 years, using a decadal time-step. To capture the general trend and range of variability in process occurrences, simulation of each scenario was repeated 100 times. This combination of time and replication represents up to 1,000 state changes for each vegetation community, and ensures that even low probability events are represented in the simulations.

The boundary of every analysis watershed was used to extract data from the landscape-level vegetation layer, so that each watershed was represented by two distinct vegetation datasets. The first dataset (WAT) represents the watershed in isolation from the surrounding landscape. That is, stands sharing an exterior boundary are not influenced by adjacent stands. Therefore, processes occurring inside the watershed will not be affected by processes occurring outside that watershed. The second dataset (LND) contains identical values for all stands in the selected watershed, except that it is connected the surrounding landscape. In fact, this is the vegetation layer covering the entire landscape, but where processes occurring in the analysis watershed are being tracked independently. With this simulation configuration, processes occurring in adjacent watersheds have the ability to influence processes inside analysis watersheds. By comparing simulation results of the same vegetation communities modeled with and without adjacent stands, the influence of landscape processes was investigated.

COMPARISON OF SIMULATION SCENARIOS

Summing all processes occurring in each decade, estimates of total decadal disturbance were generated. Taking the sum of all disturbed areas over all decades, divided by the number of decades gives the mean decadal amount of total disturbance over the simulation time period. Due to the generalization that results from averaging and summing results of 100 model runs, comparisons of simulation sets are comparisons of the general trend resulting from each simulation context scenario.

Both representations of analysis watersheds (WAT and LND) are identical except for their context. Between context alternative, multiple response permutation procedures (MRPP) (Mielke and Berry, 2001) were used to compare differences in the distribution of

disturbed areas associated with suites of processes, and paired sample t-tests (Ott, 1993) compared differences in total areas affected by simulated disturbance processes.

In both testing situations, significant differences between WAT and LND simulations indicate that a watershed behaves differently when it is not connected to its surrounding landscape. This may also be interpreted as an indication that processes are likely to propagate across watersheds divides to an extent that long-term vegetation dynamics are altered to a noticeable extent. Differences between scenarios can be interpreted as the influence of context and conceptually, the amount by which they vary represents the level of connectivity between watershed and landscape processes.

Comparison of Individual Process Distributions

Multiple-response permutation procedures (MRPP) do not require assumptions of normality or homogeneity of variances, making them well suited for analysis of natural resource data (Biondini et al., 1985; Zimmerman et al., 1985). MRPP provide a nonparametric multivariate technique for testing the hypothesis of no difference between two or more groups of entities. With MRPP, analyses are based on a distance matrix, where treatment alternatives define the groups. Components of this technique yield a test statistic (*T*), *p*-value, and associated measure of "effect" size (*A*). The null hypothesis is one of no difference in process distributions between groups. If this hypothesis is rejected, it indicates that the distributions between groups are not the same. Differences were considered significant when $\alpha \leq 0.05$. Similar to a t or F-test, the purpose of MRPP is to detect concentration within a priori groups, and the MRPP metric is calculated as:

$$\delta = \sum_{i}^{g} C_i \left(\frac{n_i}{2} \right)^{-1} \sum_{K<L} \left[\sum_{j}^{r} \left(X_{K,j} - X_{L,j} \right) \right]^{u/2} \qquad \text{(Eqn. 1)}$$

Where:

δ =	*linear combination of average within-group distance measures for g groups*
C_i =	n_i / N
u =	*distance measure (value of 2 yields squared Euclidian distance)*
r =	*number of measurements taken on the* K^{th} *object (2 in this case)*
K and L	*are objects with measurements* $X_{K,1}$, …, $X_{K,r}$
n_i =	*number of objects in each group*
N =	*total number of objects over all groups*
g =	*number of groups*

After δ is determined, the probability of obtaining a δ value of this magnitude or smaller is approximated (i.e. the expected delta) from a continuous Pearson Type III distribution. This permutation distribution accommodates datasets that are asymmetrical, and incorporates the mean, standard deviation, and skewness of δ under the null hypothesis (McCune et al., 2002).

The test statistic, *T*, describes the separation between groups. When calculated, *T* is the difference between the observed and expected deltas divided by the standard deviation of delta:

$$T = \frac{(\delta - m_\delta)}{s_\delta} \qquad \text{(Eqn. 2)}$$

where m_δ and s_δ represent the mean and standard deviation of δ under the null hypothesis. In this form, m_δ is taken as the expected delta. Increasingly negative values of *T* indicate stronger separation between groups.

Also based on the Pearson Type III distribution, the *p*-value associated with *T* is useful for evaluating how likely it is that an observed difference is due to random chance, however it is strongly influenced by sample size. To provide a measure of treatment effect size that is independent of the sample size, the chance-corrected within-group agreement statistic, *A*, is calculated as:

$$A = 1 - \frac{\delta}{m_\delta} \qquad \text{(Eqn. 3)}$$

This effect size statistic describes within-group homogeneity. When all items are identical within groups, then $A = 1$, the highest possible value. If heterogeneity within groups equals expectation by chance, then $A = 0$. With less agreement within groups than expected, $A < 0$. Put simply, differences between groups become more evident as *A* gets larger. In community ecology, values for '*A*' are commonly below 0.1, even when p-values are significant. Values of $A > 0.3$ are fairly high, and indicative of detectable differences between groups (McCune et al., 2002).

In this application of MRPP, groups were defined by the isolated watershed (WAT) and landscape context (LND) simulation sets, and separation between groups was measured with Euclidian distance. With this method, MRPP tested for differences in the

responses of 12 processes over ten time-steps, between the 2 groups (Table 4). Principle components analysis (PCA) determined how individual processes contributed to treatment differences. Comparisons were made for each of the 38 analysis watersheds, and differences between the two scenarios were considered significant when $p < 0.05$, assessed relative to *'A'*. Computations necessary to perform MRPP and associated analyses were coded and executed as a Visual Basic for Applications macro in spreadsheet format (King, 2000; Bullen et al., 2003).

Table 4. *MRPP test structure, where areas disturbed by each simulated process are reported across columns, and simulation time-steps (TS) are recorded in rows, and context groups (WAT, LND) split the sample. Data from watershed 2_1 are shown.*

Mean Area Disturbed per Simulation Time-Step (1-10) by each Process (1-12)													
TS	**1**	**2**	**3**	**4**	**5**	**6**	**7**	**8**	**9**	**10**	**11**	**12**	**Group**
1	3	63	0	0	463	67	8	330	421	704	2405	1195	WAT
2	2	56	0	0	2630	72	25	379	493	6722	4338	5991	WAT
3	7	100	0	0	995	43	52	441	495	6246	4191	5566	WAT
4	27	183	0	1	1166	78	227	703	498	6310	4106	5370	WAT
5	29	203	0	1	1866	83	336	757	492	5521	3753	5544	WAT
6	39	268	0	4	2110	101	729	835	482	5533	3932	5697	WAT
7	20	237	0	6	1897	83	474	889	430	5862	4000	6719	WAT
8	20	285	0	11	1912	105	594	1056	398	5188	3773	6022	WAT
9	20	299	0	8	1908	99	637	1093	379	5083	3621	5763	WAT
10	13	330	0	11	1634	89	817	1055	352	5058	3777	5973	WAT
1	2	62	0	0	464	57	4	297	404	1141	3526	1712	LND
2	0	43	0	0	2019	61	15	293	358	10435	6777	8031	LND
3	2	97	0	1	877	46	49	376	419	7339	5368	4747	LND
4	22	172	0	2	1039	54	168	560	345	9534	6408	7150	LND
5	15	216	0	3	1325	69	321	673	358	7054	5588	5504	LND
6	17	221	0	4	1634	79	499	705	331	8021	5826	7090	LND
7	14	237	0	4	1591	78	442	820	300	7377	5075	6528	LND
8	16	262	0	12	1596	76	447	865	249	8011	5643	7504	LND
9	12	304	0	15	1576	98	516	857	243	7199	4971	6410	LND
10	11	312	0	6	1424	86	603	901	231	7276	5188	7038	LND

Comparison of Combined Disturbance Proportions

Paired sample t-tests assessed differences in the amount of disturbed areas between scenarios. By combining occurrences of all types, the total watershed area affected by disturbance processes was determined for every time-step (decade). Considering all time-steps, the mean decadal area disturbed over the simulation period was also computed.

Two-tailed tests for differences between paired scenarios were applied individually to each of the 38 analysis watersheds, where the distribution of total decadal

disturbed area was compared over the simulation period (ten time-steps). The null hypothesis being tested was that no difference exists between paired simulations sets at $\alpha \leq 0.05$.

An additional two-tailed test was computed to compare the mean decadal area affected by disturbances in analysis watersheds when watershed responses were grouped by WAT and LND context simulations. In this comparison, one test was applied to a set of 38 pairs. The null hypothesis was that no difference exists between groups. Each modeled alternative represented the mean decadal area disturbed over the simulation period, and differences in affected area between the two watershed context scenarios were considered significant when $\alpha \leq 0.05$.

RELATING WATERSHED AND DISTURBANCE CHARACTERISTICS

Multiple linear regression procedures were used to model the interaction between watershed characteristics, and differences in the mean decadal amount of watershed area affected by disturbances when simulated in a landscape context versus when it is simulated in isolation. Differences between scenarios can be interpreted as the influence of context and the amount by which they vary represents an index of landscape connectivity (LC). Conceptually, LC can be expressed as relative differences in watershed area disturbed due to context. As LC increases so does the connectivity between watershed and landscape processes. This index can potentially be calculated for other watersheds in the region to assess the potential for connection to landscape processes.

For analysis purposes, a database of watershed properties was populated with characteristics of each watershed and a buffer area encompassing its respective hydrologic divide, and related disturbance measures including test statistics describing differences between scenarios. Landscape connectivity (LC) was predicted as a function of several watershed characteristics using multiple linear regression techniques. The magnitude of the standardized regression coefficients in this final prediction equation indicate the influence that those watershed characteristics have on the interaction between landscape and watershed disturbance processes.

Watershed Characterization

Each analysis watershed was described by shape, drainage pattern, elevation, slope, aspect, terrain ruggedness, current landcover distribution and configuration (3 landscape metrics), mean temporal disturbance process distribution, and mean decadal differences between process distributions in the two context treatment simulations.

Shape

Watershed shape affects rainfall runoff patterns (Strahler, 1964) such that narrow watersheds tend to have more flashy responses than round ones. Shape can also be related to parent materials and therefore offer some regional stratification. To describe shape, a circularity index (CI), that is based on the compactness coefficient described by Black (1996) was used. CI compares the dimensions of a watershed to a round circle with the same area. As values of the index approach the high of one, the measured watershed shape becomes more round. The index is calculated as:

$$\mathbf{CI} = \frac{\text{perimeter of a circle with same area as watershed}}{\text{perimeter of watershed}} \qquad \text{(Eqn. 4)}$$

Drainage network

Drainage networks are indicators of climate, parent materials, and vegetation characteristics (Wohl, 2000). Using 1:100,000 scale linear stream features of the NHD, and HUC5 watershed boundaries, a drainage density index (DD) was calculated:

$$\mathbf{DD} = \frac{\text{total length of streams in a watershed (km)}}{\text{total watershed area (sqkm)}} \qquad \text{(Eqn. 5)}$$

Topographic attributes

Elevation, slope, aspect, and ruggedness were derived from a digital elevation model with 30 m grid cells. For elevation, measures of the mean, median, and range were calculated. Average watershed slope (degrees) and median aspect represented the inclination and direction of watersheds. Indices of terrain ruggedness (TRI) have been

used to study the movements of wildlife (Beasom, et al., 1983); (Nellemann and Cameron, 1996); (Nellemann and Fry, 1995); (Nellemann and Thomsen, 1994); (Nielsen et al., 2004), forest productivity (McNab, 1993), and drainage patterns (Patton and Baker, 1976). Landform characteristics have the potential to encourage or hinder the spread of disturbance processes across landscapes (Turner and Romme, 1994), and three forms of TRI were used to describe third and fourth orders of land surface complexity (Blaszczyski, 1997) in analysis watersheds:

TRI 1 = Drainage density * Basin Relief (Melton, 1957) (Eqn. 6)

$$\textbf{TRI 2} = \left[\sum \left(x_{ij} - x_{00)}\right)^2\right]^{1/2} \text{ (Riley et al., 1999)} \qquad \text{(Eqn. 7)}$$

where $_{xij}$ = elevation of each neighbor to cell (0,0)

$$\textbf{TRI 3} = \frac{\text{aspect variety} \times \text{percent slope}}{\text{aspect variety} + \text{percent slope}} \text{ (Ahl et al., 2005)} \qquad \text{(Eqn. 8)}$$

where variety = number of observed categories in the analysis window

Landcover composition and configuration

Relative proportions of landcover categories, produced from the SIMPPLLE input data by the SMAC conversion algorithm, represent the current land and vegetation composition of the analysis watersheds. Possible landcover types include places where no data exist, barren ground, water, grassland, shrubland, savannah, riparian shrubs, riparian forest, quaking aspen forest, spruce-fir forest, lodgepole pine forest, Douglas fir forest, ponderosa pine forest, and disturbed forest. For more generalized landcover patterns, components were aggregated into non-vegetation, non-forest, and forest vegetation groupings.

The characterization of patterns can be an important component of landscape evaluation and management (Farina, 2000) because landscape configuration can generally be related to ecological processes (Forman and Gordon, 1986; Zonneveld and Forman, 1990). Many metrics have been developed that describe the proportions and configuration of patches, classes of patches, and landscape-level system properties

(McGarigal and Marks, 1995). Because each metric measures a specific characteristic of heterogeneity, simultaneous consideration of several indices is often instructive (Gustafson, 1998). Three landscape-level indices were computed for each analysis watershed with FRAGSTATS software, version 3 (McGarigal et al., 2002). The Largest Patch Index (LPI) measures the percentage of total landscape area comprised by the largest patch. Landscape Shape Index (LSI) values can be interpreted as a measure of patch aggregation; as LSI increases, patches become increasingly disaggregated. Lastly, the Contagion Index (CONTAG) assesses overall landscape clumpiness. When Contagion is high, large clumps exist (Turner et al., 1989; McGarigal and Marks, 1995).

Disturbances

Mean decadal disturbance area as a percent of the total watershed area was computed for all processes simulated by SIMPPLLE in each watershed (Table 2). The sum of all disturbances per decade, and the mean area disturbed per decade, and the difference between mean decadal disturbed areas due to simulation context were also computed. Disturbances due to mountain pine beetle and western spruce budworm infestation were modeled at various severities, but in the final analysis, both light and severe occurrences were simply lumped into MPB and WSBW categories.

Test statistics

Other included analysis watershed attributes were the MRPP test statistic, its *p*-value and associated effect size statistic (*A*), paired-sample t-test value and its *p*-value.

Buffer Characterization

Structural elements of the biophysical environment can affect the propagation of process across landscapes. To account for properties of the divide that separate watersheds from their surroundings, a 1-km buffer was established around their boundary centerline (Figure 2). Within the buffer, the same topographic, and landcover characteristics describing the analysis watershed were also computed. Properties of the boundary buffer were associated with the corresponding watersheds in the database.

Factors Affecting Disturbance Differences

A multiple regression approach was used to relate watershed and ridgeline characteristics to the mean decadal difference in watershed area disturbed by natural processes between the two simulation scenarios. When significant differences in disturbance proportions between the isolated and landscape context watershed simulations were observed, a high level of connection between landscape and watershed processes was inferred. This condition can also be interpreted as a high likelihood of process propagation across the watershed divide. In contrast, small differences between disturbance processes distributions were viewed as an indication that processes within a watershed are not strongly connected to those occurring in the surrounding landscape.

The percent difference between mean decadal relative watershed areas affected by all disturbances when the watersheds were simulated in isolation versus when the same watersheds were simulated in the context of their surrounding landscapes (DIFF) was modeled as a function of independent variables describing watershed and boundary characteristics. Variables that did not contribute to the prediction of differences were eliminated in a backward stepwise fashion until a parsimonious model became evident.

RESULTS

VEGETATION CHARACTERIZATION

Analysis watersheds tended to have significant proportions of grassland and forest types, and relatively little barren ground (Figure 3). In general, grassland occupied between 35 and 45%, and the combination of various forest types constituted another 35 – 45% of watersheds. Among the forest types, lodgepole pine was generally the most prevalent, covering an average area of roughly 20%. Rocky or barren ground was a small component of most watersheds, but given that such conditions are usually associated with ridge crests it is understandable that this cover type only extends over 3% of areas. The spatial arrangement of landcover can generally be described as having grass or shrub cover types at lower elevations and as elevation increased there was a vertical stratification of forest cover types, changing from ponderosa pine, to Douglas-fir, lodgepole pine, and spruce-fir forest. South and west facing slopes had grassland, shrubland, or ponderosa pine components. High, exposed and rocky ridge lines framed some watersheds.

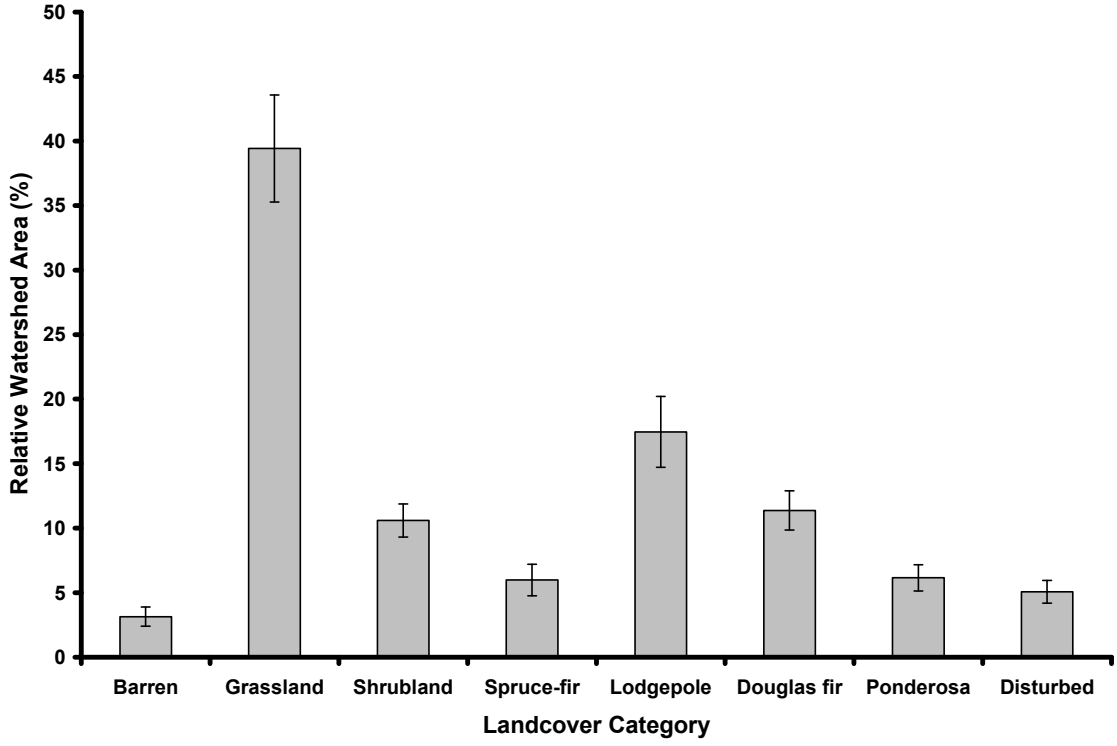

Figure 3. *Mean relative watershed area by landcover type derived from 38 analysis watersheds across central Montana, USA. Error bars represent the std. error of estimate.*

Figure 4. *Typical landcover patterns found in study area watersheds (analysis unit 2_1 is shown here). Shrub and grassland are represented by light shades of green and brown, mature forest is dark green, and barren and recently disturbed areas are red.*

COMPARISON OF SIMULATION SCENARIOS

SIMPPLLE modeled up to 12 disturbance processes (Table 2), but not all had notable extents over the simulation time-steps. To illustrate the distribution of processes occurring over the decadal time-steps, mountain pine beetle, and western spruce budworm types and severities were combined. Mountain pine beetle and fire are the dominant vegetation disturbance processes across the study area watersheds. Light severity and stand replacing fire tended to occur more often than mixed severity fire.

The mean decadal watershed area affected by fire tended to be greater in watersheds when they were simulated in the context of their surrounding landscape (LND), but this was not true for all disturbance processes (Figure 5).

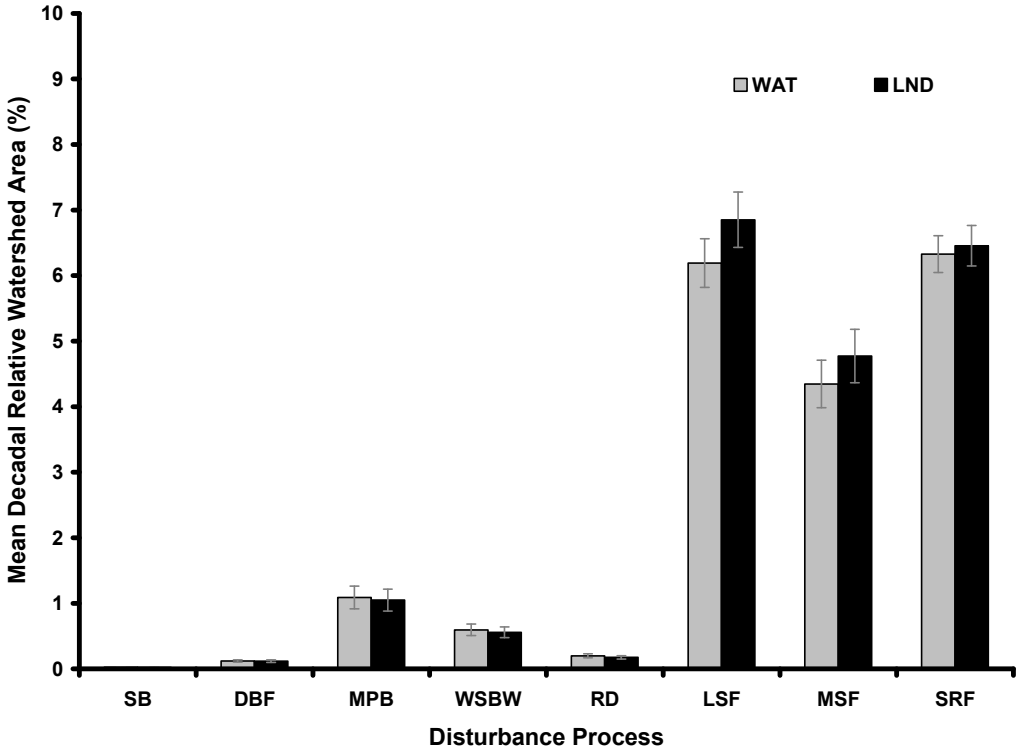

Figure 5. *Mean decadal relative watershed areas affected by disturbance process types for 38 analysis watersheds, based on LND and WAT context simulations. Error bars represent the standard error of estimate.*

Comparison of Individual Process Distributions

Multiple response permutation procedure (MRPP) tests for differences between disturbance process distributions were applied to all watershed simulation sets (WAT vs. LND). Vegetation responses were highly variable, with some watersheds exhibiting extreme differences, while little change in disturbance pattern could be detected in others (Figs.e 6a, and b). For example, disturbance process patterns in watershed 1 located within landscape 2 (coded as 2_1) were strongly differentiated by context (Figure 6a). The *p*-value derived from MRPP was 0.0012, and the chance corrected statistic, A = 0.153. Together these scores reinforced the clear distinction between processes distributions resulting from each context simulation alternative. Exhibiting a very different response, virtually no differences between disturbance processes were observed in watershed 1 located with landscape 4 (coded as 4_1). MRPP derived p= 0.865, and A = 0.039 were clear indicators that simulation context had little effect on how disturbance processes were distributed in this watershed (Figure 6b).

(A)

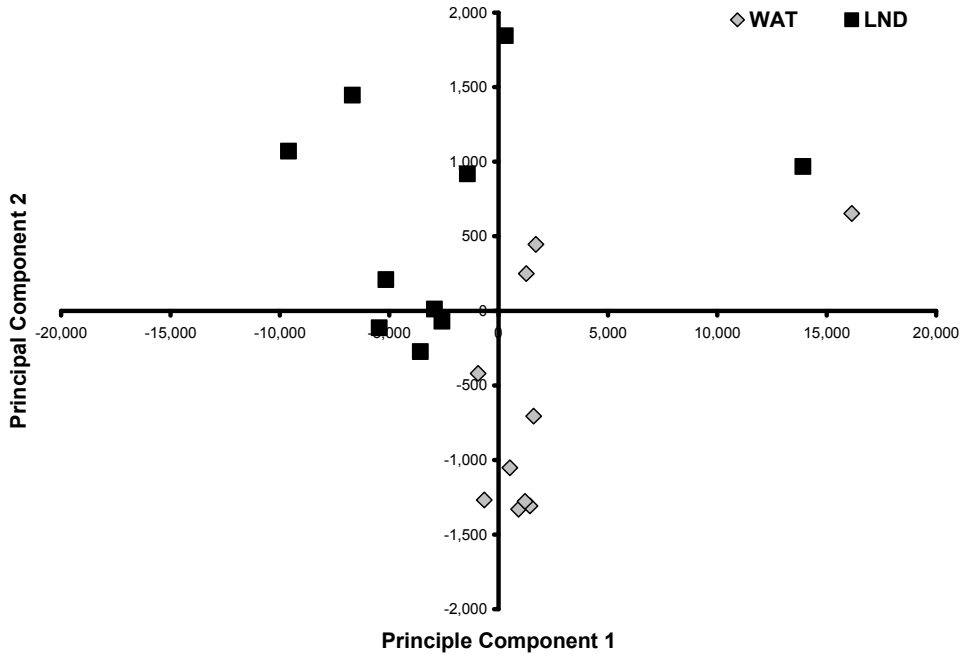

(B)

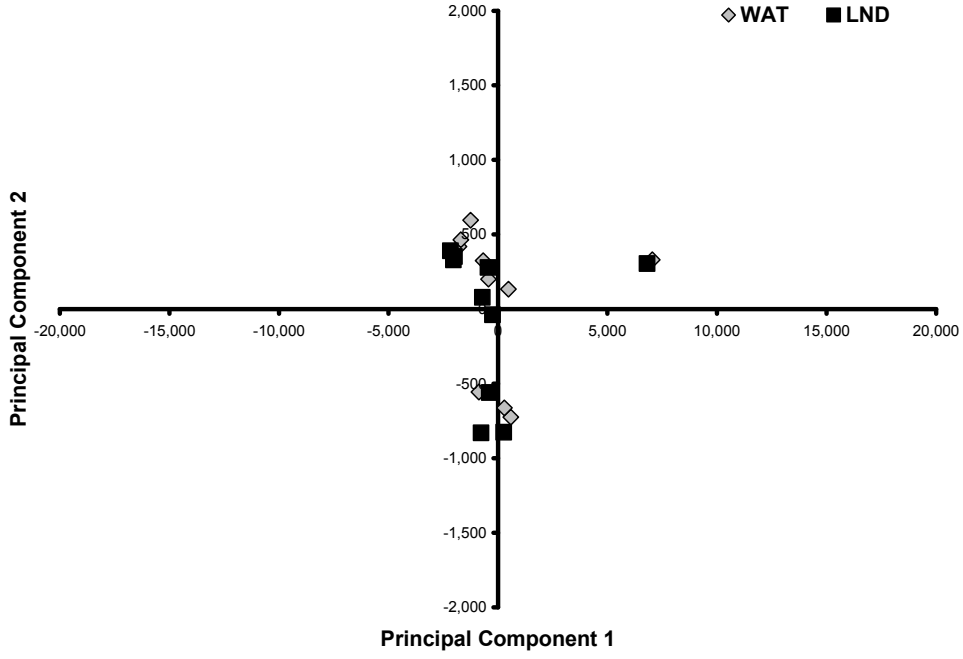

Figure 6. *Principal components plots of MRPP tests comparing the distribution of 12 disturbance processes over ten decadal time-steps, between landscape context and isolated watershed simulations: (A) comparison of Landscape 2, watershed 1 on top, and (B) Landscape 4, watershed 1 (p = 0.865, A = 0.039) is shown below.*

Although a wide range of MRPP test values were encountered in all 38 comparisons, clear separation between WAT and LND simulation groups was not apparent across all watersheds. Combining all disturbance processes into one category simply called 'disturbance', differences in the decadal distribution, and mean decadal magnitude of disturbances were compared with paired-sample t-tests.

Comparison of Combined Disturbance Proportions

Differences between decadal distributions

Paired sample t-tests applied to all simulation sets indicated that significant differences in the amount of area disturbed on a decadal basis were detectable in 32 of 38 pairs, representing 84% of analysis watersheds (Table 5). Grouping *p*-values into no (>0.05), somewhat (≤ 0.05), strong (≤ 0.01), and very strong (≤ 0.001) significant differences indicated that 16% of the watersheds exhibited little to no difference between simulation types, 16% were somewhat different, 45% were strongly different, and 24% were very strongly different.

Table 5. *Influential watershed attributes, and comparisons of decadal disturbance distributions between WAT and LND simulations scenarios using paired sample t-tests. Terrain ruggedness (TRI 3) and LSI are unitless measures, but BRRN, LPFR, DFFR, describe the relative watershed areas (%) occupied by those landcover categories. FV is the sum of all forest types. Underscore designations refer to summarizations of watershed boundary (b), and watershed interior (i) characteristics. Mean decadal differences in relative watershed areas affected by disturbances between paired WAT and LND simulations are given as DIFF (%) and t values. P-values were grouped into sig. levels.*

LND	WAT	TRI 3_b	LSI	BRRN_b	LPFR_i	DFFR_i	FV_i	DIFF	Paired t	Sig.
6	6_2	254	17.1	13	10	15	36	0.2	0.633	NS
6	6_5	220	30.4	2	1	10	13	0.1	-1.061	NS
12	12_1	158	16.2	1	0	0	1	0.0	-0.199	NS
12	12_2	380	52.2	6	4	10	27	0.1	-0.435	NS
6	6_1	268	28.5	1	2	18	26	0.6	1.730	NS
11	11_3	244	22.6	4	2	4	7	0.6	1.718	NS
4	4_1	562	32.3	45	11	31	54	0.5	2.244	0.05
5	5_3	222	21.3	1	6	6	16	0.5	2.330	0.05
6	6_4	156	23.5	3	0	2	2	0.4	-2.224	0.05
10	10_3	182	17.4	0	2	4	7	0.6	2.446	0.05
12	12_3	380	36.7	2	14	10	50	0.7	2.066	0.05
16	16_1	354	33.1	12	15	4	29	0.5	2.237	0.05
6	6_3	228	25.1	7	1	21	27	0.9	4.007	0.01
6	6_6	250	40.4	3	1	15	19	0.6	3.005	0.01
7	7_2	174	38.7	4	34	28	75	1.8	4.166	0.01
7	7_3	182	32.4	0	49	8	81	1.7	3.793	0.01
7	7_5	174	22.7	3	56	13	82	2.1	3.852	0.01
7	7_6	158	29.3	2	39	3	55	1.0	3.662	0.01
8	8_1	170	20.3	0	18	18	41	1.2	3.524	0.01
8	8_2	198	13.3	0	5	7	14	0.8	3.482	0.01
8	8_4	280	25.5	5	25	29	86	2.8	3.393	0.01
9	9_1	244	29.9	5	38	1	75	1.4	4.220	0.01
9	9_2	384	43.9	23	41	1	83	0.7	3.867	0.01
10	10_1	366	24.4	24	2	13	35	0.7	3.045	0.01
10	10_2	342	25.0	14	4	4	17	0.4	3.925	0.01
10	10_4	376	33.9	7	8	11	31	1.1	4.228	0.01
11	11_1	196	18.5	2	4	5	11	1.4	3.251	0.01
11	11_2	244	11.0	2	0	0	1	1.0	3.035	0.01
17	17_1	196	38.2	5	17	9	35	0.7	4.247	0.01
2	2_1	446	29.7	3	34	29	72	5.6	5.842	0.001
5	5_1	434	36.3	15	22	23	65	1.7	4.394	0.001
5	5_2	228	35.0	4	31	24	60	1.6	6.369	0.001
6	6_7	218	5.6	1	0	0	0	1.2	-9.079	0.001
7	7_1	218	28.1	1	43	28	74	2.6	6.349	0.001
7	7_4	182	24.9	1	48	8	74	1.8	4.449	0.001
8	8_3	260	22.8	1	20	13	44	2.2	4.916	0.001
9	9_3	204	32.4	3	37	0	74	2.4	6.104	0.001
10	10_5	218	22.7	1	17	8	29	1.4	4.772	0.001

Mean decadal differences between context groups

Differences in the mean decadal amount of disturbance due to context were examined with a paired sample t-test. Averaged over all analysis units, watersheds with vegetation dynamics simulated in the landscape context tended to have 20% of their area disturbed every decade, compared to 18.9% for the same watersheds when simulated in isolation. The two-tailed t-test on paired watershed responses showed the difference between scenarios to be significant ($t = -6.003$, $df = 37$, $p < 0.001$).

A box plot illustrates the differences between disturbed areas over the simulation period in each context scenario (Figure 7). Vegetation dynamics simulated in the landscape context exhibited more disturbed area, and patterns of disturbance that were more variable over time than when vegetation communities were simulated in isolation form their surrounding landscape.

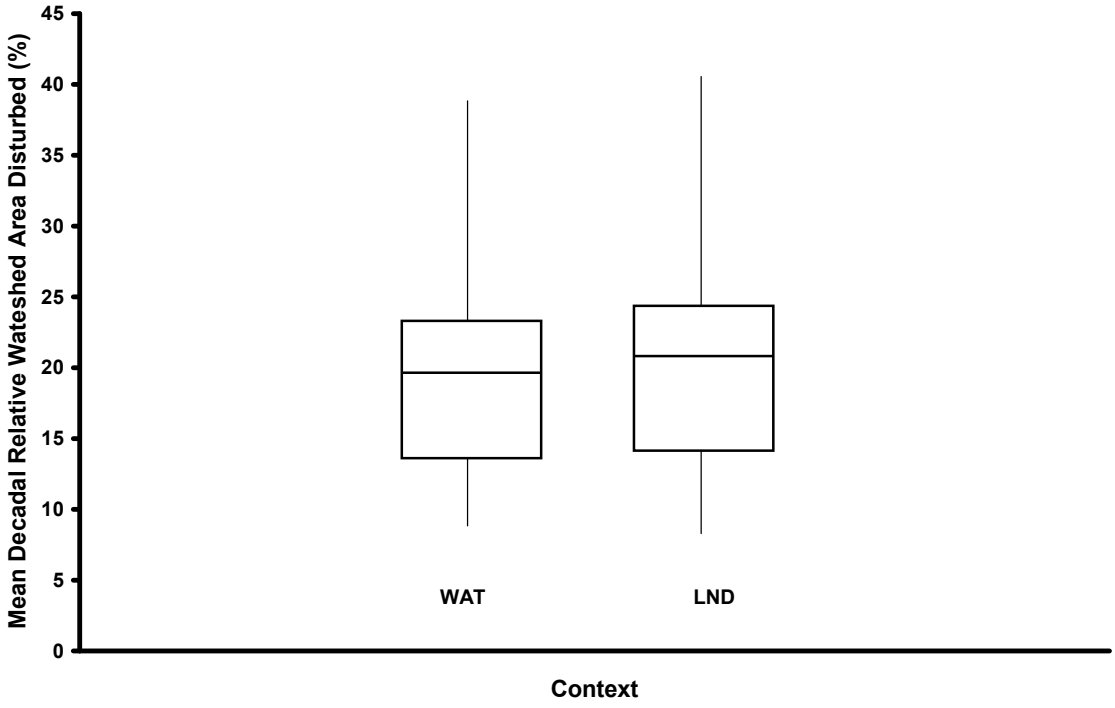

Figure 7. *Mean decadal relative watershed area affected by the sum of all disturbances, across all watersheds for WAT and LND contexts over the 100-year simulation period.*

RELATING WATERSHED AND DISTURBANCE CHARACTERISTICS

Internal and ridgeline attributes were used to construct an equation that predicts differences in the mean decadal disturbed relative watershed areas due to vegetation simulation context (DIFF). The magnitude of differences may be thought of as levels of watershed vegetation process connectivity to the landscape processes. When differences are small, the watershed appears to function in a manner that is independent of its surroundings. Conversely, as differences between simulation contexts become larger, processes within watersheds are increasingly connected to landscape processes. As such, the equation can be considered a predictor of landscape connectivity (LC), where larger values are indicative of increasing connectivity between watershed and landscape processes.

The final regression equation predicted LC as a function of five variables. Summed over the simulation time period, total disturbance differences in total areas affected by disturbances due to simulation context was the dependent variable. The independent variables were 1) the proportion of barren ground, and 2) ruggedness of watershed divides (Eqn. 8), along with 3) the proportion of lodgepole pine and, 4) Douglas fir forest inside watersheds, and 5) the aggregation of patches in the current watershed mosaic (LSI). The final prediction equation for LC was:

$$\mathbf{LC} = -0.480 + (0.007925)\,\mathbf{TRI\ 3\_b} + (0.03995)\,\mathbf{LPFR\_i} + (0.04072)\,\mathbf{DFFR\_i} + (-0.0843)\,\mathbf{BRRN\_b} + (-0.0385)\,\mathbf{LSI} \quad \text{(Eqn. 9)}$$

The regression was significant ($F = 15.43$, $p < 0.001$), and accounted for 69% of the variation in mean decadal disturbance differences due to simulation context (Table 6). The standard error of estimate indicates that predictions are within 0.6% of the mean measured difference in decadal disturbances. There was no evidence of collinearity with independent variables, as variance inflation factors (VIF) ranged between 1.2 and 2.8, which is well below the standard cutoff of 10 (Kleinbaum et al., 1988).

Table 6. *Landscape Connectivity (LC) model description.*

N	DF	R	R^2	Adjusted R^2	Standard error of the estimate
38	32	0.86	0.74	0.69	0.57

Standardized regression coefficients of the 5 independent variables included in the final model show that the proportion of barren ground and terrain ruggedness in the watershed perimeter, along with proportions of lodgepole pine forest cover had the greatest influence on estimates of connectivity between landscape and watershed disturbance processes (Table 7). Douglas fir proportions within watersheds were also significant, but the influence of this variable was roughly half that of lodgepole pine forest cover. The last variable of consequence was the aggregation of current landcover patches (LSI). Small values of LSI indicate aggregated landcover patches. The model showed that as values of LSI increased, differences in disturbed area due to context decreased. As such, increased patch aggregation led to increased differences, and hence landscape connectivity.

Table 7. *Landscape Connectivity (LC) multiple regression model coefficients.*

	Unstandardized Coefficients		*Standardized Coefficients*		
Predictor	**B**	**Std. Error**	**Beta**	**Sig.**	**VIF**
Constant	-0.480000	0.461		0.307	
BRRN_b	-0.084300	0.017	-0.754	< 0.001	2.370
TRI 3_b	0.007925	0.002	0.744	< 0.001	2.831
LPFR_i	0.039950	0.007	0.654	< 0.001	1.333
DFFR_i	0.040720	0.011	0.373	0.001	1.151
LSI	-0.038500	0.015	-0.298	0.018	1.442

DISCUSSION

MODEL JUSTIFICATION

The SIMPPLE model was selected for use in this study because it is being institutionally applied throughout the Rocky Mountain region, its underlying philosophy and architecture, and user support provided by system developers. This modeling system was originally developed for the U.S. Department of Agriculture (USDA) to simulate vegetation changes in the Northern Region (R1) of the Forest Service. Since its inception, SIMPPLE has been an effective component in landscape planning and analysis efforts throughout the Rocky Mountain region. National Forest managers have found the model to be particularly good at integrating current knowledge and using it to capture vegetation patterns and projecting them over time. It can be used to clearly display interactions between management alternatives and the effect they may have on future landscape patterns of vegetation (Lee et al., 2003).

Simulation of vegetation patterns over large areas requires either substantial computing resources, or models that can process data efficiently. SIMPPLLE uses polygons to represent spatial patterns of landcover, pathways to advance stands through developmental stages, and probabilities to impart disturbance processes. With this design, landscape-level changes can be modeled with relative efficiency. This approach, however, does forego some detail. For example, once stand boundaries are defined by the initial landcover, they remain static over the course of simulation. Stand attributes change as pathway states are altered, but the dimension of stands remains constant. This is unrealistic, and may inhibit some interpretations of ecological processes. Although highly detailed models can be informative, they can be difficult to parameterize and run over large areas, due to limitation in data, and processing requirements. Overall, SIMPPLLE offers a good compromise between detail and efficiency, and provides ample information about vegetation changes across large areas for long time periods.

SITE SELECTION

There is no clear definition of how a landscape should be defined. In general, landscape is the subject of the applied discipline of land evaluation (Zonneveld and Forman, 1990), and is simply defined as 'the total character of a patch of the earth'. Outlines of the landscapes used in this study were originally defined by USDA Forest Service planners for a regional assessment of the management situation that is mandated by the National Forest Management Act (USDA-FS, 1982). These landscape-level planning units intended to capture unique ecological characteristics of central Montana, and were useful for stratifying the region into individual landscapes.

Watersheds provide natural sub-divisions of the landscape, and are thus useful for the analysis of ecological processes. In Montana, three levels of watershed hierarchies are available, ranging from river basins (HUC4), to watersheds (HUC5), and sub-watersheds (HUC6). River basins on average cover 365,000 ha, and such a large analysis unit would not be appropriate for examining the effects of disturbance processes on landscapes. Rather, management is often planned over areas that resemble the dimensions of watersheds and sub-watersheds. At the time this study was initiated, HUC6 delineations were not available for the entire study area, and so HUC5 delineations were used instead. The average size of HUC5 watersheds (40,500 ha), is somewhat larger than most management units, but nonetheless offers a good compromise because they are not too large yet represent functioning ecological systems.

The watershed level of sub-division yielded a sufficient number of units so that wholly interior watersheds could be identified in all study area landscapes. This was important, because the connection between landscapes and watersheds could only be studied if analysis watersheds were completely surrounded by vegetation in adjacent watersheds. If the edge of a watershed was at the periphery of a defined landscape, as exterior watersheds were, then no disturbance process could originate in or spread from them because no data are present there. For this reason, only interior watersheds were selected, and processes within them individually simulated and analyzed.

COMPARISON OF SIMULATION SCENARIOS

Data management

One of the useful features of SIMPLLE is that individual simulations are stochastic, and multiple simulations can be run to capture a range of variability in model output, while all model elements are held constant. Running 100 simulations over 10 decades with 12 disturbance processes produced a large amount of output that needed to be organized. One problem of datasets having very large sample sizes is that tests can detect minute differences that may be statistically significant, but physically or ecologically have no practical significance. Previous analyses of SIMPPLLE output have shown that process predictions based on large numbers of simulations tend to be normally distributed and can be described with parametric measures (Zuuring and Sweet, 2000).

Through a series of summarizations, the relative watershed areas affected by the disturbance processes simulated with SIMPPLLE were analyzed at three levels of aggregation, comparing 1) the temporal suit of all process distributions, 2) the decadal distribution of the total area affected by all disturbances processes, and 3) the average area disturbed per decade. The definitions of the three levels of aggregation are:

(1) **Process Distributions**: *the relative area affected by every process is summarized every decade by the mean of 100 simulations*

(2) **Disturbed Area Distribution**: *areas affected by all disturbance processes are summed to yield total disturbed area every decade (based on values from (1).*

(3) **Mean Decadal Disturbed Area**: *the total area disturbed over the simulation period (sum of (2) over decades) divided by the number of decades to yield the mean area that is disturbed every decade.*

These levels of aggregation reduced the dimensionality and variability in model output, and made results of analytical procedures more realistic. Upon summarization, simulation sets produced for each watershed were grouped into those that were simulated in isolation from the surrounding landscape (WAT), and those that were conducted in the landscape context but tracked disturbance processes in the watershed of interest (LND).

For each scenario a non-parametric test was used to compare process distributions and a parametric test was employed to evaluate differences in more generalized measures of disturbed areas.

Test application

Natural resource data rarely follow normal distributions, and important assumptions are often violated when standard parametric tests are used to compare responses. Testing for differences between suites of vegetation responses (processes) to a treatment (context) over time (decades) represented an analytical challenge that was addressed with multiple response permutation procedures (MRPPs). MRPPs are particularly useful for analyzing ecological data because they do not require assumptions of normality or homogeneity of variance (Mielke and Berry, 2001). Over the years, MRPP has been used to interpret a variety of differences in vegetative community responses to treatments. Biondini et al. (1985) compared sagebrush community responses to four levels of treatments, while Zimmerman et al. (1985) investigated prairie vegetation community responses to fire severities, and differences in old-growth and secondary forest species composition were examined with MRPP by Lesica et al. (1991). The similarity of these other applications suggested that MRPP was an appropriate means of comparing the distribution of disturbed area by each process over time between the context treatment scenarios.

Two sets of simulations were produced for each of the watersheds, and comparisons of generalized differences in amounts of relative watershed area disturbed over the course of simulation, and over an average decade were well suited for paired-sample t-tests. The paired-sample t-test is relatively sensitive, as it assumes no difference between the paired data. Values examined by this test were based on averages taken from averages, which removed outliers, and greatly reduced the variability in each sample. Being able to detect small, but meaningful differences was therefore useful in this application of paired-sample t-tests.

Comparing Process Distributions

Areas affected by individual disturbance processes between context scenarios were very different in some watersheds, while differences in others were not apparent, and overall a systematic pattern was difficult to detect. Most notable, however, was the fact that light, mixed and stand-replacing fire tended to be more abundant in LND vs. WAT simulations. This indicates that all the analyzed watersheds are strongly influenced by fire in the landscape. It suggests that regardless of watershed context and characteristics, fire processes move about the landscape and invariably influence internal watershed processes, even if the fires that burn in watersheds do not originate within them. The question then becomes, how important is that influence.

Although the simulated impact may be small, the magnitude of that impact may be a result of data resolution, and model conceptualization. In other words, observed differences in disturbed areas due to the context treatment may actually be due to the ecology of the systems, but also related to the data used to represent it, and the tools used to simulate it. What the model shows may or may not resemble the real system, but until there is an opportunity to empirically test this, it will be difficult to know for sure.

Comparing Disturbance Proportions

Aggregating all the simulated disturbance processes into a combined total of disturbance vs. succession permitted more generalized analyses to be conducted. First, the distributions of total disturbed area produced per decade by each context scenario were compared for each watershed. In 32 out of 38 watersheds (84%) LND and WAT context simulations produced significantly different patterns of disturbance. In all cases where differences were significant, LND simulations created more disturbed areas than WAT simulations. This difference may be related to elevated amounts of fire that occurred when the watershed was connected to the landscape mosaic.

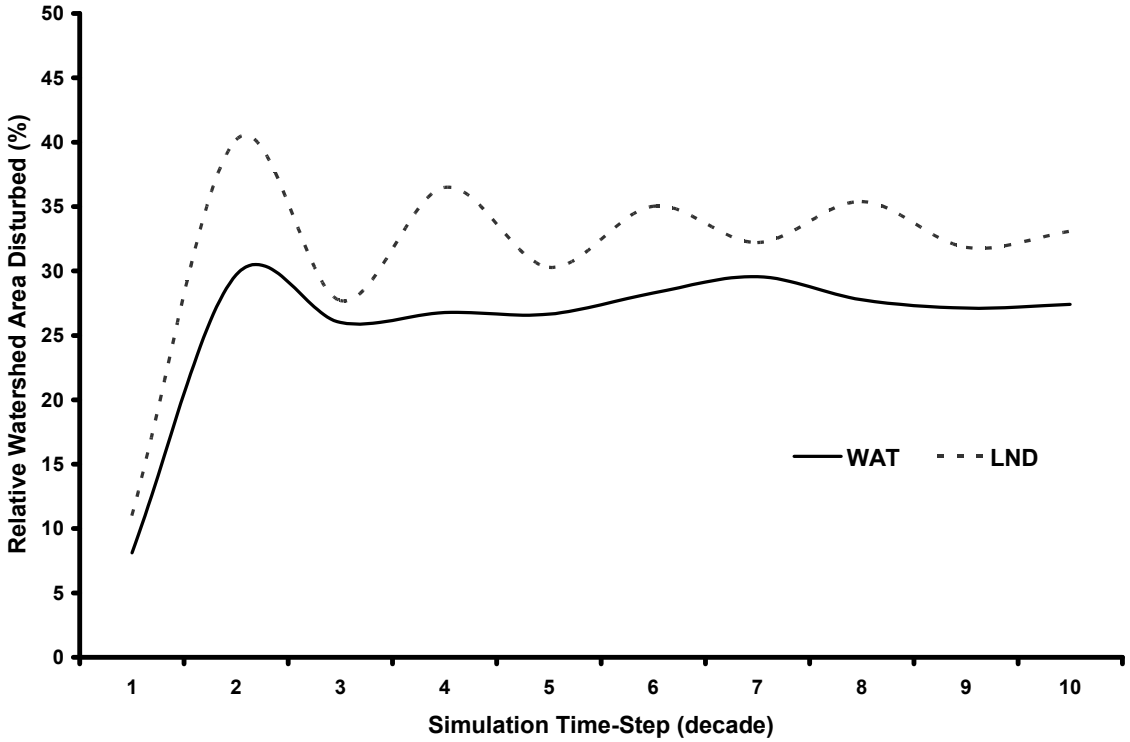

Figure 8. *A comparison of relative watershed area disturbed over decadal time steps by context, showing data from watershed 2_1.*

In a comparison of the average decadal amount of disturbed area between watersheds grouped by context, LND simulations produced significantly more disturbed area than WAT-based simulations. For example, watershed 2_1, located in the Little Belt Mountains, consistently demonstrated significantly different patterns of disturbed area between context scenarios (Figure 8). Over time, larger and more frequent disturbances occurred when the watershed was simulated in the context of the surrounding landscape. The cyclical pattern of disturbance in watershed 2_1 is indicative of periodic episodes of fire, perhaps in grasslands. When connected to the surrounding landscape, disturbances such as fire can spread across large areas of connected and susceptible landcover, like grassland or mature forest, if strong barriers are not present. The frequency of disturbance illustrated in Figure 8 resembles that of grassland ecology, and may indicate that the difference between contexts may be related to the spreading of grassland fires that originate elsewhere and spread to adjoining patches of susceptible cover. At lower

elevations where extensive grasslands are more likely to exist, topography may provide little resistance to disturbances that can spread.

RELATING WATERSHED AND DISTURBANCE CHARACTERISTICS

A multiple regression approach was used to predict landscape connectivity (LC), measured by differences in the aerial extent of disturbance due to simulation context, expressed in relative watershed proportions. Characteristics describing topographic and landcover elements within and around watersheds were calculated from nationally available DEMs and satellite image products that in turn became the independent variables in the predictive equation. A large number of variables were included at the onset of the procedures, and non-significant contributors to the relationship were removed through stepwise, backward elimination. In the final model, the combination of 5 variables accounted for roughly 70% of the variation in landscape connectivity across the 38 watersheds in the mountains of central Montana.

Variables in the LC equation (Eqn. 9) represented elements contained within a 1 km buffer around the watershed divide together with corresponding measures for certain attributes of the watershed itself. Along the periphery, the proportion of barren ground, and ruggedness of the terrain were important. On the inside of watersheds the important variables consisted of the proportions of lodgepole pine and Douglas fir forest, and a measure of landcover patch aggregation. In general, variables identified by the analysis seemed realistic. They represent the important topographic and physiographic landscape components that lead to the propagation of disturbance processes in forested watersheds (Turner and Romme, 1994).

Direct comparison of regression coefficients was not possible because not all variables were measured with like units. According to the equation's standardized coefficients, however, the most influential predictor variables described barren ground and ruggedness components along the watershed perimeter. Of these, a consistent pattern relative to LC was most noticeable for barren ground. As the amount of barren ground increased, landscape connectivity decreased. An index of terrain ruggedness (Eqn. 8) was used to describe topography because it incorporates elements that cannot be detected by

measures of elevation, slope, and aspect alone. The ruggedness index used here was based on an automated procedure initially developed by Riley et al. (1999). Taking into consideration some improvements suggested by Nielsen et al. (2004), variation in terrain aspect was also incorporated. This produced an index that described the vertical (slope) and horizontal axes (aspect) of terrain elements. Perhaps this is why it accounted for more variability than other topographic metrics. Ruggedness along the watershed perimeter was positively related with landscape connectivity, although the linear association was weak.

On the inside of watersheds lodgepole pine and Douglas-fir proportions were important attributes. Lodgepole pine is the most abundant forest cover type in the analysis watersheds, often forming large, continuous stands, and is highly susceptible to motile disturbances like fire and mountain pine beetle. Douglas-fir is also a common species in this region, and is similarly susceptible to fires and other insect pests. Interpreting vegetation as forest or non-forest illustrates a general trend. As the proportion of forest cover increased in watersheds, the differences in disturbed areas between context scenarios also increased, indicating greater levels of connectivity. Using percolation theory (Strauss et al., 1989), Turner et al. (1989) illustrated a similar effect with sets of synthetic landscape simulations. Two dimensional arrays representing landscapes with resistant and susceptible habitat patches were generated over a range of configurations. As the proportion of susceptible landscape patches approached 60% the likelihood that once initiated, a disturbance could spread across the entire landscape through connected patches became very high. They postulated that in natural landscapes where susceptible patches have shapes that are more irregular than the square grid cells and the threshold value for spread could be lower than 60%. Indeed, differences in WAT and LND simulations were apparent even when the sum of all forest cover was as low as 30%, but most significant as that proportion approached 60% (Table 8).

Table 8. *Mean relative watershed areas of influential explanatory landscape connectivity (LC) model variables, averaged over significance groupings.*

Sig. Group	LPFR_i	DFFR_i	FV_i	BRRN_b
0.05	8	12	30	10
0.01	20	11	45	6
0.001	32	17	61	4

Averaging values of the LC equation's predictor variables over the 0.05, 0.01, and 0.001 significance groups reveals a general trend between landcover components in and around the watersheds, and differences in disturbed area due to context, referred to as landcover connectivity. Large or increasingly significant differences indicated increasing connectivity between watershed and landscape disturbance processes. The pattern revealed by averaging predictor variable values and then combining all forest cover types shows that the greatest levels of landscape connectivity occur with increasing watershed proportions of forest cover, and decreasing levels of barren ground in the watershed perimeter. When there was less than 30% forest cover in watersheds or more than 10% barren ground in the watershed perimeter, the likelihood of landscape connectivity was low. Conversely, internal forest proportions of 45% or more, and less than 6% barren ground in the watershed perimeter were associated with high landscape connectivity.

CONCLUSIONS

Management and planning at the watershed scale is beneficial because it incorporates a systems approach in which it acknowledges the multitude of interactions between upland, riparian and aquatic processes. All too often, however, selected watersheds are treated as discrete entities and characterized and modeled accordingly. Yet natural systems rarely function in isolation and tend to be influenced by processes occurring in their surroundings. By ignoring adjacent landscapes, connections between landscape and watershed processes may not be properly accounted for, especially when disturbances that have the potential to spread through connected patches of susceptible habitat are considered. Failure to document the full range of disturbances that may occur in a natural setting can change the outcome of even the most careful planning strategies.

Examination of 38 watersheds across Montana showed that landscape context and adjacency are important considerations. Although it was difficult to establish a pattern of disturbance processes, a connection to the landscape generally produced more disturbed area in 84% of the watersheds studied, especially due to fire, than when context was ignored.

Watersheds of interest should be modeled with at least one layer of adjacent watersheds on all sides to ensure that the full range of ecological processes is accounted for in long-term simulations. Expanding the spatial extent in simulations of natural processes may require more data and processing time but should help capture processes like fire that readily spread across landscapes when positive conditions for propagation exist.

To help determine the role of context on individual watersheds, a predictive equation was developed that estimates landscape connectivity as a function of watershed content and watershed boundary conditions that can be calculated from readily attainable data. The final equation was driven by the amount of barren ground and ruggedness of terrain in the watershed perimeter, and proportions of lodgepole pine and Douglas-fir forest, and landcover patch aggregation measured by the Landscape Shape Index inside the watershed. The index measures context influences on the amount of relative watershed area that may be affected by disturbance processes due to the influence of the surrounding landscape. Given results presented here, values of 5 % and above are indicative of strong connections between landscape and watershed processes. Simulation of vegetation dynamics for watersheds with high levels of connectivity should be simulated in a broad spatial context. Following that, when low levels of connectivity are estimated for a watershed, a more constrained (i.e. narrower perimeter around the area of interest) simulation context may be acceptable.

Based on the variables included in the landscape connectivity equation, vegetation dynamics of analysis watersheds with large forest components and gentle topographic divides with little barren landcover tend to be more connected to those of the surrounding landscape. Watersheds with less interior forest, specifically lodgepole pine, and more abundant barren ridge components with rugged terrain will be more independent from landscape disturbance processes. As a general rule of thumb, if a landscape is composed of 60% landcover that is disturbance prone, once initiated, a single disturbance may propagate across the entire landscape. When analyzing landcover composition, assessing the proportions of susceptible landcover should be a first step in determining landscape connectivity.

LITERATURE CITED

Ahl, R.S., H.R. Zuuring, and W. Chung. 2005. A terrain ruggedness index that captures vertical and horizontal topographic axes. Unpublished manuscript. College of Forestry and Conservation, Department of Forest Management, The University of Montana, Missoula, MT, USA.

Anderson, J.R., E.E. Hardy, J.T. Roach, and R.E. Witmer. 1976. A land use and land cover classification system for use with remote sensor data. Geological Survey Professional Paper 964. U.S. Government Printing Office, Washington, D.C.

Arno, S.F. and C.E. Fiedler. 2005. Mimicking Nature's Fire: Restoring Fire-Prone Forests in the West. Island Press, Washington, D.C.

Barrett, T.M. 2001. Models of vegetative change for landscape planning: a comparison of FETM, LANDSUM, SIMPPLLE, and VDDT. U.S. Department of Agriculture, Forest Service, General Technical Report RMRS-GTR-76-WWW.

Beasom, S.L., E.P. Wiggers, and J.R. Giardino. 1983. A technique for assessing land surface ruggedness. Journal of Wildlife Management 47: 1163-1166.

Bergeron, Y., and J. Brisson. 1990. Fire regime in Red Pine stands at the northern limit of the species' extent. Ecology 71: 1352-1364.

Biondini, M.E., C.D. Bonham, E.F. Redente. 1985. Secondary successional patterns in a sagebrush (*Artemisia tridentata*) community as they relate to soil disturbance and soil biological activity. Plant Ecology 60(1): 25-36.

Black, P.E. 1996. Watershed Hydrology. CRC Press, 2nd Edn. Taylor and Francis, London. 449 pp.

Blaszczynski, J.S. 1997. Landform characterization with geographic information systems. Photogrammetric Engineering and Remote Sensing 63: 183-191.

Bullen, S., J. Bovey, and R. Rosenberg. 2003. EXCEL 2002 VBA: Programmer's Guide. Wiley Pub. Co. Indianapolis IN

Chew, J.D., K. Moeller, C. Stalling, E. Bella, and R. Ahl. 2002. Simulating Patterns and Processes at Landscape Scales: User Guide for SIMPPLLE V2.2. U.S. Department of Agriculture, Forest Service, Rocky Mountain Research Station, Forest Ecology and Management, Missoula, MT, USA.

Chew, J.D., C. Stalling, and K. Moeller. 2004. Integrating knowledge for simulating vegetation change. Western Journal of Applied Forestry 19(2): 102-108.

Farina, A. 2000. Landscape Ecology in Action. Kluwer, Dordrecht. 317 pp.

Forman, R. T.T. 1995. Land Mosaics: The ecology of landscapes and regions. Cambridge University Press, London.

Forman, R.T.T. and M. Gordon. 1986. Landscape Ecology. John Wiley and Sons, New York.

Gesch, D., M. Oimoen, S. Greenlee, C. Nelson, M. Steuck, and D.D. Tyler. 2002. The National Elevation Dataset. Photogrammetric Engineering and Remote Sensing 68: 5-11.

Gustafson, E.J. 1998. Quantifying landscape spatial pattern: What is the state of the art? Ecosystems 1: 143-156.

Heinselman, M. L. 1973. Fire in the virgin forests of the Boundary Waters Canoe Area. Quaternary Research 3: 329-382.

Hunter, M.L. Jr. 1993. Natural fire regimes as spatial models for managing boreal forests. Biological Conservation 65: 115-120.

Jones, J. 2002. Personal Communication. Landscape Ecologist, U.S. Department of Agriculture, Forest Service, Flathead National Forest, 406-758-5341.

King, R. 2000. Comparison of simulation results among EXCEL worksheets using MRPP. U.S. Department of Agriculture, Forest Service, Rocky Mountain Research Station, Statistics Unit, Fort Collins, CO.

Kleinbaum, D.G., L.L. Kupper and K.E. Muller. 1988. Applied Regression and Other Multivariable Methods. 2nd Edn. PWS-Kent, Boston. 718 pp.

Klijn, F. and H.A. Udo de Haes. 1994. A hierarchichal approach to ecosystems and its implications for ecological land classification. Landscape Ecology 9: 89-104.

Lee, B., B. Meneghin, M. Turner, T. Hoekstra. 2003. An evaluation of landscape dynamic simulation models. U.S. Department of Agriculture, Forest Service, Inventory and Monitoring Institute, Natural Resources Research Center, Fort Collins, CO. Available for download at: http://www.fs.fed.us./institute/pag/landscape_dynamics.shtm.

Lesica, P., B. McCune, S.V. Cooper, and W.S. Hong. 1991. Differences in lichen and bryophyte communities between old-growth and managed second-growth forests in the Swan Valley, Montana. Canadian Journal of Botany 6(8): 1745-1755.

Lundquist, J.E., L.R. Lindner, and J. Popp. 2001. Using landscape metrics to measure suitability of a forested watershed: a case study for old growth. Canadian Journal of Forest Research 31: 1786-1792.

McCune, B., G. James, D.L Urban. 2002. Analysis of Ecological Communities. MJM Software Design. ISBN 0-9721290-06.

McGarigal, K., S. A. Cushman, M. C. Neel, and E. Ene. 2002. FRAGSTATS: Spatial Pattern Analysis Program for Categorical Maps. Computer software program produced by the authors at the University of Massachusetts, Amherst. Available at the following web site: www.umass.edu/landeco/research/fragstats/fragstats.html

McGarigal, K. and B. J. Marks. 1995. FRAGSTATS: Spatial pattern analysis program for quantifying landscape structure. U.S. Department of Agriculture, Forest Service, General Technical Report PNW-351.

McNab, W.H. 1993. A topographic index to quantify the effect of mesoscale landform on site productivity. Canadian Journal of Forest Research 23: 1100-1107.

Melton, M.A. 1957. An Analysis of the ecological relations among elements of climate, surface properties, and geomorphology. Project NR 389-042, Technical Report 11. Columbia University, Department of Geology, New York, USA. 102 pp.

Mielke, P.W. Jr. and K.J. Berry. 2001. Permutation Methods: A Distance Function Approach. Springer-Verlag, New York. 352 pp.

Nellemann, C. and R.D. Cameron. 1996. Effects of petroleum development on terrain preferences of calving caribou. Arctic 49(1): 23-28.

Nellemann, C. and G. Fry. 1995. Quantitative analysis of terrain ruggedness in reindeer winter grounds. Arctic 48(2): 172-176.

Nellemann, C. and M.G. Thomsen. 1994. Terrain ruggedness and caribou forage availability during snowmelt on the arctic coastal plain, Alaska. Arctic 47(4): 361-367.

Nielsen, S.E., S. Herrero, M.S. Boyce, R.D. Mace, B. Benn, M.L. Gibeau, and S. Jevons. 2004. Modelling the spatial distribution of human-caused grizzly bear mortalities in the Central Rockies Ecosystem of Canada. Biological Conservation 120 (1): 101-113.

Ott, R.L. 1993. An introduction to statistical methods and data analysis. Duxbury Press, Belmont, CA.

Pastor, J. and C.A. Johnston. 1992. Using Simulation Models and Geographic Information Systems to Integrate Ecosystem and Landscape Ecology, in Watershed Management: Balancing Sustainability and Environmental Change. R.J. Naiman, Editor. Springer-Verlag, New York.

Patton, C. and V.R. Baker. 1976. Morphometry and floods in small drainage basins subject to diverse hydrogeomorphic controls. Water Resources Research 12(5): 941-952.

Pfister, R. D., B.L. Kovalchik, S.F. Arno, and R.C. Presby. 1977. Forest Habitat Types of Montana. U.S. Department of Agriculture, Forest Service, General Technical Report INT-34. 174 pp.

Redmond, R.L., C.L. Winne, C. Fischer. 2001. Existing vegetation and landcover of west-central Montana. Final scene reports submitted to U.S. Department of Agriculture, Forest Service, Northern Regional Office, Missoula, MT, USA.

Riley, S. R., S.D. DeGloria, and R. Elliot. 1999. A terrain ruggedness index that quantifies topographic heterogeneity. Intermountain Journal of Sciences 5(1-4): 23-27.

Seaber, P.R., F.P. Kapinos, and G.L. Knapp. 1987. Hydrologic Unit Maps: U.S. Geological Survey Water-Supply Paper 2294. 63 pp.

Stauffer, D. 1985. Introduction to Percolation Theory. Taylor and Francis, London.

Strahler, A.N. 1964. Quantitative geomorphology of drainage basins and channel networks, *In* Handbook of Applied Hydrology, edited by V.T. Chow, McGraw-Hill, New York.

Strauss, D., L. Bednar, and R. Mees. 1989. Do One Percent of the Forest Fires Cause Ninety-Nine Percent of the Damage? Forest Science 35(2): 318-328.

Turner, M.G. 1989. Landscape Ecology: The effect of pattern on process. Annual Review of Ecology and Systematics 20: 171-197.

Turner, M.G., R.H. Gardner, V.H. Dale, and R.V. O'Neil. 1989. Predicting the spread of disturbances across heterogeneous landscapes. Oikos 55: 121-129.

Turner, M.G. and R.H. Gardner. 1991. Quantitative Methods in Landscape Ecology. Springer-Verlag, New York.

Turner, M.G. and W.H. Romme. 1994. Landscape dynamics in crown fire ecosystems. Landscape Ecology 9(1): 59-77.

USDA-FS, 1982. U.S. Department of Agriculture, Forest Service. National Forest Management Act. 16 U.S.C 528-531 1982.

White, P.S., J. Harrod, W.H. Romme, and J. Betancourt. 1999. Disturbance and Temporal Dynamics, in Ecological Stewardship: A Common Reference for Ecosystem Management, R.C. Szaro R.C., N.C Johnson, W.T. Sexton, and A.J. Malk, editors, Elsevier Science, Oxford.

Wohl, E. 2000. Mountain Rivers. American Geophysical Union, Washington, D.C.

Zimmerman, G.M., H. Goetz, and P.W. Mielke Jr. 1985. Use of an improved statistical method for group comparisons to study effects of prairie fire. Ecology 66(2): 606–611.

Zonneveld, I.S. and R.T.T. Forman. 1990. Changing Landscapes: An Ecological Perspective. Springer-Verlag, New York.

Zuuring, H.R., J.G. Jones, and J.D. Chew. 2000. Applying simulation and optimization to address Forest Health issues at landscape scales. U.S. Department of Agriculture, Forest Service, General Technical Report NC-GTR-205.

Zuuring, H. and M. Sweet. 2000. An Evaluation of Landscape Metrics and Spatial Statistics for Interpreting SIMPPLLE output. Final Report to U.S. Department of Agriculture, Forest Service, Rocky Mountain Research Station, Forest Ecology and Management, Missoula MT, USA. 33 pp.

Zuuring, H.R., W.L. Wood, and J.G. Jones. 1995. An overview of MAGIS: A Multi-Resource Analysis and Geographic Information System. U.S. Department of Agriculture, Forest Service, Research Note INT-RN-427.

CHAPTER 2

Hydrologic Calibration and Validation of SWAT in a Snow-Dominated Rocky Mountain Watershed

ABSTRACT

The Soil and Water Assessment Tool (SWAT) has a long track record of successful application in lowland and temperate environments, but little is known about the model's performance in forested mountain watersheds where hydrologic patterns are dominated by seasonal cycles of snow accumulation and melt. In this study, the ability of SWAT to simulate annual, monthly, daily, and seasonal streamflow in a snow-dominated upland watershed that represents conditions commonly found in high elevation environments in the Rocky Mountains of North America was evaluated. The model was calibrated with 4 years of continuous daily climate data collected within the Tenderfoot Creek Experimental Forest (TCEF), and corresponding streamflow records measured at the defined outlet. Hydrologic flow predictions were assessed graphically and with relative error (RE), mean paired deviation (Dv), and Nash-Sutcliffe model efficiency (NS) statistics. The calibrated model was validated with an independent dataset spanning an additional 4 years, using both traditional performance criteria obtained over the calibration and validation time periods, and objective regression-based methods. After calibration, model performance was very good, with a relative simulation period error of 2%, mean deviations of 36% and 31%, and Nash-Sutcliffe efficiencies of 0.90 and 0.86 for monthly and daily streamflow predictions, respectively. Model predictions were validated over annual, monthly ($_m$), and daily ($_d$) time steps with RE 4%, Dv_m 43 and Dv_d 32 and NS_m 0.90 and NS_d. 0.76. Seasonally, SWAT performed well during the snowmelt-induced runoff periods, but could not be validated for baseflow simulation. Assessment of key factors indicated that adjustment of snow process parameters contributed most significantly to model calibration. Other important parameters were surface runoff lag, groundwater recession, soil conductivity, and curve number parameters, in decreasing order of influence. Model results indicate that when calibrated SWAT can predict annual, monthly, and daily hydrologic processes in forested mountain watersheds with efficiency levels that are similar to those obtained in other regions where it has been applied. Refinement of the model components representing snowmelt infiltration, and groundwater discharge during baseflow may further improve model performance and the physical representation of hydrologic processes within this and similar watersheds.

INTRODUCTION

Watershed simulation models are commonly used to investigate interactions between components of the hydrologic cycle. Once calibrated, watershed models make it possible to evaluate the impacts of natural or management-induced changes in watershed condition in a way that cannot be done through field experiments and direct observation. With the use of simulations, a variety of scenarios can be evaluated before they are enacted, and unwanted outcomes may therefore be avoided. Following early watershed conceptualizations (Crawford and Linsley, 1966), contemporary watershed models have become increasingly comprehensive tools (Singh, 1995) that are vital components of integrated environmental assessments (Jakeman and Letcher, 2003). To become versatile tools, however, models must be evaluated over a broad range of settings and applications.

While an abundance of models are currently available the Soil and Water Assessment Tool (SWAT) is among the most widely used. SWAT is a river basin model designed to assess the impact of land management and climate patterns on water supply and non-point source pollution in large, complex watersheds with varying soil, landcover, and management conditions over long periods (Arnold et al., 1993; Srinivasan and Arnold, 1994; Arnold et al. 1998; Srinivasan et. al., 1998; Di Luzio et. al., 2002; Arnold and Fohrer, 2005). In the United States, SWAT is commonly being used in Total Maximum Daily Load (TMDL) analyses (Di Luzio et al., 2002), to investigate the effectiveness of best management and conservation practices (Arabi et al. 2006), and evaluate the hydrologic effects of climate change (Jha et al., 2006). Internationally, this model has also been applied with success (Gassman et al., 2005).

Despite the wide-spread use of SWAT, most applications have been associated with agricultural, grass and rangeland management, and climate change impacts in lowland and temperate environments (Gassman et al., 2005). There are, however, few examples where SWAT has been used to evaluate the streamflow hydrology of forested, mountainous, snowmelt-driven watersheds.

Much of the water available for runoff in the Rocky Mountain region of western North America is deposited and temporarily stored as snow in remote, high elevation watersheds that are largely forested. Understanding the inter-relationships among snowfall, snowmelt, forest structure, and streamflow generation is therefore necessary to

effectively integrate forest and water resource management in the region. Decades of research have focused on this and shown that the changing extent, composition, and configuration of forest cover have the potential to alter water yield and runoff patterns (Bosch and Hewlett, 1982; Stednick, 1996). Specifically, timber harvest, fires or other stand-replacing disturbances are often associated with increased streamflow due to the reduced canopy interception and evapotranspiration in cleared and low density stands (Golding and Swanson, 1978; Troendle, 1983; Troendle and King, 1985; Troendle and King, 1987; Pomeroy et al., 2002). Because possibilities for evaluating of management scenarios through experimental manipulation are limited, reliable modeling tools are essential for providing otherwise unattainable assessment data. Given its development philosophy and model architecture, SWAT may be useful for evaluating the effects of forest management on water resources in the Rocky Mountains.

To predict the streamflow hydrograph in this environment, models must adequately describe forest and snowmelt dynamics. The ability of the SWAT model to simulate snowmelt has been enhanced by algorithms that account for the effects of elevation on snowmelt in mountainous terrain (Fontaine et al., 2000). Streamflow simulations based on these routines have only been evaluated in a Minnesota watershed with little relief and mixed landcover (Wang, 2005), so there is still a need to assess the performance of SWAT in forested mountain watersheds.

The Tenderfoot Creek research watershed is instrumented with a well-distributed array of climate and stream gauging stations and thus provides an opportunity for calibration and validation of the SWAT model in an environment where little is known about its ability to simulate the water balance along with timing and magnitude of annual peak flows associated with snowmelt runoff. Climate, ecological trajectory and vegetation patterns within the study area are representative of high elevation lodgepole pine (*Pinus contorta*) forests east of the Continental Divide across southwest Alberta, Montana, and Wyoming, making inferences from this research applicable to similar watersheds throughout the North American Rocky Mountains.

The aim of this study is to evaluate the ability of SWAT to simulate streamflow in a forested mountain watershed with snowmelt-driven hydrology. SWAT was first parameterized and calibrated with detailed and locally derived data representing current

forest, climate, and streamflow conditions. Model performance was evaluated over annual, monthly, and daily time steps with traditional and objective hypothesis-testing procedures. Using similar criteria, seasonal performance of the model was assessed through separation of baseflow and runoff flow regimes. Key factors that influenced calibration in this environment are also described in this chapter.

METHODS

STUDY AREA DESCRIPTION

Tenderfoot Creek is a headwater tributary of the Missouri River that drains the Little Belt Mountains of central Montana in a westerly direction (Figure 1). The Tenderfoot Creek Experimental Forest (TCEF) encompasses the upper reaches of this creek, and the outlet of the research watershed was defined by a flume at the downstream extent of the TCEF administrative area (McCaughey, 1996). The delineated basin has a dendritic stream network and is bisected by a steep canyon along its main channel. A headwater reach and two major tributaries on each north and south aspect make up the 2,251 ha that contribute flow to the main outlet. Steep 25° to 30° slopes are found along the main canyon and upper headwalls, but most of the area is inclined less than 15°. Elevations range from 1,991 m at the watershed outlet to 2,420 m on the ridge crest.

The natural vegetation mosaic of this region is strongly influenced by periodic forest fires (Arno and Fiedler, 2005). Over the past four centuries a succession of fires have consumed most of the vegetation in the watershed, but it has been nearly 120 years since the last major burn (Barrett, 1993). In the absence of severe disturbances, forest stands of varying developmental stages now cover 85% of the watershed. Approximately 65% of the area is composed of lodgepole pine (*Pinus contorta*) which represents the most recently initiated forest cover. Over time, shade tolerant subalpine fir (*Abies lasiocarpa*) and Englemann spruce (*Picea engelmannii*) have emerged underneath the oldest pine stands, and these mixed communities make up the remaining 20% of mature forest cover. Disturbed or low density forest stands constitute another 10% of the watershed. Shrubby meadows and small riparian areas (1%) surround many of the creek bottoms, while drier grassland openings (1%) tend to occur on higher ground. Talus slopes (2%) line the main canyon and some high, exposed ridges.

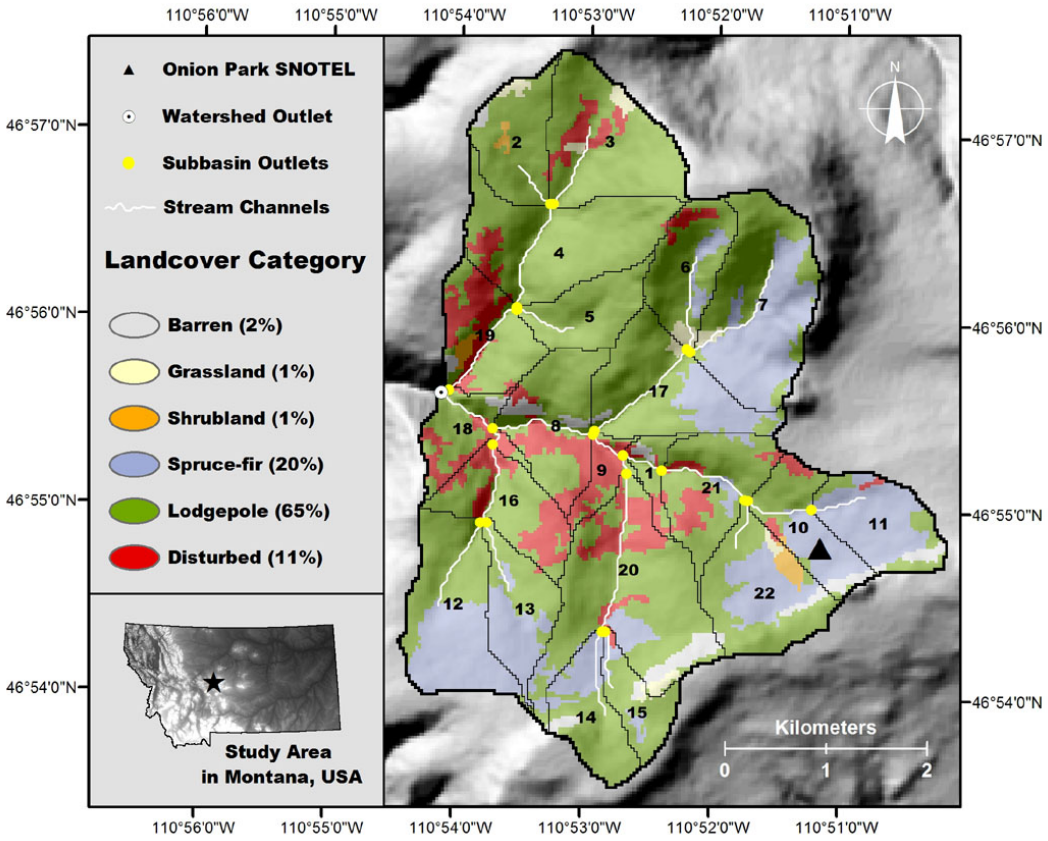

Figure 1. *Delineation, configuration, and landcover characteristics of the Tenderfoot Creek research watershed, located in the Little Belt Mountains of central Montana, USA.*

Geologically, the Tenderfoot Creek research watershed is underlain by Precambrian meta-sedimentary rocks of the Belt Supergroup (Alt and Hyndman, 1986). Field surveys conducted at TCEF indicate that the most extensive soil groups in the watershed are loamy skeletal, mixed Typic Cryochrepts and clayey, mixed Aquic Cryoboralfs (Farnes and McCaughey, 1995).

Climate patterns are continental and total annual precipitation averages close to 800 mm. Almost 70% of the annual precipitation falls as snow, which accumulates between November and May. The snowpack is drier and less dense than what is found west of the continental divide but more moist than that of the Utah and Colorado Front Ranges (Kosnik, 1995; Moore and McCaughey, 1997).

Runoff patterns in this watershed are strongly influenced by the seasonal cycle of snow accumulation and snowmelt. Peak discharge occurs in response to snowmelt and spring rainfall between May and early June, creating a sharply peaked runoff hydrograph

with steep rising and falling limbs. The baseflow period begins in August and persists through April. Summer rainfall is limited, generally occurs as brief, high intensity thunderstorms, and contributes little to streamflow. In that sense, the hydrology of this watershed does not have the typical rainfall-runoff patterns that are common in more temperate environments (Figure 2).

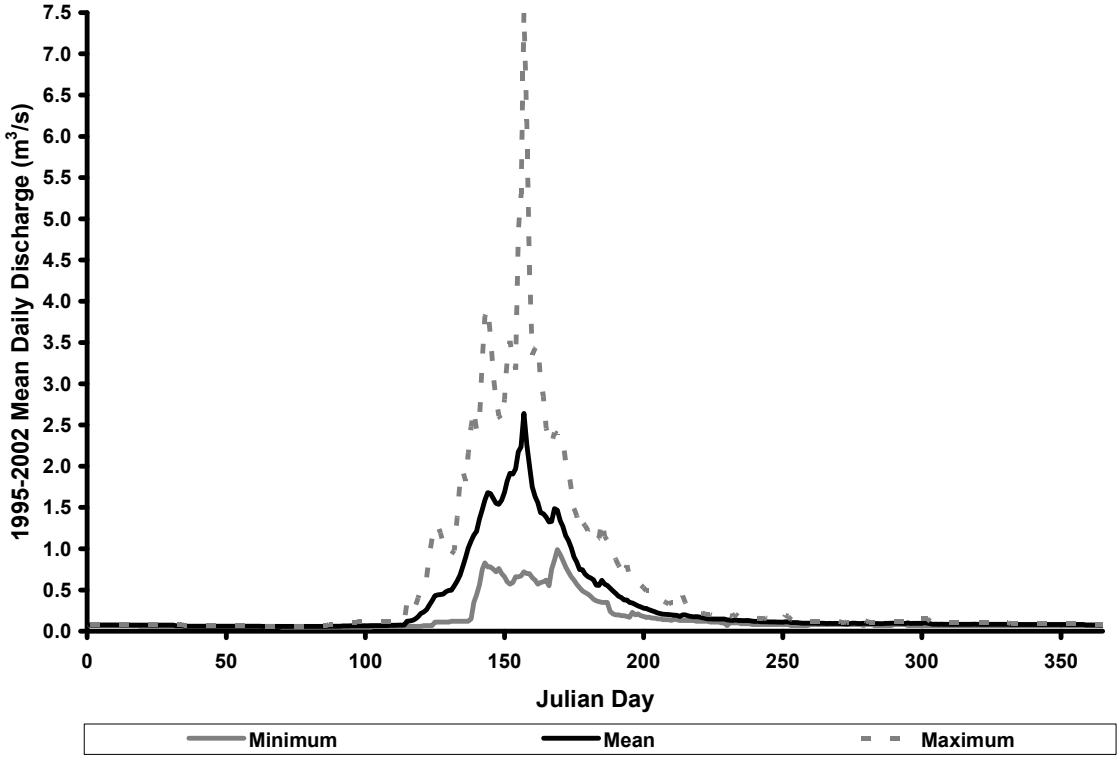

Figure 2. *Minimum, mean, and maximum daily streamflow patterns in the Tenderfoot Creek research watershed spanning one year beginning in January and ending in December based on daily records from 1995-2002*

MODEL DESCRIPTION

SWAT is a physically based, distributed parameter, continuous time, river basin model. It was developed to assess the impact of land management and climate patterns on water supply and non-point source pollution in large, complex watersheds with varying soil, landcover, and management conditions over long periods (Arnold et al., 1993; Srinivasan and Arnold, 1994; Arnold et al. 1998; Srinivasan et. al., 1998; Di Luzio et. al., 2002; Arnold and Fohrer, 2005). SWAT represents the culmination of over 30 years of

modeling efforts within the United States Department of Agriculture, Agriculture Research Service (USDA-ARS), and is an outgrowth of previous models such as the Simulator for Water Resources in Rural Basins (SWRRB) (Williams et al., 1985), and Groundwater Loading Effects of Agricultural Management Systems (GLEAMS) (Leonard et al., 1987). By combining proven agricultural management models with simple, yet realistic routing components SWAT expands the spatial domain of past field-scale models to that of river basins.

With a goal of being a useful management tool, SWAT was designed with a flexible architecture. It uses readily available data that describe the physical and climatic characteristics of watersheds. Using physically based inputs SWAT can obtain reasonable results in remote basins where calibration is not possible. The code is computationally efficient, allowing continuous simulation over large areas and long time periods. By simulating watershed processes over the long-term, impacts of management practices can be evaluated (Arnold and Fohrer, 2005).

SWAT runs on a daily time step, and can be configured with spatially-referenced topographic, soil, landcover and climate data available from government agencies worldwide, although customized information can also be included. With a GIS interface (Di Luzio et al., 2002, 2004) the model integrates these data to simulate major components of the hydrologic cycle as simply and realistically as possible.

In a SWAT simulation the driving force of watershed function is the water balance, which is divided into land, and water routing phases of the hydrologic cycle. The land phase controls the amount of water, sediment, nutrient, and pesticide loadings to the main channel by simulating hydrology, climate, erosion, soil temperature, plant growth, nutrients, pesticides, as well as land and water management. Movement of water and its constituents through the watershed is controlled by the stream and reservoir routing phases of the model.

To account for the spatial variability of properties that influence the water balance, a watershed may be partitioned into a number of sub-watersheds. These sub-divisions form the basic spatial unit of the model, and each is attributed with specific climatic, topographic, landcover, soil, and channel network characteristics. Within sub-watersheds, unique combinations of soil, landcover, and management practices are called

Hydrologic Response Units (HRUs), and each is assumed to have uniform hydrologic characteristics (Leavesley et al., 1983; Maidment, 1993; Niche et al., 2002). HRUs are the fundamental modeling unit within SWAT, and sub-watersheds can be composed of one dominant or multiple HRUs by specifying relative area thresholds for each defining component (Neitsch et. al., 2002).

A daily water balance is calculated by considering precipitation, snowmelt, soil percolation, lateral subsurface and groundwater flow to streams from a shallow aquifer, surface runoff, evapotranspiration, transmission losses and water diversions. Streamflow reported at drainage outlets is the product of surface runoff, lateral flow, baseflow from shallow aquifers, and open channel processes. Water flow predictions from each HRU are summed for the individual sub-watersheds and systematically routed through the watershed, yielding basin-wide estimates (Arnold et al., 1998).

Surface runoff and infiltration can be estimated by SWAT using either the SCS curve number (USDA-SCS, 1972) or Green-Ampt infiltration (Green and Ampt, 1911) methods. With the SCS curve number method, a rainfall-runoff relationship is determined by landcover characteristics, soil hydrologic group, and soil moisture condition for every HRU in the watershed. The Green and Ampt method requires sub-daily runoff to calculate infiltration as a function of the wetting front matric potential and effective hydraulic conductivity. Because data at the daily time-step are more readily available, the SCS curve number method is most frequently used to estimate surface runoff. Various potential evapotranspiration models exist, and SWAT can utilize the Hargreaves (Hargreaves et al. 1985), Priestley-Taylor (Priestley and Taylor, 1972) or Penman-Monteith (Monteith, 1965) methods. Channel flow routing may be accomplished with either variable storage, or Muskingum methods (Neitsch et al., 2002).

The SWAT model has been in the public domain for over a decade, and many versions of this tool are currently available. In this study, SWAT2005 was used in conjunction with the AVSWAT interface (Di Luzio et al., 2004). This GIS-based graphical user interface facilitated watershed delineation, subdivision and initial parameterization. AVSWAT also incorporated sensitivity analysis, auto-calibration, and uncertainty assessment procedures (van Griensven et al., 2006). These routines were originally formulated to automate SWAT calibration in a European watershed with

typical rainfall-runoff hydrology (van Griensven and Bauwens, 2003), but to date have not been applied in a mountainous, snowmelt dominated watershed like Tenderfoot Creek. More detailed accounts of SWAT development, version enhancements, and model applications can be found in Arnold and Fohrer (2005), Jayakrishnan et al. (2005) and Gassmann et al. (2005).

MODEL CONFIGURATION

The model set-up process described below is composed of five basic steps, namely: data collection, watershed delineation, subdivision, parameterization, and initiation. The first step is to assemble the necessary spatially referenced climate, topographic, soil, and landcover data. Once an outlet has been identified, the watershed is delineated. The spatial context and diversity of land units is accounted for through a series of nested divisions, first into logical sub-watersheds and then into unique combinations of soil and landcover (hydrologic response units - HRUs). Watershed elements are then systematically parameterized with characteristics derived from the input data. After the initial, or default parameterization, evapotranspiration, surface runoff, and channel routing methods must be selected before the model can be initiated. Simulations are continuous and operate at the daily time-step, but output can be aggregated for monthly or annual periods. Although generated climate inputs can run the model, actual measured temperature and precipitation with corresponding streamflow data are required for calibration.

Input Data

To reduce input uncertainty the model was parameterized with values measured onsite, derived from reliable data, and other physically-realistic estimates. Thus, SWAT was configured with a standard digital elevation model (DEM), soil, and stream network data obtained from national agency databases. With a focus on forest hydrology, a detailed landcover map based on a reclassification of multiple stand attributes provided the landcover input. Daily temperature and precipitation input data were measured onsite, and streamflow records were collected at the watershed outlet (Table 1).

The DEM was extracted from the National Elevation Dataset (NED) (Gesch et al., 2002), and used for watershed delineation, subdivision, characterization, and routing. Linear elements of the National Hydrography Dataset (NHD) were overlain on the DEM to assist segmentation into logical sub-watersheds. Channel dimensions were first modeled, and later refined with actual measurements within each sub-watershed. Soil characteristics from the State Soil Geographic Database of Montana (STATSGO) (USDA-NRCS, 1994) were used to estimate parameters affecting infiltration, water holding capacity, evapotranspiration, and other hydrologic processes. Parameters influencing productivity, interception, evapotranspiration, and runoff characteristics were associated with each category of the customized landcover map.

The Onion Park snow telemetry site (SNOTEL: 1008) is located within the research watershed and provided a continuous record of daily minimum and maximum temperature, and precipitation from October 1, 1993 to December 31, 2002. Average annual summaries from this site were compared to a National Weather Service site (NWS: 248927) to estimate local temperature and precipitation lapse rates. Daily discharge data measured at the Lower Tenderfoot Creek (LTC) flume spanned the same time period, and made it possible to calibrate SWAT for streamflow in this watershed. During delineation, the location of LTC also defined the watershed outlet (Figure 1).

Table 1. *Model configuration data: Description of data used to configure SWAT for streamflow simulation in the Tenderfoot Creek research watershed.*

Information Type	Dataset	Source	Resolution / Units
Raster \ Landcover	Custom	USDA-FS	30m
Raster \ Topography	NED	USDI-GS	30m
Raster \ Soil	STATSGO	USDA-NRCS	1:100,000 / 30m
Route \ Hydrography	NHD	USDI-GS	1:24,000 / m
Route \ Channels	Custom	USDA-FS	Width, depth / m
Hydrology \ Flow	LTC Flume	USDA-FS	Daily m^3/s
Climate	SNOTEL	USDA-NRCS	
Temperature	Site 1008	USDA-NRCS	Daily min °C
Temperature	Site 1008	USDA-NRCS	Daily max °C
Precipitation	Site 1008	USDA-NRCS	Daily mm
Climate	NWS	USDC-NCDC	
Temperature	Station Number 248927	USDC-NCDC	Ave. annual °C
Precipitation	Station Number 248927	USDC-NCDC	Ave annual mm

Watershed Delineation and Subdivision

Coordinates of the LTC flume defined the watershed outlet, and topographic delineation produced a 2,251 ha drainage basin. Sub-watersheds are the smallest aerial unit that SWAT considers, and a high level of subdivision is necessary to capture spatially explicit watershed processes (Mangurerra and Engel, 1998; Haverkamp, et al. 2002; Arabi, et al. 2006). By specifying a critical source area delineation threshold with a relative area of approximately 1.5% (30 ha), the watershed was configured with 22 sub-watersheds (Figure 1). This level of segmentation created subdivisions that on average represented 4.5% of the watershed (range ~1% – 10%), which is roughly what Arabi et al. (2006) suggested as the minimum relative area required to detect the influence of management practices in watersheds.

Sub-watershed Characterization

Elevation Bands

Snow accumulation and melt are dominant hydrologic processes in mountainous watersheds (Wohl, 2000) that are strongly influenced by changes in elevation (Pomeroy and Brun, 2001). Refined snow process algorithms and the ability to define as many as 10 elevation bands within each subbasin have enhanced the performance of SWAT in watersheds with complex topography and large elevation gradients (Fontaine, et al. 2002). To account for a 425 m elevation gain within the watershed, three elevation bands were defined for each of the 22 sub-watersheds.

Climate and Lapse Rates

Unless otherwise specified, SWAT applies either the mean sub-watershed elevations, or average elevation of bands within sub-watersheds, and default laps rates to distribute climatic variables across a watershed. Due to the importance of orographic precipitation in mountainous environments, data from the SNOTEL site (1008) and the National Weather Service (NWS) cooperative station at White Sulphur Springs (248927) were used to estimate local temperature and precipitation lapse rates for more representative climate forcing (Table 2).

Table 2. *Mean annual temperature (TMP), and precipitation (PCP), temperature and precipitation lapse rates (TLPAS and PLAPS respectively) for two recording sites that provided climate forcing data for SWAT. Default lapse rates are shown in parentheses.*

Climate Site	Elev. (m)	TMP (C)	PCP (mm)	TLAPS (°C/km)	PLAPS (mm/km)
Onion Park	2,259	0.50	846	-7.14 (-6.0)	765 (0)
White Sulphur Springs	1,582	5.33	328		

Stream Channel Characteristics

Routing within SWAT requires information concerning main channel dimensions within each sub-watershed (Niche 2002). Geo-processing capabilities of the AVSWAT interface provided initial estimates based on an analysis of the input DEM. Width and depth were later measured at three evenly distributed locations within all sub-watersheds, and mean values for each dimension and their ratios updated the estimated inputs.

Management Scenarios

The research watershed is representative of undisturbed forest conditions, and the goal of this study was to determine if streamflow generated by the natural biophysical processes in this basin could be replicated. Hence, no management was prescribed and plant growth was governed by vegetation database parameters (Neitsch et al., 2002).

Landcover Characteristics

While they are distinct, the terms *landuse* and *landcover* are often used interchangeably. In essence, *landuse* implies some form of land management, whereas *landcover* refers to a land classification category (Anderson et al., 1976). Because no management was specified, the mapped distribution of vegetation, rock, and barren ground is referred herein as landcover.

SWAT uses a vegetation database to define the parameters for mapped landcover categories. Most of the forested land in the upper Tenderfoot watershed is coniferous, but options for representing different conifer forest types with the standard database are limited. To account for differences in canopy and other vegetation characteristics, detailed stand-level and remotely sensed data (Redmond, et al. 2001) described the existing forest and non-forest features of the watershed. Multiple attributes were used to

classify each stand into landcover categories that resemble those of Anderson Level II classification (Anderson et al., 1976), but offer greater forest type diversity. The final landcover map was processed as raster data with 30 m resolution, and categories represented in the watershed included barren ground, grassland, shrubland, spruce-fir forest, lodgepole pine forest, and disturbed forest. Upon classification, site-specific parameters were estimated for each landcover category (Table 3).

Table 3. *Seven estimated site-specific characteristics of landcover with the Tenderfoot Creek research watershed. In order of appearance they are: maximum canopy height in meters, maximum and minimum leaf area index in m2/m2, the proportion of annual precipitation intercepted by the canopy, minimum mean daily temperature required for plant growth in degrees Celsius, Manning's coefficient for ground surface roughness, and SCS curve number for moisture condition II on hydrologic soil group B.*

Landcover	Max HT (m)	Max LAI	Min LAI	Int. (%)	Base T °C	OVN	CN2B
Barren	0	0	0	0	0	0.10	96
Grassland	0.75	1.50	0.75	3	10	0.12	70
Shrubland	3.50	2.00	1.00	5	10	0.13	65
Lodgepole	22	2.80	1.80	25	3	0.16	58
Spruce-fir	26	3.0	1.95	28	3	0.17	55
Disturbed	10	2.0	1.00	10	3	0.14	69

The standard range grass and range brush parameter sets within SWAT were modified to describe the grassland and shrubland categories. Similarly, the standard evergreen forest parameters were modified to better represent the characteristics of pure or mixed stands of Engleman spruce (*Picea engelmannii*), sub-alpine fir (*Abies lasiocarpa*), and whitebark pine (*Pinus albicaulis*) which were classified as spruce-fir, and lodgepole pine (*Pinus contorta*) forest types found within the watershed. The barren landcover category is a modification of the dirt road transportation parameter set in SWAT and represents bare ground, rock outcrops, and alpine conditions. The fraction of total impervious area is set to 0.98, while the fraction of connected impervious area is set to 0.95. The space between the impervious areas is represented by the generic Bermuda grass (*Cynodon dactylon*) parameters. The disturbed category is based on the Anderson Level II (Anderson, et al. 1976) transitional classification and represents decadent, burned, or regenerating forest stands. Like the other conifer forest categories, it is based on a modification of the standard evergreen forest parameter set.

Interception is an important hydrologic process in forested areas because it reduces the amount of snow or rain available to recharge soil moisture and contribute to streamflow (Golding and Swanson, 1978). The forest canopy intercepts 25 to 30% of the annual snowfall within the Tenderfoot Creek watershed (Moore and McCaughey, 1997; McCaughey and Farnes, 2001; Woods et al. 2004, 2006). Leaf area index (LAI) is an indirect measure of canopy structure (White, et al. 1997; Hall, et al. 2003), and is used by SWAT as one of the variables that determines interception and canopy moisture storage (Niche 2002). Although conifer forests maintain needles yearlong, the quantity of leaf area varies seasonally (Oliver and Larson, 1990; Lowman and Nadkarni, 1995; Waring and Running, 1998). Analysis of multi-temporal satellite-derived leaf area index (LAI) data (Holsinger et al., 2005; USDI-GS, 2005) indicated that winter leaf area indices in the study area were approximately 40% lower than those of summer. This was handled in the SWAT model by including both minimum (*ALAI*) and maximum (*BLAI*) values in the parameter set for each forest cover type. This allowed LAI to vary from summer to winter, and ensured that LAI did not drop to zero during the winter months (Table 3).

LAI also influence interception, which in SWAT is defined by the maximum canopy storage parameter (*CANMX*). Values for CANMX were given for each landcover type by multiplying the mean precipitation event depth (6mm) by the annual interception fraction for each landcover type (Table 3). With positive LAI during winter, trees could intercept snow.

Soil Characteristics

The State Soil Geographic (STATSGO) database for Montana characterized the study area soils. This dataset consists of a digital general soil association map and attribute databases (USDA-NRCS, 1994). In the study area, only one soil type, the Stemple series, was described. According to STATSGO the Stemple soil type has 4 layers with very channery-loam texture. Based on infiltration characteristics, USDA-NRCS (1996) classifies soils into four hydrologic groups (A, B, C, D; ranging from high to low). Stemple soils belong to hydrologic group B, indicating they are moderately deep, and have average infiltration, and water transmission rates when thoroughly wetted.

Definition of Hydrologic Response Units (HRUs)

Due to the lack of mapped soil diversity, landcover patterns were the only distinguishing factor for HRU definition in this watershed. The number and diversity of HRUs can influence model output (Bingner, et al. 1997; Mangurerra, and Engel, 1998), and to ensure a high level of resolution, multiple HRUs were defined for each sub-watershed. By specifying a minimum 5% aerial extent for landcover categories, 54 hydrologic response units were created.

Simulation Strategy

Calibration and validation of the SWAT model for Tenderfoot Creek (TCSWAT) was based on a balanced, split-sample approach. Once the model was configured and initially parameterized, SWAT was run on a daily basis from October 1, 1993 to December 31, 2002. The first two years of simulation (1993 and 1994) allowed the model to equilibrate to ambient conditions. Calibration was based on the years 1997 to 2000, and the model was validated during the two years prior (1995, 1996) and two years following (2001, 2002) the calibration period (Table. 4).

Table 4. *Hydrologic simulation timeline, indicating the yeas over which model equilibration, calibration and validation took place.*

Equilibration		Validation		Calibration				Validation	
1993	1994	1995	1996	1997	1998	1999	2000	2001	2002

This simulation timeline encompassed a wide range of environmental conditions, including wet, dry and average years (Table 5). Despite being a fairly short period, the information richness provided by the variability in hydro-climatic conditions is more valuable than a lengthy record alone (Gupta et al., 1998).

Table 5. *Climate and hydrologic variability within the Tenderfoot Creek research watershed, represented by mean annual temperature, precipitation (PCP), peak snow-water equivalent (SWE) measured at Onion Park (SNOTEL:1008), water yield and peak stream discharge rate in cubic meters per second (m^3/s), measured at the research watershed outlet. Years codes as 'c' and 'v' were used for calibration and validation, respectively.*

Year	Mean Temp. °C	PCP (mm)	SWE (mm)	Water Yield (mm)	Peak Flow (m^3/s)
v 1995	0.4	978	457	511	7.5
v 1996	-0.1	879	399	495	3.9
c 1997	0.7	856	485	564	4.0
c 1998	1.6	831	318	430	2.4
c 1999	1.4	757	330	336	2.1
c 2000	1.0	714	373	357	2.0
v 2001	2.1	677	285	288	2.0
v 2002	1.2	727	351	339	2.4
Min	-0.1	677	285	288	2.0
Mean	1.0	803	375	415	3.3
Max	2.1	978	485	511	7.5

Initial model simulations were conducted using default values for most of the model parameters. Potential evapotranspiration (PET) was modeled with the Penman-Monteith algorithm because it uses, in part, canopy height to estimate PET and this made it possible to impart differential values for locally described landcover types. Surface runoff was modeled with the standard SCS Curve Number approach, and the variable storage channel routing method.

MODEL PERFORMANCE CRITERIA

Model performance was evaluated through visual interpretation of hydrographs scatter plots, and commonly used statistical measures of agreement between measured and simulated data pairs (ASCE, 1993; Coffey, et al., 2004;White and Chaubey, 2005). Following a traditional approach, the same criteria used for calibration were also applied to the validation periods, spanning annual, seasonal, monthly, and daily time-steps. In addition to standard methods, objective validation that incorporated a regression-based model invalidation procedure was also used. Seasonal evaluation was based on flow separation into base and runoff periods, and both methods of validation were applied to each hydrologic regime.

Graphical evaluation focused first on matching the shape and magnitude of annual rising, peak, and recession hydrograph limbs of the snowmelt-induced runoff period, and secondly on maintenance of baseflow through the remaining year. Scatter plot analysis helped to determine the linear relationship between measured and simulated streamflow.

Although no standard suite of statistical criteria currently exists, the American Society of Civil Engineers (ASCE, 1993) has recommended using the Nash-Sutcliffe model efficiency (NS), and average runoff volume deviation (Dv) metrics for gauging hydrologic model performance. These statistics, along with a measure of relative difference (RE) were therefore employed to quantitatively evaluate model performance. A brief description of these metrics is provided below, and variables in the notation are defined as:

y = *individual measured values*
$\bar{y}$ = *mean measured values*
$\hat{y}$ = *individual simulated values*
$\bar{\hat{y}}$ = *mean simulated values*

Relative error (RE) is a measure that describes the percent difference between measured and simulated values over a specified time period, where smaller values are an indication of better model performance. When RE is < 20%, model estimates are usually judged as realistic. In this study, it was used to quantify differences in total water yield over annual and seasonal simulation periods, and is calculated as:

$$\mathrm{RE} = \frac{|y - \hat{y}|}{y}(100) \qquad \text{(Eqn. 1)}$$

The average percent deviation between individual data pairs over a specified time period is quantified with the (Dv) statistic. A value of zero indicates a perfect model fit, and larger values describe greater average differences between measured and simulated values. Calibration studies using this metric for evaluation have reported satisfactory results when Dv is less than 40% (Coffey et al., 2004). The Dv is calculated as:

$$Dv\,(\%) = \frac{\sum |y - \hat{y}|}{\sum y}(100) \qquad \text{(Eqn. 2)}$$

The Nash-Sutcliffe (1970) coefficient was developed as a relative sum of squares model efficiency measure to evaluate the fit between observed and simulated hydrographs. Values of the coefficient can range from negative infinity to a high of 1, which corresponds to a perfect fit. This statistic can be negative because if pair wise differences between the observed and simulated values are mostly greater than those between the observed and mean observed values then the quantity subtracted from 1 will be > 1 and the resultant coefficient will be negative. Coefficients greater than 0.75 are said to be "good", while values between 0.75 and 0.36 are considered "satisfactory" (Motovilov, et al., 1999; Wang and Melesse, 2006). When calculated coefficients are 0 or less, model predictions are no better than the mean of the observed data. The Nash-Sutcliffe coefficient (NS) was used to compare the fit of seasonal, monthly, and daily hydrographs. Relative NS changes also helped to evaluate the influence of calibration parameters on model performance. NS is calculated as:

$$NS = 1 - \left[\frac{\sum (y - \hat{y})^2}{\sum (y - \bar{y})^2} \right] \qquad \text{(Eqn. 3)}$$

MODEL CALIBRATION

The usefulness and reliability of a watershed model depends upon how well it is calibrated and subsequently validated. Calibration involves the selection and adjustment of influential model parameters until simulated outputs match field observations to the satisfaction of some pre-defined performance criteria. Validation is similar to calibration in that simulated and measured data are compared, however no parameter adjustment is carried out, and the comparison dataset represents a different time series, or set of environmental conditions than the calibration period. Ultimately, validation determines the reliability of the calibrated model when applied to an independent dataset.

Parameter Selection through Sensitivity Analysis

Complex hydrologic models like SWAT require a large number of parameters to describe the spatial distribution of watershed characteristics. Because it is neither possible, nor meaningful, to independently calibrate all parameters, sensitivity analysis helps identify the parameters that influence model outputs most strongly (Eckhardt and Arnold, 2001; Muleta and Nicklow, 2005). Sensitivity analysis permits an examination of change rates in model output with respect to changes in model input, where larger changes in output indicate greater model sensitivity. Those parameters with high sensitivity ranking should be considered for calibration, and adjusted until performance criteria are met.

Following initial parameterization, a suite of parameters commonly recommended for streamflow calibration (Table 6) were varied over their potential ranges with automated Latin Hypercube One-factor-At-a-Time (LH-OAT) global sensitivity analysis procedures (van Griensven et al., 2006). Latin Hypercube (LH) sampling is computationally efficient, and One-At-a-Time procedures (OAT) ensure that a change in model output is unambiguously attributed to the change in an input parameter. The range of values associated with any parameter may impart changes to model output that are physically unreasonable. This may cause false interpretation of model sensitivity and care should be taken when specifying parameter ranges.

Rankings associated with the LH-OAT analysis indicated that the timing and magnitude of streamflow were sensitive to variation in snow process, surface lag, groundwater, soil, and SCS curve number parameters. Given the sensitivity of model output, parameters within the above functional groups were selected for calibration.

Table 6. *Parameter ranges for sensitivity analysis of the uncalibrated SWAT model.*

Component	Parameter Name	Description	Range
Basin	ESCO	Soil evaporation compensation factor	0 - 1
Basin	EPCO	Plant uptake compensation factor	± 50%
Basin	SURLAG	Surface lag coefficient	0 - 4
Basin / Snow	SMFMX	Maximum snow melt rate (mm/C/day)	0 - 10
Basin / Snow	SMFMN	Minimum snow melt rate (mm/C/day)	0 - 10
Basin / Snow	SFTMP	Snow fall temp (C)	0 - 5
Basin / Snow	SMTMP	Snow melt temp (C)	0 - 5
Basin / Snow	TIMP	Snowpack temp lag factor	0.01 - 1
Basin / Snow	TLAPS	Temp lapse rate (C/km)	± 50%
Subbasin	SLOPE	Average Slope Steepness (m/m)	± 50%
Subbasin	SLSUBBSN	Average slope length (m)	± 50%
HRU	CN2	Initial SCS curve number II for moisture	± 10%
HRU	CANMX	Maximum canopy storage (mm)	0 - 10
HRU	BLAI	Maximum potential leaf area index (LAI, m2/m2)	± 50%
HRU	BIOMIX	Biological mixing efficiency	0 - 1
Channel	CH_N	Manning's "n" for main channel	± 20%
Channel	CH_K2	Hydrologic conductivity for main channel (mm/hr)	0 - 150
Groundwater	ALPHA_BF	Baseflow recession constant	0 - 1
Groundwater	GW_DELAY	Groundwater delay time (days)	0 - 100
Groundwater	RCHRG_DP	Deep aquifer percolation fraction (%)	0 - 1
Groundwater	GWQMN	Threshold depth in shallow aquifer for return flow (mm)	0 - 5000
Groundwater	GW_REVAP	Groundwater re-evaporation coefficient	0.02 – 0.2
Groundwater	REVAPMN	Threshold depth in shallow aquifer for re-evaporation (mm)	0 - 500
Soil	SOL_AWC	Soil available water capacity (mm)	± 50%
Soil	SOL_K	Saturated hydraulic conductivity (mm/hr)	± 50%
Soil	SOL_Z	Soil depth (mm)	± 50%
Soil	SOL_ALB	Moist soil albedo	0 - 1

Parameter Adjustment for Calibration

Selected parameters were adjusted over a range of values through a stepwise process that utilized both automated methods (van Griensven and Bauwens, 2003), and manual refinement until an optimal parameter set was obtained (Table 7).

Table 7. *Default value, calibration range and final calibration estimate of selected SWAT model parameters, by watershed component.*

Component	Parameter Name	Default Value	Calibration Range	Final Estimate
Basin	SURLAG	4	0 – 4	0.05
Snow	SFTMP	1	0 – 5	1.0
	SMTMP	0.5	0 – 5	2.5
	SMFMX	4.5	0 – 10	3.0
	SMFMN	4.5	0 – 10	2.9
	TIMP	1	0.01 – 1	0.06
	SNOCOVMX	1	0 - 500	200
	SNO50COV	0.5	0 – 1	0.1
Groundwater	ALPHA_BF	0.048	0 – 1	0.01
	GW_DELAY	31	0 – 100	1
	RCHRG_DP	0.05	0 – 0.20	0.15
Soil	SOL_AWC			
	Layer 1	0.09	0.05 – 0.20	0.18
	Layer 2	0.06	0.02 – 0.15	0.12
	Layer 3	0.06	0.02 – 0.15	0.12
	Layer4	0.05	0.02 – 0.15	0.10
Soil	SOL_K			
	Layer 1	23	10 - 100	75
	Layer 2	11	5 - 75	50
	Layer 3	6	5 - 50	25
	Layer4	3.5	5 - 25	20
Landcover	*CN2B*			
	Barren	98	95 – 100	96
	Grassland	69	68 – 72	70
	Shrubland	61	63 – 67	65
	Spruce-fir	55	53 – 57	55
	Lodgepole pine	55	57 – 60	58
	Disturbed forest	55	67 – 74	69

Focusing on the parameters sets identified by the sensitivity analysis, field measurements from Woods et al. (2006) and Sappington (2006) gave potential ranges for most of the snow parameters, and baseflow filter techniques (Arnold et al., 1995; Sloto and Crouse, 1996; Arnold and Allen, 1999) provided initial estimates for the baseflow recession constant and runoff fractions. Development guidelines (Neitsch et al., 2002) and literature reviews (Arnold et al., 1998; Mangurerra and Engel 1998; Santhi et al., 2001; Eckhardt and Arnold, 2001; White and Chaubey, 2005) helped identify reasonable ranges for remaining surface lag, soil and groundwater parameters.

The uncalibrated model was tuned by initially minimizing the difference between measured and modeled annual precipitation, snowmelt and water yield. This was accomplished by defining elevation bands within sub-watersheds, while also setting temperature and precipitation lapse rates based on local estimates. Further model

refinement focused on matching the simulated timing of streamflow to measured monthly and daily values with iterative variation of the selected calibration parameters that optimized model evaluation criteria. After appropriate parameter ranges were defined, optimum values were estimated with automated methods based on the Shuffled Complex Evolution (SCE) algorithm (Duan et al., 1992, 1994; van Griensven and Bauwens, 2003). With only a single residual sum of squares objective function (SSQ), results derived from this algorithm strongly weighted the snowmelt driven hydrograph peaks and failed to match low flow periods. Final parameter estimates were therefore reached by manually refining the automated calibration.

MODEL VALIDATION

The reliability of hydrologic predictions generated by the calibrated model was assessed via two distinct means of comparison. First, the performance statistics calculated from model output in the validation period (1995, 1996, 2001, and 2002) were compared to those generated during the calibration phase (1997-2000). When calibration and validation performance criteria are reasonably similar the model is considered validated. While this is the most common method of validation, it is subjective. Second, an alternative technique that is objective because it relies on a regression-based hypothesis-testing procedure to invalidate model predictions was employed with a confidence level of 0.05. With the traditional method, model validation considered annual, seasonal, monthly, and daily time steps. Due to data limitations, objective validation focused on seasonal and monthly model predictions.

Regression-Based Model Invalidation

Calibration established the final parameter values, and analysis of model performance during the validation time period provides an independent check on the robustness of those parameter estimates. With this concept, the relationship between streamflow estimated by SWAT during the validation and measured streamflow for corresponding periods is evaluated. A simple liner regression model is developed, where simulated values predict the actual values for each time frame being tested. When

modeled and measured values are closely matched, the y-intercept, b_0, of the above relationship should be close to zero and the slope, b_1, near 1. The following null hypotheses were simultaneously constructed and jointly tested:

H_0: $\beta_0 = 0$ and $\beta_1 = 1$ versus H_1: not H_0 at a specified α level

Next the following test statistic, **Q**, is computed (Draper and Smith, 1981):

$$\mathbf{Q} = (\beta - b)' \, X'X \, (\beta - b) \sim p \, S^2 \, F_{p, v, 1-\alpha} \qquad \text{(Eqn. 4)}$$

Where:

β	= *hypothesized values for y-intercept and slope, i.e. 0 and 1*
b	= *vector of actual regression coefficients*
X'X	= *matrix term in independent variables (predicted y's)*
S^2	= *residual mean square*
p	= *number of regression coefficients – 1*
$v = n - p$	= *residual degrees of freedom (DF)*
α	= *significance level*

For meaningful interpretation of this parametric test, applied datasets must meet the assumptions of normality and independence. When analyzed appropriately, failure to reject the above joint null hypothesis indicates that model behavior is not data bound and the model satisfactorily describes the underlying processes.

Seasonal Streamflow Separation

Calibration trials revealed that improvements in model output for the snowmelt runoff period were often obtained at the expense of reduced performance in the baseflow period, and vice versa. To determine how well the final calibration replicated streamflow in each of the two major flow regimes, model performance was therefore evaluated when they were considered in isolation. Baseflow was separated from runoff on a monthly and daily basis and individually compared to observed values. For monthly separation, October through April, along with August and September were categorized as baseflow months, while May, June and July were considered runoff months. Based on interpretation of the flow duration curve for actual streamflow from 1993 to 2002, following a method similar to that of Hay et al. (2006), discharge of < 0.2 m^3/s was

classified as baseflow, and values ≥ 0.2 m^3/s were assigned to runoff (Figure 3). The same quantitative measures used to evaluate overall streamflow predictions were also used in this analysis of individual hydrograph components.

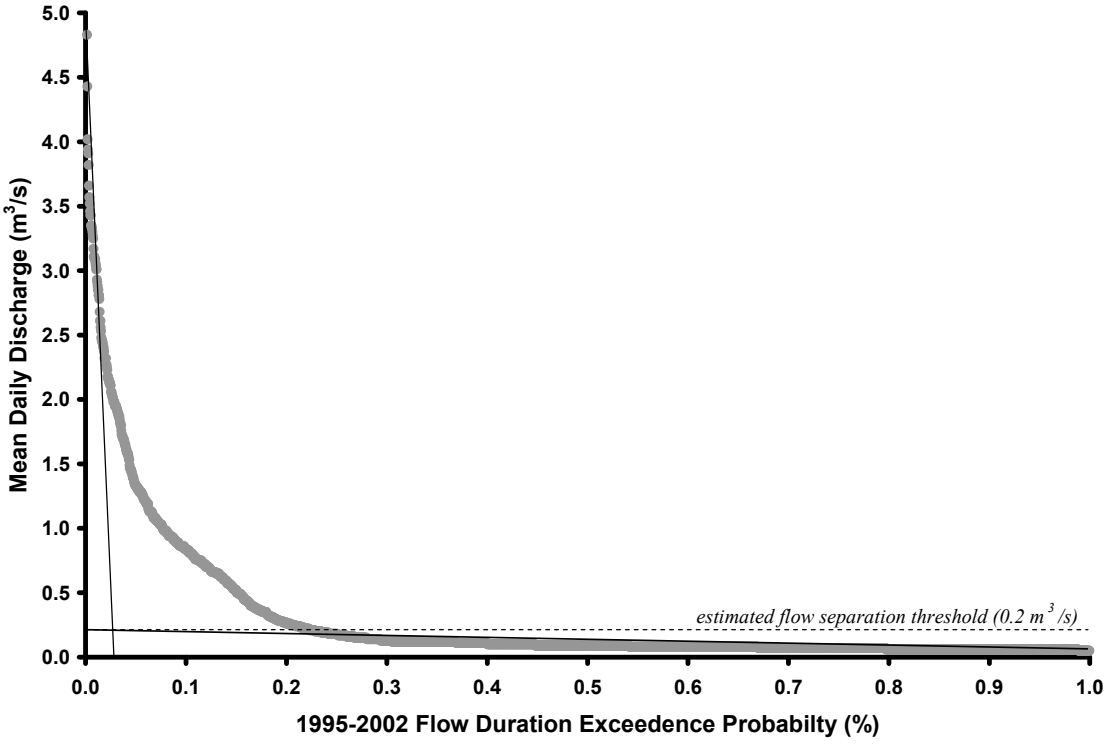

Figure 3. *Flow duration exceedence probability of measured mean daily discharge for the period 1995-2002 to indicate the separation between baseflow and runoff periods. Note: A high discharge value of 7.5 m^3/s measured in the spring of 1995 is not plotted to maintain scale.*

MODEL PERFORMANCE DECOMPOSITION

The relative influence of individual and grouped parameters associated with the final calibrated model was assessed through a stepwise decomposition. Following calibration, partial model sensitivities were quantified by systematically resetting parameter groups, and individual parameters within them, to their default values, and running the model with the other parameters groups in their calibrated state. Output from each partially calibrated model run was then compared to the fully calibrated model, and relative performance differences were noted through interpretation of changes in the NS statistic. Assessment focused on the snow, surface runoff lag, groundwater, soil, and SCS curve number parameter groups.

RESULTS

MODEL CALIBRATION

Over the period of record, the year 1999 represented standard precipitation, snow accumulation, water yield and runoff conditions within the research watershed (Table 5). Baseflow, rising, and falling components of the 1999 hydrograph were fairly symmetrical and represent a good example of snowmelt-induced hydrology. Throughout this section, 1999 data illustrate the peaked nature of annual streamflow patterns, hydrograph separation into baseflow and runoff components, and the impact of calibration on default model predictions.

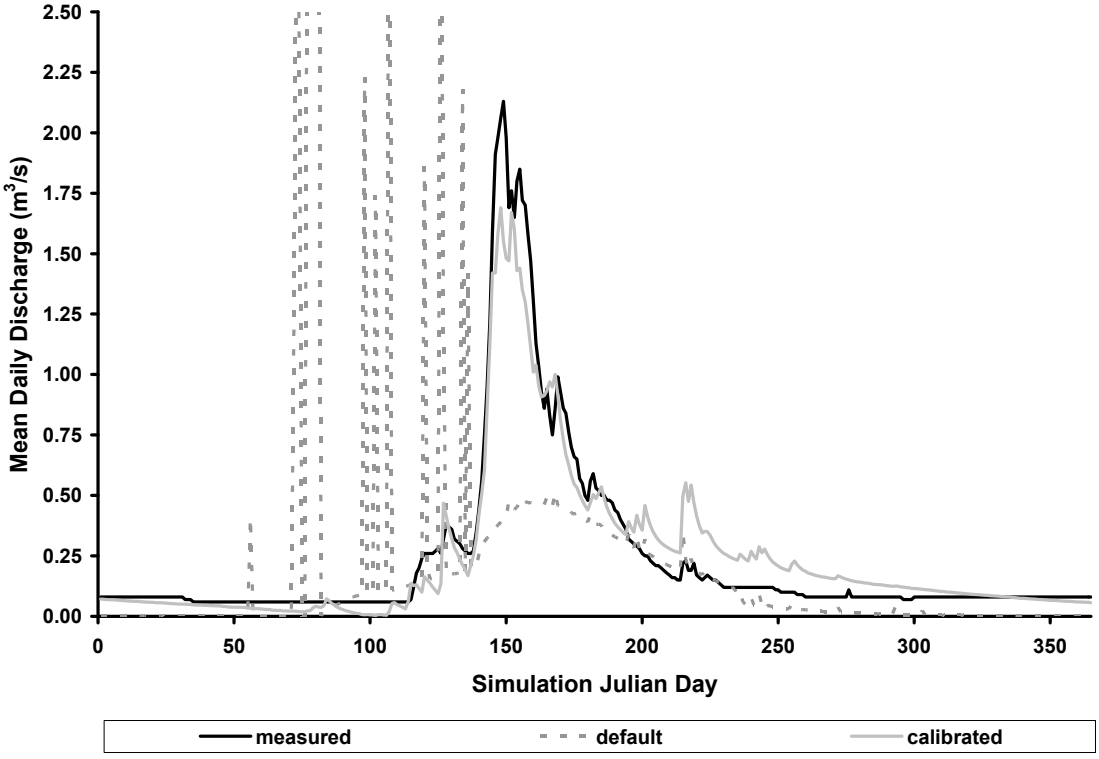

Figure 4. *Comparison of measured, default, and calibrated daily streamflow hydrographs during a year representing standard hydrologic conditions (1999).*

A visual comparison of the hydrographs obtained using the default and calibrated model parameters indicates that parameter adjustments substantially improved the fit of

modeled versus observed values (Figure 4). The 1999 hydrograph produced by the default parameterization was extremely flashy, with several short but large runoff events between Julian days 50 and 140. These events were followed by a more prolonged runoff period that corresponded with what was observed, but had a peak that was 75% smaller in magnitude. During baseflow periods the default model produced almost no runoff, and zero flows occurred for periods of up to 54 days. In contrast, the calibrated 1999 model hydrograph closely matched the observed data throughout most of the year. The best fit was obtained over the spring runoff period, particularly on the rising limb of the hydrograph. Summer recession values were overestimated, but winter and early spring baseflow components were generally underestimated. Overall, calibration reduced errors associated with the timing and magnitude of monthly water yield and daily flow rate estimates (Table 8).

Table 8. *Performance statistics for simulations with default and calibrated parameters, for the period 1997-2000. Shown are observed (Obs), and simulated (Sim) water yield, relative error (RE), mean error pair-wise error (Dv), Nash-Sutcliffe model efficiency (NS) over monthly ($_m$) and daily ($_d$) time-steps.*

Simulation Type	Year	Obs (mm)	Sim (mm)	RE (%)	Dv_m	Dv_d	NS_m	NS_d
Default	1997	564	609	8	71	123	0.53	-1.24
Default	1998	430	408	-5	73	91	0.35	-1.45
Default	1999	336	347	3	92	114	-0.48	-3.39
Default	2000	357	411	15	99	109	-0.47	-3.18
Calibration	1997	564	563	<1	34	37	0.90	0.88
Calibration	1998	430	375	-13	31	36	0.82	0.75
Calibration	1999	336	337	<1	27	30	0.92	0.92
Calibration	2000	357	374	5	30	37	0.92	0.86
Overall Default (1997-2000)		**1,688**	**1,775**	**5**	**82**	**110**	**0.23**	**-1.76**
Overall Calibration (1997-2000)		**1,688**	**1,649**	**-2**	**31**	**36**	**0.90**	**0.86**

Annual Water Yield

Over the four yeas spanning 1997-2000, the total water yield estimated by SWAT with default parameterization was within 5% of the recorded volume. While already within acceptable limits, calibration brought the relative error of estimate (RE) for the same period down to 2%. The default model overestimated water volumes in each year of the simulation. Calibration reduced the relative error but reversed its directionality so that overall the model predicted less water yield than what was observed (Table 8).

Monthly Water Yield

Calibration significantly increased model performance at the monthly time step (Table 8). The average difference between monthly estimates (Dv_m) produced by the default model was approximately 80%. After calibration, average monthly deviations were reduced to roughly 30%. Over the simulation period, the monthly Nash-Sutcliffe (NS_m) model efficiency coefficient increased from 0.23 for the default model to 0.90 upon calibration. The reduction in estimated deviations, and increase in efficiency indicate considerable improvement over the default parameterization, and a high level of model performance at the monthly time step.

Daily Streamflow

Model calibration had its greatest impact on performance during the daily time step (Table 8). The average percent deviation in daily estimates (Dv_d) produced by the default model was 110%. Calibration reduced average daily deviations by a factor of three, down to 36%. With uncalibrated parameters, the overall Nash-Sutcliffe coefficient for simulation at the daily time step (NS_d) was -1.76. Showing good performance and substantial improvement over the default model, the efficiency of calibrated daily simulations was 0.86 for the whole time period.

MODEL VALIDATION

Following calibration, SWAT was applied to the years 1995, 1996, 2001 and 2002 for validation. Over the simulation period, model performance for the validation years was similar to that achieved during calibration, at annual, monthly and daily time steps (Table 9).

Table 9. *Performance statistics for calibration and validation simulation time periods.*

Simulation Type	Year	Obs (mm)	Sim (mm)	RE	Dv_m	Dv_d	NS_m	NS_d
Calibration	1997	564	563	0	37	34	0.90	0.88
	1998	430	375	-13	36	31	0.82	0.75
	1999	336	337	0	30	27	0.92	0.92
	2000	357	374	5	37	30	0.92	0.86
Validation	1995	511	517	1	45	32	0.95	0.78
	1996	495	460	-7	50	39	0.83	0.74
	2001	288	234	-19	42	31	0.83	0.70
	2002	339	354	4	31	22	0.97	0.94
Overall Calibration (1997-2000)		**1688**	**1649**	**-2**	**36**	**31**	**0.90**	**0.86**
Overall Validation (1995-96, 2001-02)		**1632**	**1565**	**-4**	**43**	**32**	**0.90**	**0.76**

Annual Water Yield

Annually, the model tended to underestimate water yield, with a relative error of 4% over the validation years. This was 2% worse than calibrated simulations, but offered a 1% increase in accuracy over predictions from the default model. In a year-by-year comparison, the greatest errors during calibration and validation occur in 1998 (-13%), and 2001 (-19%), respectively (Figure. 5). In either case, relative errors for annual estimates were less than 20% and model predictions are therefore validated.

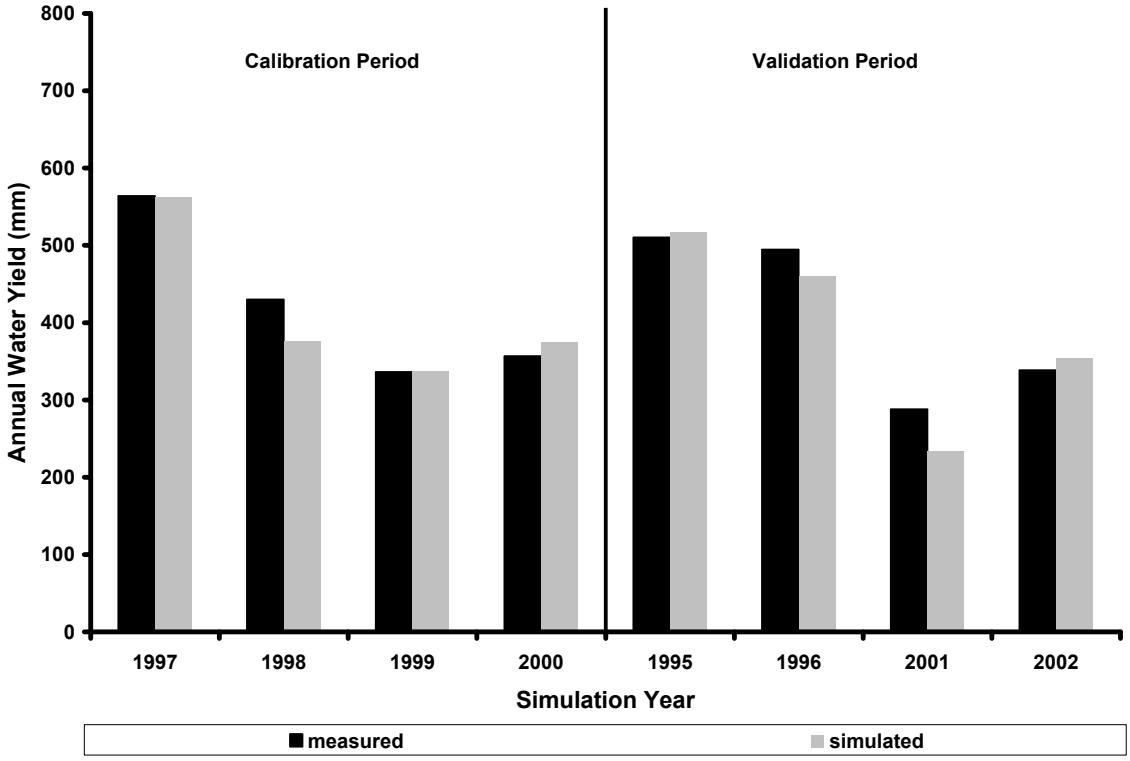

Figure 5. *Comparison of measured and simulated annual water yield (mm) by calibration and validation period.*

Monthly Water Yield

At the monthly time step, the calibrated model performed well when applied to the validation period (Table 9). The average percent difference (Dv_m) statistic changed less than 10%, going from 36% for the calibration, to 43% for the validation period. Temporally, the distribution of model flow predictions tracked observed monthly volumes well (Figure 6). Monthly NS_m values ranged from 0.83 to 0.97, and at 0.90 the overall validation efficiency was identical to that for the calibration period. The model was therefore validated for monthly estimates.

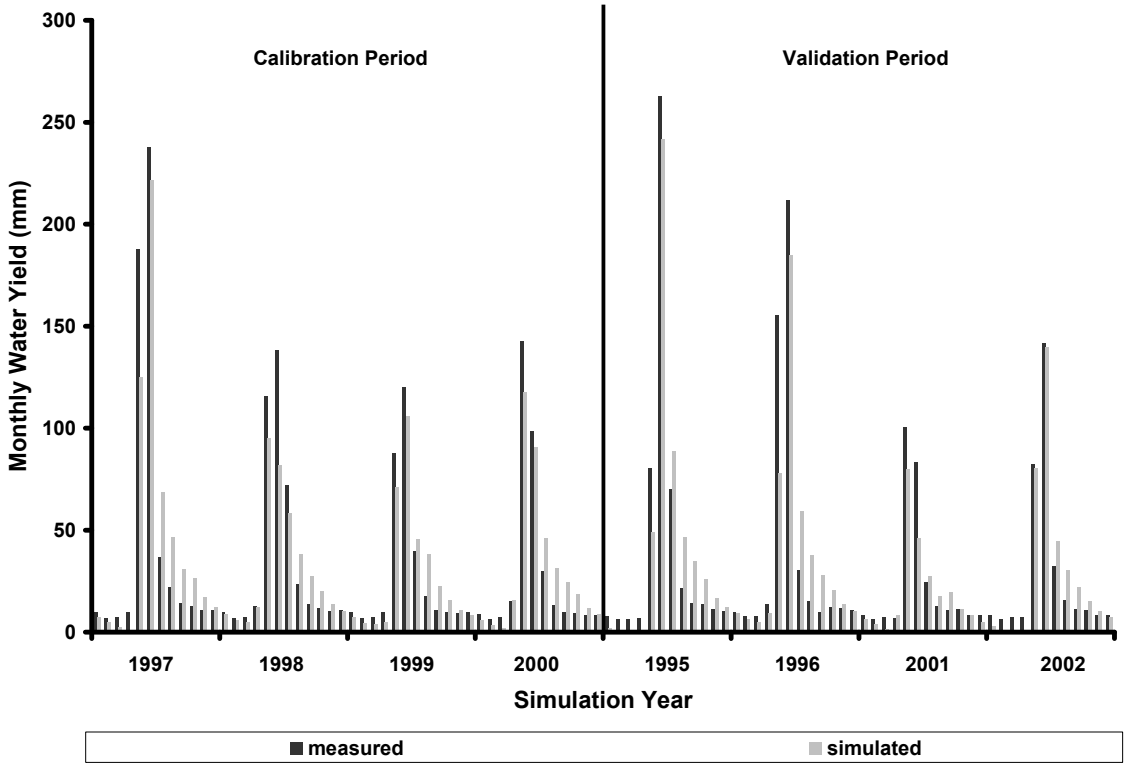

Figure 6. *Comparison of measured and simulated monthly water yield (mm) by calibration and validation period.*

Deviation between measured and simulated monthly water volumes was lowest during the spring runoff period in May and June, and greatest during recession flows of August and September. In a cyclical manner, the model consistently failed to predict adequate water yield from January through June, yet overestimated the water yield from July through November (Figure 7).

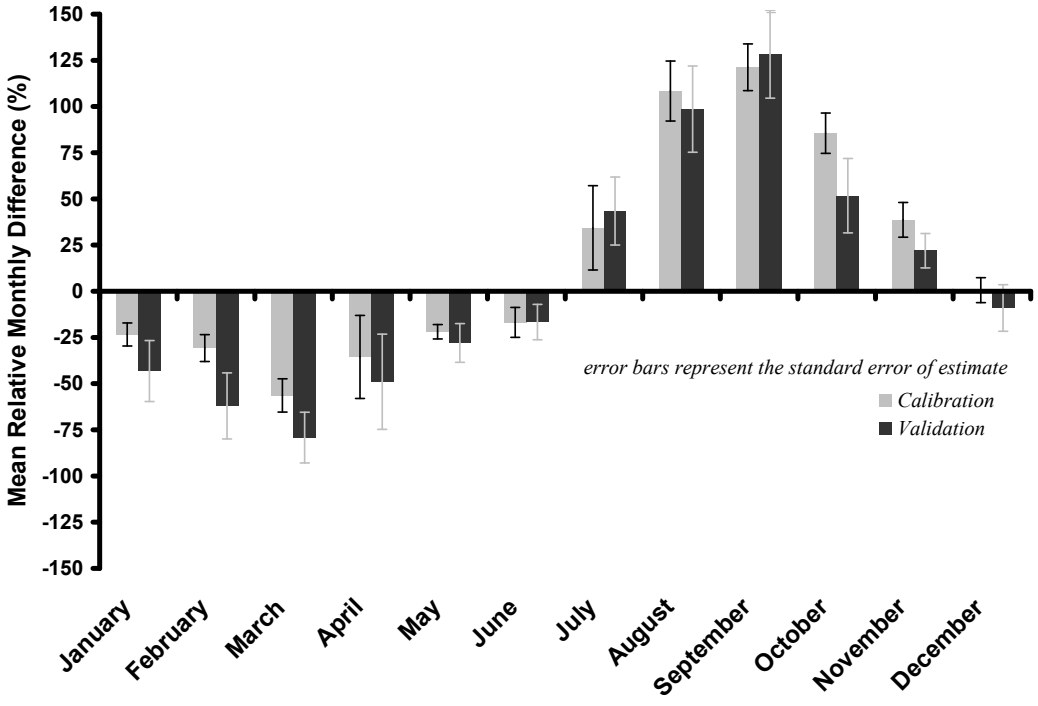

Figure 7. *Relative mean monthly deviation from measured streamflow (%) and their associated standard errors for the calibration and validation periods.*

Daily Streamflow

An approximate 10% reduction in performance was detected when the calibrated model was applied to the validation period and evaluated at the daily time step. While evaluation measures were slightly lower during validation, model results still represent good overall performance (Table 9). The mean relative deviation between daily model estimates (Dv_d) increased from 36% in the calibration as compared to 43% during the validation period. Efficiency of daily streamflow predictions (NS_d) dropped from 0.86 to 0.76 when model output was evaluated over the calibration and validation time periods.

Comparison of observed and predicted daily flows indicates that the closest match occurred during the runoff period between May and early July (Figure 8). Simulated annual peaks tended to be lower than observed peaks, especially in wetter years with high annual peak flows. In 1995 and 1996, for example, annual peaks of 7.5 and 4.0 m^3/sec

were recorded, but the model predicted peak flows were just 3.5 m^3/sec and 2.5 m^3/sec, respectively. The model also underestimated the rate of decline in the falling limb of the snowmelt-induced hydrograph peak, so that predicted flows were consistently higher than the observed values during the recession period. In contrast, the calibrated model did not produce sufficient baseflows in winter and early spring.

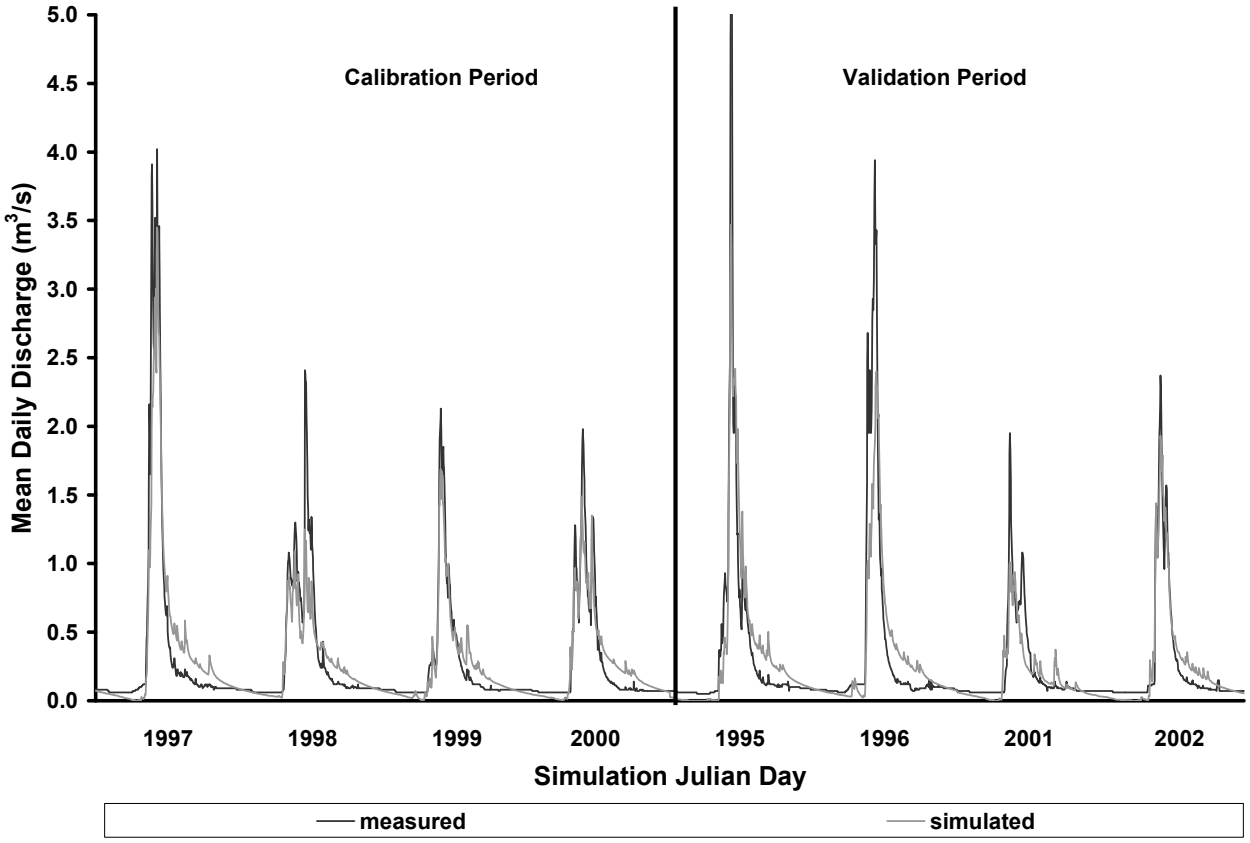

Figure 8. *Measured and simulated daily streamflow during calibration and validation periods.*

Seasonal Streamflow

For illustration, the 1999 hydrograph was separated into baseflow and runoff components through analysis of measured daily streamflow records (Figure 9). Streamflow components were validated by comparing the similarity of calculated performance measures between the calibration and independent validation dataset.

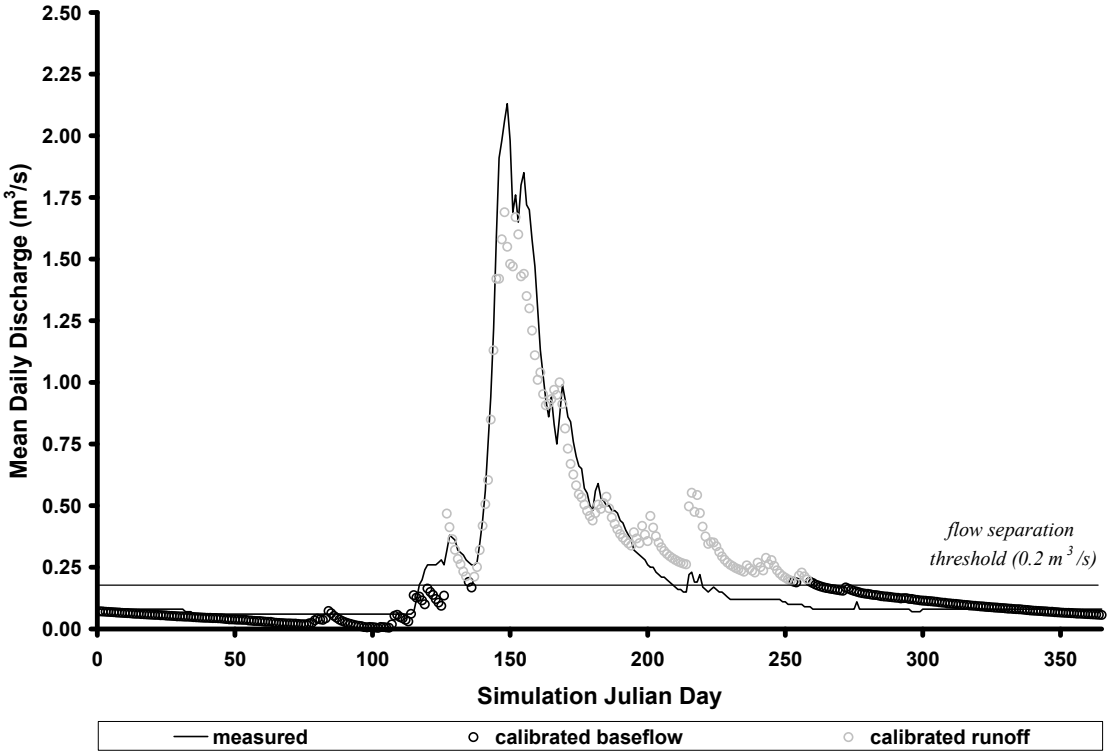

Figure 9. *Streamflow separation and evaluation of simulated components during representative hydrologic conditions in year 1999.*

Comparison of measured and simulated streamflow during the runoff period indicates a generally good fit, especially on the rising limb of the hydrograph (Figure 9). Although the timing of peaks is generally correct, the major difference between observed and predicted values is that the maximum simulated flow is lower than the measured peak flow. In addition, simulated flows are generally higher than observed flows in the latter part of the recession limb of the snowmelt hydrograph.

Unlike streamflow in the runoff period, baseflow was not well represented (Figure 9). SWAT produced too much flow in the lower part of the recession limb, but underestimated flow during the winter and early spring baseflow period.

Performance Measures

Model performance statistics for the runoff period reflected generally good fit between observed and predicted flows. The mean differences between monthly measured and simulated runoff estimates (Dv_m) in calibration and validation runs were both less than 25% at the monthly time step. Monthly calibration and validation efficiency scores (NS_m) were also around 0.80. With nearly identical performance measures, traditional analyses suggest that monthly runoff estimates have been validated by an independent time series. Relative errors (Dv_d) and model efficiencies (NS_d) for daily flows were slightly lower than what was achieved for the monthly values, but also indicated satisfactory model performance (Table 10).

Mean monthly difference between baseflow estimates were more than twice as large as those generated during runoff, where the model produced mean errors of nearly 65% for both the calibration and validation periods (Table 10). Daily scenarios were similar to those reported for the monthly time step, and the calibration and validation model runs still had ~70% error in predicted streamflow. Although the average efficiency of daily predictions was increased by two orders of magnitude in the calibrated model compared to the default model, the negative NS_d efficiency scores for the calibration and validation periods indicate that model performance was no better than an average of the observed values; in fact it was worse. Given poor performance, SWAT predictions cannot be validated over baseflow periods at monthly or daily time steps.

Table 10. *Performance statistics for baseflow and runoff hydrograph components. At the monthly time step, baseflow was defined as January - April, and August - December, while the runoff component was defined by the months of May, June and July. Daily flow baseflow was separated from runoff by a 0.2 m^3/s threshold, where runoff was captured by values equal to or greater than the threshold.*

		Baseflow Period		Runoff Period	
Monthly Simulation	**Year**	**Dv_m**	**NS_m**	**Dv_d**	**NS_d**
Calibration	1997-2000	62	-4.73	24	0.80
Validation	1995-96, 2001-02	66	-6.90	24	0.83
		Baseflow (<0.2 m^3/s)		**Runoff (≥0.2 m^3/s)**	
Daily Simulation	**Year**	**Dv_m**	**NS_m**	**Dv_d**	**NS_d**
Calibration	1997	80	-7.15	29	0.81
	1998	51	-4.86	32	0.42
	1999	59	-5.59	19	0.89
	2000	86	-11.99	23	0.69
Validation	1995	93	-9.09	34	0.70
	1996	70	-14.65	44	0.48
	2001	52	-4.36	38	0.16
	2002	73	-5.17	15	0.89
Calibration (1997-2000)		**69**	**-6.93**	**27**	**0.78**
Validation (1995-96, 2001-02)		**72**	**-8.58**	**34**	**0.63**

Regression-Based Model Invalidation

Considering simulations at the monthly time-step the regression-based model invalidation test suggests that streamflow predictions at that resolution are reliable. This is verified by the fact that most p-values are greater than 0.05 (Table 11) which indicates a failure to reject the joint null hypotheses of a zero y-intercept and slope equal to 1, i.e. the calibrated model behavior is confirmed by the independent validation dataset. These results are consistent for the overall simulation period, and individual years (Table 11).

Table 11. *Validation statistics for overall monthly streamflow prediction with SWAT.*

Monthly Simulation Year	**F-Statistic**	**DF**	**p-Value**
1995	0.56	10	0.47
1996	2.24	10	0.17
2001	9.26	10	0.01
2002	0.44	10	0.84
All Months (1995-96, 2001-02)	**3.88**	**46**	**0.06**

Due to the peaked nature of the annual hydrograph, streamflow predications were evaluated during the two most pronounced flow components on a monthly time-step; the baseflow and runoff periods. Consistency among the whole simulation time period and annual comparisons indicated no significant differences between observed and predicted water yield during the validation runoff period (all p-values greater than 0.05). Validation of the baseflow component was, however, not successful since all p-values were less than 0.05 indicating a rejection of the joint null hypotheses of a zero y-intercept and slope equal to 1 (Table 12). As shown with other evaluation measures, this analysis revealed that the calibrated model produced more favorable results during runoff rather than baseflow periods.

Table 12. *Seasonal streamflow validation of SWAT estimates at the monthly time-step.*

	Baseflow Period*			Runoff Period**		
Monthly Simulation Year	**F-Statistic**	**DF**	**p-Value**	**F-Statistic**	**DF**	**p-Value**
1995	1,015.97	7	0.00	0.29	1	0.69
1996	214.09	7	0.00	0.37	1	0.65
2001	103.94	7	0.00	1.77	1	0.41
2002	574.13	7	0.00	2.02	1	0.39
All Months (1995-96, 2001-02)	**1,413.86**	**34**	**0.00**	**2.41**	**10**	**0.15**

***** *January, February, March, April, August, September, October, November, December*
****** *May, June, July*

MODEL PERFORMANCE DECOMPOSITION

Calibration of the snow parameter set had the greatest effect on model performance in the Tenderfoot Creek research watershed. In decreasing order of influence, snow parameters were followed by the surface lag coefficient (SURLAG*)*, and the groundwater, soil, and curve number parameter sets (Table 13).

Table 13. *Relative influence of factors affecting model calibration. Model performance was evaluated for daily streamflow in representative year, 1999 through analysis of the model efficiency statistic (NS_d). Changes in performance due to parameter set decomposition are described in relative terms. Results of simulations where all parameters in a group have been decomposed are shown in bold face. Results from variation of individual parameters within a composite are italicized. Only values for the primary layer are given for the groundwater and soil parameter sets.*

	Default Value	Calibrated Value	NS_d	NS_d Change (%)
CALIBRATED MODEL			**0.92**	
Composite Snow			**-0.06**	**106**
Timp	*1.0*	*0.06*	*0.52*	*43*
Smtmp	*0.5*	*1*	*0.71*	*23*
Snocov50	*0.5*	*0.1*	*0.73*	*20*
Smfmx	*4.5*	*3*	*0.89*	*3*
Snocovmx	*1.0*	*200*	*0.93*	*-2*
Smfmn	*4.5*	*2.9*	*0.91*	*1*
Composite SURLAG	**4.0**	**0.05**	**0.19**	**79**
Composite Groundwater			**0.80**	**13**
Alpha_BF	*0.05*	*0.01*	*0.81*	*12*
GW_Delay	*31*	*1*	*0.85*	*7*
Composite Soil			**0.88**	**4**
Sol_K	*23*	*75*	*0.88*	*4*
Sol_awc	*0.09*	*0.18*	*0.91*	*1*
Composite CN2			**0.89**	**3**
Lodgepole pine	*55*	*58*	*0.90*	*2*
Disturbed forest	*55*	*69*	*0.91*	*1*
Shrubland	*61*	*65*	*0.92*	*0*
Grassland	*69*	*70*	*0.92*	*0*
Spruce-fir	*55*	*55*	*0.92*	*0*

Snow Parameters

Setting the snow parameters to their default values reduced the daily NS efficiency from 0.92 to -0.06. With the default snow values the snowmelt driven runoff peak occurred 75-80 days earlier than the calibrated and observed peaks, and the recession limb was extended by a similar number of days longer (Figure 10). The snow parameter with the greatest impact on model calibration was the snow pack temperature lag factor (TIMP), followed by the snow melt temperature (SMTMP), and the snow cover depletion curve (SNCOV50). Use of the default values for the maximum and minimum snowmelt rate factors (SMFMX and SMFMN) had only a minimal effect on model

performance, while setting the snow covered area parameter back to the default value of 1 improved the model efficiency by 1%.

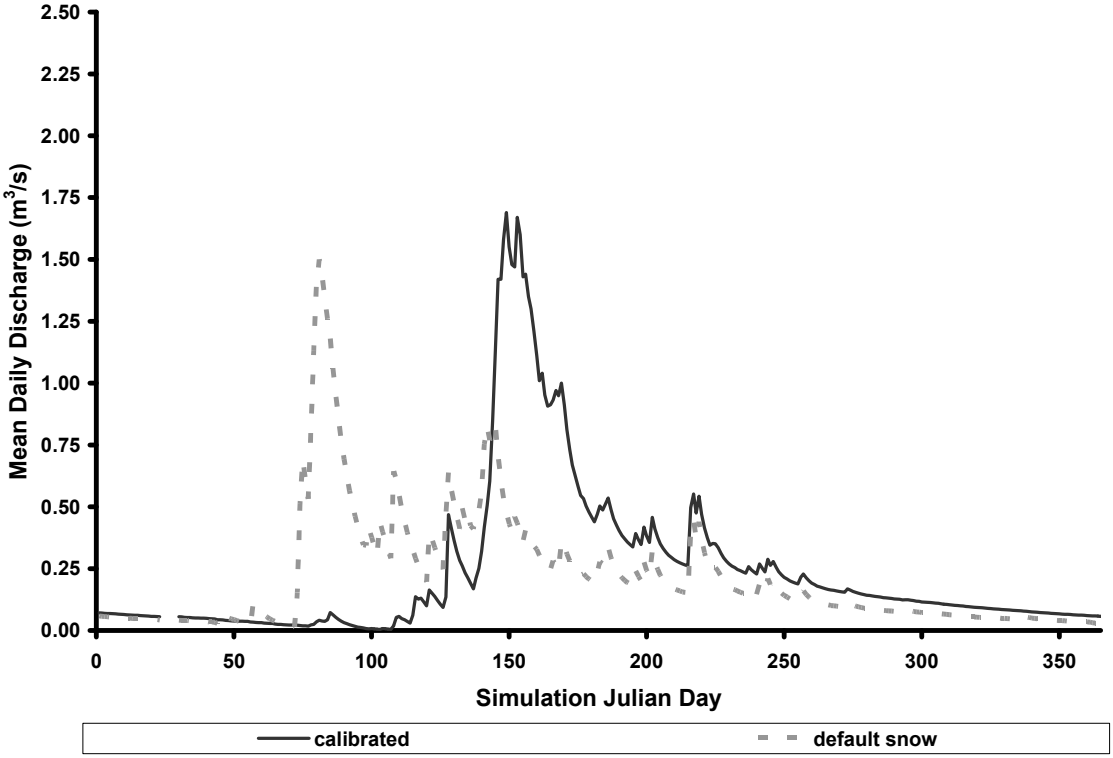

Figure 10. *Impact of the snow parameter set decomposition on the calibrated daily streamflow hydrograph simulated in 1999.*

Surface Runoff Lag Factor

Re-setting the surface lag factor (SURLAG) from the calibrated value of 0.05 to the default value of 4.0 reduced the model efficiency from 0.92 to 0.19. Comparison of the hydrographs obtained using the default and calibrated values for SURLAG shows that the primary effect of the calibration of surface lag was to smooth the hydrograph by slowing the rate of runoff during the snowmelt period, when there was a large quantity of water potentially available for streamflow (Figure 11).

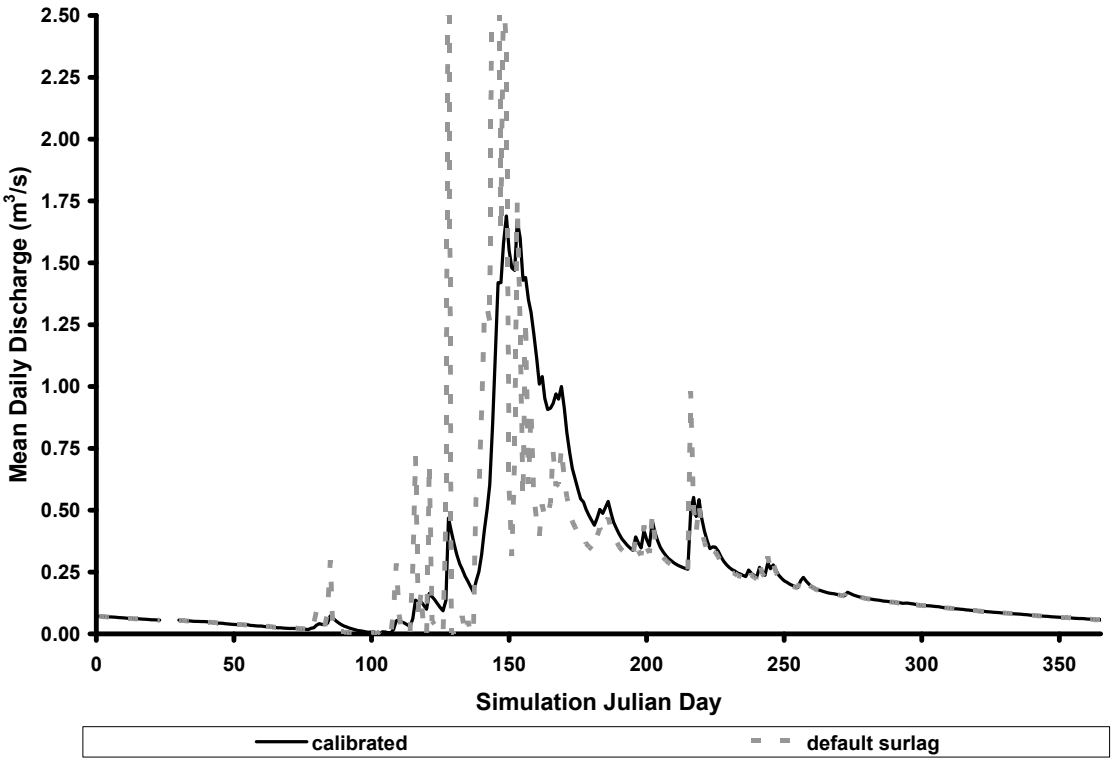

Figure 11. *Daily streamflow hydrographs for 1999 water year with default and calibrated values for the surface lag coefficient (SURLAG). For the default hydrograph all other parameters were set to their calibrated values.*

Groundwater Parameters

When compared with the snow and surface parameters, re-setting the groundwater parameters to their default values had relatively little effect on model performance. The model efficiency with the default parameters was only 12% lower than with the calibrated parameter set (Table 13). However, calibration of the groundwater parameter set improved the model fit during the streamflow recession period, and made more water available for baseflow (Figure 12). Of the calibrated groundwater parameters, adjustment of the ALPHA_BF parameter yielded the greatest improvement in model performance. Reducing ALPHA_BF from the default value of 0.048 to 0.01 slowed the shallow aquifer response to recharge, causing a reduction in the annual runoff peak during snowmelt and making more water available for streamflow later in the year. Reducing the value of

GW_DELAY from the default of 31 days to 1 day affected both the width of the peak discharge and the quantity of water available for baseflow.

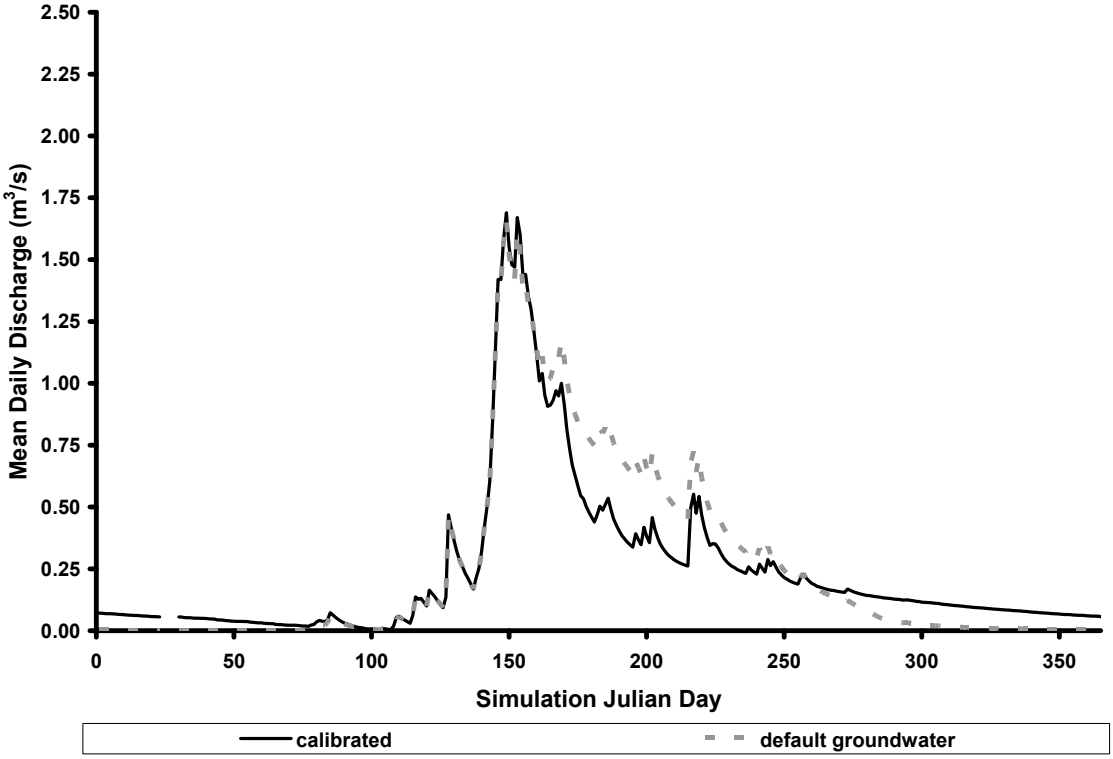

Figure 12. *Impact of the groundwater parameter set decomposition on the calibrated daily streamflow hydrograph simulated in 1999.*

Soil Parameters

Use of the default soil parameters reduced the overall model efficiency by just 4%. Calibration of the soil parameters primarily improved the fit to the observed daily stream flows on the recession limb of the snowmelt hydrograph. Of the two soil parameters adjusted, the soil hydraulic conductivity (SOL_K) had the greatest influence on model fit. Increasing SOL_K from the default value of 23 to the calibrated value of 75 increased the modeled peak flows during the snowmelt season. Increasing the available water holding capacity (SOL_AWC) made more water available for streamflow in the baseflow period, but the improvement in model efficiency was less than 1% (Figure 13).

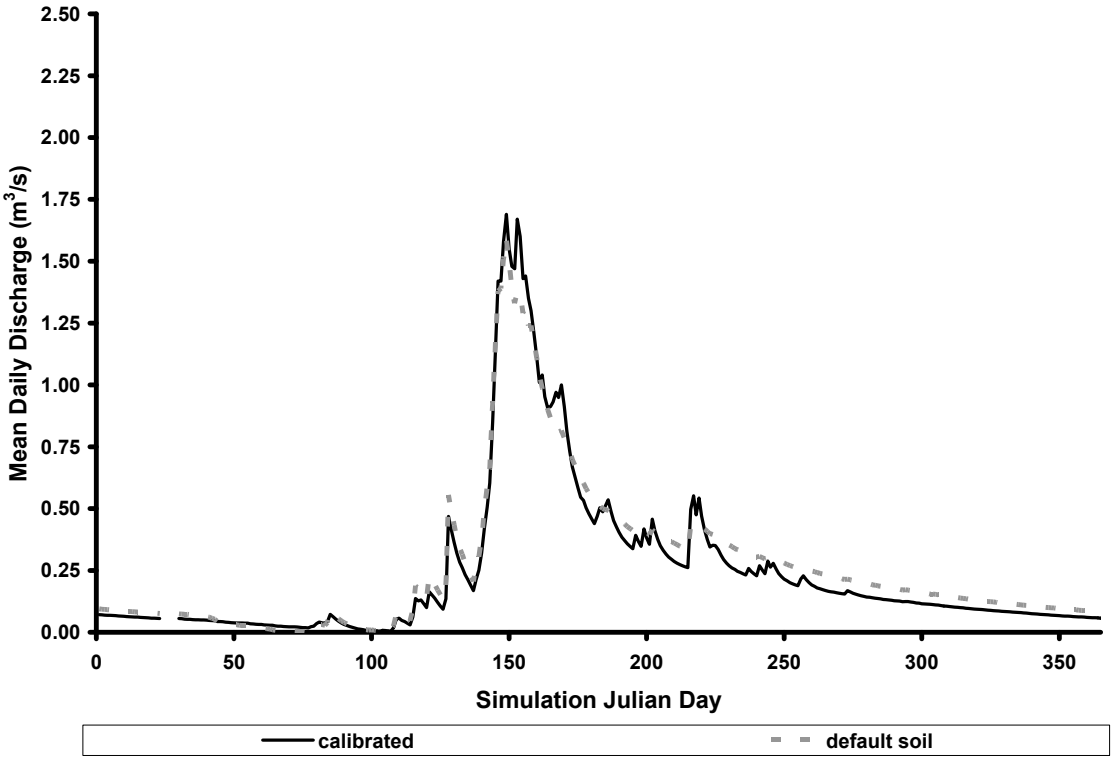

Figure 13. *Impact of the soil parameter set decomposition on the calibrated daily streamflow hydrograph simulated in 1999.*

SCS Curve Numbers

When curve numbers for all represented landcover types were set to their default values, the decrease in model efficiency was just 2.5%. The only detectable effect on model fit was a reduction in the early runoff peaks (Figure 14). Lodgepole pine forest covers the majority of the watershed, and changing the default curve number for evergreen forest from 55 to 58 yielded the greatest increase in model performance. Following lodgepole pine, introduction of the disturbed forest landcover produced the second largest improvement in efficiency. While this landcover type occupies only 10% of the watershed, the change in curve number from 55 to 69 had a noticeable effect on the model fit to observed values.

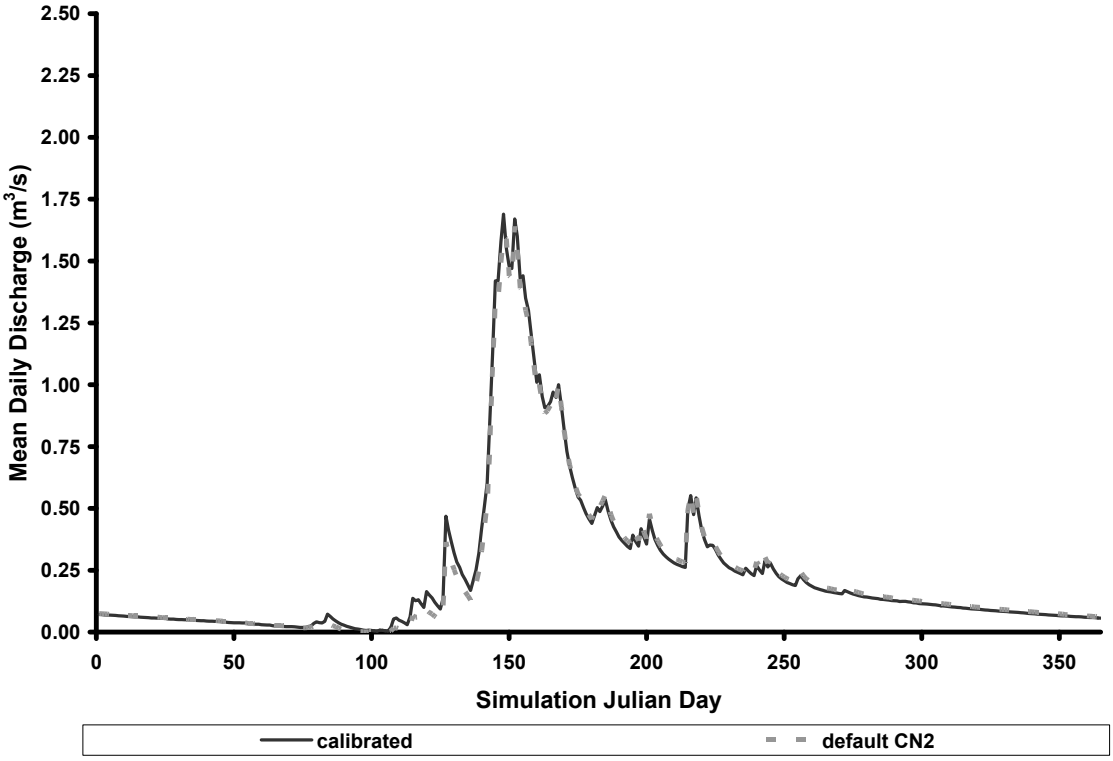

Figure 14. *Impact of the SCS curve number set decomposition on the calibrated daily streamflow hydrograph simulated in 1999.*

DISCUSSION

The goal of this study was to evaluate SWAT performance in previously untested conditions to determine if it would be suitable for streamflow prediction in a forested snow-dominated mountain environment at a scale commonly used in natural resource planning and management; the watershed scale.

Mountainous watersheds in western North America are generally remote, forested, and have hydrologic patterns dominated by snowmelt. Shifts in vegetation patterns due to periodic fires, timber harvest, or natural succession can alter the hydrologic behavior of upland watersheds, and understanding the interactions between streamflow and forest structure is important for integrated water resource management.

Because opportunities to experimentally evaluate the impact of management or policy scenarios on watershed function are limited, modeling tools are needed. The Soil and Water Assessment Tool (SWAT) is based on over three decades of institutional research and was designed to help evaluate the hydrologic impacts of land management (Arnold et al., 1998). SWAT has a long track record of successful application in lowland and temperate regions, but little is known about its performance in forested mountain watersheds where streamflow patterns are driven by snowmelt, and forest dynamics are the primary management alternatives (Gassmann, 2005). Few examples of calibration in upland watersheds exist because reliable climate and streamflow data necessary for calibration are rare. First, not many mountain watersheds are gauged for streamflow over meaningful time periods, and second, rugged terrain makes it difficult to accurately extrapolate climate data from distant locations.

The Tenderfoot Creek Experimental Forest research watershed is instrumented with climate and hydrologic monitoring sites that provided an unusually comprehensive dataset with which to calibrate SWAT. Climate and ecological characteristics of this site are similar to those found throughout the eastern slope of the Rocky Mountains, and this should make results from the study broadly applicable to comparable watersheds.

MODEL CONFIGURATION

Among the first steps in the SWAT configuration process is to delineate and partition the watershed. Resulting sub-watersheds are the smallest aerial unit that SWAT considers, and a high level of subdivision is necessary to capture spatially explicit watershed processes (Mangurerra and Engel, 1998; Haverkamp, et al. 2002; Arabi, et al. 2006). The level of sub-division should be proportionate to the changes in sub-watershed condition that will be evaluated from model scenarios. For example, reductions of 20% or more forest cover in Rocky Mountain watersheds are assumed to elicit detectable changes in streamflow (Bosh and Hewlett, 1982; Stednick, 1996). Using this proportion suggests that a model designed to evaluate the impact of forest removal on streamflow should be configured with sub-watersheds that are not larger than 5 times the size of anticipated forest disturbances. In this calibration, sub-watershed size was roughly equal to 5% of the total watershed area, which is similar to what Arabi et al., (2006) proposed as the minimum relative area required to detect the influence of management practices.

Once the spatial structure of the model was established, each sub-watershed was attributed with physical properties based on the required input data. To reduce input uncertainty, measured and physically realistic parameters were used whenever possible.

Sub-watershed Characterization

To account for the influence of orographic precipitation, configured sub-watersheds were stratified into three elevation bands, and locally derived lapse rate information were used to provide the necessary climate forcing elements (Table 2).

Channel dimensions are one aspect of the physical environment that can be easily quantified. Specifically, measured channel width and depth and their ratios were used to update inputs estimated by the geo-processing capabilities of AVSWAT interface.

SWAT uses a vegetation database to define the parameters for mapped landcover categories. Most of the forested land in the upper Tenderfoot watershed is coniferous, but options for representing different conifer forest types with the standard database are limited. To account for differences in canopy and other vegetation characteristics, the final landcover map used in this study represented barren ground, grassland, shrubland, spruce-fir forest, lodgepole pine forest, and disturbed forest. Each landcover category was

associated with site-specific parameters, focusing on the interaction between vegetation characteristics and atmospheric inputs (Table 3).

In the study area, only one soil type, the Stemple series, was described. This assumption of uniform soil characteristics across the study area is an obvious shortcoming, and likely the least accurate representation of physical properties within the model.

Hydrologic Response unit Definition

After characterization, sub-watersheds were further sub-divided into hydrologic response units (HRUs) to establish the basic SWAT modeling elements. Due to the lack of mapped soil diversity, landcover patterns were the only distinguishing factor for HRU definition in this watershed. The number and diversity of HRUs can influence model output (Bingner, et al. 1997; Mangurerra and Engel, 1998). To ensure a high level of resolution, multiple HRUs were defined for each sub-watershed by specifying a minimum 5% aerial extent for landcover categories.

MODEL CALIBRATION

Simulations based on default parameterization produced 105 percent of the observed water yield. While already within acceptable limits, calibration brought the relative error of estimate (RE) for the same period down to 2%. Calibration for annual intervals focused on adjustment of lapse rates. Increasing the PLAPS from -6.0 to -7.25 forced more realistic orographic precipitation patterns in the watershed, and as a result overall water yield estimates became more accurate.

A global sensitivity analysis indicated that model predictions were sensitive to changes in snow, surface runoff lag, groundwater, soil, and curve number parameters. Adjustment of snow parameters affected the timing of the dominant annual hydrograph feature; the runoff peak occurring between late May and early June. Tuning the surface runoff lag coefficient reduced the flashiness of the default parameterization.

One of the major problems in calibrating SWAT in this watershed was matching the baseflow component of the hydrograph. While peak flows could be matched by

adjusting the snowmelt and runoff parameters, baseflow estimates were affected by groundwater parameters. With default settings, no baseflow was maintained for winter flow and too much water was held and released in late summer. For calibration, slowing the response to recharge by lowering ALPHA_BF and reducing the groundwater delay time, GW_DELAY, caused the runoff peak to become narrower and taller, while also maintaining reasonable baseflow rates.

Soil infiltration and water holding capacity parameters affected early runoff peaks and late summer recession flows. According to the STATSGO database, soil properties were uniform throughout the watershed and this is obviously one of the least well represented aspects of the watershed model.

Calibration of snowmelt, surface runoff, groundwater, soil, and curve number parameter groups improved model performance at the monthly, and most noticeably the daily time steps. After calibration, model performance was very good, with Nash-Sutcliffe efficiencies of 0.90 and 0.86 for monthly and daily streamflow predictions.

Automated calibration procedures offer many advantages over manual methods. However, the auto-calibration algorithm embedded in the current version of the AVSWAT interface cannot be used effectively in watersheds with snowmelt dominated hydrology like TCSWAT with a strongly seasonal, unimodal hydrograph. Currently, the auto-calibration algorithm uses only a single sum of squares objective function. With that format, very little weight is given to model performance during low flow periods because the errors associated with those values are an order of magnitude smaller than those of the runoff period, and this leads to an inability to simultaneously calibrate the model for both high and low flows. However, baseflows can be just as important as snowmelt driven peak flows when considering the effects of management on fish populations and riparian condition in mountainous watersheds (Tennant, 1976; Binns and Eiserman, 1979). Instead, an algorithm with multiple, rather than a single objective function(s) could yield more favorable results. One function could be used to calibrate the rising limb and peak of the hydrograph, another for the recession limb focusing on the inflection between runoff and groundwater dominated flow regimes, and a third to account for the baseflow period. Hay et al, (2006) used a similar multi-objective function approach with another model, where various components of the physical system were calibrated

independently. In addition to improving model performance during baseflow periods a multiple objective function approach would facilitate more effective automated calibration when time or expertise are lacking for extensive manual refinement.

MODEL VALIDATION

Model performance was validated with two distinct techniques, focusing on annual, monthly, daily, and seasonal periods. Using the traditional validation approach, model performance measures derived over the calibration period were compared to those generated when SWAT was applied to an independent dataset. With this method no significant decline in model performance was detected at annual, monthly or daily time steps and the model was considered validated for prediction at these temporal resolutions. However, a closer examination of monthly performance revealed that the model consistently failed to predict adequate monthly water yield from January through June, and overestimated the water yield from July through November (Figure 7). Because there is a water deficit in winter, not enough water is available for spring runoff. Recharge from snowmelt alone was insufficient for model simulation to match the annual peaks. Additional water needed to be made available to the baseline flow to which snowmelt water would be added. Most of the water in the system is a result of snowmelt, and a component that improves the model's ability to store and transmit groundwater would be helpful for hydrologic simulation in this environment.

At the daily time step, simulated annual peak flows tended to be lower than the observed ones, particularly in wetter years with high annual peak flows. This may be explained by the inability to fully represent snowmelt groundwater processes, and climatic conditions that cannot be accounted for with daily data. In 1995 and 1996, for example, annual peak discharges of 7.5 and 4.0 m^3/s were recorded, but the model predicted peak flow rates to be just 3.5 and 2.5 m^3/s, respectively. The unusually high flow rates occurring in those years were the product of high-intensity, short duration rain during the peak of spring runoff (McCaughey, personal communication, 2007). Such rain-on-snow events are difficult to capture with weather data representing average daily conditions, and the temperature-based snowmelt model is not able to replicate the

processes that are responsible for producing this type of discharge pattern. This indicates that successful application of SWAT for streamflow prediction in watersheds with a high frequency of rain-on-snow events may be limited.

Seasonality is defined by the dominant features of the annual hydrograph. In this watershed, there are two distinct flow regimes; baseflow and snowmelt-induced runoff. Months were classified as either baseflow or runoff months by the dominant process occurring in them. When streamflow was separated into baseflow and runoff components, traditional validation was only possible for monthly and daily predictions during the runoff period.

To provide an objective test of model performance, a regression-based invalidation procedure was applied to monthly data. Model performance was evaluated for the whole validation period, and over the two hydrograph components. Because the model invalidation test is based on simple linear regression, assumptions of normality and independence must be met to produce meaningful results. Parametric tests and performance measures designed with these assumptions in mind are most suited for annual and monthly data (Coffey et al, 2002). At the annual time-step, only four data points were used for calculation, leaving few degrees of freedom. Conversely, many degrees of freedom are available for analysis at the daily time-step, but assumptions of normality and especially independence are violated. Without a suitable transformation, daily streamflow data tend to exhibit skewness and kurtosis that preclude assumptions of normality. Likewise, lagging by up to a week is required to remove serial autocorrelation within daily records. Analysis of the monthly time-step therefore provides the most reliable indicator of model validation when at least 2 years of validation data are available (so that $n = 24$).

Conclusions derived from this test were similar to those obtained from the traditional model assessment. Results indicated no significant differences between simulated and observed values, and model output could therefore not be invalidated (i.e. model was validated at the monthly time step). Objective evaluation of hydrograph components with monthly data also supported traditional comparisons, where the model preformed well during runoff periods, but failed to represent baseflow periods adequately.

MODEL PERFORMANCE DECOMPOSITION

The snowmelt-induced peak is the most prominent feature of the annual streamflow hydrograph of the Tenderfoot Creek research watershed, and adjustment of snowmelt parameters increased the calibration efficiency of the Tenderfoot Creek SWAT model (TCSWAT) more than any other parameter group. Calibration of the whole snowmelt parameter group substantially improved the timing of the simulated runoff during the rising limb and peak of the hydrograph. Insufficient infiltration during snowmelt required significant surface runoff attenuation, and model sensitivity to SURLAG adjustments followed second behind that of the snow parameter group. Calibration of the SURLAG parameter primarily affected hydrograph flashiness during runoff. In decreasing order of influence, the groundwater and soil parameter groups changed the shape of the peak flow recession and baseflow components, while soil parameters affected recession flows and instantaneous responses to precipitation and snowmelt. Curve number (CN) parameters had relatively little influence on the final calibration, but primarily affected streamflow responses to precipitation and snowmelt runoff. At the conclusion of the calibration it was evident that matching the large annual hydrograph peak had the greatest impact on the generation of favorable performance statistics. Once snow process and surface lag parameters were calibrated, acceptable model performance statistics could be achieved even when baseflow estimates were poor, because the large annual snowmelt peak was well matched.

Despite generating favorable statistics, two aspects of SWAT performance in the research watershed warrant further examination. These areas of interest are first the representation of snowmelt infiltration and runoff processes, and second the difficulty associated with matching the recession curve and subsequently poor representation of baseflow periods. Refinements in the handling of the snowmelt infiltration and groundwater recession elements may improve model performance in TCSWAT and similar mountainous, snow-dominated, forested environments.

Snowmelt Infiltration and Runoff Processes

Of all the snowmelt parameters, adjusting the snowpack temperature lag factor parameter (TIMP), and the threshold temperature for the onset of snowmelt (SMTMP) yielded the greatest improvement in model performance during calibration (Table 13). Snowpack of TCSWAT tends to be light and dry, and to reflect these characteristics TIMP was set to a low value nearly one tenth that of the default, while SMTMP was increased 2.5 times over the default to account for large diurnal temperature ranges during the snowmelt season. Both of these changes had the effect of decreasing or eliminating snowmelt during isolated warm days in the early spring, and is consistent with the observed behavior of the snowpack at TCEF, which is initially dry and does not become ripe and produce melt until mid to late May each year (Sappington, 2005). In the translation to streamflow, adjustment of the snowmelt parameters caused delayed snowmelt generated runoff and shifted the annual peak from winter to spring (Figure 10).

Although calibration of the snow parameter set substantially improved the timing of snowmelt conversion to streamflow, the decomposition analysis indicated that the calibrated hydrograph would still have been extremely flashy without adjustment of the surface runoff lag coefficient (SURLAG). The sensitivity analysis also identified SURLAG as a critical calibration parameter. SURLAG dampens the streamflow response by delaying the delivery of a portion of the surface runoff produced each day to the stream. The fact that SURLAG played such an important role in the model calibration therefore indicates that simulated streamflow was routed to the stream primarily as surface runoff. This is inconsistent with field observations at TCEF and in other pristine forested environments in western North America, where little or no overland flow is generated even during the period of maximum snowmelt because infiltration rates are extremely high (Stadler et al., 1996). Rather, snowmelt is routed to the stream by a combination of lateral flow and shallow groundwater flow. This inconsistency is likely because SWAT assumes an infiltration rate of zero in frozen soils (Neitsch et al., 2002). Soil temperatures in SWAT are calculated as a lagged function of the air temperature, adjusted for the effects of surface litter cover and snow cover (Neitsch et al., 2002). During the calibration and validation periods, SWAT modeled near-surface soil temperatures were below freezing during 95% of the snowmelt runoff period (Figure 15).

Much of that snowmelt runoff was therefore routed to the stream as overland flow, and. the SURLAG parameter was set to a value well below that used in comparable studies (e.g. Eckhardt and Arnold, 2001) so that simulated surface runoff rates were similar to the slower, shallow subsurface flows that predominate in this environment. The absence of infiltration into frozen soils also explains why, in contrast with many other studies, the calibrated SWAT model was relatively insensitive to the curve number parameter set. In situations where the infiltration rate is zero, SWAT ignores the curve number parameter defined for the HRU.

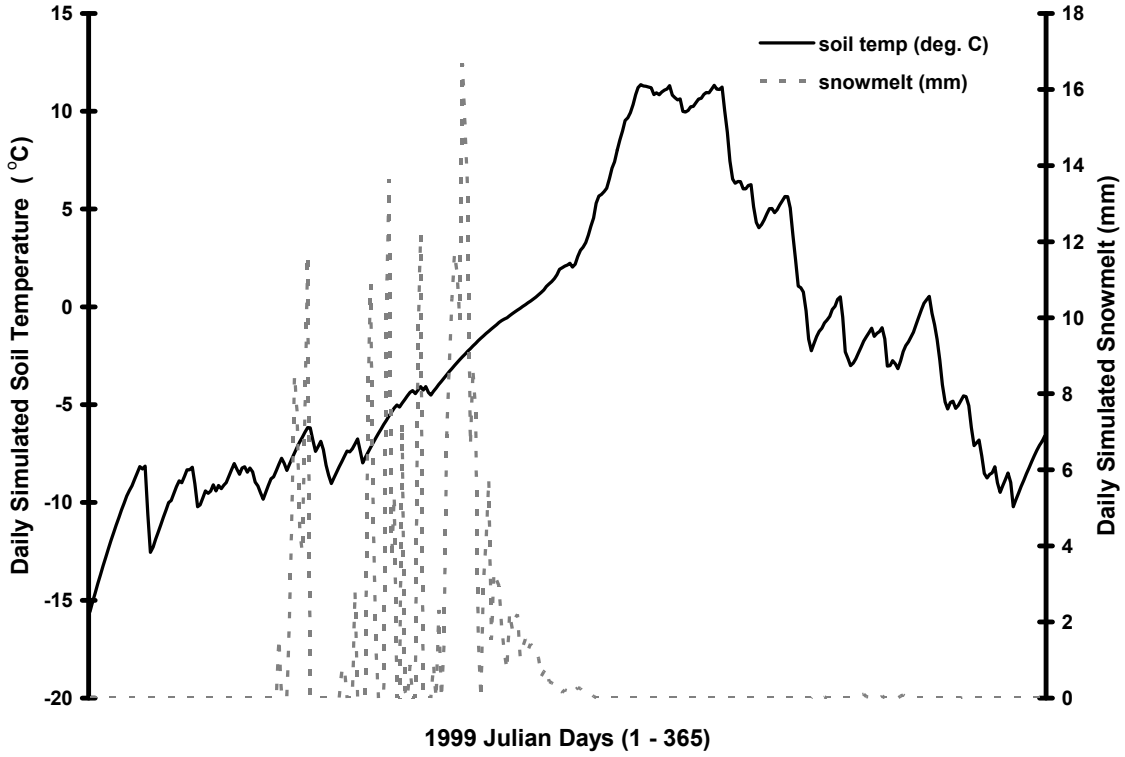

Figure 15. *Simulated daily soil temperature (°C) and snowmelt (mm) in a lodgepole pine forest HRU (# 8) within TCSWAT's sub-watershed 4, during the year 1999.*

Data from the Onion Park SNOTEL site indicate that mean daily winter temperatures at TCEF are well below freezing for extended periods, so it is reasonable to assume that soils within the study area are frozen for much of the winter. However the model assumption that there is no snowmelt infiltration into these frozen soils may not

apply in this environment for two reasons. First, in the relatively dry summer environment of central Montana, soils are usually well drained immediately prior to the first snowfall. This reduced the extent to which frozen interstitial water could constrict the matrix flow of infiltration during snowmelt (Gray et al., 2001). Second, like most forest soils, those at TCEF contain an abundance of macropores that typically facilitate infiltration rates in frozen soils comparable to those in unfrozen soils of the same type, regardless of the extent to which the soil matrix is clogged by ice (Popov, 1972; Roberge and Plamondon, 1987; Stadler et al., 1996). Modification of SWAT to allow infiltration into frozen forest soils, using the approaches outlined by Gray et al., (2001) would lead to improved model performance and better representation of runoff processes in forested upland watersheds. Such a change would also increase the model sensitivity to differences in landcover as represented by the curve number parameters, and hence to the effects of disturbance events such as fire and forest management.

Recession Curve and Baseflow Periods

The recession limb of the streamflow hydrograph peak produced by TCSWAT was primarily controlled by groundwater processes, and the ALPHA_BF and GW_Delay parameters were most useful for adjusting groundwater flow. With the current model structure, there is however considerable difficulty associated with matching the rapid transition between shallow subsurface flow during and shortly after the snowmelt period and the baseflow regime of the remaining portions of the year dominated by groundwater flow. Modification of the groundwater handling routine to include separate recession constants (ALPHA_BF) for the transition and, baseflow periods may facilitate improved hydrologic process representation in Rocky Mountain watersheds.

SWAT consistently underestimated monthly water yields from January through June, and overestimated the monthly water yields from July through November. The same trends were observed in the daily flow simulations, where the model consistently underestimated runoff peaks, overestimated flows during the snowmelt recession period, and then underestimated baseflows. Both of these trends can be explained in terms of the partitioning of water into runoff and baseflow components during snowmelt, and the effect of groundwater parameters that control the timing of the delivery of groundwater to

the stream. In general, the model apportioned too little water to baseflow during the snowmelt runoff period, in part due to the frozen soil effect previously described. With steep slopes in this watershed, the model also routed water out of the groundwater reservoir faster than occurs under field conditions. Lowering the value of the baseflow runoff coefficient (ALPHA_BF) dampened the model response to snowmelt induced recharge, increasing the amount of runoff available for baseflow later in the year. However, this also decreased the snowmelt runoff peak by reducing the groundwater contribution, and increased the runoff during the snowmelt recession period when runoff is rapidly changing from a shallow subsurface flow dominated regime to one dominated by groundwater flow. Reducing the value of GW_DELAY partially offset the effect of the low baseflow recession on the runoff peak, but improvements in model performance during the baseflow period were largely achieved at the expense of reduced model performance during the runoff period, and vice-versa. A better fit between observed and simulated flows in the recession period of the snowmelt hydrograph and during baseflow may be achieved by incorporating two baseflow recession constants into the SWAT groundwater parameter set, with one for the recession limb of snowmelt driven runoff and the other for the maintenance of baseflow.

CONCLUSIONS

Configuration is important, as it affects the spatial arrangement of watershed elements, and therefore influences the model's ability to represent the diversity of terrain, parent materials, and vegetation and management practices. When this is important, a high level of subdivision is advisable.

Although annual water yield predictions based on default parameterization were acceptable, calibration increased model performance in all time steps over which streamflow predictions were evaluated, especially at the daily level of prediction. Calibration was most strongly influenced by snow process, and surface runoff lag parameters in this watershed, as they were most responsible for matching the large annual hydrograph peak, and smoothing the streamflow response to snowmelt. Once runoff peaks were well represented, reasonable performance statistics could be generated

regardless of baseflow accuracy. Evaluation of model performance against a validation dataset provides an independent check on the robustness of the calibrated parameter set. With an objective regression-based hypothesis testing procedure model performance can be evaluated objectively, and add rigor to validation statements.

Nash-Sutcliffe (NS) efficiency statistics reported for the Tenderfoot Creek site for both the calibration and validation periods compare favorably with others reported in the literature (Table 14). This confirms that SWAT can predict annual, monthly, and daily hydrologic processes in forested snow-dominated mountain watersheds with efficiency levels that are similar to those obtained in other regions where it has been successfully applied. A relatively small drop in performance from the calibration to independent validation also suggests that the calibrated parameter set is robust across the 1995-2002 period. Future studies may be able to use SWAT with these calibrated parameters to investigate various biophysical interactions at the watershed scale. For example, the effects of management associated with forest disturbances on runoff could be evaluated before policies are enacted, so that desired future conditions may be reached with minimal negative streamflow consequences. It should be noted, however, that relationships between frozen soil and snowmelt infiltration, along with groundwater recession and baseflow maintenance still require refinement.

Table 14. *TCSWAT calibration statistics compared to published studies.*

		Area	*Calibration Period*		*Validation Period*	
Reference	**Location**	**(sq. km)**	**NSm**	**NSd**	**NSm**	**NSd**
Cao et al. (2006)	New Zealand	2,075		0.78		0.72
Eckhardt and Arnold (2001)	Germany	81		0.70		0.73
Eckhardt et al. (2002)	Germany	81		0.76		0.81
Muleta and Nicklow (2006)	IL, USA	133		0.74		
Arabi et al. (2006)	IA, USA	6	0.84		0.73	
		7	0.73		0.63	
Fontaine et al. (2002)	WY, USA	4,999	0.86			
Santhi et al. (2001)	TX, USA	926	0.79		0.87	
		2,997	0.83		0.62	
Srinivasan et al. (1998)	TX, USA	238	0.84		0.82	
White and Chaubey (2005)	AR, USA	362	0.89		0.85	
		684	0.89		0.72	
		1,020	0.86		0.87	
Jha et al. (2006)	IL, USA	447,500	0.69	0.58	0.81	0.65
Van Liew and Garbrecht (2003)	OK, USA	160	0.75	0.60	0.83	0.71
Wang and Melesse (2005)	MN, USA	2,419	0.86	0.64	0.90	0.62
		4,040	0.86	0.67	0.83	0.50
Wang and Melesse (2006)	MN, USA	515	0.88	0.51	0.50	0.31
		515	0.92	0.49	0.49	0.26
Wu and Xu (2006)	LA, USA	3,435	0.93	0.92	0.85	0.78
		662	0.94	0.90	0.81	0.71
		1,682	0.96	0.83	0.87	0.69
NSd = daily	min	6	0.69	0.49	0.49	0.26
NSm = monthly	**TCSWAT**	**22.5**	**0.90**	**0.86**	**0.90**	**0.76**
	max	447,500	0.96	0.92	0.90	0.81

RECOMMENDATIONS

While the existing model produces acceptable results, the assumption that there is no infiltration in frozen soils means that the model does not properly represent the snowmelt infiltration and runoff process. In addition, the model does not perform well during baseflow periods. Refinement of the model components representing snowmelt infiltration and runoff and groundwater discharge during baseflow would further improve model performance and the physical representation of hydrologic processes within this and similar Rocky Mountain watersheds. Model calibration using the auto-calibration procedures in SWAT could also be improved by incorporating multiple objective functions to simultaneously calibrate the three major components of the annual streamflow hydrograph; the runoff, recession, and baseflow periods.

LITERATURE CITED

Alt, D. and D.W. Hyndman. 1986. Roadside Geology of Montana. Mountain Press, Missoula, MT.

Anderson, J.R., E.E. Hardy, J.T. Roach, and R.E. Witmer. 1976. A land use and land cover classification system for use with remote sensor data. Geological Survey Professional Paper 964. U.S. Government Printing Office, Washington, D.C.

Arabi, M., R.S. Govindaraju, M.M Hantush, and B.A. Engel. 2006. Role of watershed subdivision on modeling the effectiveness of best management practices with SWAT. Journal of the American Water Resources Association 42(2): 513-528.

Arno, S.F. and C.E. Fiedler. 2005. Mimicking Nature's Fire: Restoring Fire-Prone Forests in the West. Island Press, Washington, D.C.

Arnold, J.G. and P.M. Allen. 1999. Automated methods for estimating baseflow and groundwater recharge from streamflow records. Journal of the American Water Resources Association 35(2):411-424.

Arnold, J.G., P.M. Allen, and G. Bernhardt. 1993. A comprehensive surface-groundwater flow model. Journal of Hydrology 142(1-4): 47-69.

Arnold, J.G., P.M. Allen, R. Muttia, and G. Bernhardt. 1995. Automated base flow separation and recession analysis techniques. Ground Water 33(6): 1010-1018.

Arnold, J.G. and N. Fohrer. 2005. SWAT2000: Current Capabilities and Research Opportunities in Applied Watershed Modeling. Hydrological Processes 19(3): 563-572.

Arnold, J.G., R. Srinivasan, R. Muttiah, and J.R. Williams. 1998. Large Area Hydrologic Modeling and Assessment Part I: Model Development. Journal of the American Water Resources Association 34(1): 73-89.

ASCE, 1993. Criteria for evaluation of watershed models. Journal of Irrigation and Drainage Engineering 119(3): 429-442.

Barrett, S.W. 1993. Fire History of Tenderfoot Creek Experimental Forest, Lewis and Clark National Forest. Systems for Environmental Management, Research Joint Venture Agreement No. INT-92679-RJVA.

Bingner, R.L., J. Garbrecht, J.G. Arnold, and R. Srinivasan. 1997. Effect of watershed subdivision on simulation runoff and fine sediment yield. Transactions of the ASAE 40(5): 1329-1335.

Binns, N.A. and F.A. Eiserman. 1979. Quantification of fluvial trout habitat in Wyoming. Transactions of the American Fisheries Society 108:215–228.

Bosch, J.M. and J.D. Hewlett. 1982. A review of catchment experiments to determine the effect of vegetation changes on water yield and evapotranspiration. Journal of Hydrology 55: 3-23.

Cao, W., W.B. Bowden, T. Davie, and A. Fenemor. 2006. Multi-variable and multi-site calibration and dalidation of SWAT in a large mountainous catchment with high spatial variability. Hydrological Processes 20: 1057-1073.

Coffey, M.E., J.L. Workman, A.W. Taraba, and A. W. Fogel. 2004. Statistical procedures for evaluating daily and monthly hydrologic model predictions. Transactions of the ASCE 47(1): 59-68.

Crawford, N.H. and R.S. Linsley. 1966. Digital Simulation in Hydrology: Stanford Watershed Model IV, Stanford Univ., Dept. Civ. Eng. Palo Alto, CA. Technical Report 39.

Di Luzio, M., J.G. Arnold, and R. Srinivasan. 2005. Effect of GIS data quality on small watershed stream flow and sediment simulations. Hydrological Processes 19(3): 629-650.

Di Luzio, M., R. Srinivasan, and J.G. Arnold. 2002. Integration of Watershed Tools and SWAT model into BASINS. Journal of the American Water Resources Association 38(4): 1127-1141.

Di Luzio, M., R. Srinivasan, and J.G. Arnold. 2004. A GIS-coupled hydrological model system for the watershed assessment of agricultural nonpoint and point sources of pollution. Transactions in GIS 8(1): 113-136.

Draper, N.R. and H. Smith. 1981. Applied Regression Analysis. 2nd Edn., John Wiley and Sons, New York. 709 pp.

Duan, Q., S. Sorooshian, and V. Gupta. 1992.Effective and efficient global optimization for conceptual rainfall-runoff models. Water Resources Research 28(4): 1015-1031.

Duan, Q., S. Sorooshian, and V. Gupta. 1994. Optimal use of the SCE-UA global optimization method for calibrating watershed models. Journal of Hydrology 158(3-4): 265-284.

Eckhardt, K. and J.G. Arnold. 2001. Automatic calibration of a distributed catchment model. Journal of Hydrology 251(1-2): 103-109.

Eckhardt, K., S. Haverkamp, N. Fohrer, Frede, H.G. 2003. SWAT-G, a version of SWAT99.2 modified for application to low mountain range catchments. Physics and Chemistry of the Earth 27(9-10): 641-644.

Farnes, P.E. and W.W. McCaughey. 1995. Hydrologic and geologic characterization of Tenderfoot Creek Experimental Forest, Montana. Unpublished Report. U.S. Department of Agriculture, Forest Service, Rocky Mountain Research Station, Forestry Sciences Laboratory, Bozeman, MT. 200 pp.

Fontaine, T.A., T.S. Cruickshank, J.G. Arnold, and R.H. Hotchkiss. 2002. Development of a snowfall-snowmelt routine for mountainous terrain for the soil water assessment tool (SWAT). Journal of Hydrology 262(1-4): 209-223.

Gassman, P.W., M.R. Reyes, C.H. Green, and J.G. Arnold. 2005. Review of peer-reviewed literature on the SWAT model. in: R. Srinivasan, J. Jacobs, D. Day, and K. Abbaspour. Proceedings of the 3rd International SWAT Conference Zurich, Switzerland: Swiss Federal Institute for Environmental Science and Technology (EAWAG) 1-8.

Gesch, D., M. Oimoen, S. Greenlee, C. Nelson, M. Steuck, and D. Tyler. 2002. The National Elevation Dataset. Photogrammetric Engineering and Remote Sensing 68(1): 5-11.

Golding, D.L. and R.H. Swanson. 1978. Snow accumulation and melt in small forest openings in Alberta. Canadian Journal of Forest Research 8(4): 380-388.

Gray, D.M., B. Toth, L. Zhao, J.W. Pomeroy and R.J. Granger. 2001. Estimating areal snowmelt infiltration into frozen soils. Hydrological Processes 15: 3095-3111.

Green, W.H. and G.A. Ampt. 1911. Studies on soil physics, 1. The flow of air and water through soils. Journal of Agricultural Sciences 4: 11-24.

Gupta, H.V., S. Sorooshian, and P.O. Yapo. 1998. Toward improved calibration of hydrologic models: Multiple and noncommensurable measures of information. Water Resources Research 34(4): 751-764.

Hall, R.J., D.P. Davidson, and D.R. Peddle. 2003. Ground and remote estimation of leaf area index in Rocky Mountain forest stands, Kananaskis, Alberta. Canadian Journal of Remote Sensing 29(3): 411-427.

Hargreaves, G.L., G.H. Hargreaves, and J.P. Riley. 1985. Agricultural benefits for Senegal River Basin. Journal of Irrigation and Drainage Engineering 111(2): 113-124.

Haverkamp, S., R. Srinivasan, H.G. Frede, and C. Santhi. 2002. Subwatershed Spatial Analysis Tool: Discritization of a Distributed Hydrologic Model by Statistical Criteria. Journal of the American Water Resources Association 38(6): 1723-1733.

Hay, L.E., G.H. Leavesley, M.P. Clark, S.L. Markstrom, R.J. Viger, and M. Umemoto. 2006. Step wise, multiple objective calibration of a hydrologic model for a snowmelt dominated basin. Journal of the American Water Resources Association 42(4): 877-890.

Holsinger, L., R.E. Keane, R. Parsons, and E. Karau. 2005. Development of Biophysical Gradient layers. *In:* Rollins, M.G.; Frame, C.K., tech. eds. 2006. The LANDFIRE Prototype Project: nationally consistent and locally relevant geospatial data for wildland fire management. Gen. Tech. Rep. RMRS-GTR-175 U.S. Department of Agriculture, Forest Service, Rocky Mountain Research Station. Fort Collins, CO.

Jakeman, A.J. and R.A. Lechter. 2003. Integrated assessment and modelling: features, principles and examples for catchment management. Environmental Modelling & Software 18(6): 491-501.

Jayakrishnan, R., R. Srinivasan, C. Santhi, J.G. Arnold. 2005. Advances in the application of the SWAT model for water resources management. Hydrological Processes 19(3): 749-762.

Jha, M., J.G. Arnold, P.W. Gassman, F.Giorgi, and R.R. Gu. 2006. Climate Change Sensitivity Assessment on Upper Mississippi River Basin Streamflows Using Swat. Journal of the American Water Resources Association 42(4): 997-1015.

Jha, M., Z. Pan, E. Takle, and R. Gu. 2004. Impact of climate change on streamflow in the upper Mississippi River Basin: a regional climate model perspective. Journal of Geophysical Research 109 1-12 (doi:10.1029/2003JD003686).

King, K.W. and J.C. Balogh. 2001. Water quality impacts associated with converting Farmland and forests to turfgrass. Transactions of ASCE 44(3): 569-576.

Kirsch, K.J. and A.E. Kirsch, 2001. Using SWAT to predict erosion and phosphorous Loads in the Rock River Basin, Wisconsin. ASAE 701P0007, ASAE St. Joseph, Michigan. p. 54-57.

Kosnik, K.E. 1995. Continentality and the snowpack density distribution in the western United States. Proceedings 63rd Western Snow Conference. p. 66-77.

Leavesley, G.H., R.W. Litchey, M.M. Troutman, and L.G. Saindon, 1983. Precipitation-Runoff Modeling System: User's Manual. U.S. Geological Survey Water-Resources Investigations Report 83-4238. 207 pp.

Leonard, R.A., W.G. Knisel, and D.A. Still. 1987. Gleams: Groundwater loading effects on agricultural management systems. Trans. ASAE 30(5): 1403-1428.

Lowman, M.D. and N.M. Nadkarni. 1995. Forest Canopies. Academic Press, San Diego.

Maidment, D.R. 1993. Handbook of Hydrology. McGraw- Hill, New York.

Mangurerra, H.B. and B.A. Engel. 1998. Hydrologic parameterization of watersheds for runoff prediction using SWAT. Journal of the American Water Resources Association 34(5): 1149-1162.

McCaughey, W.W. 1996. Tenderfoot Creek Experimental Forest. *In* Experimental forests, ranges, and watersheds in the Northern Rocky Mountains: A compendium of outdoor laboratories in Utah, Idaho, and Montana. W.C. Schmidt and J.L. Friede, Compilers. U.S. Department of Agriculture, Forest Service, Gen. Tech. Rep. INT-GTR-334. p. 101-108.

McCaughey, W.W. and P.E. Farnes. 2001. Snowpack comparison between an opening and a lodgepole stand. Proceedings 69th Western Snow Conference. p. 59-64.

Monteith, J.L., 1965. Evapotranspiration and the environment. p. 205-234. *In* The state and movement of water in living organisms. 19th Symposia of the Society for Experimental Biology. Cambridge University Press, London.

Moore, C.A. and W.W. McCaughey. 1997. Snow Accumulation under various forest stands densities at Tenderfoot Creek Experimental Forest, Montana, USA. Proceedings 66th Western Snow Conference. p. 42-51.

Motovilov, Y.G., L. Gottschalk, K. Engeland, and A. Rodhe. 1999. Validation of a distributed hydrological model against spatial observations. Agricultural and Forest Meteorology 98-99: 257-277.

Muleta, M.K. and J.W. Nicklow. 2005. Sensitivity and uncertainty analysis coupled with automatic calibration for a distributed watershed model. Journal of Hydrology 306(1-4): 127-145.

Nash, J.E. and J.V. Sutcliffe. 1970. River flow forecasting through conceptual model part 1 - A discussion of principles. Journal of Hydrology 10(3): 282-290.

Neitsch, S.L., J.G Arnold, J.R Kiniry, J.R Williams, and K.W. King. 2002. Soil and Water Assessment Tool Theoretical Documentation, Version 2000. Texas Water Resources Institute, College Station, Texas, TWRI Report TR-191, GSWRL Report 02-01, BRC Report 02-05.

Oliver, C.D. and B.C. Larson, 1990. Forest Stand Dynamics. McGraw-Hill, New York.

Pomeroy, J.W. and E. Burn. 2001. Physical Properties of Snow. *In* Snow Ecology: An Interdisciplinary Examination of Snow-Covered Ecosystems. Jones H., J.W. Pomeroy, D.A. Walker, and R.W. Hoham, Eds. Cambridge University Press, London.

Pomeroy, J.W., D.M. Gray, N.R. Hedstrom, and J.R. Janowicz. 2002. Prediction of seasonal snow accumulation in cold climate forests. Hydrological Processes 16(18): 3543-3558.

Popov, E.G. 1972. Snowmelt runoff forecasts – theoretical problems. In: The Role of Ice and Snow in Hydrology, Proceedings Banff Symposium, Vol. 2 UNESCO-WMO-IASH, 829-839.

Priestley, C.H.B. and R.J. Taylor. 1972. On the assessment of surface heat flux and evapotranspiration using large-scale parameters. Mon. Weather Rev. 100: 81-92.

Redmond, R.L., C. Winne, and C. Fisher. 2001. Existing Vegetation and Landcover of West-Central Montana. Final Scene Reports Submitted to U.S. Department of Agriculture, Forest Service, Northern Regional Office, Missoula, MT, USA.

Roberge, J. and A.P. Plamondon. 1987. Snowmelt runoff pathways in a boreal forest hillslope, the role of pipe throughflow. Journal of Hydrology 95: 39-54.

Santhi, C., J.G. Arnold, J.R. Williams, W.A. Dugas, R. Srinivasan, and L.M. Hauck. 2001a. Validation of the SWAT model on a large river basin with point and non-point sources. Journal of the American Water Resources Association 37(5): 1169-1187.

Santhi, C., J.G. Arnold, J.R. Williams, L.M. Hauck, and W.A. Dugas. 2001b. Application of a watershed model to evaluate management effects on point and nonpoint source pollution. Transactions of ASCE 44(6): 1559-1570.

Sappington, J. 2005. Snow accumulation and snowmelt in thinned lodgepole pine stands, west central Montana. M.S. Thesis. The University of Montana. 54 pp.

Singh, V.P. 1995. Computer Models of Watershed Hydrology. Water Resources Publications, Highlands Ranch, CO.

Sloto, R.A. and M.Y. Crouse. 1996. HYSEP: A Computer Program for Streamflow Separation and Analysis. U.S. Geological Survey -Water Resources Investigations Report 96-4040.

Srinivasan, R. and J.G. Arnold. 1994. Integration of a basin-scale water quality model with GIS. Water Resources Bulletin 30(33): 453-462.

Srinivasan, R., T.S. Ramanarayanan, J.G. Arnold, and S.T. Bednarz. 1998. Large Area Hydrologic Modeling and Assessment Part II: Model Application. Journal of the American Water Resources Association 34(1): 91-101.

Stadler, D., H. Wunderli, A. Auckenthaler and H. Flühler. 1996. Measurement of frost-induced snowmelt runoff in a forest soil. Hydrological Processes 10: 1293-1304.Stednick, J.D. 1996. Monitoring the effects of timber harvest on annual water yield. Journal of Hydrology 176: 79-95.

Stednick, J.D. 1996. Monitoring the Effects of Timber Harvest on Annual Water Yield. Journal of Hydrology 176:79-95.

Tennant, D.L. 1976. Instream flow regimens for fish, wildlife, recreation and related environmental resources. Fisheries 1: 6-10.

Troendle, C.A. 1983. The Potential for water yield augmentation from forest management in the Rocky Mountains. Water Resources Bulletin 19(3): 359-373.

Troendle, C.A. and R.M. King. 1985. The effect of timber harvesting on the Fool Creek watershed, 30 years later. Water Resources Research 21(12):1915-1922.

Troendle, C.A. and R.M. King. 1987. The effect of partial and clearcutting on streamflow at Deadhorse Creek, Colorado. Journal of Hydrology 90(1/2):145-157.

USDA-NRCS (U.S. Department of Agriculture, Natural Resource Conservation Service). 1994. State Soil Geographic Data base (STATSGO): Data Use Information. U.S. Department of Agriculture, National Soil Survey Center, Miscellaneous Publication Number 1492. 113 pp.

USDA-NRCS (U.S. Department of Agriculture, Natural Resource Conservation Service). 1996. National soil survey handbook, title 430-VI. U.S. Government Printing Office, Washington, D.C.

USDA-SCS (U.S. Department of Agriculture, Soil Conservation Service), 1972. SCS National Engineering Handbook, Section 4, Hydrology. Chapter 10, Estimation of Direct Runoff from Storm Rainfall. U.S. Department of Agriculture, Soil Conservation Service, Washington D.C. p. 10.1-10.24.

USDI-GS, (U.S. Department of the Interior, Geological Survey) 2005. MODIS/Terra Leaf Area Index/FPAR 8-day L4 Global 1km ISIN Grid. United States Geological Survey, Center for Earth Observation and Science (EROS), 47914 252nd Street, Sioux Falls, SD 57198-0001. Available for download at: http://LPDACC.usgs.gov

van Griensven, A. and W. Bauwens. 2003. Multiobjective autocalibration for semidistributed water quality models. Water Resources Research 39(12): 1348.

van Griensven, A., A. Francos, and W. Bauwens. 2002. Sensitivity analysis and auto-calibration of an integral dynamic model for river water quality. Water Science Technology 45(9): 325-32.

van Griensven, A., T. Meixner, S. Grunwald, T. Bishop, M. Di Luzio, and R. Srinivasan. 2006. A global sensitivity analysis tool for the parameters of multi-variable catchment models. Journal of Hydrology 324(1-4): 10-23.

Van Liew, M.W., J. Garbrecht. 2003. Hydrologic Simulation of the Little Washita River Experimental Watershed Using SWAT. Journal of the American Water Resources Association 39(2): 413-426.

Wang, X. and A.M. Melesse. 2005. Evaluation of the SWAT model's snowmelt hydrology in a northwestern Minnesota watershed. Transactions of the ASAE 48(4): 1359-1376.

Wang, X. and A.M. Melesse. 2006. Effects of STATSGO and SSURGO as inputs on SWAT model's snowmelt simulation. Journal of the American Water Resources Association 42(5):1217-1236.

Waring, R.H. and S.W. Running. 1998. Forest Ecosystems: Analysis at Multiple Scales. Academic Press, San Diego.

White, K.L. and I. Chaubey. 2005. Sensitivity Analysis, Calibration, and Validations for a Multisite and Multivariable SWAT Model. Journal of the American Water Resources Association 41(5): 1077-1089.

White, J.D., S.W. Running, R. Nemani, R.E. Keane, and K.C.Ryan. 1997. Measurement and remote sensing of LAI in Rocky Mountain montane ecosystems. Canadian Journal of Forest Research 27: 1714-1727.

Williams, J.R., A.D. Nicks, and J.G. Arnold. 1985. Simulator for water resources in rural basins. Journal of Hydraulic Engineering 111(6): 970-986.

Woods, S.W., R. Ahl, J. Sappington, and W. McCaughey. 2006. Snow Accumulation in thinned lodgepole pine stands, Montana, USA. Forest Ecology and Management 235: 202 – 211.

Woods, S.W., W.W. McCaughey, R. Ahl, and J. Sappington. 2004. Effect of alternative sivilcultural treatments on snow accumulation in lodgepole pine stands, Montana, U.S.A. Proceedings 72nd Western Snow Conference. p. 65-73.

Wu, K., Y.J. Xu. 2006. Evaluation of the Applicability of the SWAT Model for Coastal Watersheds in Southern Louisiana. Journal of the American Water Resources Association 42(5): 1247-1260.

Yapo, P.O., H.V. Gupta, and S. Sorooshian. 1998. Multi-Objective Global optimization for hydrologic models. Journal of Hydrology 204: 83-97.

Zhao, L. and D.M. Gray. 1999. Estimating snowmelt infiltration into forest soils. Hydrological Processes 13: 1827-1842.

CHAPTER 3

Simulating Long-Term Landcover Change and Forest Hydrology Dynamics in a Rocky Mountain Watershed

ABSTRACT

Snow is the dominant source of water in the Rocky Mountains. In forested watersheds, patterns of snow accumulation, melt and evapotranspiration are strongly influenced by canopy and other vegetation characteristics. Changes in the extent, composition, and configuration of the forest canopy over time due to succession or disturbance processes can lead to measurable changes in streamflow and water yield. Removal of forest cover generally increases streamflow due to reduced canopy interception and evapotranspiration. Water, yield increases and advanced peak discharge are attributed to increased snow accumulation, and enhanced melt rates in forest openings. Because knowledge of long-term watershed-level streamflow responses to landcover dynamics is limited by relatively short-term gauge data, a modeling approach that takes advantage of existing data and combines vegetation and hydrologic simulation systems to evaluate these interactions is presented. Results of this study suggest that both vegetation and hydrologic characteristics of the research watershed are at the limits of their estimated natural ranges. Although simulated species composition remained fairly stable over time, the size and connectivity of current landcover patches are at the upper end of their estimated temporal distribution. The large proportion and continuous extent of forest cover associated with current conditions coincide with water yield, peak discharge rates, and flow variability that are at the low end of their modeled distributions. The integrated modeling approach described herein should be applicable in other ecosystems given knowledge of biophysical interactions and availability of appropriate data. By gaining an understanding of the possible range of variability due to natural conditions, management plans may be designed to maintain resources within estimated and desirable bounds.

INTRODUCTION

Vegetation characteristics are one of the key factors affecting the amount and timing of runoff from forested mountain watersheds. The forest canopy moderates the precipitation-infiltration-runoff continuum by influencing interception, deposition, and evapotranspiration, while also providing insulation from incident solar radiation and wind scour (Kimmins, 1997). Timber harvest can result in increased streamflow due to the reduction in canopy interception and evapotranspiration in clearcuts and stands with reduced density (Golding and Swanson, 1978; Troendle, 1983; Troendle and King, 1985; Troendle and King, 1987; Pomeroy et al., 2002). Similarly, natural disturbance mechanisms such as fire, insects, and disease affect basin-wide runoff and water yield by periodically thinning or creating openings in the forest canopy (Bosch and Hewlett, 1982; Troendle, 1983; Stednick, 1996; Troendle 1983). A reduction in the frequency of natural disturbance events due to human intervention or climatic variability may lead to denser stands and an increase in forest area, with a consequent decline in watershed runoff (Farnes et al., 2000). While the hydrologic effects of forest harvest have been widely studied, very little work has been done to determine how natural disturbance processes, and human influences on those processes, may affect the magnitude and the range of variability in runoff and water yield from forested watersheds.

Fire is the primary natural disturbance agent in the Rocky Mountains of western North America (Arno and Fiedler, 2005). Since the early 1930s, fire suppression programs in the United States and Canada have attempted to curtail the occurrence of fire in the region, and evidence suggests that there has been a concurrent increase in the extent, continuity, and density of forested stands, and an invasion of shrubs and trees into grasslands (Keane et al., 2002). Presumably, these changes in the disturbance regime and associated change in vegetation characteristics have affected watershed runoff.

Evaluating the effect of changes in forest structure on runoff and water yield requires understanding of the natural range of variability in vegetation conditions and hydrologic response. However, even the longest streamflow records are shorter than the 100-400 year natural fire return intervals in the region's high elevation forests, and there are no streamflow records from the period prior to European settlement. Evaluating the

natural range of variability in watershed runoff from forested watersheds in the Rocky Mountain region therefore depends on the use of models capable of simulating conditions at time scales of many hundreds of years. In this paper, a modeling approach that uses a 300-year simulation of vegetation dynamics to provide time-series landcover data for a watershed scale hydrologic simulation model is introduced. This method is used to compare the current hydrologic response of a forested, snowmelt dominated, Rocky Mountain watershed to the range of variability that would occur given an unmanaged long-term vegetation scenario that encompasses the region's approximate 100-400 yr. fire cycle (Arno and Fiedler, 2005).

Vegetation dynamics were modeled with SIMPPLLE (Simulating Patterns and Processes at Landscape Scales). SIMPPLLE is a regionally calibrated vegetation dynamics simulation system that models the long-term impact of landscape management over large areas (Chew et al., 2004) at annual or decadal time-steps. SIMPPLLE integrates data from a diversity of sources. Vegetation is defined by stand-level inventory data whenever possible, but algorithms have been developed to extract the necessary information from classified satellite imagery when full coverage is otherwise not available. Management logic, environmental conditions, and physiognomic data (Pfister et al., 1977) in combination with dominant stand species, size class, and canopy density are used to advance vegetation through calibrated pathways with conditional probabilities to simulate succession, and natural or planned disturbances over periods of up to 500 years (Chew et al., 2002). Depending on ecosystem properties and project needs, the model can advance vegetation at annual or decadal time steps. Simulations derived from SIMPPLLE are presently being used by the Northern Region of the USDA Forest Service to assess forest management alternatives (Barrett, 2001).

Watersheds boundaries provide logical landscape divisions for natural resource assessment, but analyses based on SIMPPLE indicate that natural processes influence the character and distribution of vegetation at scales that are larger than individual watersheds. Forest fires, destructive insect, and to a lesser extent disease outbreaks generally span multiple watersheds, and to capture the full range of occurrences, a watershed must be considered in the context of its surrounding landscape. Recognizing this connection allows important processes to occur and propagate across the landscape,

providing a more realistic representation of natural dynamics than when a watershed is analyzed in isolation. When forest cover is continuous, a landscape perspective is especially important because fire and insects damage can readily spread across connected patches. Vegetation dynamics were therefore simulated at the landscape scale, and subsequently analyzed at the watershed level.

Hydrologic modeling was conducted using the Soil and Water Assessment Tool (SWAT), a physically based, distributed, continuous, river basin model developed to predict the impact of land management practices on hydrologic processes in potentially large, complex watersheds with varying soils, landcover and management practices (Arnold et al., 1998; Srinivasan et al., 1998; Di Luzio et al., 2004). The model runs on a daily time step, and the hydrologic processes mimicked by the model include snow accumulation and melt, interception, evapotranspiration, surface runoff, soil percolation, lateral and groundwater flow, and river routing. Model configuration is achieved with topographic, soil, landcover and climate data available from government agencies worldwide, although more detailed information can also be included. The model partitions a watershed into sub-watersheds, river reaches and hydrologic response units (HRUs). Sub-watershed delineation provides the spatial context, while further sub-division into HRUs is based on threshold proportions of mapped landcover and soil types within sub-watersheds, without regard to their topologic arrangement (Neitsch et. al., 2002).

SWAT is often used to study the impact of land management on watershed processes. This type of assessment is traditionally accomplished by altering management or landuse practices associated with mapped landcover patterns. In this study, the approach is rather different. First, landuse is defined as natural seasonal plant development. Second, rather than prescribing changes in management to a static HRU configuration, changing patterns of landcover are supplied over time by an independent vegetation simulator. Landcover patterns, driven by ecological biophysical interactions, are updated on a decadal basis, and new HRUs are reconfigured with each change. Using this method, basin-wide hydrologic responses to the changing diversity of landcover patterns can be accounted for. With appropriately scaled subdivision, the spatial distribution of watershed processes can be assessed as well.

Focusing on the headwaters of Tenderfoot Creek, located at the core of the Little Belt Mountains of central Montana, the interaction between changing landcover patterns due to natural ecological processes, and watershed streamflow response was studied with a two-tiered approach. The SIMPPLLE model was used to project current vegetation conditions forward for 300 years, across the Little Belt Mountain landscape. At a decadal time-step, simulated vegetation characteristics were converted into raster-based maps of generalized landcover categories, and extracted for the research watershed. Time-series maps produced by SIMPPLE simulations were used to drive the land-phase of the SWAT hydrologic model for the Tenderfoot Creek research watershed. Patterns of predicted landcover proportions, configuration, and associated streamflow responses were analyzed and compared to current conditions.

Application of this procedure provides a means for establishing the range of probable watershed conditions and places the current conditions in the context of possible conditions over time. With sufficient data and ecological understanding, this approach should also be applicable in other biomes. By gaining an understanding of the possible range of variability due to natural conditions, management plans may be designed to maintain resources, especially water flow, within desirable bounds.

METHODS

STUDY AREA DESCRIPTION

Vegetation dynamics were simulated across 376,450 ha of the Little Belt Mountain landscape in central Montana (Figure 1). To map current landcover conditions scaled, multi-attribute classification (SMAC) logic was applied to the descriptions of existing stands that were used to parameterize the SIMPPLE model (Appendix A).

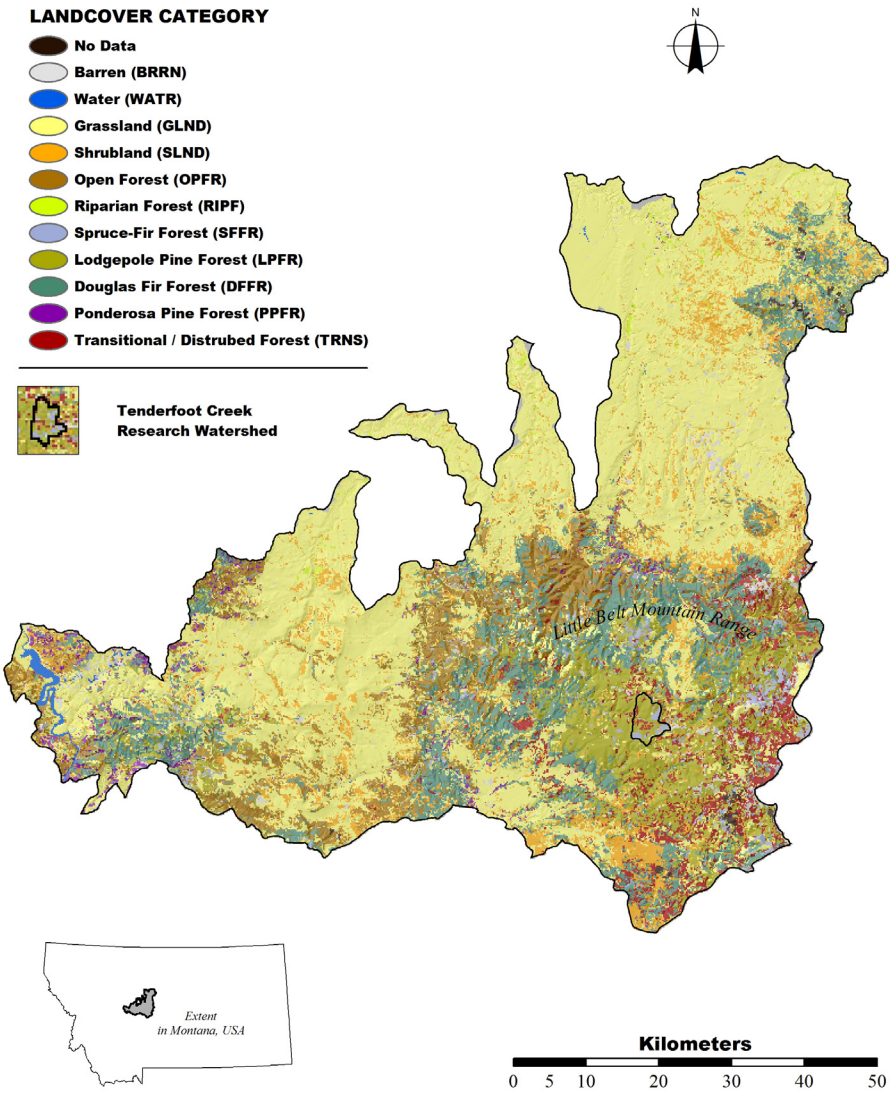

Figure 1. *Geographic extent of vegetation simulations encompassing the Little Belt Mountain Range of central Montana, USA, and Tenderfoot Creek research watershed.*

The Tenderfoot Creek research watershed lies within the Tenderfoot Creek Experimental Forest (McCaughey, 1996), on the west slope of the Little Belt Mountains in central Montana, USA (Figures 2). This broad basin-like watershed is oriented to the northwest, and bisected by a steep canyon along the main channel. An upper reach and two major tributaries on each north and south aspects make up the 2,251 ha that contribute flow to the main outlet.

The watershed is underlain by Precambrian age sedimentary rocks of the Belt Supergroup (Alt and Hyndman, 1986). Soils are characteristic of cool, moist environments, and the most extensive groups are loamy skeletal, mixed Typic Cryochrepts and clayey, mixed Aquic Cryoboralfs (Farnes and McCaughey, 1995).

Several large (800 to 1,500 ha) fires have occurred in the watershed over the past four centuries but nearly 120 years have elapsed since the last major stand replacing fire (Barrett, 1993). Forest stands of varying developmental stages presently cover 85% of the watershed. Approximately 65% of the watershed is composed of lodgepole pine (*Pinus contorta*), which generally represent the most recently initiated stands. Over time, shade tolerant subalpine fir (*Abies lasiocarpa*) and Englemann spruce (*Picea engelmannii*) emerge underneath decadent pine and now make up about 20% of the landcover. Decadent, low density and disturbed stands constitute another 11% of the watershed. The remaining 4% of the watershed consists of shrubby meadows and small riparian areas along creek bottoms (1%), drier grasses on higher ground (1%) and talus slopes (2%).

Climate patterns are continental, and almost 70% of the 800mm mean annual precipitation is deposited as snow between October and April. The annual peak discharge is driven by snowmelt and occurs between mid-May and early June, while the low flow period begins in August and persists through April. Annually, the mean water yield from the research watershed is approximately 400 mm.

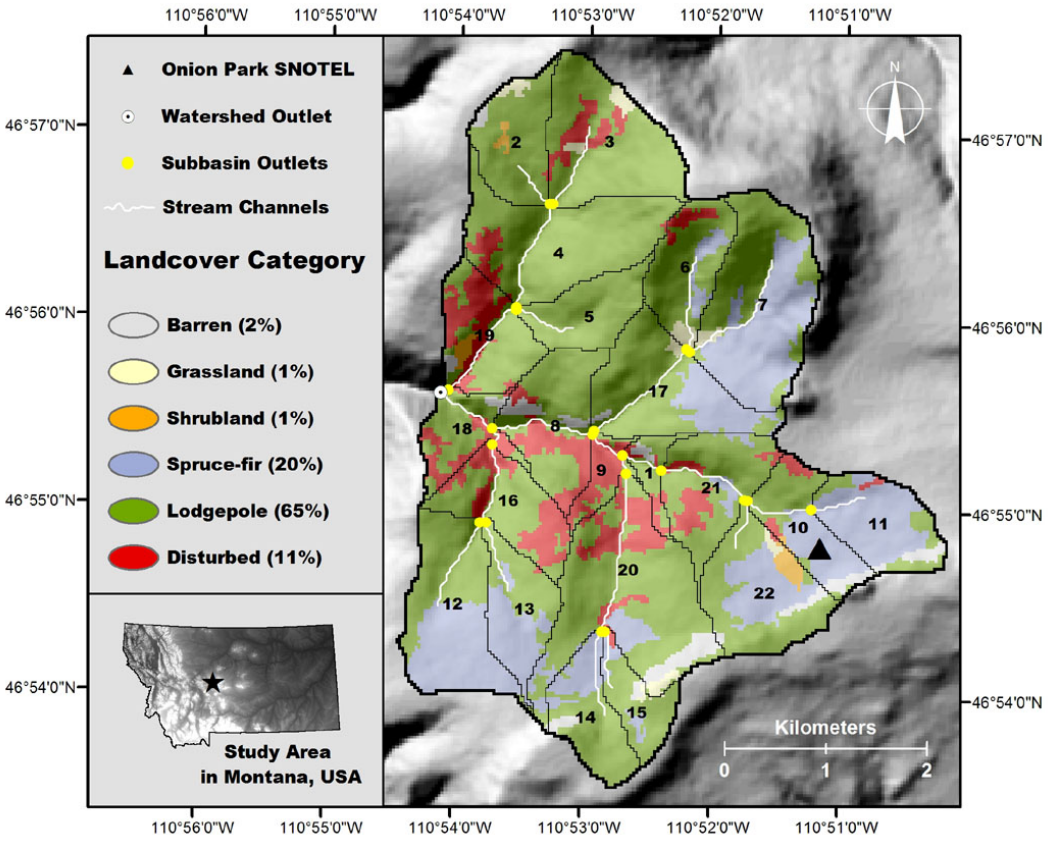

Figure 2. *Delineation, configuration, and landcover characteristics of the Tenderfoot Creek research watershed, located in the Little Belt Mountains of central Montana, USA.*

LANDCOVER SIMULATION

The SIMPPLLE model has the capability to simulate both managed and unmanaged vegetation dynamics. Since the goal of the study was to determine the range of variability in the absence of human disturbance, the model was run forward in time once for 300 years at decadal time steps, assuming an unmanaged scenario and starting with the current landscape cover characteristics.

To parameterize SIMPPLLE, forest inventory information, satellite imagery, spatial and statistical modeling are used to provide Habitat Type, dominant species, size class, and canopy density descriptions for every stand. The model then uses biophysical input data, user-specified logic, and conditional probabilities to stochastically advance each stand in the landscape through states of succession and disturbance processes at the

time-step of the model. Because state advancement is probabilistic, multiple simulations can be initiated to capture the potential range of vegetation characteristics over time. Zuuring and Sweet (2000) have shown that output from 30 to 100 iterations tends to be normally distributed and can be described with parametric methods (Ott, 1993). This suggests that a single long-term simulation could produce a similar range of conditions as multiple runs over shorted time periods. Running a simulation that produced 30 iterations of landcover patterns should therefore produce a set of conditions that approaches their probable range.

The simulation encompassed the entire Little Belt mountain range so that disturbance process propagation into the research watershed from the surrounding landscape was accounted for. To capture the ecological processes simulated by SIMPPLE, and translate them into data that could be mapped, analyzed, and used for hydrologic modeling, vegetation characteristics predicted for each stand were reclassified with an algorithm that automated the SMAC logic used to describe the current landscape condition. The SMAC algorithm produced raster-based maps with 30 m pixel resolution that represent vegetation as generalized landcover at every time-step of the model (Figure 3). The classes produced by the algorithm closely resemble the Level II landcover categories developed by the United States Geological Survey (Anderson et al., 1976), but have been refined to include more detailed differentiation among forest types.

After reclassification, data overlaying the research watershed were extracted from each of the time-series landcover depictions. The landcover map representing current watershed conditions included barren ground, grassland, shrubland, spruce-fir forest, lodgepole pine forest, and disturbed forest (Figure 2). Over time, succession process modeled by SIMPPLE predicted the emergence of quaking aspen, and Douglas fir stands would occupy roughly 3% of the watershed.

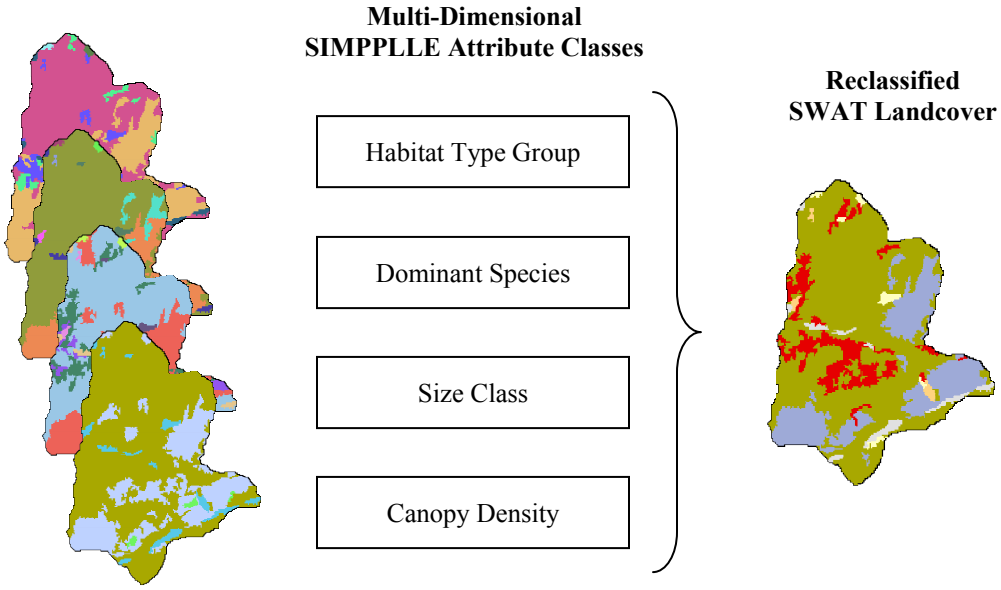

Figure 3. *A diagram of the reclassification algorithm used to convert multi-dimensional stand attributes produced by the SIMPPLLE vegetation simulator into generalized landcover categories.*

Each landcover category was attributed with regionally estimated maximum canopy height (HT; m), seasonal effective maximum and minimum leaf area index (LAI; m^2/m^2) derived through remote sensing (Hall et al., 2003), relative annual interception capacity based on field measurements (Moore and McCaughey, 1997; McCaughey and Farnes, 2001; Woods et al., 2004, 2006), base temperature (°C) for the onset of productivity, Manning's roughness coefficient (OVN) for overland flow (Neitsch et al., 2002), and SCS curve numbers (CN2B) for soil hydrologic group B with level II moisture condition (USDA-SCS, 1972), for use in hydrologic modeling (Table 1).

Table 1. *Landcover characteristics of the Tenderfoot Creek research watershed.*

Landcover	Max HT (m)	Max LAI	Min LAI	Int. (%)	Base T °C	OVN	CN2B
Barren	0	0	0	0	0	0.10	96
Grassland	0.75	1.50	0.75	3	10	0.12	70
Shrubland	3.50	2.00	1.00	5	10	0.13	65
Aspen	15	2.00	1.00	15	10	0.15	64
Lodgepole	22	2.80	1.80	25	3	0.16	58
Douglas fir	35	3.10	2.00	25	3	0.15	58
Spruce-fir	26	3.0	1.95	28	3	0.17	55
Disturbed	10	2.0	1.00	10	3	0.14	69

EVALUATION OF SIMULATED LANDCOVER

The categorical relative watershed distribution and spatial pattern of simulated landcover was quantified for each of the 30 reclassified time-series maps, and compared to that of the current mosaic. These evaluations show how the composition and structure of the current landscape compares to the modeled range of natural variability. To assess landcover composition, relative areas occurring currently were compared to the central tendency, and variation of areas occupied by each category over the course of the long-term simulation. Over the course of the 300-year simulation, aspen and Douglas fir stands emerged, but their relative proportions were insignificant and thus not compared.

Quantification of patterns can be an important component of landscape evaluation and management (Farina, 2000) because landscape configuration can generally be related to ecological processes (Forman and Gordon, 1986; Zonneveld and Forman, 1990). Many metrics have been developed that describe the proportions and configuration of patches, classes of patches, and landscape-level system properties (McGarigal and Marks, 1995). Because each metric measures a specific characteristic of heterogeneity, simultaneous consideration of several indices is often instructive (Gustafson, 1998). Three landscape-level indices were used to describe proportions, aggregation, and connectivity of the current and simulated vegetation mosaic over time. The Largest Patch Index (LPI) measures the percentage of total landscape area comprised by the largest patch. Landscape Shape Index (LSI) values can be interpreted as a measure of patch aggregation; as LSI increases, patches become increasingly disaggregated. Lastly, the Contagion Index (CONTAG) assesses overall landscape clumpiness. When Contagion is high, large clumps exist (Turner et al., 1989; McGarigal and Marks, 1995).

HYDROLOGIC MODEL CALIBRATION

Model Configuration

The 2,251 ha drainage was configured with 22 subbasins, and 54 unique combinations of subbasin, landcover and soil types, referred to as hydrologic response

units (HRUs). SWAT was calibrated for streamflow using spatially explicit current landcover characteristics, soil characteristics defined by the Montana STATSGO dataset (USDA-NRCS, 1994), and four years of daily temperature, precipitation, and streamflow data. Climate data were obtained from the Onion Park snow telemetry site (SNOTEL) located within the research watershed. Streamflow data from a flume at the watershed outlet were used for calibration and subsequent model validation.

The configured and initially parameterized SWAT model was used to simulate hydrologic processes for the period from January 1, 1993 to December 31, 2002. The first two years of the simulation were used to ramp up the model and allow it to equilibrate to ambient conditions (White and Chaubey, 2005).Years 1997 through 2000 were used for model calibration, and model validation was performed by running the calibrated model for the two years prior to (1995-96) and two years beyond (2001-02) the calibration period (Table. 2). The time period used for model calibration and validation encompassed a wide range of environmental conditions, including wet, dry and average years. Despite being a fairly short period of time, research into calibration data requirements has shown that information richness of this type is more valuable than lengthy records alone (Gupta et al., 1998).

Table 2. *Hydrologic simulation timeline, indicating the yeas over which model equilibration, calibration and validation took place.*

Spin-Up		Validation		Calibration				Validation	
1993	1994	1995	1996	1997	1998	1999	2000	2001	2002

In this study, SWAT2005 was used in conjunction with the AVSWAT interface (Di Luzio et al., 2004). This GIS-based graphical user interface facilitated watershed delineation, subdivision and initial parameterization. AVSWAT also incorporated sensitivity analysis, auto-calibration, and uncertainty assessment procedures (van Griensven et al., 2006).

Initial model simulations were conducted using default values for most of the model parameters. Potential evapotranspiration (PET) was modeled with the Penman-Monteith algorithm because it incorporates, in part, canopy height to estimate PET and

this made it possible to impart differential values for locally described landcover types. Surface runoff was modeled with the standard SCS Curve Number approach, and the variable storage channel routing method (Neitch et al., 2002).

Model Performance Criteria

Model performance was evaluated through visual interpretation of hydrograph scatter plots, and commonly used statistical measures of agreement between measured and simulated data pairs (ASCE, 1993; Coffey et al., 2004; White and Chaubey, 2005). Criteria for calibration were also applied to the validation periods, spanning annual, monthly, and daily time-steps.

A report issued by the American Society of Civil Engineers (ASCE, 1993) recommended using the Nash-Sutcliffe model efficiency (NS), and average runoff volume deviation (Dv) metrics for gauging hydrologic model performance. These statistics, along with a measure of relative difference (RE) were therefore employed to quantitatively evaluate model predictions.

The Nash-Sutcliffe (NS) measure of model efficiency is among the most commonly discussed in the hydrologic literature, and to permit comparison with results from other studies, evaluation of model performance was primarily based on this metric. With NS, the similarity of measured and simulated hydrograph silhouettes is assessed quantitatively. Values of the coefficient can range from negative infinity to a high of 1.0, which corresponds to a perfect fit between paired time-series data. When NS values are 0 or less, model predictions are no better than the mean of the observed data. Coefficients greater than 0.75 are said to be "good", and values between 0.75 and 0.36 are considered "satisfactory" (Motovilov et al., 1999; Wang and Melesse, 2006). NS is calculated as:

$$NS = 1 - \left[\frac{\sum (\hat{y} - y)^2}{\sum (y - \bar{y})^2} \right]$$

where individual and mean measured values are y and $\bar{y}$, and simulated individual and mean values are $\hat{y}$ and $\bar{\hat{y}}$, respectively

Model Calibration

Global sensitivity analysis procedures (van Griensven et al., 2006) indicated that model predictions were strongly influenced by snowmelt, surface runoff lag coefficient, groundwater, soil, and SCS curve number parameter values. Given the sensitivity of model output to the flux of their values, parameters within the above functional groups were selected for calibration.

The model was first calibrated by minimizing the relative error (RE) between measured and simulated annual precipitation, snowmelt, and water yield. Further model refinement focused on matching the simulated timing of streamflow to measured monthly and daily values with iterative modifications of the selected calibration parameters that optimized model evaluation criteria. After appropriate parameter ranges were defined, optimum values were estimated with automated methods based on the Shuffled Complex Evolution algorithm (Duan et al., 1992, 1994; van Griensven and Bauwens, 2003). With only a single residual sum of squares objective function, results derived from this algorithm strongly weighted the snowmelt driven hydrograph peaks and failed to match low flow periods. Final parameter estimates were therefore reached by manually refining the automated calibration.

Model Validation

Model performance during the validation period (1995, 1996, 2001, and 2002) was compared to that of the calibration phase (1997-2000). When calibration and validation performance criteria were reasonably similar the model was considered validated by the independent time-series dataset.

HYDROLOGIC ASSESSMENT OF LANDCOVER CHANGE

The calibrated SWAT model was used to simulate streamflow in response to each of the 30, 10-year time-step landcover maps. For every 10-year representation of landcover, a new SWAT model was established, using the same watershed delineation, sub-watershed configuration, soil, and climate forcing data. Unique landcover patterns in each map required HRUs to be redefined for each 10-year time-step landcover map.

Calibrated parameters were then assigned to all model elements and SWAT was run from 1993-2002. This is a departure from how long-term simulations are generally handled by SWAT, but nonetheless, use of the same physical inputs ensures that streamflow variability can be unambiguously attributed to changes in landcover. To further isolate hydrologic response due to landcover dynamics, output from a single year that represented typical climate and hydrologic patterns (1999) was employed in the evaluation procedures.

Daily hydrographs were constructed for each landcover representation to show the range of streamflow responses to varying vegetation patterns. With values from each representation, a composite hydrograph of mean daily streamflow was plotted against the hydrograph of calibrated conditions to illustrate how current streamflow relates to the central tendency of a range of possible patterns. Time-series annual water yield, peak discharge rate and flow regime variability were also assessed and compared to current conditions.

RESULTS

LANDCOVER PATTERNS

Vegetation dynamics modeled with SIMPPLLE indicated that, under an unmanaged scenario, the Tenderfoot Creek research watershed would have considerably less mature forest cover, more disturbed forest, and a greater area of shrublands than at present (Figure 4). In addition, under the current conditions, many of the dominant vegetation cover types within the Tenderfoot Creek research watershed are either at the limit or outside of the natural range of variability. Total forest cover, which is presently 85% of the watershed, is nearly twice as high as the long term mean of 46%. Present day values for both lodgepole pine (65%) and spruce fir forest (20%) are more than two standard deviations from the simulated long term means of 41% and 5%. Shrublands, which presently encompass only 1% of the watershed, would average 19% under natural conditions, so that current conditions are more than two standard deviations below the mean. The only general landcover category that is similar under both the current and simulated unmanaged conditions is grassland, which encompasses only about 1% of the watershed.

The largest patch index (LPI) for the current landscape is more than two standard deviations above the mean, indicating that landscape patches are much larger than would occur across most of the range of conditions in an unmanaged landscape (Table 3 and Figure 5). Similarly, the current landscape shape index (LSI) is more than two standard deviations below the mean, and the contagion index is nearly two standard deviations above the mean, indicating that under an unmanaged scenario landscape vegetation patches would be more disaggregated and less clumpy than they are at present.

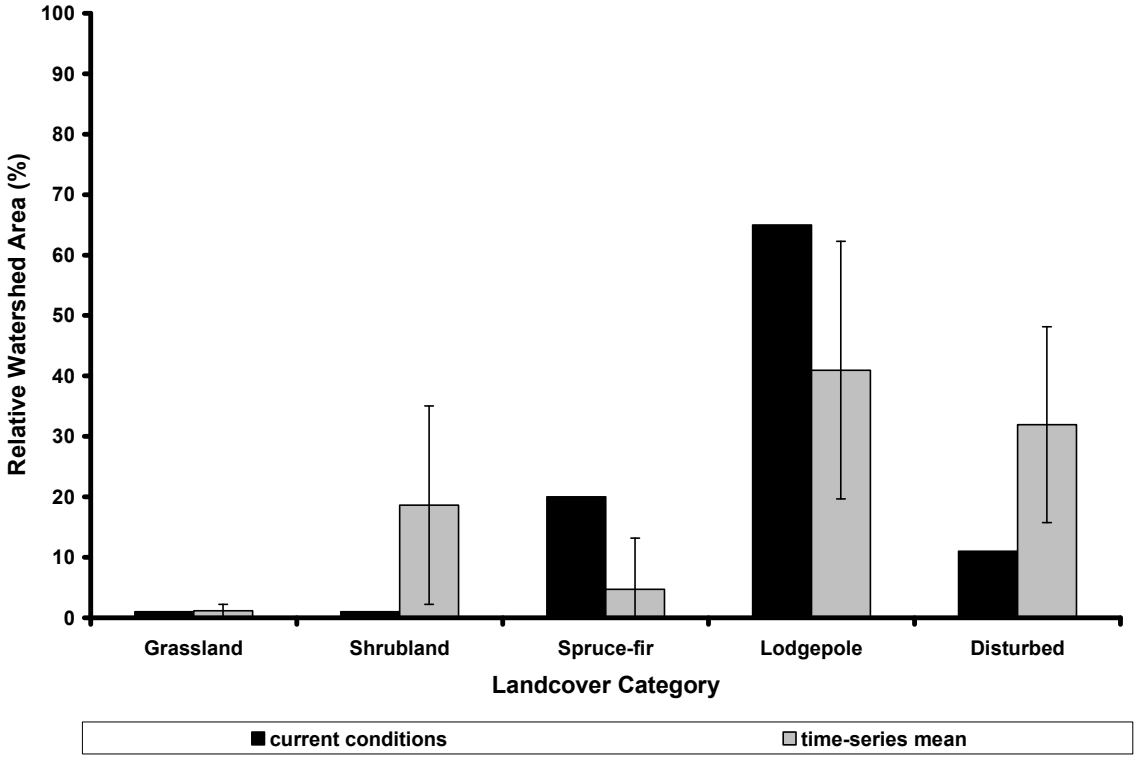

Figure 4. *Comparison of relative watershed area occupied by the current and mean times-series landcover categories. Error bars represent ± two standard deviations of the mean, capturing the full range of data.*

Table 3. *Summary statistics for largest patch index (LPI), Landscape Shape Index (LSI) and Contagion (CONTAG) for the current mosaic and simulated unmanaged conditions over 300 years of simulation at decadal time steps*.

Landscape Metric	Current	Mean	SD	Min	Max
Largest Patch Index (LPI)	62.61	33.77	10.96	21.20	62.61
Landscape Shape Index (LSI)	7.23	8.88	0.77	6.82	9.69
Contagion (CONTAG)	62.50	55.17	3.99	49.35	64.33

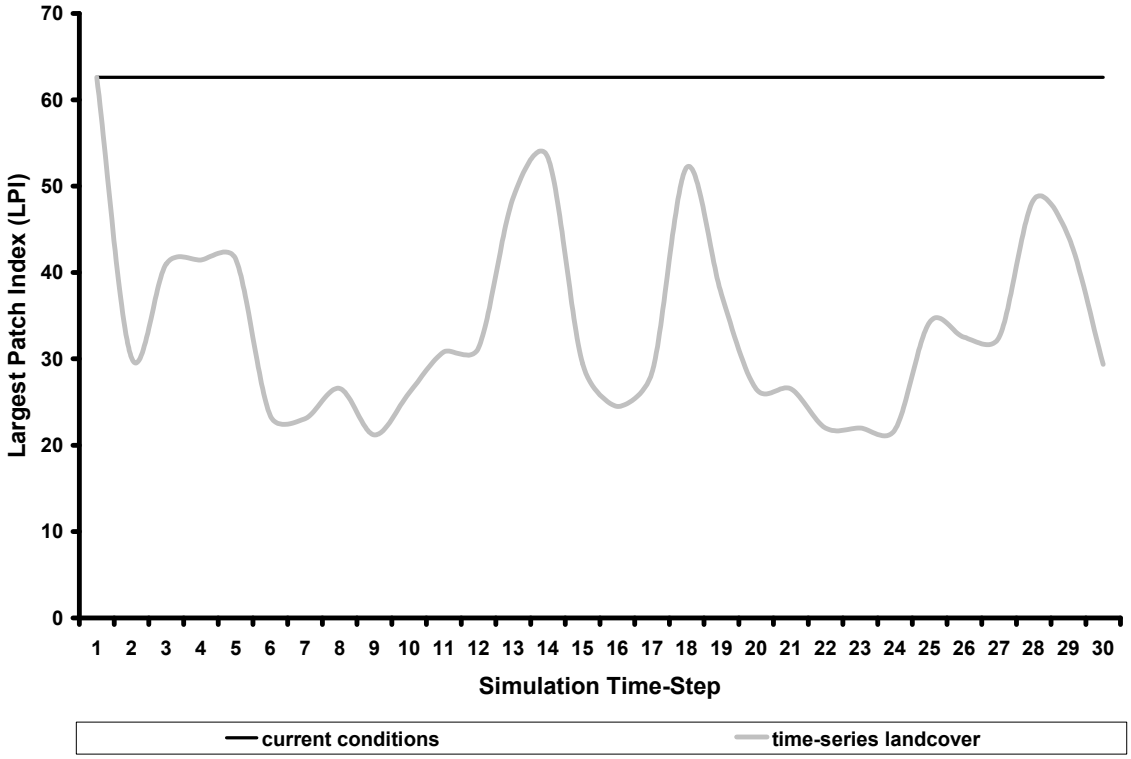

Figure 5. *Comparison of the landscape-level Largest Patch Index (LPI) that describes the current and simulated landcover configuration in the research watershed. The straight line illustrates the metric's current value while the undulating, line depicts time-series values.*

HYDROLOGIC MODEL CALIBRATION AND VALIDATION

The calibrated SWAT model produced very realistic estimates of annual, monthly, and daily hydrologic patterns over individual years, and the overall simulation period. During the calibration phase, SWAT predicted 98% of the measured water yield, with monthly (NS_m) and daily (NS_d) model efficiency scores of 0.90 and 0.86, respectively. In the subsequent validation, the model simulated monthly and daily streamflow with respective overall monthly and daily NS efficiencies of 0.90 and 0.76, and produced 96% of the measured water yield (Table 4).

Table 4. *Performance statistics for calibration and validation simulation time periods.*

Simulation Type	Year	Obs (mm)	Sim (mm)	RE	NS_m	NS_d
Calibration	1997	564	563	0	0.90	0.88
	1998	430	375	-13	0.82	0.75
	1999	336	337	0	0.92	0.92
	2000	357	374	5	0.92	0.86
Validation	1995	511	517	1	0.95	0.78
	1996	495	460	-7	0.83	0.74
	2001	288	234	-19	0.83	0.70
	2002	339	354	4	0.97	0.94
Overall Calibration (1997-2000)		**1,688**	**1,649**	**-2**	**0.90**	**0.86**
Overall Validation (1995-96, 2001-02)		**1,632**	**1,565**	**-4**	**0.90**	**0.76**

While the overall hydrograph fit was good for daily estimates, the model tended to perform better during the runoff rather than baseflow periods. The rising limb of the annual hydrograph peak was generally well matched, although some of the highest runoff rates were underestimated. Model performance decreased on the recession limb, and baseflow periods of the annual hydrograph, but was still acceptable (Figure 6).

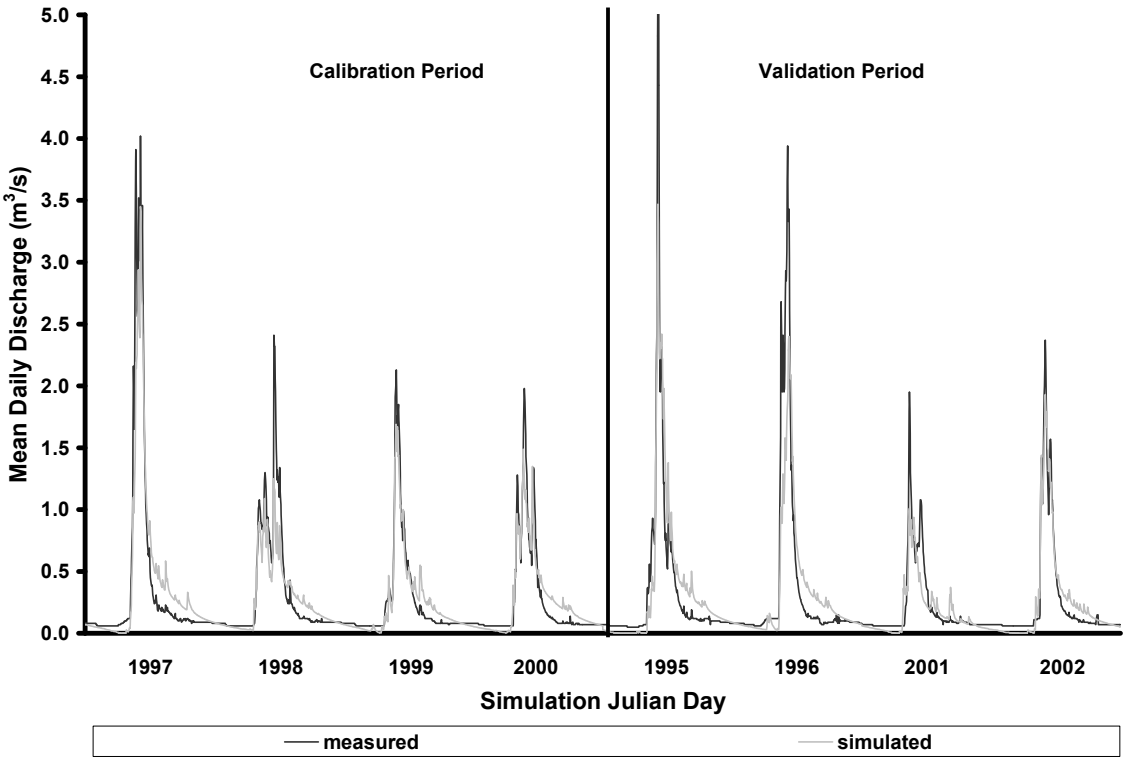

Figure 6. *Simulated mean daily discharge hydrograph during calibration (1997-2000) and validation (1995-96, 2001-02).*

TIME-SERIES HYDROLOGIC VARIABILITY

Over the range of simulated landcover scenarios, peak flow rates for the modeled water year (1999) varied approximately 12%, from 1.70 to 2.19 m^3/s, while variation in annual yield varied 4% from 337 to 349 mm. Compared to current conditions, time-series models yielded between 1.5% and 4% more water annually, and peak flow rates up to 22% greater in magnitude (Figure 7).

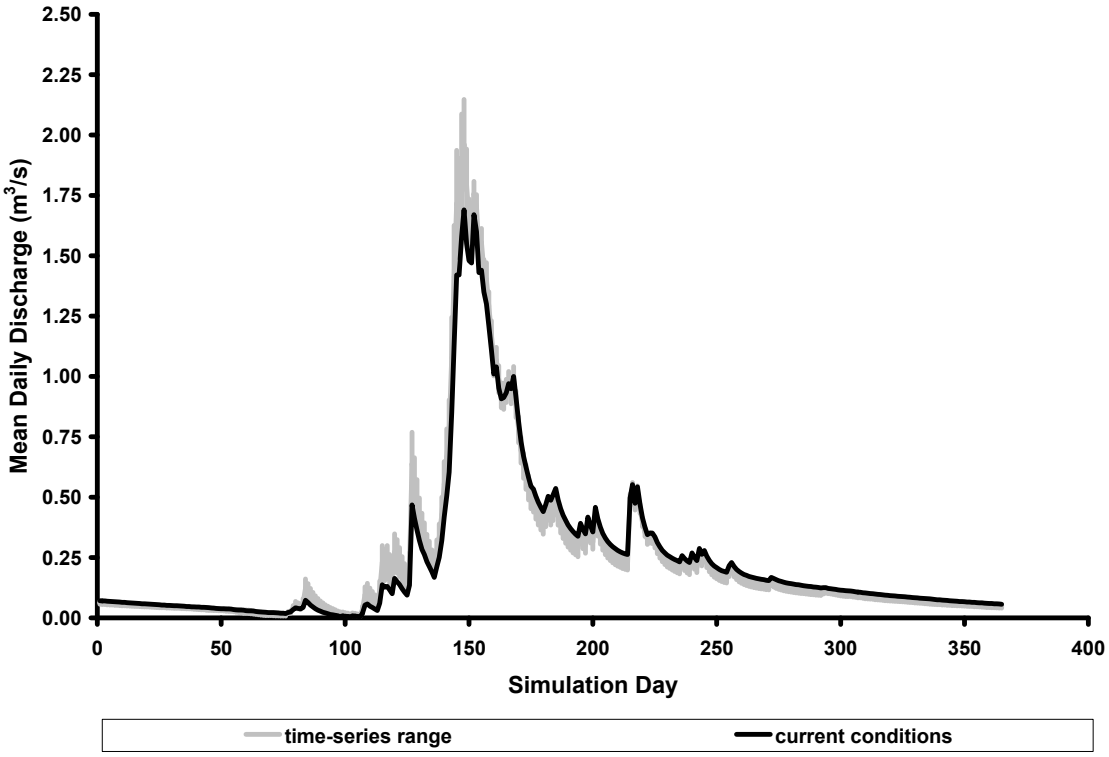

Figure 7. *Simulated streamflow range (min and max) associated with the time-series landcover, plotted against current streamflow values for representative year 1999.*

Time-series landcover scenarios were associated with streamflow patterns that had, on average, 5% greater discharge rates, and the median flow between the 95-99th percentile was about 10% larger (Figure 8).

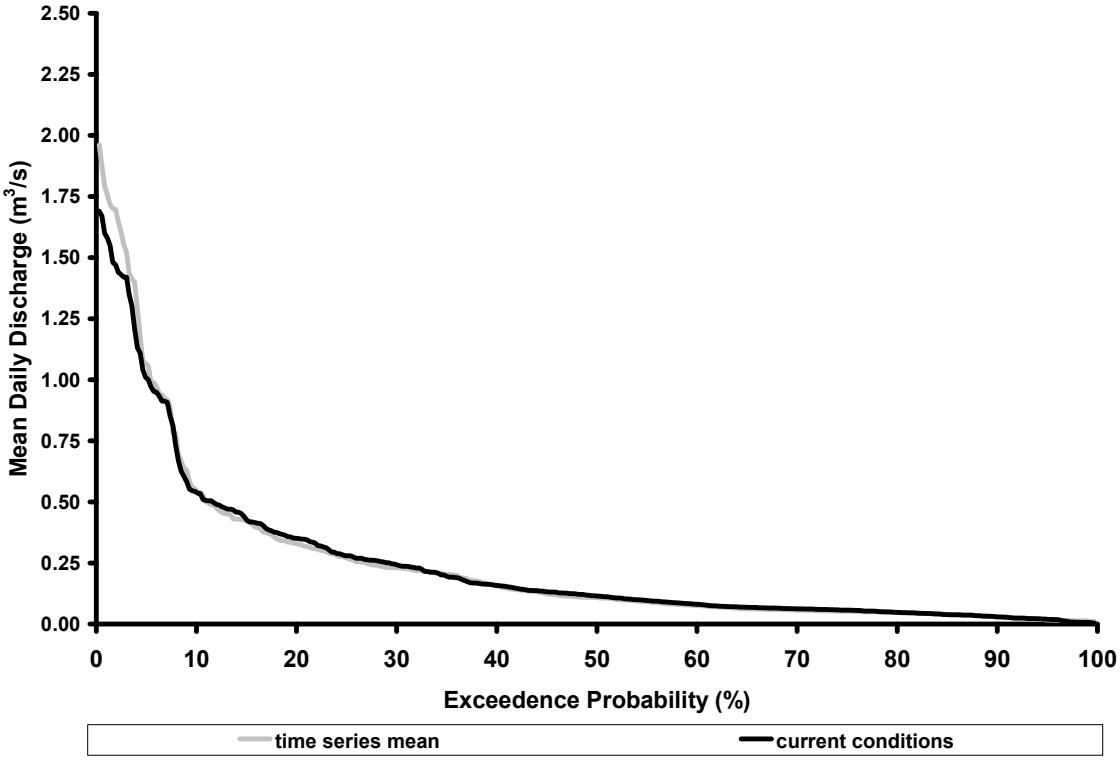

Figure 8. M*ean time-series streamflow exceedence probability relative to the current streamflow distribution for the representative year, 1999.*

DISCUSSION

Much of the water that supplies western North America originates as snow that is deposited and temporarily stored in forested mountain watersheds. The high value of water resources has encouraged nearly a century of research focusing on the relationships between conifer forest characteristics and their influence on the magnitude and timing of basin-wide runoff. This work has shown that removal of threshold levels of forest cover tends to advance the timing of snowmelt runoff, increase the magnitude of peak flows, and elevate total annual water yield. Similarly, when undisturbed for long periods of time, the process of succession may increase the extent of forest cover, and cause stands to become denser. Relative to other types, conifer forests intercept more precipitation and transpire more water, and increased relative abundance of this landcover can therefore lead to reduced watershed runoff.

While the interactions between forest and hydrologic characteristics have been well documented, the dynamic range over which this relationship occurs naturally is less well known. Fire is the dominant disturbance agent that imparts changes to the mosaic of Rocky Mountain forests, but our ability to empirically evaluate the interactions between varying vegetation patterns and watershed-level streamflow response is limited by the relatively short duration of continuous streamflow measurements in upland watersheds. Most gauge records only reflect an 80-year history, but estimated fire cycles range between 100 – 400 years. Over the period of measurement relatively few large watershed-altering forest fires have been observed. Regardless of whether this is because of effective suppression efforts or an intrinsically low probability of occurrence (Strauss, 1989), there are insufficient data to estimate the natural range of streamflow variability in forested mountain watersheds. Using current knowledge of watershed processes and available data, a modeling framework has been developed to ascertain a potential range of streamflow variability in forested mountain watershed, based on a natural, long-term vegetation dynamics scenario.

LANDSCAPE VEGETATION DYNAMICS

Simulations of landcover change using the SIMPPLLE model are based on successional pathways and disturbance probabilities related to stand characteristics including history, topology, habitat type, composition and structure. The relationships embedded in the model have been defined by scientists across the Northern Region of the USDA Forest Service, and represent the current state of knowledge (Chew et al. 2004).

The stochastic structure of the model makes it possible to estimate the range of vegetation conditions over time by running multiple simulations of a defined landscape over short periods, or individual long-term simulations. To estimate the range of landcover patterns, a single simulation was run. It spanned a 300-year time frame, and encompassed the probable fire cycle of this region. Using a decadal time step, this procedure yielded a set of 30 time-series landcover maps. Given the tendency for normally distributed output (Zuuring and Sweet, 2000), 30 time-step landcover maps are likely to encompass the range of possible conditions in the research watershed.

Recognizing the connection between landscape and watershed processes is important in environments where disturbances have the potential to propagate over large regions. Without the influence of the surrounding landscape, disturbances such as fires that originate outside the boundaries cannot spread into the watershed as they naturally would. When forest cover is continuous, a landscape perspective is especially important because fire and insects damage can readily spread across connected patches. To represent natural landscape function as accurately as possible, vegetation dynamics were simulated at the landscape scale, and then analyzed at the watershed level.

Simulated patterns of watershed level landcover composition and configuration, measured by relative abundance and landscape-level spatial pattern metrics, appear to be cyclical and punctuated by rare but large fluctuations. Assessment of fire history in the research watershed estimated roughly 4 distinct episodes over a period of roughly 400 years that disturbed more than 25% of the area (Barrett, 1993). Analysis of the predicted landcover shows a pattern of disturbance that is quite similar, where large changes in forest extent and configuration are evident approximately 3 times over the 300 year simulation period. It therefore appears that these landcover simulations portray a level of landcover stochasticity that is similar to what has been observed in the fire record, and resulting maps span the potential range of conditions likely to occur in the research watershed over time. The distribution of values from these maps, thus, provides the context in which we assess current watershed landcover patterns and associated hydrologic characteristics.

The existing landcover mosaic in the research watershed has been influenced by nearly 120 years of relatively disturbance-free succession. Due to biophysical variables and a fairly long time since disturbance almost 85% of this watershed is covered by coniferous forest, composed largely of lodgepole pine (*Pinus contorta*), subalpine fir (*Abies lasiocarpa*) and Engelman spruce (*Picea engelmannii*). When compared to future simulated distributions of landcover composition and configuration, it is clear that current patterns are poised to change dramatically.

In terms of composition, when the relative abundance of landcover categories was averaged over the simulation period, mature forest was reduced by 45%, and generally replaced by shrubland and disturbed forest cover types. The current proportions of forest

cover types exceed the distribution of their simulated abundance. Conversely, the abundance of shrubland, and disturbed forest is currently lower than that predicted over time.

Assessment of landcover configuration also shows that current patterns are at the extreme ends of their simulated distributions. Compared to future patterns, the current landcover pattern is characterized by larger, more aggregated, and clumpy patches. Of all the metrics evaluated, LPI may be the most informative. For maps classified into categories of suitable and unsuitable patches (i.e. forest and non-forest) the primary determinant of spatial pattern is the proportion of the class of interest (Gustafson, 1998). The compositional component determines the probable range of many patch configuration characteristics. If the proportion is low, the patches are generally small and isolated, and do not have enough area to form convoluted shapes.

According to percolation theory (Stauffer, 1985), if a suitable habitat patch (i.e. forest) occupies 59% of the landscape, then a process such as fire may easily spread across the entire landscape (Turner et al., 1989). The largest patch in the existing landscape occupies 62% of the watershed, and furthermore, 85% of current landcover is composed of mature forest. This combination of composition and configuration creates a situation that is highly conducive for propagation of fire across the watershed. If the simulated patterns are an indication of this watershed's landcover trajectory, it is plausible that a large stand-replacing disturbance is likely to occur in the future. Major changes in landcover composition and structure have the potential to alter the watershed hydrologic response

WATERSHED RESPONSE TO VEGETATION CHANGE

Simulated streamflow was calibrated to the current landcover conditions, using regionally derived estimates of important hydrologic parameters. The resulting model produces outcomes that are well within the range of what other authors have reported. A review of contemporary literature by White and Chaubey (2005) lists NS values ranging between 0.58 and 0.98 for monthly yield estimates. Eckhardt and Arnold (2001) used automated methods and achieved daily values of 0.70 for a small forested watershed in

Germany. In our calibration, we obtained monthly and daily NS values of 0.90 and 0.86, respectively. Validation of the model, using independent data suggested that the calibration was robust. Despite good overall performance statistics, the model seemed to most accurately represent the snowmelt runoff portion of the hydrograph, while matching low flows was problematic.

A global sensitivity analysis of the uncalibrated model identified parameters that govern snow processes, surface runoff, groundwater, and soil properties as highly influential components of the streamflow simulation. Results of a post-calibration parameter set decomposition clearly show that in this forested mountain watershed, parameters that estimate snow fall accumulation, and melt rates have at least 20% more influence on model performance than other evaluated parameter sets (Chapter 2, Table 13). This may partially explain why model predictions were generally better for runoff rather than baseflow periods. Without the recent incorporation of enhanced snow process routines, streamflow calibration in a snow-dominated watershed, such as ours, may have been less successful (Fontaine et al., 2002).

Forests are dynamic, and their structure and configuration are a function of climate, topography, and disturbance processes. When long-term watershed simulations are intended to evaluate the hydrologic response of watersheds to ecological trajectories of forested ecosystems, patterns of forest growth, disturbance, and species composition must be taken into consideration. Rather than altering landuse characteristics of hydrologic response units (HRUs) defined by the initial model set up, the method used in this study assumes that HRU management (i.e. natural growth) does not change, but instead the processes that govern landcover patterns are simulated separately, and new landcover patterns are supplied at regular intervals. In this way, the only model element that changes is the extent, composition, and spatial arrangement of landcover. With each shift in pattern, HRUs are reconfigured. Although the arrangement of HRUs within sub-watersheds is not considered, basin-wide hydrologic responses to the changing diversity of landcover patterns can be accounted for with this method. With appropriate subdivision, the spatial distribution of watershed processes may also be assessed. To track the spatial distribution of processes affecting streamflow, considering the approximate nature of expected changes in landcover patterns can guide the degree to

which a watershed should be subdivided. In the Rocky Mountains for example, roughly 20% cover must be removed in order to elicit detectable changes in streamflow from watersheds with coniferous forest (Stednick, 1996). To account for such changes spatially with SWAT, sub-watersheds should be no coarser than 5 times the dimension of the smallest change that is expected to have an impact.

Running the calibrated hydrologic model separately with each of the 30 landcover representations produced an envelope of streamflow responses that was used to estimate the range of streamflow variability given landcover change over the course of natural disturbance cycles in this watershed. Streamflow predictions related to simulations of landcover change appear to be similar to those reported by authors conducting catchment studies in other parts of the world, and especially in the Rocky Mountain region.

Matheussen et al. (2000) simulated the change between current and historic landcover and hydrologic response and found that forest reduction increased water yield 1-7% in the Columbia River Basin. Recognizing vast differences in scale, results from our simulations are comparable, with annual water yield increases between 1.5 - 4.0%. Experimental manipulation in watersheds located in Colorado and Wyoming showed an average increase of 23% in peak flow rates as a result of removing 50% of the forest (Troendle and King, 1985), and an 8% increase due to 24% forest reduction (Troendle et al., 2001), respectively. On average, simulated landcover in our watershed was about 45% less forest and peak flow rates varied 12%, and increased up to 22% over calibrated conditions. Additionally, analysis of daily flows from 28 paired watershed experiments showed that the median increase in the 95-99th percentiles of daily flows was about 10-15% (Austin, 1999). A comparison of current with future flow duration shows a very similar trend, where the median difference between the same percentile range is roughly 10%.

Given that simulations are reasonable, it appears that current landcover and streamflow patterns are at the extreme ends of their probable distributions, and a long-term perspective that encompasses natural cycles is necessary to capture the range of possible conditions likely to occur in the watershed. Currently, forest covers more area than is forecast over time and it is anticipated that its extent will inevitably be reduced by cyclical disturbances. Hydrologic patterns observed currently resemble annual yield and

peak flow rate values at low end of the estimated range of variability. Temporal landcover change associated with natural disturbances such as fire, insect and disease outbreaks may cause annual water yield and peak discharge rates to fluctuate up to 4% and 12%, respectively. Compared to current conditions, forest cover may be reduced by up to 45%, and this could increase annual water yield between 1.5 and 4% annually, while also increasing peak flow rate by up to 22%.

CONCLUSIONS

Long-term simulations of landcover change indicate that natural disturbances create landcover patches that are smaller, less aggregated, and less clumpy than current patterns. Over time, forest cover is expected to occupy less area than it does currently. These simulations also illustrate that patterns of landcover compositions and configuration are cyclical and periodic disturbances, while they are rare, create major changes in landscape mosaic. With a low probability of occurrence, a temporal perspective that encompasses natural disturbance cycles is necessary to capture the range of possible conditions.

The hydrologic model used to simulate streamflow response to landcover change was well calibrated for conditions in this Rocky Mountain watershed. Its performance was most strongly influenced by parameters that govern snow accumulation and melt, relative to other important parameters that describe surface runoff, groundwater or soil characteristics and SCS curve numbers. The incorporation of improved snow process algorithms in the recent versions of the model is therefore likely to encourage its use in other snow-dominated watersheds.

To study long-term watershed dynamics in a forested ecosystem, a landscape perspective is necessary to estimate the full range of processes that are likely to occur over time. Without a connection to the surrounding landscape, disturbances that originate outside a watershed cannot spread into it, given the probability of natural percolation. Failing to account for process propagation across landscapes can lead to an underestimation of watershed disturbances over time. A mechanism that captures not only the different stages of plant development, but also the spatial dynamics of species

composition and arrangement is also needed. SWAT uses an internal simulator to grow vegetation in defined HRUs. The standard SWAT method accounts for changes in management associated with existing HRUs, but does not consider changing patterns of landcover over time. Procedures in this study used an independent vegetation simulator, SIMPPPLE to supply a time-series of landcover representations based on a natural succession and disturbance processes scenario. Each time a new landcover map was introduced, a separate SWAT model was established, using the calibrated parameters and all the same configuration, soil, and climate data. The only difference between successive SWAT models was the updated landcover and associated HRU definitions. Changes in watershed-level hydrologic response could therefore be unambiguously attributed to variation in landcover patterns.

When compared to other published studies of streamflow response to landcover change, this integrated modeling approach produced reasonable results. Results suggest that when landcover patterns are regulated by natural processes over time, and forest cover is reduced, annual water yield may increase by up to 4%, and peak flow rates may be up to 22% greater when compared to current watershed conditions. Using the approach described here, similar assessments may be conducted in other regions.

LITERATURE CITED

Alt, D. and D.W. Hyndman. 1986. Roadside Geology of Montana. Mountain Press, Missoula, MT.

Anderson, J.R., E.E. Hardy, J.T. Roach, and R.E. Witmer. 1976. A land use and land cover classification system for use with remote sensor data. Geological Survey Professional Paper 964. U.S. Government Printing Office, Washington, D.C.

Austin, S.A. 1999. Streamflow response to forest management: a meta-analysis using published data and flow duration curves. M.S. thesis, Department of Earth Resources, Colorado State University, Fort Collins, CO. 121 pp. plus appendices.

Arno, S.F., and C.E. Fiedler. 2005. Mimicking Nature's Fire: Restoring Fire-Prone Forests in the West. Island Press, Washington, D.C.

Arnold, J.G., R. Srinivasan, R.S. Muttiah, and J.R. Williams. 1998. Large Area Hydrologic Modeling and Assessment Part I: Model Development. Journal of the American Water Resources Association 34(1): 73-89.

ASCE, 1993. Criteria for evaluation of watershed models. Journal of Irrigation and Drainage Engineering 119(3): 429-442.

Barrett, S.W. 1993. Fire History of Tenderfoot Creek Experimental Forest, Lewis and Clark National Forest. Systems for Environmental Management, Research Joint Venture Agreement No. INT-92679-RJVA.

Barrett, T.M. 2001. Models of vegetative change for landscape planning: a comparison of FETM, LANDSUM, SIMPPLLE, and VDDT. U.S. Department of Agriculture, Forest Service, General Technical Report RMRS-GTR-76-WWW.

Bosch, J.M. and J.D. Hewlett. 1982. A Review of catchment experiments to determine the effect of vegetation changes on water yield and evapotranspiration. Journal of Hydrology 55(1-4): 3-23.

Chew, J.D., K. Moeller, C. Stalling, E. Bella, and R. Ahl. 2002. Simulating Patterns and Processes at Landscape Scales: User Guide for SIMPPLLE V2.2. U.S. Department of Agriculture, Forest Service, Rocky Mountain Research Station, Forest Ecology and Management, Missoula, MT, USA.

Chew, J.D., C. Stalling, and K. Moeller. 2004. Integrating knowledge for simulating vegetation change. Western Journal of Applied Forestry 19(2): 102-108.

Coffey, M.E., J.L. Workman, A.W. Taraba, and A. W. Fogel. 2004. Statistical procedures for evaluating daily and monthly hydrologic model predictions. Transactions of the ASCE 47(1): 59-68.

Di Luzio, M., R. Srinivasan, and J.G. Arnold. 2004. A GIS-coupled hydrological model system for the watershed assessment of agricultural non-point and point sources of pollution. Transactions in GIS 8(1): 113-136.

Duan, Q., S. Sorooshian, and V. Gupta. 1992. Effective and efficient global optimization for conceptual rainfall-runoff models. Water Recourses Research 28: 1015-1031.

Duan, Q., S. Sorooshian, and V. Gupta. 1994. Optimal use of the SCE-UA global optimization method for calibrating watershed models. Journal of Hydrology 158(3-4): 265-284.

Eckhardt, K. and J.G. Arnold. 2001. Automatic calibration of a distributed catchment model. Journal of Hydrology 251(1-2): 103-109.

Farnes, P.E., R.C. Shearer, W.W. McCaughey and K.J. Hansen. 1995. Comparisons of Hydrology, Geology and Physical Characteristics between Tenderfoot Creek Experimental Forest (East Side) Montana, and Coram Experimental Forest (West Side) Montana. Final Report RJVA-INT-92734. U.S. Department of Agriculture, Forest Service, Rocky Research Station, Forestry Sciences Laboratory, Bozeman, Montana. pp 19.

Farnes, P. E., W.W. McCaughey, and K.J. Hansen. 2000. Role of Fire in Determining Annual Water Yield in Mountain Watersheds. *In* After the Fires: The Ecology of Change in Yellowstone National Park. Yale University Press, New Haven.

Farina, A. 2000. Landscape Ecology in Action. Kluwer, Dordrecht. 317 pp.

Fontaine, T.A., T.S. Cruickshank, J.G. Arnold and R.H. Hotchkiss. 2002. Development of a snowfall-snowmelt routine for mountainous terrain for the soil water assessment tool (SWAT). Journal of Hydrology 262: 209-223.

Forman, R.T.T. and M. Gordon. 1986. Landscape Ecology. John Wiley and Sons, New York.

Golding, D.L. and R.H. Swanson. 1978. Snow accumulation and melt in small forest openings in Alberta. Canadian Journal of Forest Research 8: 380-388.

Gupta, H.V., S. Sorooshian, and P. O. Yapo. 1998. Toward improved calibration of hydrologic models: Multiple and noncommensurable measures of information. Water Resources Research 34(4): 751-764.

Gustafson, E.J. 1998. Quantifying landscape spatial pattern: What is the state of the art? Ecosystems 1: 143-156.

Hall, R.J., D.P. Davidson, and D.R. Peddle. 2003. Ground and remote estimation of leaf area index in Rocky Mountain forest stands, Kananaskis, Alberta. Canadian Journal of Remote Sensing 29(3): 411-427.

Keane, R.E., K.C. Ryan, T. Veblen, C. Allen, J. Logan, and B. Hawkes. 2002. Cascading effects of fire exclusion in Rocky Mountain ecosystems: A literature review. U.S. Department of Agriculture, Rocky Mountain Research Station, General Technical Report RMRS-GTR-91.

Kimmins, J.P. 1997. Forest Ecology: A foundation for sustainable management. Prentice-Hall, Upper Saddle River, NJ.

MacDonald, L.H. and J.D. Stednick. 2003. Forest and Water: A State-of the-Art Review for Colorado. Colorado Water Resources Research Institute Completion Report No. 196. Colorado State University, Fort Collins, CO. 65 pp.

Matheussen, B., R.L. Kirschbaum, I.A. Goodman, G.M. O'Donnell and D.P. Lettenmaier. 2000. Effects of land cover change on streamflow in the interior Columbia River Basin (USA and Canada). Hydrological Processes 14(5): 867-885.

McCaughey, W.W. 1996. Tenderfoot Creek Experimental Forest. *In* Experimental forests, ranges, and watersheds in the Northern Rocky Mountains: A compendium of outdoor laboratories in Utah, Idaho, and Montana. W.C. Schmidt and J.L. Friede ,Compilers. U.S. Department of Agriculture, Forest Service, Gen. Tech. Rep. INT-GTR-334. p. 101-108.

McCaughey, W.W. and P.E. Farnes. 2001. Snowpack comparison between an opening and a lodgepole stand. Proceedings 69th Western Snow Conference. p. 59-64.

McGarigal, K. and B. J. Marks. 1995. FRAGSTATS: Spatial pattern analysis program for quantifying landscape structure. U.S. Department of Agriculture, Forest Service, General Technical Report PNW-351.

Moore, C.A. and W.W. McCaughey. 1997. Snow Accumulation under various forest stands densities at Tenderfoot Creek Experimental Forest, Montana, USA. Proceedings 66th Western Snow Conference. p. 42-51.

Motovilov, Y.G., L. Gottschalk, K. Engeland, and A. Rodhe. 1999. Validation of a distributed hydrological model against spatial observations. Agricultural and Forest Meteorology 98-99: 257-277.

Nash, J.E. and J.V. Sutcliffe. 1970. River flow forecasting through conceptual model part 1 - A discussion of principles. Journal of Hydrology 10(3): 282-290.

Neitsch, S.L., J.G Arnold, J.R Kiniry, J.R Williams, and K.W. King. 2002. Soil and Water Assessment Tool Theoretical Documentation, Version 2000. Texas Water Resources Institute, College Station, Texas, TWRI Report TR-191, GSWRL Report 02-01, BRC Report 02-05.

Ott, R.L. 1993. An introduction to statistical methods and data analysis. Duxbury Press, Belmont, CA. 1184 pp.

Pfister, R. D., B.L. Kovalchik, S.F. Arno, and R.C. Presby. 1977. Forest Habitat Types of Montana. U.S. Department of Agriculture, Forest Service, General Technical Report INT-34. 174 pp.

Pomeroy, J.W., D.M. Gray, N.R. Hedstrom, and J.R. Janowicz. 2002. Prediction of seasonal snow accumulation in cold climate forests. Hydrological Processes 16(18): 3543-3558.

Srinivasan, R., T.S. Ramanarayanan, J.G. Arnold, and S.T. Bednarz. 1998. Large Area Hydrologic Modeling and Assessment Part II: Model Application. Journal of the American Water Resources Association 34(1): 91-101.

Stauffer, D. 1985. Introduction to Percolation Theory. Taylor and Francis, London.

Stednick, J.D. 1996. Monitoring the effects of timber harvest on annual water yield. Journal of Hydrology 176: 79-95.

Strauss, D., L. Bednar, and R. Mees. 1989. Do One Percent of the Forest Fires Cause Ninety-Nine Percent of the Damage? Forest Science 35(2): 318-328.

Troendle, C.A. 1983. The Potential for water yield augmentation from forest management in the Rocky Mountains. Water Resources Bulletin 19(3): 359-373.

Troendle, C.A. and R.M. King. 1985. The effect of timber harvesting on the Fool Creek watershed, 30 years later. Water Resources Research 21(12):1915-1922.

Troendle, C.A. and R.M. King. 1987. The effect of partial and clearcutting on streamflow at Deadhorse Creek, Colorado. Journal of Hydrology 90(1/2):145-157.

Troendle, C.A., M.S. Wilcox, G.S. Bevenger, and L.S. Porth. 2001. The Coon Creek water yield augmentation project: implementation of timer harvesting technology to increase streamflow. Forest Ecology and Management 143: 179-187.

Turner, M.G., R.H. Gardner, V.H. Dale, and R.V. O'Neil. 1989. Predicting the spread of disturbances across heterogeneous landscapes. Oikos 55: 121-129.

USDA-NRCS (U.S. Department of Agriculture, Natural Resource Conservation Service). 1994. State Soil Geographic Data base (STATSGO): Data Use Information. U.S. Department of Agriculture, National Soil Survey Center Miscellaneous Publication Number 1492. 113 pp.

USDA-SCS (U.S. Department of Agriculture, Soil Conservation Service), 1972. SCS National Engineering Handbook, Section 4, Hydrology. Chapter 10, Estimation of Direct Runoff from Storm Rainfall. U.S. Department of Agriculture, Soil Conservation Service, Washington D.C. p. 10.1-10.24.

van Griensven, A. and W. Bauwens. 2003. Multiobjective autocalibration for semidistributed water quality models. Water Resources Research 39(12): 1348.

van Griensven, A., T. Meixner, S. Grunwald, T. Bishop, M. Di Luzio, and R. Srinivasan. 2006. A global sensitivity analysis tool for the parameters of multi-variable catchment models. Journal of Hydrology 324(1-4): 10-23.

Wang, X. and A.M. Melesse. 2006. Effects of STATSGO and SSURGO as inputs on SWAT model's snowmelt simulation. Journal of the American Water Resources Association 42(5):1217-1236.

White, K.L. and I. Chaubey. 2005. Sensitivity Analysis, Calibration, and Validations for a Multisite and Multivariable SWAT Model. Journal of the American Water Resources Association 41(5): 1077-1089.

Woods, S.W., R. Ahl, J. Sappington, and W. McCaughey. 2006. Snow Accumulation in thinned lodgepole pine stands, Montana, USA. Forest Ecology and Management 235: 202 – 211.

Woods, S.W., W.W. McCaughey, R. Ahl, and J. Sappington. 2004. Effect of alternative sivilcultural treatments on snow accumulation in lodgepole pine stands, Montana, U.S.A. Proceedings 72nd Western Snow Conference. p. 65-73.

Zonneveld, I.S. and R.T.T. Forman. 1990. Changing Landscapes: An Ecological Perspective. Springer-Verlag, New York.

Zuuring, H. and M. Sweet. 2000. An Evaluation of Landscape Metrics and Spatial Statistics for Interpreting SIMPPLLE output. Final Report to U.S. Department of Agriculture, Forest Service, Rocky Mountain Research Station, Forest Ecology and Management, Missoula MT, USA. 33 pp.

CHAPTER 4

Evaluating Long-Term Forest Management through Integrated Vegetation and Hydrologic Modeling

ABSTRACT

Changes in the frequency and magnitude of natural and human-induced disturbance processes can significantly alter water yield from forested watersheds. Analytical procedures that integrate vegetation simulation, landscape ecology, and hydrologic modeling to quantify changes in basin-scale landcover and water yield dynamics, which can be associated with eco-hydrologic processes, are presented in this study. Using forest fire management alternatives as an example, the proposed method has shown potential as an adaptive management tool, enabling managers to evaluate impacts of various forest management proposals on both terrestrial and aquatic resources during the planning process. The SIMPPLLE (Simulating Patterns and Processes at Landscape Scales) model was used to simulate landcover change 300 years forward from current conditions for 1) fire suppression and 2) natural succession management scenarios. Spatial pattern analysis was conducted on grid-based maps which were produced for each scenario at decadal intervals, and used as input to the SWAT (Soil and Water Assessment Tool) hydrologic simulation model. The SWAT model was calibrated using current landcover data and five years of daily streamflow records, and a Nash-Sutcliffe model efficiency of 0.86 was achieved. The calibrated SWAT model was then used to simulate the hydrologic output for each 10-year time step over the 300-year simulation period for both management scenarios. Results suggest significant differences in landcover composition, spatial configuration, and ultimately water yield when forest fires were suppressed. Compared to the unmanaged scenario, reduced levels of disturbance created larger stand sizes, greater levels of aggregation, and increased the likelihood of process propagation across the landscape when fire suppression was simulated. From a hydrologic perspective, fire suppression reduced annual water yield, streamflow variability, and the magnitude of annual peak flows.

INTRODUCTION

Vegetation characteristics are a primary control on the amount and timing of runoff in forested mountain watersheds. Forest vegetation moderates the precipitation-infiltration-runoff continuum by influencing air turbulence patterns, interception, and evapotranspiration, while also providing insulation from incident solar radiation and wind scour (Kimmins, 1997). Changes in the extent, composition, and configuration of forest cover over time due to succession, natural disturbances caused by fire, insects, and disease or forest management activities can result in measurable differences in runoff and water yield (Bosch and Hewlett, 1982; Stednick, 1996; Troendle, 1983). Removal of forest cover generally increases streamflow due to the effect of reduced canopy interception and evapotranspiration on the water budget. In Rocky Mountain watersheds, water yield increases and earlier, exaggerated peak discharge are attributed to increased snow accumulation in clearings or stands with low density, as compared to undisturbed areas, and more rapid snowmelt because of enhanced energy transfer in the openings (Golding, and Swanson, 1978; Troendle, 1983; Trondle and King, 1985, 1987). Conversely, when stands become denser and relative forest area increases in the absence of cyclical disturbances, watershed runoff may be reduced (Farnes et al., 2000).

Forest fire is the dominant disturbance agent in the Rocky Mountains of North America (Arno and Fiedler, 2005), but beginning in the early 1930s, fire suppression programs in the United States and Canada have reduced its occurrence in this region. The exclusion of fire has increased the extent, continuity, and density of forested stands, while concurrently reducing the extent and vigor of fire dependent seral species, and encouraging the invasion of shrubs and trees into grasslands (Keane et al., 2002). Changes in the frequency and magnitude of disturbance processes due to management leads to changes in forest structure, and may result in long term alterations in water yield from forested watersheds.

Adaptive management is an iterative learning process in which feedback from attempted management actions yields knowledge that guides subsequent actions to produce desired results (McLain and Lee, 1996). The effects of forest management can be long lasting, and to avoid the loss or degradation of valuable resources, current and planned actions should be based on the best available knowledge. The goal in this chapter

is to present methods for evaluating the long-term terrestrial and eco-hydrologic consequences of forest management alternatives through an integration of vegetation and hydrologic modeling and analysis procedures.

SIMPPPLLE (Simulating Patterns and Processes at Landscape Scales) is a spatially explicit, continuous simulation system that models the long-term impact of vegetation management over large areas (Chew et al., 2004). SIMPPLLE integrates data from a diversity of sources. Vegetation is defined by stand-level inventory data whenever possible, but algorithms have been developed to extract necessary data from classified satellite imagery when full coverage is otherwise not available. Management logic, environmental conditions, and physiognomic data (Pfister et al., 1977) in combination with dominant stand species, size class, and canopy density are used to advance vegetation through regionally calibrated pathways and conditional probabilities to simulate succession, and natural and planned disturbances over annual or decadal time-steps (Chew et al., 2002). In the Northern Region of the USDA Forest Service (Region 1), simulations derived from SIMMPLE are used to assess the range of natural variability and forest management alternatives (Barrett, 2001).

The Soil and Water Assessment Tool (SWAT) is a physically based, distributed, continuous, river basin model developed to predict the impact of land management practices on hydrologic processes in potentially large, complex watersheds with varying soils, landcover and management practices on a daily time step (Arnold et al., 1998). As a minimum requirement for model configuration, SWAT, via the associated GIS interface (AVSWAT; Di Luzio et al., 2004), imports topographic, soil, landcover and climate data that are available from government agencies worldwide. Hydrologic processes are represented by interception, evapotranspiration, surface runoff, soil percolation, lateral and groundwater flow, and river routing processes. For simulation, a watershed is partitioned into subbasins, river reaches and Hydrologic Response Units (HRUs). Sub-watershed delineation provides the spatial context, while further sub-division into HRUs is based on threshold proportions of mapped landcover and soil types in sub-watersheds, without regard to their topologic arrangement (Neitsch et al., 2002).

By combining these powerful tools managers can run simulations of vegetation change and use them to assess the impact of those changes on hydrologic processes. In

this way, various scenarios can be evaluated before any management takes place to ensure that planned actions produce desired outcomes in the future.

Using forest fire management as an example, this study illustrates how SIMPPLLE can produce future landcover scenarios for various management plans. The simulated outcomes can help determine if vegetation management goals are met over time. Following that, the time-series landcover data produced by SIMPPLLE can be incorporated into SWAT to evaluate the long-term hydrologic response of the stated forest management plans.

METHODS

To evaluate the cascading impact of fire suppression on vegetation and corresponding hydrologic dynamics, two alternative planning strategies, consisting of 30 landcover grids each, were generated to represent 1) unmanaged and 2) fire-suppressed landscape management scenarios, at a decadal time-step for a total of 300 years (i.e. current, 10, 20, 30…). Patterns of landcover proportions, configuration, and associated hydrologic response for the two management scenarios were compared within the research watershed.

STUDY AREA DESCRIPTION

The Tenderfoot Creek research watershed is located on the west slope of the Little Belt Mountains in central Montana, USA (Figure 1). It is a broad basin that is oriented to the northwest, and bisected by a steep canyon along the main channel. An upper reach and two major tributaries on each north and south aspects make up the 2,251 ha area that contributes flow to the main outlet. For representation in SWAT, the watershed was divided into 22 subbasins, and 54 hydrologic response units (HRUs).

Geologically, the watershed's core is basement material set within a mantle of Precambrian age sedimentary rock known as the Belt Series formation (Alt and Hyndman, 1986). The most extensive soil groups are loamy skeletal, mixed Typic Cryochrepts and clayey, mixed Aquic Cryoboralfs (Farnes and McCaughey, 1995).

Forest fire is the main disturbance agent that shapes the vegetation mosaic of this region (Arno and Fiedler 2005). Several large fires between 800 and 1,500 ha in size have occurred in the watershed over the past four centuries but nearly 120 years have elapsed since the last major outbreak (Barrett, 1993). In the long absence of stand replacing disturbances, forest stands of varying developmental stages cover most of the watershed (85%). Approximately 65% of the forest is composed of lodgepole pine (*Pinus contorta*), which generally represent the most recently initiated stands. Over time, shade tolerant subalpine fir (*Abies lasiocarpa*) and Englemann spruce (*Picea engelmannii*) have emerged underneath decadent pine and now make up about 20% of the landcover. Disturbed or low density stands constitute another 11% of the area. Shrubby meadows

(1%) and small riparian areas surround many of the creek bottoms, while drier grasses (1%) occur on higher ground. Talus (2%) frames the main canyon and exposed ridges.

Climate patterns are continental, and close to 70% of the annual precipitation, which averages about 800mm, is deposited in the form of snow between November and May. The annual hydrograph of this watershed is strongly influenced by snowmelt runoff. Peak discharge occurs in May or early June, while the low flow period begins in August and persists through April.

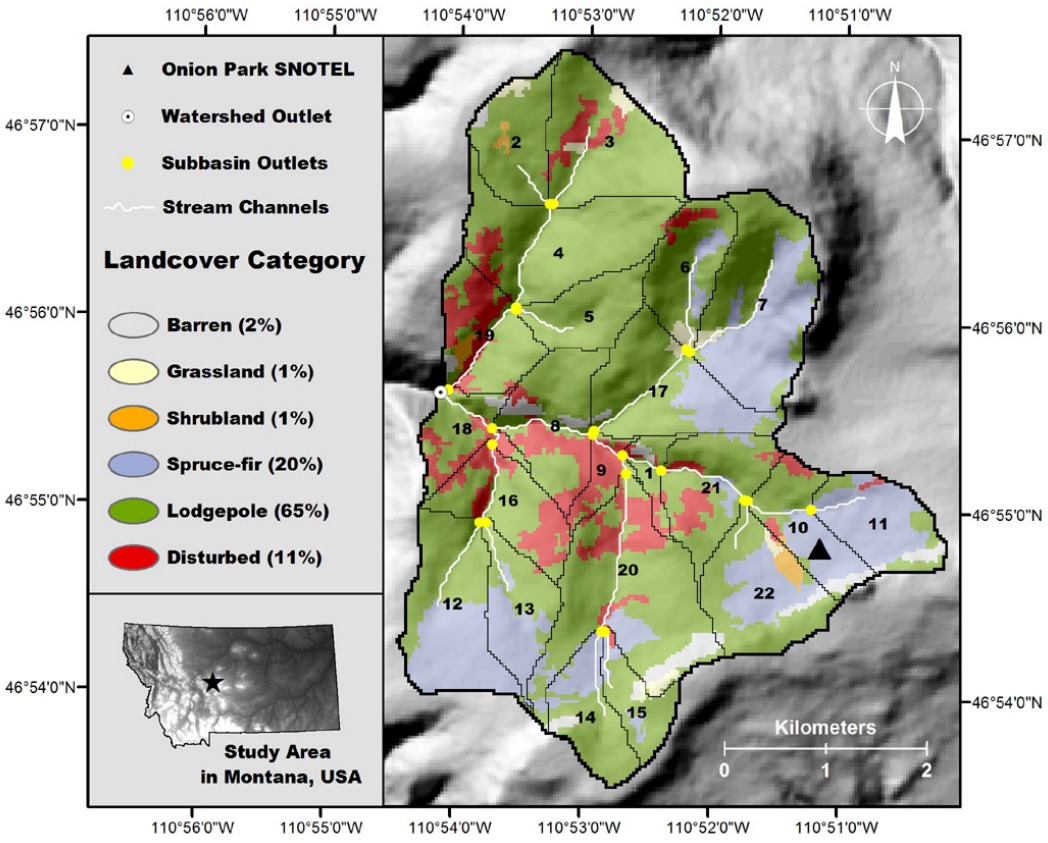

Figure 1. *Delineation, configuration, and landcover characteristics of the Tenderfoot Creek research watershed, located in the Little Belt Mountains of central Montana, USA.*

LANDCOVER SIMULATION

The regionally calibrated SIMPPLLE model (Chew et al., 2004) was used to project current vegetation conditions forward for 300 years of landcover change across

the entire Little Belt Mountain range. Simulated results spanning the research watershed were extracted from the larger spatial extent to account for disturbance process propagation from the surrounding landscape. For every stand, SIMPPLLE characterizes species composition, size class, and canopy coverage, and uses logic to stochastically simulate succession under both natural and planned disturbances. At every time-step, multi-dimensional SIMPPLLE output was reclassified into generalized landcover categories by a conversion algorithm (Figure 2, Appendix A). The resulting classes closely resemble the Level II landcover categories developed by the United States Geological Survey (Anderson et al., 1976), but have been refined to include more detailed differentiation among forest types. Including standard parameterization, each predicted landcover type was attributed with regional estimates of canopy height, minimum and maximum annual leaf area index (LAI), overland roughness (OVN), canopy interception capacity (CANMX), and SCS curve numbers (USDA-SCS, 1972) for use in hydrologic modeling with SWAT (Appendix A).

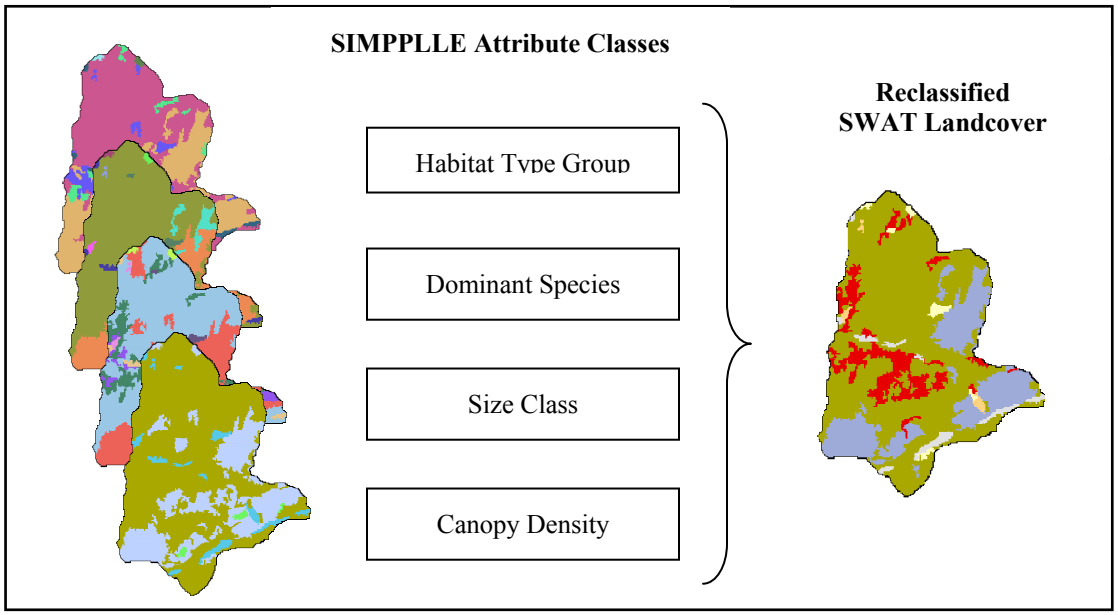

Figure 2. *A diagram of the reclassification algorithm used to convert multi-dimensional stand attributes produced by the SIMPPLLE vegetation simulator into generalized landcover categories.*

COMPARISON OF SIMULATED LANDCOVER SCENARIOS

Multiple response permutation procedures (MRPP) (Mielke and Berry, 2001), and landscape metrics (McGarigal and Marks, 1995) were used to compare the distribution, and spatial pattern of simulated landcover trajectories for the two management scenarios. The MRPP provided nonparametric tests for assessing differences between landcover distributions of scenarios, while variation between landscape-level metrics was quantified with paired-sample t-tests.

Landcover Distribution

The categorical relative watershed area of simulated fire-suppressed and unmanaged landcover was quantified for each of the 30 landcover maps of the two scenarios. Landcover distributions of the 30 time-series maps, produced for each scenario, were compared using 1) MRPP and, 2) comparison of the average watershed area occupied by each type of cover.

Multi-response permutation procedures (MRPP) provide a nonparametric multivariate technique for testing the hypothesis of no difference between two or more groups of entities. MRPP does not require assumptions of normality or homogeneity of variances, making them well suited for analysis of natural resource data (Biondini et al., 1985; Zimmerman et al., 1985). With MRPP, analyses are based on a distance matrix, where treatment alternatives define the groups. Components of this technique yield a test statistic, *p*-value, and associated measure of "effect" size.

The purpose of MRPP is to detect concentration within a priori groups (like a t- or F-test), and the MRPP metric is calculated as:

$$\delta = \sum_{i}^{g} C_i \left(\frac{n_i}{2} \right)^{-1} \sum_{K<L} \left[\sum_{j}^{r} \left(X_{K,j} - X_{L,j} \right) \right]^{u/2} \quad \text{(Eqn. 1)}$$

Where:

δ =	*linear combination of average within-group distance measures for g groups*
C_i =	n_i / N
u =	*distance measure (value of 2 yields squared Euclidian distance)*
r =	*number of measurements taken on the* K^{th} *object (2 in this case)*
K and L	*are objects with measurements* $X_{K,1}, \ldots, X_{K,r}$
n_i =	*number of objects in each group*
N =	*total number of objects over all groups*
g =	*number of groups*

After δ is determined, the probability of obtaining a δ value of this magnitude or smaller is approximated (i.e. the expected delta) from a continuous Pearson Type III distribution. This permutation distribution accommodates datasets that are asymmetrical, and incorporates the mean, standard deviation, and skewness of δ under the null hypothesis (McCuen et al., 2002).

The test statistic, *T*, describes the separation between groups. When calculated, *T* is the difference between the observed and expected deltas divided by the standard deviation of delta:

$$T = \frac{(\delta - m_\delta)}{s_\delta} \quad \text{(Eqn. 2)}$$

where m_δ and s_δ represent the mean and standard deviation of δ under the null hypothesis. In this form, m_δ is taken as the expected delta. Increasingly negative values of *T* indicate stronger separation between groups.

Also based on the Pearson Type III distribution, the *p*-value associated with *T* is useful for evaluating how likely it is that an observed difference is due to random chance, however it is strongly influenced by sample size. To provide a measure of treatment effect size that is independent of the sample size, the chance-corrected within-group agreement statistic, *A*, is calculated as:

$$A = 1 - \frac{\delta}{m_\delta} \quad \text{(Eqn. 3)}$$

This effect size statistic describes within-group homogeneity. When all items are identical within groups, then $A = 1$, the highest possible value. If heterogeneity within groups equals expectation by chance, then $A = 0$. With less agreement within groups than expected, $A < 0$. Put simply, differences between groups become more evident as A gets larger. In community ecology, values for 'A' are commonly below 0.1, even when p-values are significant. Values of $A > 0.3$ are fairly high, and indicative of detectable differences between groups (McCuen et al., 2002).

In this application of MRPP, groups were defined by the fire suppression and unmanaged treatment alternatives, and separation was measured with Euclidian distance. Ultimately, watershed proportions of simulated landcover, spanning 7 possible categories (columns) over 30 time-steps (rows) were compared between the two treatment groups. Principle components analysis (PCA) determined how individual landcover types contributed to treatment differences. Computations necessary to perform MRPP and associated analyses were coded and executed as a Visual Basic for Applications macro in spreadsheet format (King, 2000; Bullen et al., 2003).

Landcover Patterns

Quantification of patterns can be an important component of landscape evaluation and management (Farina, 2000) because landscape configuration can generally be related to ecological processes (Forman and Gordon, 1986; Zonneveld and Forman, 1990). Many metrics have been developed that describe the proportions and configuration of patches, classes of patches, and landscape-level system properties (McGarigal and Marks, 1995). Because each metric measures a specific characteristic of heterogeneity, simultaneous consideration of several indices is often instructive (Gustafson, 1998). Three landscape-level indices were used to describe proportions, aggregation, and connectivity of the current and simulated vegetation mosaic over time. The Largest Patch Index (LPI) measures the percentage of total landscape area comprised by the largest patch. Landscape Shape Index (LSI) values can be interpreted as a measure of patch aggregation; as LSI increases, patches become increasingly disaggregated. Lastly, the Contagion Index (CONTAG) assesses overall landscape clumpiness. When Contagion is high, large clumps exist (Turner et al., 1989; McGarigal and Marks, 1995).

HYDROLOGIC CALIBRATION AND VALIDATION

The Soil and Water Assessment Tool was run from October 1, 1993 to December 31, 2002 using daily precipitation and temperature obtained from a remote snow telemetry station (SNOTEL) located within the watershed. Streamflow data from the gauge that marked the watershed outlet was used to calibrate the model for streamflow. Topography was represented by a 30-m resolution digital elevation model extracted from the National Elevation Dataset (Gesch et al., 2002). Soil characteristics were defined by the State Soil Geographic database for Montana (USDA-NRCS, 1994). Reclassified output from the vegetation simulator was used to depict current and projected landcover within the watershed. The 2,251-ha drainage was configured with 22 subbasins, and 54 hydrologic response units (HRUs). The first two simulation years were used to equilibrate the model, while the years 1997-2000 were used for calibration.

A global sensitivity analysis indicated that the uncalibrated model was most strongly influenced by variation in the snow process, surface runoff lag factor, groundwater, soil and curve number parameters. The model was therefore calibrated with a blend of automated procedures based on the Shuffled Complex Evolution (SCE) algorithm (Duan et al., 1992; van Griensven et al., 2006), and manual refinement that focused on adjustments of these influential parameter sets (Chapter 2).

The calibrated model was validated with two years of data prior and two years beyond the calibration period (1995-96, 2001-02). Results were evaluated graphically and with commonly used goodness-of-fit and performance statistics (ASCE, 1993). For ready comparison to other studies, model performance is described by the Nash-Sutcliffe (1970) coefficient (NS). This performance metric quantifies the similarity between measured and simulated hydrographs, and its values range from negative infinity to a high of 1.0. Coefficients ≤ 0 indicate that simulated output is no better than an average of the observed dataset. Value of ≥ 0.75, however indicate good model performance.

In this study, SWAT2005 was used in conjunction with the AVSWAT interface (Di Luzio et al. 2004). This GIS-based graphical user interface facilitated watershed delineation, subdivision and initial parameterization. AVSWAT also incorporated

sensitivity analysis, auto-calibration, and uncertainty assessment procedures (van Griensven et al. 2006).

Initial model simulations were conducted using default values for most of the model parameters. Potential evapotranspiration (PET) was modeled with the Penman-Monteith algorithm because it uses, in part, canopy height to estimate PET and this made it possible to impart differential values for locally described landcover types. Surface runoff was modeled with the standard SCS Curve Number approach, and the variable storage channel routing method.

HYDROLOGIC COMPARISON OF LANDCOVER SCENARIOS

The calibrated SWAT model was used to simulate streamflow for each of the 30, 10-year time-step landcover maps of both scenarios. For every 10-year representation of landcover, a new SWAT model was established, using the same watershed delineation, sub-watershed configuration, soil, and climate forcing data. Unique landcover patterns in each map required HRUs to be redefined for each map. Calibrated parameters were then assigned to all model elements and SWAT was run from 1993-2002. Use of the same physical inputs ensures that streamflow variability can be unambiguously attributed to changes in landcover. After conducting climate and streamflow analyses, output from a representative year (1999) were used to evaluate differences in timing and magnitude of peak discharge and annual water yield due to landcover composition and distribution.

Hydrographs representing mean daily streamflow of 1999 were constructed for all landcover representations to examine the range of responses to varying vegetation patterns associated with each scenario. Composite hydrographs, computed from each set of 30 10-year time-steps and represented by the mean and standard error of the estimate of streamflow, were compared.

STATISTICAL SIMPPLLE-SWAT LINKAGE

To reduce the landcover and annual water yield modeling process, a statistical relationship between the dominant landcover components and annual water yield was

developed through multiple regression procedures. An established relationship between landcover distribution and annual water yield can be useful. SIMPPLLE estimates vegetation change stochastically, and multiple simulations can be produced with relative efficiency. Output created by SIMPPLLE can be converted into a time-series dataset of mapped landcover. Patterns of landcover can be evaluated based on project specific criteria. With a relationship developed from calibrated SWAT simulations, annual water yield variability can then be inferred, based on estimated landcover patterns. Through automation, this process can be readily repeated, and confidence intervals based on the result of multiple simulations could define the bounds for a large number of evaluation criteria. Multiple, linked simulations thus provide a means for estimating uncertainty.

RESULTS

LANDCOVER DISTRIBUTION

An MRPP test for differences between the 30 representations of 7 landcover classes indicated that the two management scenarios (suppression and unmanaged) produced significantly different landcover distributions ($p < 0.001$, effect size $A = 0.55$). Separation between grouped landcover proportions was distinct, as eigenvalues revealed that the first two principal components accounted for 96% of the variability between the two scenarios. An ordination plot of principal components 1 and 2 illustrates this separation clearly (Figure 3). Positive loadings on principal component 1were driven by differences in lodgepole pine cover types, and captured 91% of the total variability between groups. Principal component 2 was driven primarily by negative loadings associated with shrubland and quaking aspen cover types. Together, proportions of the two cover types only accounted for 1.1% of the variation between grouped landcover scenarios.

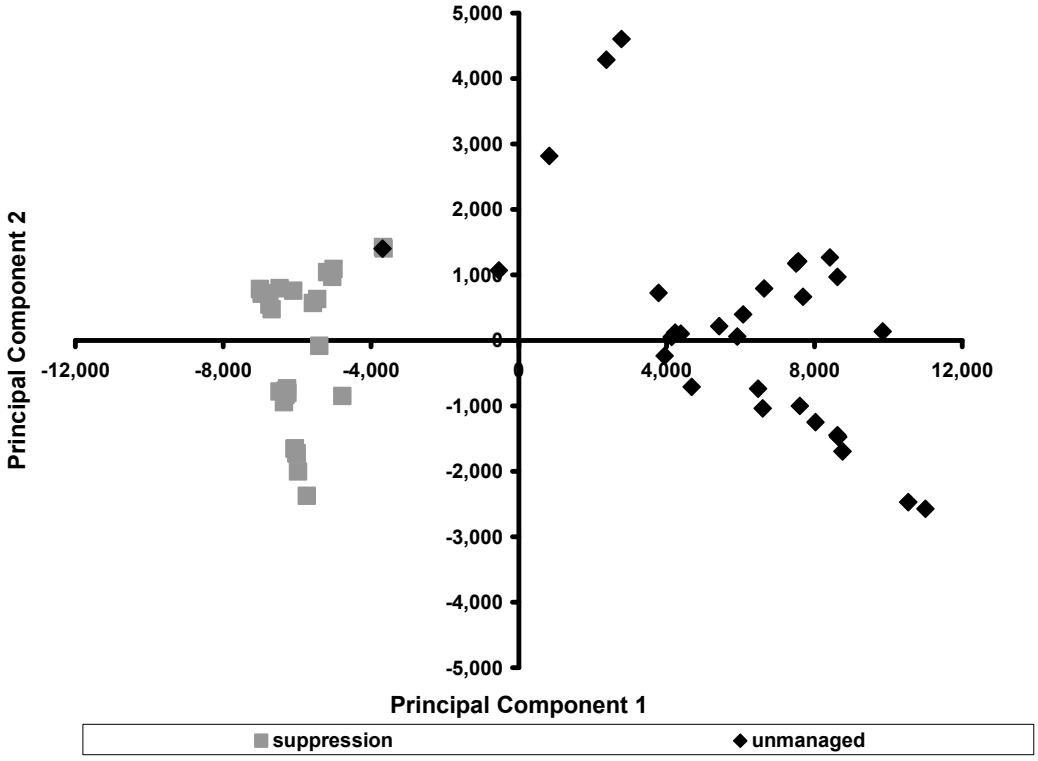

Figure 3. *Plot of the first two principal components responsible for the separation between 30 fire-suppressed and unmanaged landcover simulations scenarios.*

Averaged over the simulation period, the unmanaged landscape was occupied by approximately 50% less total mature forest, 90% more disturbed forest, and 95% more shrubland than the fire-suppressed scenario (Figure 4).

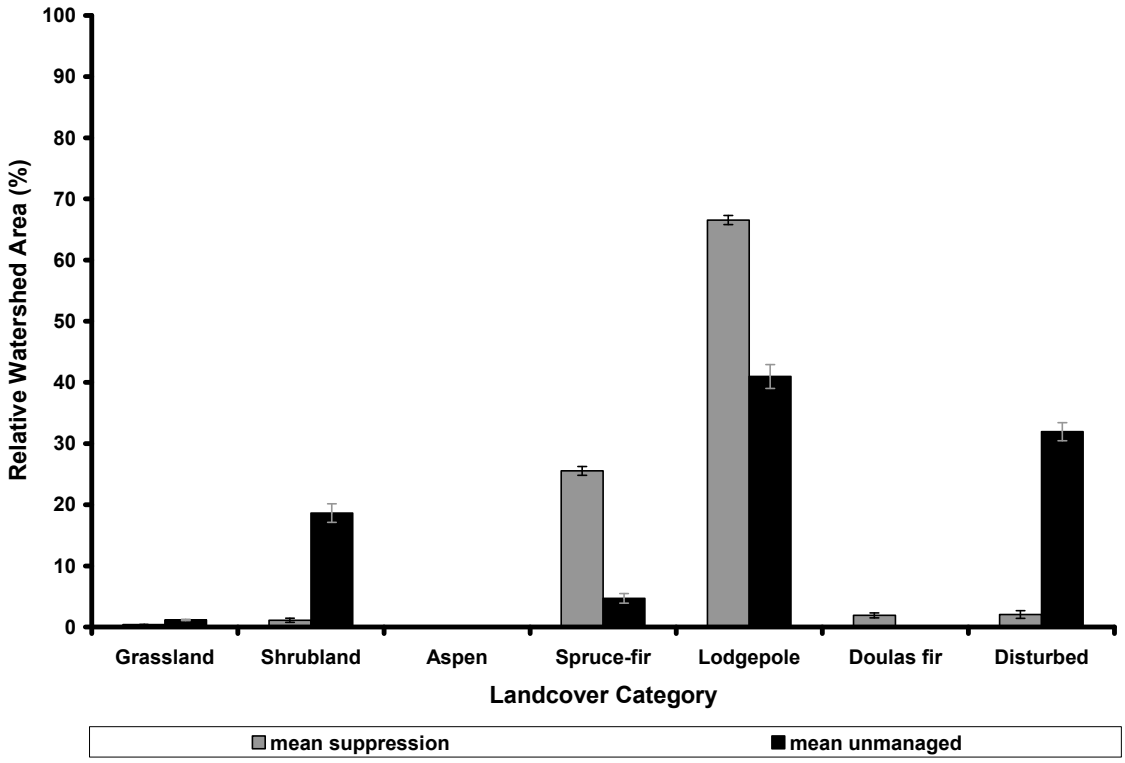

Figure 4. *Mean decadal relative aerial distribution of seven landcover types in the watershed, for fire-suppressed and unmanaged simulation scenarios. Scenario means are based on 30 landcover maps each, and error bars represent the standard error of estimate.*

LANDCOVER CONFIGURATION

Evaluation of spatial patterns, represented by patch size (Largest Patch Index, $p < 0.001$), aggregation (Landscape Shape Index, $p < 0.001$), and clumpiness (Contagion Index, $p < 0.001$) indicated highly significant differences between unmanaged and fire-suppressed landscape scenarios (Table 1).

Table 1. *Comparison of landscape metrics and paired-sample t-test scores for unmanaged and fire-suppressed landcover (n = 30, df = 29, critical t = 2.05).*

Landscape Metric	Suppression Mean and SD.	Unmanaged Mean and SD	t statistic
Largest Patch Index (LPI)	58.9 (9.5)	33.8 (11.0)	9.72
Landscape Shape Index (LSI)	6.2 (0.4)	8.9 (0.8)	-14.23
Contagion Index (CONTAG)	68.9 (3.1)	55.2 (4.0)	12.25

Compared to patterns occurring when vegetation was left to develop naturally, the configuration of fire suppressed landcover was more stable over time, with less cyclical variation in measures of patch size (LPI), aggregation (LSI), and overall clumpiness (CONTAG). Metrics for the unmanaged scenario show three episodes of disturbance, while only one major shift in landcover configuration is evident in the fire suppressed landcover over time. Patches of the unmanaged landcover were smaller (Figure 5), less aggregated (Figure 6), and not as clumpy (Figure 7) as those of the fire-suppressed scenario.

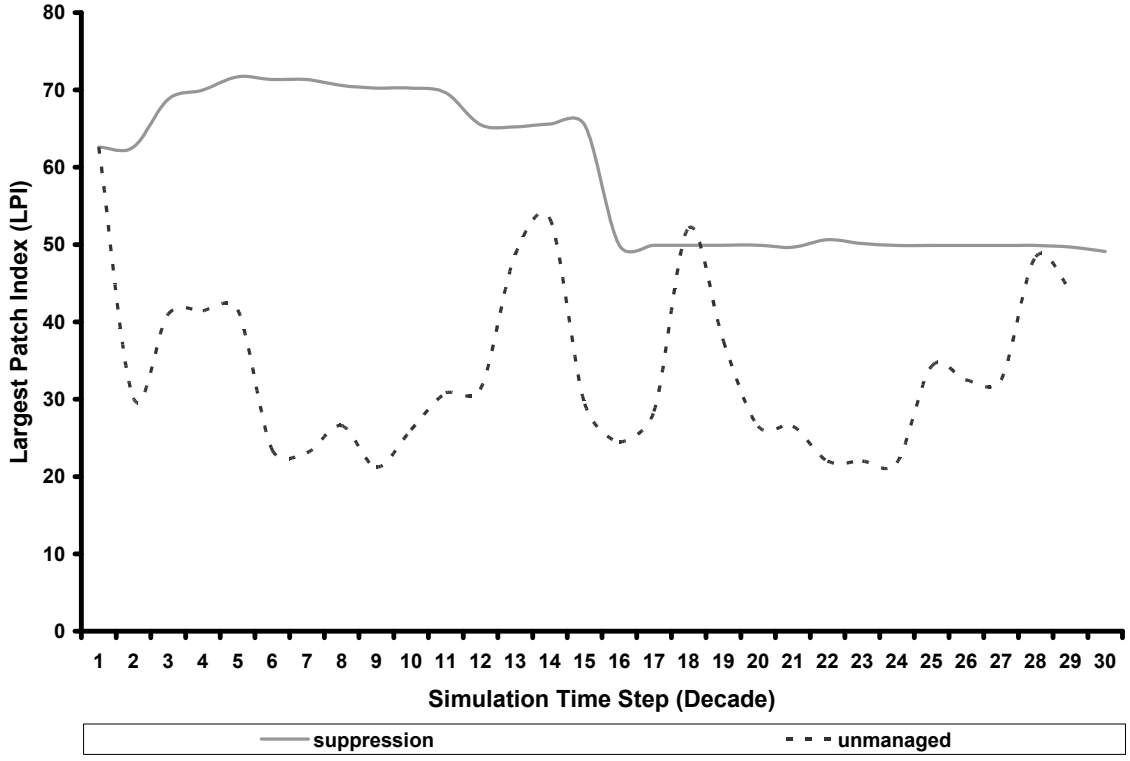

Figure 5. *The Largest Patch Index (LPI) is a measure of landscape proportion occupied by the largest landcover patch (a), where increasing values indicate larger patch sizes.*

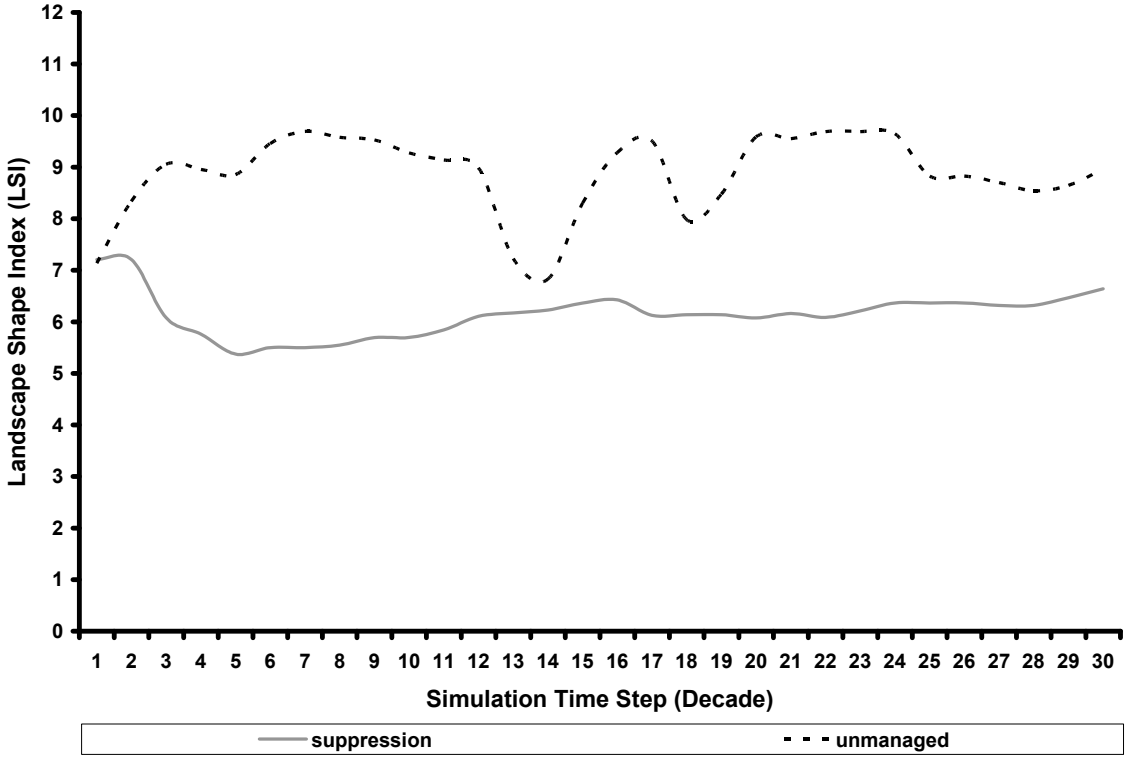

Figure 6. *Landscape Shape Index (LSI) quantifies landcover aggregation (b), where larger values indicate greater levels of disaggregation.*

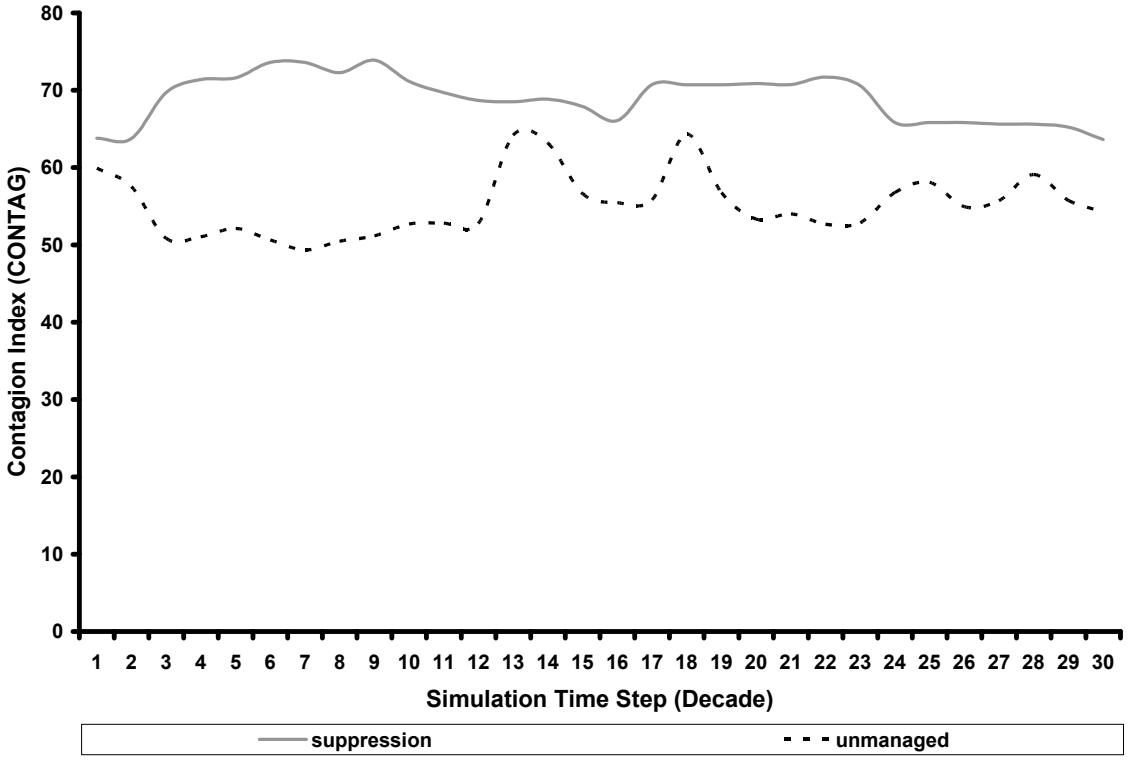

Figure 7. *Contagion Index evaluates the potential for process propagation across landscapes (c), where higher values suggest increasing contagious potential.*

HYDROLOGIC CALIBRATION AND VALIDATION

The calibrated SWAT model produced realistic estimates of annual, monthly, and daily hydrologic patterns over individual years, and the total simulation period. During calibration, SWAT predicted 98% of the measured water yield, with an overall daily Nash-Sutcliffe (1970) model efficiency score (NS) of 0.86. In validation, the model simulated streamflow with a daily NS efficiency of 0.76, and produced 96% of the measured water yield.

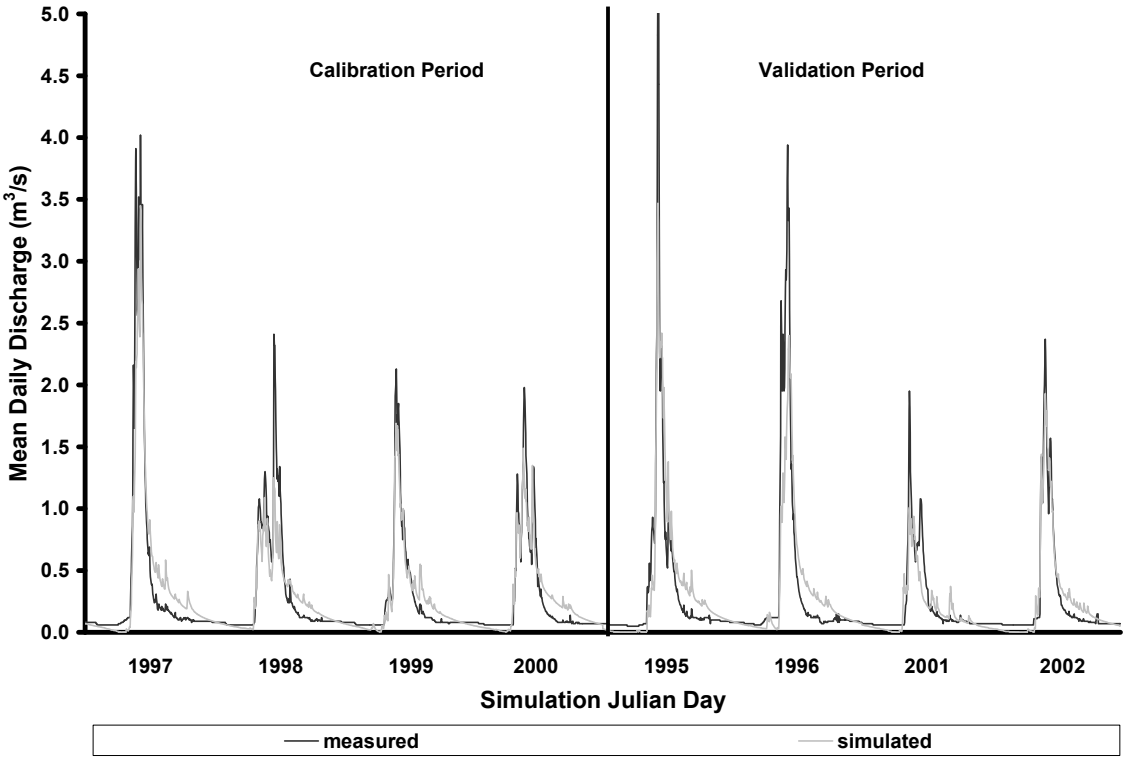

Figure 8. *Mean daily discharge during calibration and validation time periods.*

The mean daily discharge patterns were well matched for both the calibration and validation period although some of the highest runoff rates were underestimated. Specifically, model performance was lower during the recession and baseflow periods of the annual hydrograph (Figure 8).

HYDROLOGIC COMPARISONS

When averaged over the 30 landcover representations the fire suppressed scenario yielded a discharge of 338 mm annually while the unmanaged landscape produced a total annual discharge of 342 mm. While the average difference is only 1%, a paired sample t-test indicated that individual annual differences between the two scenarios were highly significant ($t = -6.08$, $p < 0.001$), where the unmanaged scenario yielded up to 3% (11 mm) more water annually.

Differences in the timing, magnitude and variability of daily discharge were observed between the two scenarios. Runoff generally rose approximately 15% higher (Figure 9) and was four times more variable in the unmanaged landscape over the 30 landcover scenarios than fire suppressed ones (Figure 10).

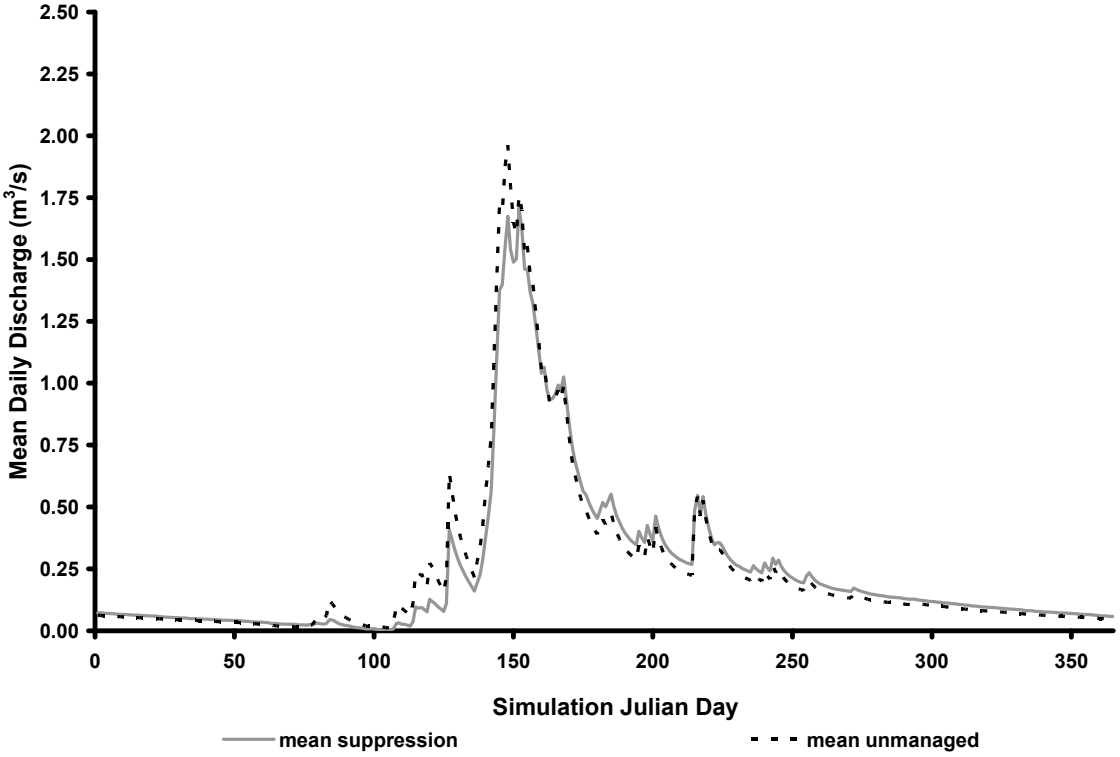

Figure 9. *Comparison of 1999 mean daily hydrographs for 30 simulations of fire suppressed and unmanaged landcover scenarios.*

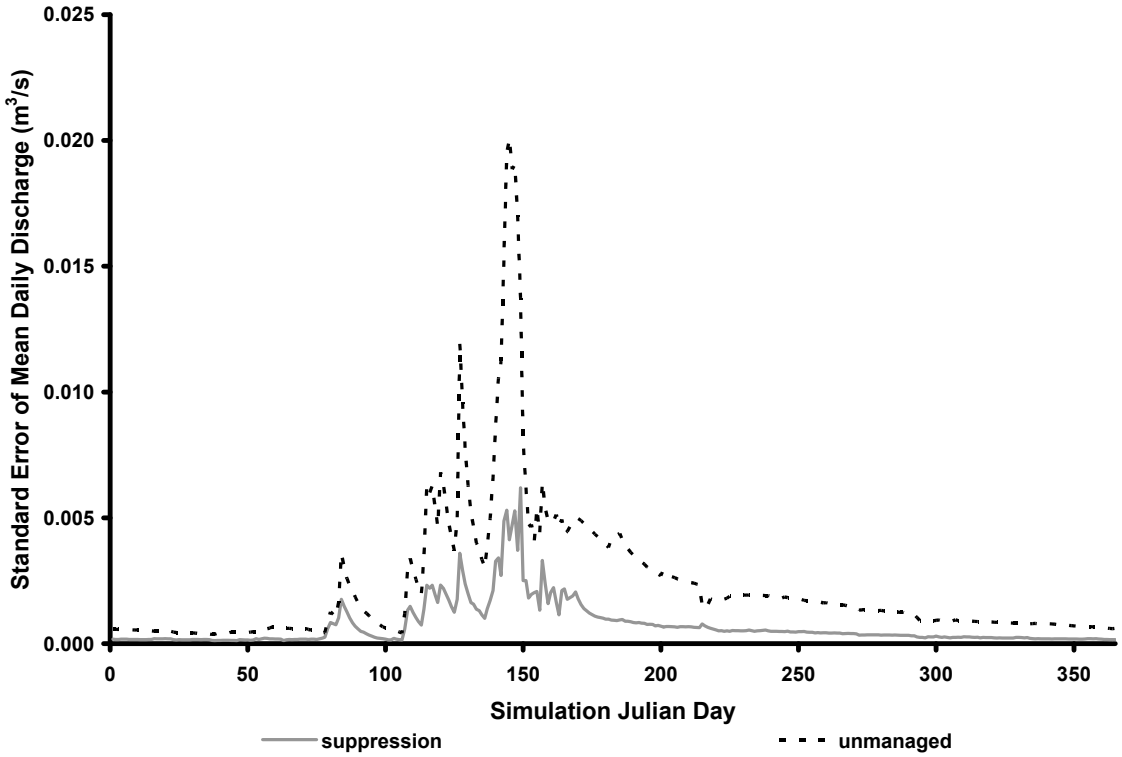

Figure 10. *Comparison of 1999 mean daily streamflow variability for 30 simulations of fire suppressed and unmanaged landcover, measured by the standard error of estimate.*

LANDCOVER - WATER YIELD REGRESSION MODEL

Data from the unmanaged landscape scenario were used to develop a prediction equation where annual water yield predicted by SWAT for the representative year (1999) is a function of relative watershed area of dominant landcover components in each of the 30 grids produced by SIMPPLLE. Multiple regression (n =30) revealed a highly significant relationship ($p < 0.0001$) between water yield and three landcover components. The regression model, based on proportions of spruce-fir (SFFR), lodgepole pine (LPFR), and disturbed forest (TRNS) for every landcover time-step captured 96% of the variation in predicted water yield SWAT. Variance inflation factors for SFFR, LPFR, and TRNS were all less than 10, indicating no evidence of collinearity (Table 2).

Table 2. *Regression model (REGMOD) summary, for annual water yield predictions of the year 1999 based on landcover proportions, where SFFR, LPFR, and TRNS represent relative watershed areas occupied by spruce-fir, lodgepole pine, and disturbed forest.*

annual water yield (mm) = 306.939 + 0.222 SFFR + 0.354 LPFR + 0.615 TRNS	
Adjusted Pearson R2	0.961
Standard Error of the Estimate	0.620
Variance Inflation Factor	SFFR = 1.382
	LPFR = 2.515
	TRNS = 2.623

Over the 30 representations of landcover the difference between the total water yield predicted by SWAT and the regression model (REGMOD) was less than 1 mm. The temporal distribution of SWAT and REGMOD water yield estimates also tracked one another very well (Figure 11).

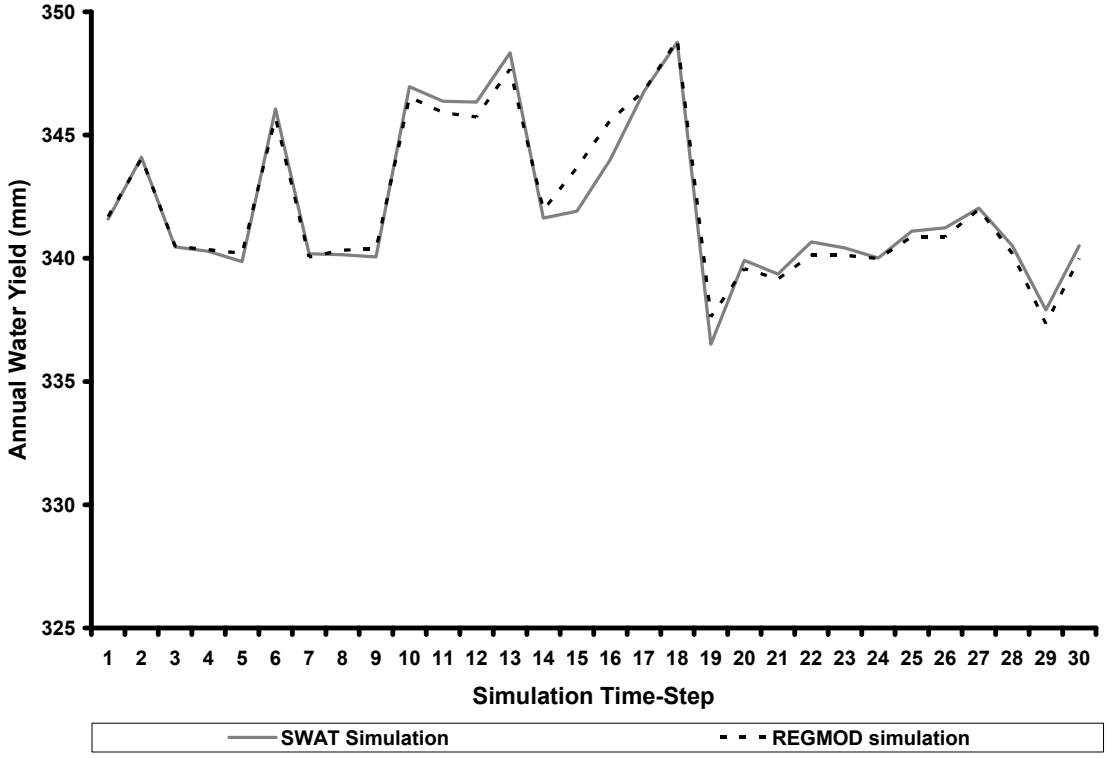

Figure 11. *Comparison of 1999 water yield predictions from the SWAT and REGMOD models for each of 30 landcover representations.*

DISCUSSION

The extent, composition and configuration of forests within a watershed can exert strong controls on terrestrial and hydrologic processes. Because the effects of forest management on these resources can be significant and long lasting, modeling procedures are necessary to evaluate various alternatives before actions are implemented to ensure that societal values are maintained over time.

Fire is the dominant natural agent of change in western North America's forests, and the long-term effects of fire suppression are of great interests to forest, wildlife, and water resource managers. Adaptive management is a process where actions and policies are based on the best available knowledge and implemented to produce new information that can inform future actions (Stankey et al., 2003). Methods described in this study offer a process that integrates existing vegetation and hydrologic models, and allows users to evaluate the expected terrestrial and aquatic consequences of proposed forest management alternatives before they are initiated, so that costly mistakes can be avoided. Although model output should be interpreted in a relative sense, the ability to experiment with and assess various strategies before implementing them reduces the likelihood that poorly planned actions will have negative, unforeseen impacts on valuable or scarce resources. Results of the modeling procedures can be synthesized by landscape ecology, hydrology and aquatic biology specialists to form an integrated assessment of proposed land management alternatives (Jakeman and Letcher, 2003).

The central theorem of landscape ecology is that patterns and processes are directly related to one another (Forman and Gordon, 1986). Comparison of the landcover simulations indicates that the fire-suppressed landscape has landcover patterns that are significantly different than those of the unmanaged scenario. Mature forests occupy almost twice as much land, and the patches of cover tend to be larger and more continuous in the fire suppressed landscape than those of the unmanaged scenario, and this is generally supported by contemporary knowledge (Keane et al., 2002). Although only three landscape indices that interpret the extent, composition, and configuration of landcover were investigated, specialists may analyze patterns that are relevant to specific resources given the reclassified output.

From a hydrologic perspective, modeling results are encouraging because they are within the realm of what other investigations have found through experimental manipulation and long-term observation (Trondle and King, 1985, 1987), and modeling in other parts of the Rocky Mountain region (Matheussen et al. 2000). In general, results show that landcover composition, especially the proportion of disturbed forest strongly influenced basin-level hydrologic response. Compared to the fire-suppressed scenario, mean annual water yield was up to 3% (11 mm) greater in the unmanaged landcover simulations. Annual peaks tended to occur earlier, and were on average 15% greater and approximately 4 times more variable in the unmanaged scenario (Figures 6a, b).

Development of a prediction relationship between the hydrologic response and simulated landcover has great potential because, once established, it essentially calibrates SWAT to SIMPPLLE for annual output. In doing so, analysts need only run landscape scenarios to get estimates of water yield and this reduces the model set up time and computational resources required to assess the long term impact of forest management on water resources. Furthermore, SIMPPLLE stochastically simulates vegetation processes, and to produce estimates of uncertainty, the model can be run multiple times to yield ensembles of potential landcover responses to management. With the estimation link, corresponding uncertainty in hydrologic response may be assessed as well without the need for more detailed hydrologic modeling.

CONCLUSIONS

Integrated assessment recognizes that management of one resource may have cascading impacts on associated resources. The effects of forest management on ecosystem function can be profound and long lasting. To ensure that societal values are maintained over the long-term, various alternatives should be assessed before management actions are implemented to avoid degradation of valuable resources.

The purpose of this study was to illustrate how two distinct but complementary modeling systems can be combined to conduct an integrated assessment of land and water resource management in a watershed. While comparison of management scenarios should be viewed in a relative sense, model results show that after calibration both land

and water resource simulations are likely to produce reasonable output. Depending on the complexity of desired analyses, the modeling process can be simplified by not only calibrating tools to environmental conditions, but also to one another. An established linkage between models can reduce the time and resources required to perform exhaustive evaluations because output from one model can be used to predict outcomes of the other model.

In this study, the relationship between landcover distribution and predicted water yield suggests that upon calibration to initial conditions, landcover proportions may be used to predict annual water yield for a chosen year. In this way, a predictive equation can be applied to simulated landcover patterns and used to derive estimates of annual hydrologic output.

LITERATURE CITED

Alt, D. and D.W. Hyndman. 1986. Roadside Geology of Montana. Mountain Press, Missoula, MT.

Arno, S.F. and C.E. Fiedler, 2005. Mimicking Nature's Fire: Restoring Fire-Prone Forests in the West. Island Press, Washington, D.C.

Arnold, J.G., R. Srinivasan, R.S. Muttiah, and J.R. Williams. 1998. Large area hydrologic modeling and assessment part I: Model development. Journal of the American Water Resources Association 34(1): 73-89.

ASCE, 1993. Criteria for evaluation of watershed models. Journal of Irrigation and Drainage Engineering 119(3): 429-442.

Barrett, S. W. 1993. Fire History of Tenderfoot Creek Experimental Forest, Lewis and Clark National Forest. Systems for Environmental Management, Research Joint Venture Agreement No. INT-92679-RJVA.

Biondini, M.E., C.D. Bonham, E.F. Redente. 1985. Secondary successional patterns in a sagebrush (*Artemisia tridentata*) community as they relate to soil disturbance and soil biological activity. Plant Ecology 60(1): 25-36.

Bosch, J.M. and J.D. Hewlett. 1982. A review of catchment experiments to determine the effect of vegetation changes on water yield and evapotranspiration. Journal of Hydrology 55: 3-23.

Bullen, S., J. Bovey, and R. Rosenberg. 2003. EXCEL 2002 VBA: Programmer's Guide. Wiley Pub. Co. Indianapolis IN.

Chew, J.D., K. Moeller, C. Stalling, E. Bella, and R. Ahl. 2002. Simulating Patterns and Processes at Landscape Scales: User Guide for SIMPPLLE V2.2. U.S. Department of Agriculture, Forest Service, Rocky Mountain Research Station, Forest Ecology and Management, Missoula, MT.

Chew, J.D., C. Stalling, and K. Moeller. 2004. Integrating knowledge for simulating vegetation change at landscape scales. Western Journal of Applied Forestry 19(2): 102-108.

Di Luzio, M., R. Srinivasan, and J.G. Arnold. 2004. A GIS-coupled hydrological model system for the watershed assessment of agricultural nonpoint and point sources of pollution. Transactions in GIS 8(1): 113-136.

Farnes, P.E. and W.W. McCaughey. 1995. Hydrologic and geologic characterization of Tenderfoot Creek Experimental Forest, Montana. Unpublished Report. U.S. Department of Agriculture, Forest Service, Rocky Mountain Research Station, Forestry Sciences Laboratory, Bozeman, MT. 200 pp.

Farnes, P. E., W.W. McCaughey, and K.J. Hansen. 2000. Role of Fire in Determining Annual Water Yield in Mountain Watersheds. *In* After the Fires: The Ecology of Change in Yellowstone National Park. Yale University Press, New Haven.

Forman, R.T.T. and M. Gordon. 1986. Landscape Ecology. John Wiley and Sons, New York.

Gesch, D., M. Oimoen, S. Greenlee, C. Nelson, M. Steuck, and D. Tyler. 2002. The National Elevation Dataset. Photogrammetric Engineering and Remote Sensing 68(1): 5-11.

Golding, D.L. and R.H. Swanson. 1978. Snow accumulation and melt in small forest openings in Alberta. Canadian Journal of Forest Research 8(4): 380-388.

Jakeman, A.J. and R.A. Letcher. 2003. Integrated assessment and modelling: features, principles and examples for catchment management. Environmental Modeling and Software 18(6): 491-501.

Keane, R.E., K.C. Ryan, T. Veblen, C. Allen, J. Logan, and B. Hawkes. 2002. Cascading effects of fire exclusion in Rocky Mountain ecosystems: A literature review. U.S. Department of Agriculture-Forest Service, Rocky Mountain Research Station, General Technical Report RMRS-GTR-91.

Kimmins, J.P. 1997. Forest Ecology: A foundation for sustainable management. Prentice-Hall, Upper Saddle River, NJ.

King, R. 2000. Comparison of simulation results among EXCEL worksheets using MRPP. U.S. Department of Agriculture, Forest Service, Rocky Mountain Research Station, Statistics Unit, Fort Collins, CO.

Matheussen, B., R.L. Kirchbaum, I.A. Goodman, G.M. O'Donnell, and D.P. Lettenmaier. 2000. Effects of landcover change on streamflow in the Interior Columbia River Basin (USA and Canada). Hydrological Processes 14(5): 867-885.

McCune, B., G. James, D.L Urban. 2002. Analysis of Ecological Communities. MJM Software Design. ISBN 0-9721290-06.

McGarigal, K. and B. J. Marks. 1995. FRAGSTATS: Spatial pattern analysis program for quantifying landscape structure. U.S. Department of Agriculture, Forest Service, General Technical Report PNW-351.

McLain, R.J. and R.G. Lee. 1996. Adaptive management: Promises and pitfalls. Environmental Management 20(4): 437-448.

Mielke, P.W. Jr. and K.J. Berry. 2001. Permutation Methods: A Distance Function Approach. Springer-Verlag, New York. 352 pp.

Nash, J.E. and J.V. Sutcliffe. 1970. River flow forecasting through conceptual models part I: A discussion of principles. Journal of Hydrology 10(3): 282-290.

Neitsch, S.L., J.G Arnold, J.R Kiniry, J.R Williams, and K.W. King. 2002. Soil and Water Assessment Tool Theoretical Documentation, Version 2000. Texas Water Resources Institute, College Station, Texas, TWRI Report TR-191, GSWRL Report 02-01, BRC Report 02-05.

Pfister, R. D., B.L. Kovalchik, S.F. Arno, and R.C. Presby. 1977. Forest Habitat Types of Montana. U.S. Department of Agriculture, Forest Service, General Technical Report INT-34. 174 pp.

Stankey, G.H., B.T. Bormann, C. Ryan, B. Shindler, V. Sturtevant, R.N. Clark, and C. Philpot. 2003. Adaptive Management and the Northwest Forest Plan: Rhetoric and Reality. Journal of Forestry 101(1): 40-46.

Stednick, J.D. 1996. Monitoring the effects of timber harvest on annual water yield. Journal of Hydrology 176(1): 79-95.

Troendle, C.A. 1983. The potential for water yield augmentation from forest management in the Rocky Mountains. Water Resources Bulletin 19(3): 359-373.

Troendle C.A. and R.M. King, 1985. The effect of timber harvesting on the Fool Creek watershed, 30 Years Later. Water Resources Research 21(12): 1915-1922.

Troendle, C.A. and R.M. King. 1987. The effect of partial and clearcutting on streamflow at Deadhorse Creek, Colorado. Journal of Hydrology 90(1/2): 145-157.

USDA-NRCS (U.S. Department of Agriculture, Natural Resource Conservation Service). 1994. State Soil Geographic Data base (STATSGO): Data Use Information. U.S. Department of Agriculture, National Soil Survey Center Miscellaneous Publication Number 1492. 113 pp.

USDA-SCS (U.S. Department of Agriculture, Soil Conservation Service), 1972. SCS National Engineering Handbook, Section 4, Hydrology. Chapter 10, Estimation of Direct Runoff from Storm Rainfall. U.S. Department of Agriculture, Soil Conservation Service, Washington D.C. p. 10.1-10.24.

Zimmerman, G.M., H. Goetz, and P.W. Mielke Jr. 1985. Use of an improved statistical method for group comparisons to study effects of prairie fire. Ecology 66(2): 606–611.

APPENDIX A

Scaled Multi-Attribute Classification (SMAC)

SIMPPLLE-SWAT LANDCOVER RECLASSIFICATION

The SIMPPLLE vegetation simulator (Chew et al., 2004) uses detailed landcover descriptions derived from a diversity of sources. Vegetation is defined by stand-level inventory data whenever possible. When full coverage is not available, remotely derived 30-meter satellite data are used to supplement missing information. Topographically derived (modeled from DEM) Habitat Type groups are used to parameterize broad potential vegetation groups. The combination of vegetative and topographic data is used to define SIMPPLLE vegetation community habitat type group, species, size-class, and canopy density attributes.

The vegetation dynamics model uses the detailed stand attributes to simulate succession and disturbance processes across the landscape. At every time step of the model, stand attribute data are written to text files that can be joined to the original vegetation data layer. Vegetation change is reported at ten year intervals. Species composition, stand size-class, canopy density, and disturbance processes are updated at every step of the model.

There is a considerable difference between the level of description required to simulate vegetation change and that needed to model hydrologic processes. In comparison to SIMPPLLE, the SWAT model (Arnold et al., 1998) does not need multi-level stand characterization. Therefore, the detailed information that SIMPPLLE carries is reclassified into general landcover categories. In a general sense, the reclassification is based on the Anderson Level II Landcover Classification supported by USGS (Anderson et al., 1976). The watersheds being simulated in this study have a large proportion of forested area, and to refine the modeling of hydrologic response to vegetation change, the number of forest categories has been expanded. In addition to increasing the diversity of forest types, forest disturbances have also been included in the reclassification. The Anderson Level II TRANSITIONAL landcover is passed on to forested vegetation communities that are in a state of disturbance that reduced canopy closure and / or replaced the stand, as in the event of high-intensity fire or severe insect or disease damage.

The satellite imagery used to supplement inventory data is composed of many scenes and was collected to avoid cloud contamination. There are nonetheless, scenes with some cloud spottiness and landcover data have not been defined where clouds exit. In these cases, No Data values have been assigned. The No Data landcover carries the same hydrologic characteristics as the BARREN landcover. This was done to avoid assignment of erroneous vegetation characteristics. The down-side of this hydrologic characterization is that some overestimation of water and sediment yield may occur if large areas are contaminated by clouds.

The following are lookup tables and logic used to convert SIMPPLLE vegetation output to landcover maps used by the SWAT hydrologic model. Resulting, raster-based maps can also be analyzed for spatial patterns, and associated with multiple resources values, not only hydrologic function.

Table 1. *Habitat Type reclassification lookup table.*

SIMP_HTG	HTG_RCLS
A1	FOREST
A2	FOREST
B1	FOREST
B2	FOREST
B3	FOREST
C1	FOREST
C2	FOREST
D1	FOREST
D2	FOREST
D3	FOREST
E1	FOREST
E2	FOREST
F1	FOREST
F2	FOREST
G1	FOREST
G2	FOREST
ND	ND
NF	NON-FOREST
NF1	NON-FOREST
NF2	NON-FOREST
NF3	NON-FOREST
NF4	NON-FOREST
NF5	NON-FOREST
NF1A	NON-FOREST
NF1B	NON-FOREST
NF1C	NON-FOREST
NF2A	NON-FOREST
NF2B	NON-FOREST
NF2C	NON-FOREST
NF2D	NON-FOREST
NF3C	NON-FOREST
NF3D	NON-FOREST
NF4E	NON-FOREST
NF5A	NON-FOREST
XX1	NON-FOREST
XX2	NON-FOREST
XX3	NON-FOREST
XX4	NON-FOREST
XX5	NON-FOREST

Table 2. *SIMPPLLE Species reclassification lookup table.*

SIMP_SPP	SPP_RCLS
ND	ND
NF	BARREN
WATER	WATER
AGR	PASTURE
AGSP	GRASSLAND
ALPINE-GRASSES	GRASSLAND
ALPINE-HERBS	GRASSLAND
ALPINE-SHRUBS	GRASSLAND
ALTERED-GRASSES	GRASSLAND
ALTERED-NOXIOUS	GRASSLAND
EARLY-SERAL	GRASSLAND
FESCUE	GRASSLAND
HERBS	GRASSLAND
JUSC-AGSP	GRASSLAND
JUSC-ORMI	GRASSLAND
LATE-SERAL	GRASSLAND
MID-SERAL	GRASSLAND
NATIVE-FORBS	GRASSLAND
NOXIOUS	GRASSLAND
UPLAND-GRASSES	GRASSLAND
FS-S-G	SHRUBLAND
GA	SHRUBLAND
JUSC	SHRUBLAND
MAHOGANY	SHRUBLAND
MESIC-SHRUBS	SHRUBLAND
MTN-FS-SHRUBS	SHRUBLAND
MTN-MAHOGANY	SHRUBLAND
MTN-SHRUBS	SHRUBLAND
XERIC-FS-SHRUBS	SHRUBLAND
XERIC-SHRUBS	SHRUBLAND
NS	OPEN_FOREST
WOODLAND	OPEN_FOREST
RIPARIAN-GRASSES	RIPARIAN_SHRUB
RIPARIAN-SHRUBS	RIPARIAN_SHRUB
RIP-GRAMS	RIPARIAN_SHRUB
RIP-S-GRAMS	RIPARIAN_SHRUB
RIP-DECID	RIPARIAN_FOREST
RIP-DECID-MC	RIPARIAN_FOREST
CW	RIPARIAN_FOREST
CW-MC	RIPARIAN_FOREST
QA	QA
QA-MC	QA

SIMP_SPP	SPP_RCLS
AF	SFFR
AF-ES-LP	SFFR
ES	SFFR
ES-AF	SFFR
ES-LP	SFFR
WB	SFFR
WB-AF	SFFR
WB-ES	SFFR
WB-ES-AF	SFFR
WB-ES-LP	SFFR
LP	LP
LP-AF	LP
PF	LP
PF-LP	LP
DF	DF
DF-AF	DF
DF-AF-ES	DF
DF-ES	DF
DF-LP	DF
DF-LP-AF	DF
DF-LP-ES	DF
DF-PP-LP	DF
DF-PP-PF	DF
PP	PP
PP-DF	PP

Table 3. *SIMPPLLE Size-Class reclassification lookup table.*

SIMP_SIZE	SIZE_RCLS
NS	NON-FOREST
UNIFORM	NON-FOREST
SCATTERED	NON-FOREST
CLUMPED	NON-FOREST
OPEN-HERB	NON-FOREST
CLOSED-HERB	NON-FOREST
OPEN-LOW-SHRUB	NON-FOREST
CLOSED-LOW-SHRUB	NON-FOREST
OPEN-MID-SHRUB	NON-FOREST
CLOSED-MID-SHRUB	NON-FOREST
OPEN-TALL-SHRUB	NON-FOREST
CLOSED-TALL-SHRUB	NON-FOREST
SS	TRANSITIONAL
POLE	FOREST
PTS	FOREST
PMU	FOREST
MEDIUM	FOREST
MTS	FOREST
MMU	FOREST
LARGE	FOREST
LTS	FOREST
LMU	FOREST
VERY-LARGE	FOREST
VLTS	FOREST
VLMU	FOREST
AGR	PASTURE
NF	BARREN
WATER	WATER

Table 4. *SIMPPLLE Canopy Density reclassification lookup table.*

SIMP_DENSITY	DENSITY_RCLS
1	NON-FOREST
2	FOREST
3	FOREST
4	FOREST

Table 5. *Reclassified Grid reclassification lookup table.*

VALUE	LANDUSE
1	NNDD
2	BRRN
3	WATR
4	PSTR
5	GLND
6	SLND
7	OPFR
8	RIPS
9	RIPF
10	QAFR
11	SAFR
12	LPFR
13	DFFR
14	PPFR
15	TRNS

RECLASSIFICATION PROCEDURE

Use the original vegetation coverage and update text file to reclassify SIMPPLLE attributes to general landcover attributes used by SWAT. For the landscape current condition the COVERNAME-0-UPDATE table is used. For all subsequent time steps the COVERNAME-1-UPDATE tables are used. The number preceding the update table indicates the time step.

An Arc/Info program, called "SMAC.aml" automated this reclassification sequence.

Repeat steps for each time-step, the number symbol (#) refers to time-step

- Copy input vegetation coverage and call it "rclsc-cov#"
- Edit "rclsc-cov#" table and add text field called "SWAT_COVER" for SWAT codes
- Join SIMPPLLE run output "Update#", use "SLINK" as join field
  (*# indicates time step*)
- Join "HTG_RCLS.DBF" table, use "SIMP_HTG" as join field
  (*the reclassification table is joined to the coverage, where a SIMP_HTG field exists*)
- Join "SPP_RCLS.DBF" table, use "SIM_SPECIES" as join field
  (*the reclassification table is joined to the already joined UPDATE table, where a SIM_SPECIES field exists – notice the difference between SIM and SIMP*)
- Join "SIZE_RCLS.DBF" table, use "SIM_SIZE" as join field
  (*the reclassification table is joined to the already joined UPDATE table, where a SIM_SIZE field exists – notice the difference between SIM and SIMP*)
- Join "DENSITY_RCLS.DBF" table, use "SIM_CANOPY as join field
  (*the reclassification table is joined to the already joined UPDATE table, where a SIM_CANOPY field exists – notice the difference between SIM and SIMP*)
- Do manually or use Arc/Info aml, "SMAC", to apply reclassification logic and calculate new attributes to "SWAT_COVER" field (*use of aml is recommended*)
- After the "SWAT_COVER" field has been populated the coverage is converted to grid format, using the "SWAT_COVER" field as attributes. (*also automated by aml*)
- Optionally, LANDUSE_LUT.DBF table can be then joined to the landcover grid. The attributes in the lookup table are descriptions of the landcover codes used by SWAT to link to supporting databases. (*also automated by aml*)

LANDCOVER DESCRIPTION AND RECLASSIFICATION LOGIC

NO DATA

This landcover is the result of clouds in remotely sensed imagery. Clouds block the view of surface features and make it impossible to determine accurate landcover characteristics.

Reclassification Logic

NO DATA		
IF	SIMP_HTG	ND
	SPP_RCLS	ND
THEN	SWAT COVER	**NNDD**
	VALUE	**1**

BARREN

The barren landcover represents bare ground, rocky areas, above tree line conditions, and any land condition that is not cloud, water or vegetation.

Reclassification Logic

BARREN		
IF	HTG_RCLS	NON-FOREST
	SPP_RCLS	BARREN
	SIZE_RCLS	BARREN
	DENSITY_RCLS	NON-FOREST
THEN	SWAT COVER	**BRRN**
	VALUE	**2**

WATER

The spectral signature of water is relatively easy to distinguish from bare ground or vegetated surfaces.

Reclassification Logic

WATER		
IF	HTG_RCLS	NON-FOREST
	SPP_RCLS	WATER
	SIZE_RCLS	WATER
	DENSITY_RCLS	NON-FOREST
THEN	SWAT COVER	**WATR**
	VALUE	**3**

PASTURE

Agricultural land is broadly reclassified as pasture.

Reclassification Logic

PASTURE		
IF	HTG_RCLS	NON-FOREST
	SPP_RCLS	AGR
THEN	SWAT COVER	**PSTR**
	VALUE	**4**

GRASSLAND

The grassland cover type designation encompasses all forms of grasses and herbs. No distinction is made between mesic and xeric conditions.

Reclassification Logic

GRASSLAND		
IF	SPP_RCLS	GRASSLAND
	SIZE_RCLS	NON-FOREST
THEN	SWAT COVER	**GLND**
	VALUE	**5**

SHRUBLAND

The shrubland cover type is assigned to stands that are naturally considered shrub given their species and size class designations.

Reclassification Logic

SHRUBLAND (NON-FORESTED)		
IF	SPP_RCLS	SHRUBLAND
	SIZE_RCLS	NON-FOREST
THEN	SWAT COVER	**SLND**
	VALUE	**6**

OPEN FOREST

The 'Open Forest' landcover is also assigned to open stands composed of forest species, which occur on non-forest habitat type groups, but are not dense enough to be considered forest stands. These types of stands tend to occur on the driest upland sites that are capable of supporting trees.

Reclassification Logic

OPEN-FOREST (TREED SHRUBLAND)		
IF	HTG_RCLS	NON-FOREST
	SPP_RCLS	SAF
		LP
		DF
		PP
		QA
	SIZE_RCLS	FOREST
THEN	SWAT COVER	**OPFR**
	VALUE	**7**

RIPARIAN SHRUB

The USGS Andersen Level II classification differentiates between woody and herbaceous riparian areas. Following this logic I separated riparian vegetation into shrub and forest communities. The 'riparian shrub' landcover is composed of riparian grasses, shrubs, and grammanoid species.

Reclassification Logic

RIPARIAN SHRUB		
IF	SPP_RCLS	RIPARIAN_SHRUB
THEN	SWAT COVER	**RIPS**
	VALUE	**8**

RIPARIAN FOREST

Landcover defined as 'riparian forest' consists of cottonwood and cottonwood / mixed conifer stands.

Reclassification Logic

RIPARIAN FOREST		
IF	SPP_RCLS	RIPARIAN_FOREST
THEN	SWAT COVER	**RIPF**
	VALUE	**9**

QUAKING ASPEN FOREST

When stands occur on either forest or non-forest habitat type groups, have stand structure indicative of forest communities, and dominated by quaking aspen, or combinations thereof, they are reclassified to the 'quaking aspen forest' landcover. Although dominant in the stand, quaking aspen may occur in combination with mixed conifers.

Reclassification Logic

QUAKING ASPEN FOREST		
IF	SPP_RCLS	QA
	SIZE_RCLS	FOREST
	DENSITY_RCLS	FOREST
THEN	SWAT COVER	**QAFR**
	VALUE	**10**

SPRUCE-FIR FOREST

The 'sub-alpine forest' landcover category encompasses the broadest range of forest species assemblages of all the forest landcover types. The relative abundance of any one species, or species combinations within this broad category tend to be fairly low in a given landscape, occur occupy similar niches, and were therefore collapsed into one landcover. Essentially, the 'spruce-fir forest' landcover represents, stands composed of Englemann spruce, sub-alpine fir, and whitebark pine.

Reclassification Logic

SPRUCE-FIR FOREST		
IF	HTG_RCLS	FOREST
	SPP_RCLS	SFFR
	SIZE_RCLS	FOREST
	DENSITY_RCLS	FOREST
THEN	SWAT COVER	**SFFR**
	VALUE	**11**

LODGEPOLE PINE FOREST

When stands occur on forest habitat type groups, have stand structure indicative of forest communities, and dominated by lodgepole pine, or limber pine, they are reclassified as 'lodgepole pine" landcover. Limber pine is included in this designation because it can be found in similar locations and is difficult to differentiate the spectral signature of these two species, and as a consequence stands are sometimes misclassified.

Reclassification Logic

LODGEPOLE PINE FOREST		
IF	HTG_RCLS	FOREST
	SPP_RCLS	LP
	SIZE_RCLS	FOREST
	DENSITY_RCLS	FOREST
THEN	SWAT COVER	**LPFR**
	VALUE	**12**

DOUGLAS FIR FOREST

When stands occur on forest habitat type groups, have stand structure indicative of forest communities, and dominated by Douglas fir, or combinations thereof, they are reclassified to the 'Douglas fir forest' landcover. Although dominant in the stand, Douglas fir may occur in combination with Englemann spruce, sub-alpine fir, lodgepole pine, ponderosa pine, and limber pine

Reclassification Logic

DOUGLAS FIR FOREST		
IF	HTG_RCLS	FOREST
	SPP_RCLS	DF
	SIZE_RCLS	FOREST
	DENSITY_RCLS	FOREST
THEN	SWAT COVER	**DFFR**
	VALUE	**13**

PONDEROSA PINE FOREST

When stands occur on forest habitat type groups, have stand structure indicative of forest communities, and dominated by ponderosa pine, or combinations thereof, they are reclassified to the 'ponderosa pine forest' landcover. Although dominant in the stand, ponderosa pine may occur in combination with Douglas fir.

Reclassification Logic

PONDEROSA PINE FOREST		
IF	HTG_RCLS	FOREST
	SPP_RCLS	PP
	SIZE_RCLS	FOREST
	DENSITY_RCLS	FOREST
THEN	SWAT COVER	**PPFR**
	VALUE	**14**

TRANSITIONAL FOREST

The USGS Andersen Level II classification defines 'transitional' as *"Areas of sparse vegetative cover (less than 25 percent of cover) that are dynamically changing from one land cover to another, often because of land use activities. Examples include forest clearcuts, a transition phase between forest and agricultural land, the temporary clearing of vegetation, and changes due to natural causes (e.g. fire, flood, etc.)".* Within this reclassification framework the 'transitional forest' state is applied to disturbed forest stands. Only natural disturbance processes, such as insect, disease, and fire are considered. When forest stands occur on forest habitat type groups, and have had a disturbance that reduced their structure to the seedling-sapling stage, the stand is considered to be 'transitional'. Change from a forested condition to a transitional condition is likely to yield hydrologic responses to landcover change.

Reclassification Logic

TRANSITIONAL OR DISTURBED FOREST		
IF	SPP_RCLS	SFFR
		LP
		DF
		PP
		QA
	SIZE_RCLS	TRANSITIONAL
	DENSITY_RCLS	FOREST
THEN	SWAT COVER	**TRNS**
	VALUE	**15**

CLASSIFIED LANDCOVER CHARACTERISTICS

Physically based attributes that influence hydrologic processes were associated with each landcover category produced by the conversion algorithm (Table 6).

Table 6. *Hydrologic properties of landcover categories produced by the SMAC algorithm. Maximum tree height (HT), minimum (1) and maximum (2) annual leaf area index (LAI), proportion of annual precipitation interception (Int%),photosynthetic base temperature, Manning's overland roughness coefficient (OV_N), and SCS curve number for antecedent moisture condition II (CN2), and soil hydrologic groups A, B, C, and D.*

Description	HT (m)	1LAI	2LAI	Int%	T°	OV_N	CN2A	CN2B	CN2C	CN2D
No Data	0	0	0	0	0	0	0	0	0	0
Barren	0	0	0	0	0	0	0	0	0	0
Water	0	0	0	0	0	0	0	0	0	0
Pasture	0.50	0.50	1.00	0.03	10	0.10	50	72	80	85
Grassland	0.75	0.75	1.50	0.03	10	0.12	49	70	79	85
Shrubland	3.50	1.00	2.00	0.05	10	0.13	42	65	76	83
Open Forest	10.00	1.10	2.20	0.15	3	0.14	35	62	76	82
Riparian Shrub	3.50	1.00	2.00	0.10	10	0.15	47	68	79	84
Riparian Forest	35.00	1.15	2.30	0.15	10	0.15	46	67	78	84
Quaking Aspen	15.00	1.00	2.00	0.15	10	0.15	44	65	76	82
Spruce-Fir	26.00	1.95	3.00	0.28	3	0.17	25	55	70	77
Lodgepole Pine	22.00	1.80	2.80	0.25	3	0.16	30	56	71	79
Douglas Fir	35.00	2.00	3.10	0.25	3	0.15	32	58	72	80
Ponderosa Pine	35.00	1.60	2.50	0.20	3	0.14	33	60	74	81
Transitional	10.00	1.00	2.00	0.10	3	0.14	48	69	78	84

Tree height was estimated based on regional measurements and literature review (1990). Leaf area index (LAI) is an efficient way to describe vegetation canopy coverage, density and stratification, and can be measured with a variety of optical and algometric techniques (White et al., 1997; Hall et al., 2003). The majority of forest cover in the Rocky Mountain region of North America is coniferous, and although needles remain on these types of trees yearlong, leaf area index fluctuates seasonally (Waring and Running,1998). To establish the range of possible LAI values for landcover categories, remotely sensed imagery (Holsinger et al., 2005; USDI-GS, 2005) representing minimum LAI in January and maximum LAI in July were analyzed. Annual interception estimates were based on field measurements in open and forested sites in central Montana (Woods et al., 2006, and published values (Kimmins, 1997; White et al., 1997). Base temperature was interpreted from basic physiological characteristics of forest and non-forest vegetation (Waring and Running, 1998). Estimates of Manning's overland roughness coefficient are less certain than other landcover characteristics given here. Assignments of "OV_N" were made by scaling default grassland, shrubland, riparian, and evergreen forest values reported in the SWAT vegetation database. Similarly, default SCS curve numbers (USDA-SCS, 1972) for forest and non-forest landcover types were scaled to more closely approximate values that are representative of regional conditions.

SMAC ALGORITHM CODE

This algorithm is written in Arc Macro Language (AML). It takes a series of output data (spatial and tabular) from the SIMPPLE model and converts them to a corresponding input data set for the SWAT hydrologic model. Output grids, which maintain polygon boundaries throughout the SIMPPLE simulation, are reclassified into a coarser categorical representation (many classes into few classes).

==========

```
&severity &error &routine bailout
&terminal 9999
&echo &off
&sv starttime = [date -vfull]
&if [show program] ne 'ARC' &then q

/*************************************************************************
/*     USER DEFINED INPUTS     *
/*************************************************************************
/* set key input variables
&sv base_dir = C:\AVSWATX\data\simp2swat\wat_only\    /* base, or parent directory
to simpple simulations
&sv base_cov = C:\AVSWATX\data\gis\tc_swat              /* common polygon cov to all
sims listed in simlist
/* Enter the list of directory basenames here (e.g. ahl\in\tchuc5)
&sv simlist = tc_unmanaged    /* simulation set subdirectories located in "in"
&sv ntimesteps = 31              /* number of 10 year timesteps per simulation
/*************************************************************************
/* NO NEED TO MESS WITH THINGS BELOW HERE!*
/*************************************************************************


/*************************************************************************
/*    MAIN PROCESS     *
/*************************************************************************
&type RUNNING SIMP2SWAT.AML
/* set sim counter
&sv i = 0
/* outer loop is process for many simulation sets, each organized in their own directory
&do sim &list %simlist%
&sv i = %i% + 1
  &type Currently processing simulation run %i%: %sim%
  &call directory_structure     /* makes new output directory for SWAT input files

  /* inner loop is process for a single sim
  &do tstep = 0 &to %ntimesteps% &by 1
    &sv indir = %base_dir%in\%sim%\
```

```
    &sv outdir = %base_dir%out\%sim%\
    &type In: %indir% out: %outdir% timestep: %tstep%

    /* routines description
    /*-----------------------------------------------------------------------------------------------
     &call luts                /* assemble luts
     &call sim_data_in         /* brings in all the spatial and tabular data from a single
SIMPPLE simulation set
     &call convert_data        /* reclasses the input data with appropriate look up tables
or whatever

  &end
&end


&sv endtime = [date -vfull]
&messages &popup
&type Process started at %starttime%. Done at %endtime%.
&messages &on
&return
/*************************************************************************
/************END PROGRAM*****************************************
/*************************************************************************


/*************************************************************************
/*              bailout routine
/*
&routine bailout
&sv line_no = %aml$errorline%
&messages &popup
&type Program crashed on line %line_no%
&messages &on

&sv curslist = [ show cursors ]
&sv curscount = [ token %curslist% -count ]
&do k = 1 &to %curscount%
  cursor [ extract %k% %curslist% ] close
  cursor [ extract %k% %curslist% ] remove
&end
&return
/*********************END ROUTINE BAILOUT************************


/*************************************************************************
/*    ROUTINE LUTS
```

```
&routine luts
&if [show program] ne 'ARC' &then q
/* check if required luts are present as info files
/* if they are not, bring them in from directory
&do lutname &list htg_rcls spp_rcls size_rcls density_rcls landuse
&if ^ [exists %lutname%.lut -info] &then
  &do
    &type Required look up table, %lutname%.lut, not found in INFO dir: bringing in
from e00 file.
    import info %base_dir%%lutname%.e00 %lutname%.lut
  &end
&end
&return
/**********END ROUTINE RMDIRECT**********************************


/*****************************************************************
/*    ROUTINE RMDIRECT
&routine rmdirect
/* goes in and wipes out the whole directory structure
/* This is a hard wipe out to clean up everything.
&if [show program] ne 'ARC' &then q
&sys del /q %base_dir%\out\%sim%\*
&sys rmdir %base_dir%\out\%sim%

&return
/**********END ROUTINE RMDIRECT**********************************


/*****************************************************************
/*    ROUTINE MKDIRECT
&routine mkdirect
/* makes directories to store each simulation run
&if [show program] ne 'ARC' &then q
&sys mkdir %base_dir%\out\%sim%
&return
/**********END ROUTINE MKDIRECT**********************************


/*****************************************************************
&routine directory_structure
&if [show program] ne 'ARC' &then q
&type now in 'Setting up directory structure for output' routine
&if ^ [exists %base_dir%\in\%sim% -DIRECTORY] &then &return &inform Input
directory %base_dir%\in\%sim% not found. Ending program.
&call rmdirect
```

```
&call mkdirect
&return
/************END ROUTINE ****************************************


/*****************************************************************
&routine sim_data_in
&if [show program] ne 'ARC' &then q

&type Bringing in landscape simulation data from %sim%-%tstep%-UPDATE.txt
/* temporarily rename file -- arc doesn't like the - "dash" symbol in the file name.
&sys rename %indir%%sim%-%tstep%-update.txt data.in
&type temporarily renaming %indir%%sim%-%tstep%-update.txt as "data.in"
&type Ignore the error message below: it is due to the header line. No big deal.
&severity &error &ignore
&if [exists tempin.tab -info] &then &type [delete tempin.tab -info]
tables
define tempin.tab
SLINK              10    10     I
SIM_SPECIES         255   255     C
SIM_SIZE            255   255     C
SIM_CANOPY           10    10     I
SIM_PROCESS         255   255     C
SIM_TREATMENT       255   255     C
~
select tempin.tab

add SLINK  SIM_SPECIES  SIM_SIZE SIM_CANOPY SIM_PROCESS
SIM_TREATMENT from %indir%data.in
select tempin.tab
resel $recno = 1
purge
y
q stop

/* rename file back
&sys rename %indir%data.in %sim%-%tstep%-update.txt
&severity &error &routine bailout  /* reset to preferred error handling

&return
/************END ROUTINE ****************************************


/*****************************************************************
&routine convert_data
&type now in 'convert data' routine
```

```
&if [show program] ne 'ARC' &then q
/* make a temporary coverage to hold various attributes
&if [exists tempcov -cov] &then kill tempcov all
copy  %base_cov% tempcov
build tempcov poly
/* build connections to look up tables
additem tempcov.pat tempcov.pat swat_cover 16 16 i # slink

joinitem tempcov.pat tempin.tab tempcov.pat slink
joinitem tempcov.pat htg_rcls.lut tempcov.pat simp_htg
joinitem tempcov.pat spp_rcls.lut tempcov.pat sim_species
joinitem tempcov.pat size_rcls.lut tempcov.pat sim_size
joinitem tempcov.pat density_rcls.lut tempcov.pat sim_canopy
/*modify values based on lookup table values
tables

select tempcov.pat

&type ASSIGNING "NO DATA" VALUES
res Simp_htg = 'ND' and Spp_rcls = 'ND'
cal swat_cover = 1
ase

&type ASSIGNING "BARREN" VALUES
res Htg_rcls = 'NON-FOREST' and Spp_rcls = 'BARREN' and Size_rcls = 'BARREN'
and Density_rcls = 'NON-FOREST'
cal swat_cover = 2
ase

&type ASSIGNING "WATER" VALUES
res Htg_rcls = 'NON-FOREST' and Spp_rcls = 'WATER' and Size_rcls = 'WATER' and
Density_rcls = 'NON-FOREST'
cal swat_cover = 3
ase

&type ASSIGNING "PASTURE" VALUES
res Htg_rcls = 'NON-FOREST' and Spp_rcls = 'AGR'
cal swat_cover = 4
ase

&type ASSIGNING "GRASSLAND" VALUES
res Spp_rcls = 'GRASSLAND' and Size_rcls = 'NON-FOREST'
cal swat_cover = 5
ase

&type ASSIGNING "SHRUBLAND" VALUES
```

```
res Spp_rcls = 'SHRUBLAND' and Size_rcls = 'NON-FOREST'
cal swat_cover = 6
ase

&type ASSIGNING "OPEN FOREST" VALUES
res Htg_rcls = 'NON-FOREST' and ( Spp_rcls = 'sffr' or Spp_rcls = 'LP' or Spp_rcls =
'DF' or Spp_rcls = 'PP' or Spp_rcls = 'QA' )
cal swat_cover = 7
ase

&type ASSIGNING "RIPARIAN SHRUB" VALUES
res Spp_rcls = 'RIPARIAN_SHURB'
cal swat_cover = 8
ase

&type ASSIGNING "RIPARIAN FOREST" VALUES
res Spp_rcls = 'RIPARIAN_FOREST'
cal swat_cover = 9
ase

&type ASSIGNING "QUAKING ASPEN" VALUES
res Spp_rcls = 'QA' and Size_rcls = 'FOREST' and Density_rcls = 'FOREST'
cal swat_cover = 10
ase

&type ASSIGNING "SPRUCE-FIR FOREST" VALUES
res Htg_rcls = 'FOREST' and Spp_rcls = 'SFFR' and Size_rcls = 'FOREST' and
Density_rcls = 'FOREST'
cal swat_cover = 11
ase

&type ASSIGNING "LODGEPOLE PINE FOREST" VALUES
res Htg_rcls = 'FOREST' and Spp_rcls = 'LP' and Size_rcls = 'FOREST' and Density_rcls
= 'FOREST'
cal swat_cover = 12
ase

&type ASSIGNING "DOUGLAS FIR FOREST" VALUES
res Htg_rcls = 'FOREST' and Spp_rcls = 'DF' and Size_rcls = 'FOREST' and Density_rcls
= 'FOREST'
cal swat_cover = 13
ase
```

```
&type ASSIGNING "PONDEROSA PINE FOREST" VALUES
res Htg_rcls = 'FOREST' and Spp_rcls = 'PP' and Size_rcls = 'FOREST' and Density_rcls
= 'FOREST'
cal swat_cover = 14
ase

&type ASSIGNING "TRANSITIONAL FOREST" VALUES
res Size_rcls = 'TRANSITIONAL' and Density_rcls = 'FOREST' and ( Spp_rcls = 'SFFR'
or Spp_rcls = 'LP' or Spp_rcls = 'DF' or Spp_rcls = 'PP' or Spp_rcls = 'QA' )
cal swat_cover = 15
ase

q stop

/* take that temporary coverage and convert it into a temporary grid for SWAT
&if [exists tempgrd -grid] &then kill tempgrd all
polygrid tempcov %outdir%swat_cover%tstep% swat_cover
30
Y

/* convert the temporary grid to an ascii grid
/* gridascii tempgrd %outdir%swat_cover%tstep%.asc
/* clean up temporary deals
&if [exists tempgrd -grid] &then kill tempgrd all
&if [exists tempcov -cov] &then kill tempcov all
&if [exists tempin.tab -info] &then &type [delete tempin.tab -info]

&return
/*************END ROUTINE ****************************************
```

SMAC ALOGITHM INSTRUCTIONS

The SMAC algorithm is designed to automate the processing of output data from the SIMPPLE landscape dynamics model into input data for the spatially explicit hydrologic model, SWAT. The process involves association of a series of attributes, contained in an ascii text file output from SIMPPLE, to a corresponding polygon coverage. This information is then greatly simplified from several hundred classes (combinations of habitat type group, cover type, structure and density for the most part) to a reduced number of classes for use with SWAT through a series of look up table operations. The output data is then converted to a raster-based output with 30 m grid cell resolution.

The underlying process and associated reclassification was developed by Robert Ahl, and the program to automate the inherent logic was coded by Russ Parsons, GIS Specialist, of U.S. Department of Agriculture, Forest Service, Fire Sciences Lab. The SMAC routine encapsulates that process in a series of simple routines and nests it in two loop structures. The outer loop structure is for a simulation set, and the inner loop is for each individual time step in a given simulation set.

DIRECTORY STRUCTURE

In general, the more complex an automated process is, the more important it is to have a consistent directory structure and set of naming conventions. The directory structure for this automated process is as follows:

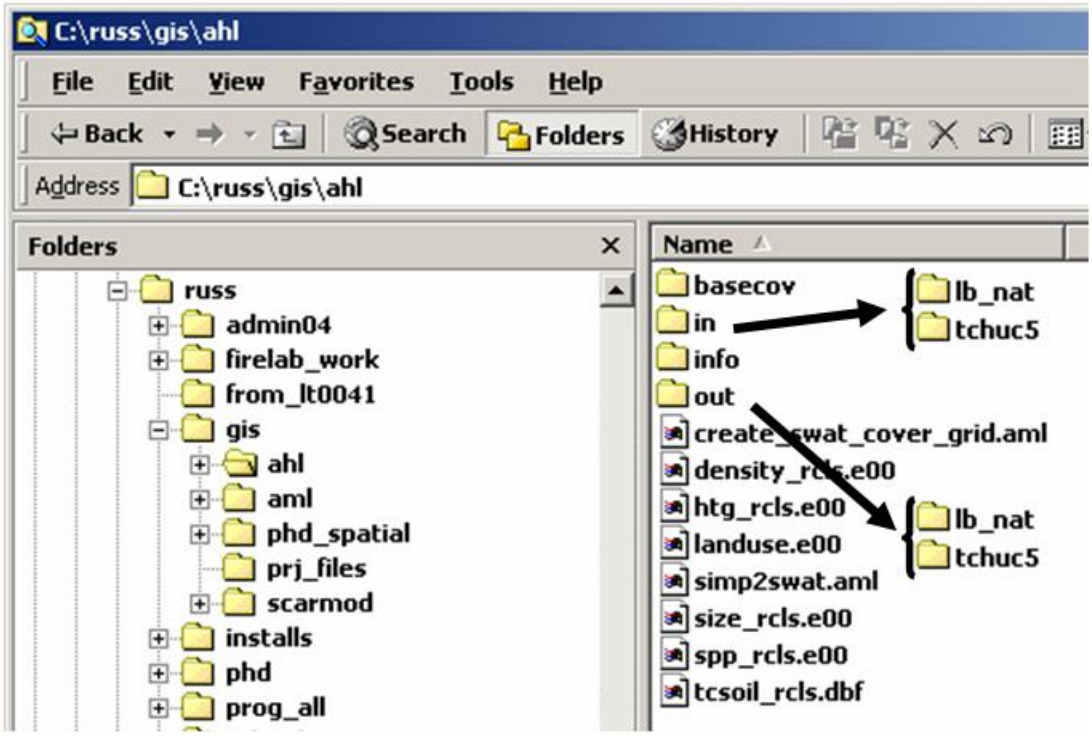

Figure 1. *SMAC algorithm directory structure schematic*.

The "base_dir"
The "base_dir" is the directory which contains the lookup tables (as info tables) and the aml, simp2swat.aml.Inside this main directory is an "in" directory and an "out" directory.

The "IN" directory
The "in" directory is the place to put each simulation set directory, for example, tchuc5 and lb_nat are simulation set directories. These directories contain all the output files from SIMPPLE for a given simulation. For example, in the tchuc5 directory shown above, there are 11 output files, labeled "tchuc5-0-update.txt" through "tchuc5-10-output.txt". The aml will read as many of these time steps from that directory, from zero to ntimesteps, which is an input parameter in the "user inputs" part of the aml. For example, using a value of 10 for the variable ntimesteps will have the aml process all timesteps 0 to 10.

The "OUT" directory
You never have to make an output subdirectory. It will be automatically made each time you run the aml. For example, the tchuc5 directory in the "out" directory was created by the aml. It contains the ascii grids of the reclassified cover maps to use in running SWAT. Note that these output directories will be deleted and overwritten if you run the aml twice with the same input subdirectory name. So be sure to rename these or save them to somewhere else. Since these output subdirectories are created when you run the aml, they do not exist on this CD ROM. But they will exist after you run the aml.

Running the AML
There are a few input parameters at the top of the aml. These are the only parts of the aml you should mess with to make it run. Of course the rest of the aml may be useful to copy and modify for your other purposes. Feel free to do so as you please.
Here is the input part:

```
/*********************************
/*    USER DEFINED INPUTS         *
/*********************************
/* set key input variables
&sv base_dir = c:\russ\gis\ahl\       /* base, or parent directory to simpple simulations
&sv base_cov = basecov                /* common polygon cov to all sims listed in simlist
/* Enter the list of directory basenames here (e.g. ahl\in\tchuc5)
&sv simlist = tchuc5  lb_nat      /* simulation set subdirectories located in "in"
&sv ntimesteps = 10                   /* number of 10 year timesteps per simulation
/*****************************************
/* NO NEED TO MESS WITH THINGS BELOW HERE!*
/*****************************************
```

USAGE NOTES

1. Set your **base dir** variable appropriately. It doesn't matter where your base dir is but you still need to maintain the in and out directory structure discussed above.

2. The **basecov** is the path to the polygon that you want to link the simple files to. ALL subdirectories listed in the variable "**simlist**" will use that same base coverage. So if you have a bunch of different landscapes you should just have one subdirectory in there. You can of course list as many subdirectories as you want in there provided they all use that same base coverage (for example, a bunch of simulations with different simulations all for the same landscape).

3. For each simulation set that you want to run the process on, you will have to copy a directory into the "**in**" directory. The name of the directory must correspond to the first part of the name of the files inside it. For example, in the tchuc5 directory shown above, there are 11 output files, labeled "tchuc5-0-update.txt" through "tchuc5-10-output.txt". If the directory name does not correspond to the first part of the file name (underlined above for clarity), the aml won't know where to look and will shut down the program. Similarly, the aml reads the timestep (0 ... n), where n is specified in the "user inputs" section of the aml as "ntimesteps". The aml is looking for files with the naming convention <simsetdirectoryname>-<timestep>-output.txt, like these ones. Since this is apparently an output file name convention for SIMPPLE, this shouldn't be any kind of problem, but just be aware of it.

LITERATURE CITED

Anderson, J. R., E.E. Hardy, J.T. Roach, and R.E. Witmer. 1976. A land use and land cover classification system for use with remote sensor data. Geological Survey Professional Paper 964. Washington, D.C., U.S. Government Printing Office.

Arnold, J.G., R. Srinivasan, R.S. Muttiah, and J.R. Williams. 1998. Large area hydrologic modeling and assessment part I: model development. *Journal of the American Water Resources Association* 34 (1), 73-89.

Burns, R.M. and B.H. Honkala. 1990. Silvics of North America, Volume 1, Conifers. United States Department of Agriculture, Forest Service, Washington, DC.

Chew, J.D., C. Stalling, and K. Moeller. 2004. Integrating knowledge for simulating vegetation change at landscape scales. Western Journal of Applied Forestry 19(2): 102-108.

Hall, R.J., D.P. Davidson, and D.R. Peddle. 2003. Ground and remote estimation of leaf area index in Rocky Mountain forest stands, Kananaskis, Alberta. *Canadian Journal of Remote Sensing* 29 (3), 411-427.

Holsinger, L., R.E. Keane, R. Parsons, and E. Karau. 2005. Development of Biophysical Gradient layers. *In:* Rollins, M.G.; Frame, C.K., tech. eds. 2006. The LANDFIRE Prototype Project: nationally consistent and locally relevant geospatial data for wildland fire management. Gen. Tech. Rep. RMRS-GTR-175 U.S. Department of Agriculture, Forest Service, Rocky Mountain Research Station. Fort Collins, CO.

Kimmins, J.P., 1997. Forest Ecology: A foundation for sustainable management. Prentice-Hall, Inc., Upper Saddle River, New Jersey 07458.

USDA-SCS (U.S. Department of Agriculture, Soil Conservation Service), 1972. SCS National Engineering Handbook, Section 4, Hydrology. Chapter 10, Estimation of Direct Runoff from Storm Rainfall. U.S. Department of Agriculture, Soil Conservation Service, Washington D.C., pp. 10.1-10.24.

USDI-GS, (U.S. Department of the Interior, Geological Survey) 2005. MODIS/Terra Leaf Area Index/FPAR 8-day L4 Global 1km ISIN Grid. United States Geological Survey, Center for Earth Observation and Science (EROS), 47914 252nd Street, Sioux Falls, SD 57198-0001. Available for download at: http://LPDACC.usgs.gov

Waring R.H. and Running, S.W. 1998. Forest Ecosystems: Analysis at Multiple Scales. Academic Press, San Diego.

White J.D., S.W. Running, R. Nemani, R.E. Keane, and K.C. Ryan, 1997. Measurement and remote sensing of LAI in Rocky Mountain montane ecosystems. Canadian Journal of Forest Research 27: 1714-1727.

Woods S.W., R. Ahl, J. Sappington, W. McCaughey, 2006. Snow Accumulation in thinned lodgepole pine stands, Montana, USA. Forest ecology and Management 235: 202-211.

APPENDIX B

TCSWAT Parameterization and Calibration

INTRODUCTION

Detailed parameterization and calibration of SWAT in the Tenderfoot Creek watershed (TCSWAT) focused on five major input types representing, snow processes, surface runoff attenuation (SURLAG), groundwater processes, soil processes, and SCS curve numbers associated with rainfall runoff relationships. Mathematical formulae, taken from the SWAT theoretical documentation (Neitsch et al., 2002), used to represent biophysical interactions, and descriptions of how relevant parameter ranges were established are presented below.

SNOW PROCESSES

Snow Accumulation and Snowmelt

Snow accumulation and melt processes within SWAT are calculated individually for each HRU. SWAT classifies precipitation as rain or snow based on whether the mean daily air temperature is greater or less than a predefined snowfall temperature parameter (SFTMP). If the mean daily air temperature is less than SFTMP then all of the precipitation falling within the HRU on that day is classified as snow and the snow water equivalent (SWE) of the precipitation is added to the snow pack. The snowpack increases with each additional snowfall or decreases with sublimation according to a mass balance of the form:

$$SNO = SNO + R_{day} - E_{sub} - SNO_{mlt} \qquad \text{(Eqn. 1)}$$

where *SNO* is the water content of the snow pack on a given day (mm), R_{day} is the amount of precipitation on a given day (mm), E_{sub} is the amount of sublimation on a given day (mm), and SNO_{mlt} is the amount of snow melt on a give day (mm).

Computation of snowmelt within a sub-basin requires information on the spatial distribution of snow cover. The factors that contribute to variable snow coverage are often consistent from year to year, making it possible to correlate the aerial coverage of snow with the amount of snow present in the subbasin at a given time. This correlation is expressed as an aerial depletion curve, which is used to describe the seasonal growth and recession of the snow pack as a function of the amount of snow present in the subbasin (Anderson, 1976; Neitsch et al., 2002). The depletion curve is based on a natural logarithm and calculated as:

$$sno_{\mathrm{cov}} = \frac{\mathrm{SNO}}{\mathrm{SNOCOVMX}} * \left(\frac{\mathrm{SNO}}{\mathrm{SNOCOVMX}} + \exp\left(\mathrm{b}_1 - \mathrm{b}_2 * \frac{\mathrm{SNO}}{\mathrm{SNOCOVMX}} \right) \right)^{-1} \qquad \text{(Eqn. 2)}$$

where sno_{cov} is the fraction of the HRU area covered by snow, *SNO* is the SWE of the snow pack (mm), SNOCOVMX is the SWE (mm) threshold depth above which there is 100% coverage (a function of topographic irregularities, aspect, wind scour, and canopy

interception that are unique to a specific watershed), and b_1 and b_2 are coefficients that define the shape of the curve. The values used for the coefficients are determined by two known points at 95% and 50% coverage at a user specified fraction of SNOCOVMX. The parameter that specifies the fraction of SNOCOVMX that provides 50% cover is referred to as SNO50COV, and its value can be approximated by interpreting the shape of the various depletion curves provided in the SWAT theoretical documentation manual (Neitsch et al., 2002). In the Tenderfoot Creek research watershed, it was assumed that 10% of SNOCOVMX would provide 50% snow coverage. The aerial depletion curve affects snow melt only when the snow pack water content is between 0.0 and SNOCOVMX. Therefore, as the value of SNOCOVMX increases, influence of the depletion curve also increases (Neitsch et al., 2002; Wang, 2005).

Snowmelt in SWAT is calculated as a linear function of the difference between the average snow pack-maximum air temperature and a threshold snow melt temperature parameter, SMTMP. Daily snowmelt (SNO_{mlt}) is calculated from:

$$SNO_{mlt} = b_{mlt} * sno_{\text{cov}} * \left[\frac{T_{snow} + T_{mx}}{2} - SMTMP \right] \qquad \text{(Eqn. 3)}$$

where b_{mlt} is the melt factor for the day, sno_{cov} is the fraction of the HRU area covered by snow, T_{snow} is the snow pack temperature for the day, T_{mx} is the maximum air temperature on a given day, and SMTMP is the snow melt temperature threshold. The value b_{mlt} varies seasonally, with maximum and minimum melt rates theoretically occurring on summer and winter solstices. The snow melt rate factor is calculated as:

$$b_{mlt} = \frac{(SMFMX + SMFMN)}{2} + \frac{(SMFMX - SMFMN)}{2} * \sin\left(\frac{2\,pie}{365} * (d_n - 81) \right) \qquad \text{(Eqn. 4)}$$

where b_{mlt} is the melt factor for the day, SMFMX is the maximum melt factor for June 21, SMFMN is the minimum melt factor for December 21, and d_n is the day number of the year. Because the snow is unlikely to melt in mid-winter the minimum melt rate should theoretically be 0.

The snow pack temperature is a function of the mean daily temperature during the preceding days and varies as a dampened function of air temperature (Anderson, 1976; Neitsch et al., 2002). The influence of the previous day's snow pack temperature is controlled by a lagging factor, TIMP. The lagging factor inherently accounts for snow pack density, snow pack depth, exposure and other factors affecting snow pack temperature. Snow pack temperature is calculated as:

$$T_{snow(dn)} = T_{snow(dn-1)} * (1 - TIMP) + \overline{T}_{av} * TIMP \qquad \text{(Eqn. 5)}$$

where $T_{snow(dn)}$ is the snow pack temperature on a given day, $T_{snow(dn-1)}$ is the snow pack temperature on the previous day, TIMP is the snow pack temperature lag factor, and $\overline{T}_{av}$ is the mean air temperature on the current day. As TIMP approaches 1.0, the mean air

temperature on the current day exerts an increasing influence on the snow pack temperature. Smaller values of TIMP mean that the model places more weight on the previous day's temperature when calculating snowpack temperature.

SURFACE RUNOFF LAG

In large sub-watersheds with a time of concentration greater than 1 day, only a portion of the surface runoff will reach the main channel on the day it is generated. SWAT incorporates a storage feature to lag a portion of the surface runoff release to the main channel. Once calculated, the amount of surface runoff released to the main channel is calculated:

$$Q_{surf} = \left(Q'_{surf} + Q_{stor,i-1}\right) * \left(1 - \exp\left[\frac{-SURLAG}{t_{conc}} -\right]\right) \qquad \text{(Eqn. 6)}$$

where Q_{surf} is the amount of surface runoff discharged to the main channel on a given day (mm), Q'_{surf} is the amount of surface runoff generated in the subbasin on a given day (mm), $Q_{stor,i-1}$ is the surface runoff stored or lagged from the previous day (mm), *SURLAG* is the surface runoff lag coefficient, and t_{cons} is the time of concentration for the subbasin. The expression in the large parentheses represents the fraction of the total available water that will be allowed to enter the reach on any one day. For a given time of concentration, as *SURLAG* decreases in value more water is held in storage. The delay in release of surface runoff will smooth the streamflow hydrograph simulated in the reach (Neitsch et al., 2002).

Lowering SURLAG from 4.0 to 0.05 increased model efficiency by nearly 80%. The default value made the hydrograph too flashy during runoff. Discharge needs to be lagged and that is why the calibrated SURLAG is such a small number. The calibrated value for this watershed is much smaller than what is reported by others. Most studies have been in watersheds with less topography than TCEF, and also do not have snowmelt hydrology. The combination of steep slopes and rapid water inputs due to snowmelt create a situation where too much runoff can be predicted unless corrective adjustments are made. In the Tenderfoot Creek watershed, SURLAG may have to be adjusted beyond physical limits because the model was designed for this type of system.

GROUNDWATER PROCESSES

Base flow Fraction

Base flow is that component of the runoff that is supplied to the channel by groundwater discharge from the surrounding upland. In forested watersheds, base flow dominates the runoff because the porous nature and roughness of forest floors encourages infiltration. Surface flow only happens in periods when the soil water capacity is exceeded and infiltration is no longer possible. In SWAT, the landcover SCS Curve

Number (CN2) estimates are adjusted so that water yield fractions resemble the values of the base flow separation. Reducing the Curve Number increases base flow contribution (Mangurerra and Engel, 1998). As such, forested landcover should have lower CN2 values than shrub or grass cover types. No data regarding the proportions of ground and surface water contribution from runoff events was available for the Tenderfoot Creek watershed. Therefore the digital base flow filter program introduced by Arnold and Allen (1999) was used to process observed mean daily discharge data from 1995-2002 and provide estimates of base and surface flow proportions (Table 1). This is one of several methods for estimating base flow contributions that have been developed (Arnold et al., 1995; Arnold and Allen, 1999; Sloto and Crouse, 1996).

Table 1. *Baseflow filter analysis for observed daily streamflow TCSWAT, 1995 – 2002, showing the estimated contribution of baseflow for runoff events for each pass of the filter. Averages of the first and second pass, along with an average of the second and third pass are shown at the bottom of the table.*

Filter Cycle	Estimated Baseflow Fraction (%)
Pass 1	76
Pass 2	61
Pass 3	51
Mean Pass 1, 2	69
Mean Pass 2, 3	56

The base flow fraction for our watershed may be lower than the 70% indicated by the filter program. Steep hillsides and a large influx of water in a short period of time may produce more 'runoff' than predicted by the filter. Therefore, it may be reasonable to compare SWAT water yield fraction output to the mean of the second and third pass, rather than the average of the first and second pass. Also, CN were developed for slope conditions of roughly 5%. As slopes in mountainous environments are generally greater than that, smaller baseflow fractions, or slightly higher curve numbers may again be appropriate.

Groundwater Recharge and Discharge

SWAT simulates two aquifers in each subbasin. The shallow aquifer is unconfined and contributes to flow in the main channel of the subbasin. The deep aquifer is confined. Water that enters the deep aquifer is assumed to contribute to streamflow somewhere outside of the watershed (Arnold et al., 1993; Neitsch et al., 2002). Calibration of groundwater processes focuses on adjustment of the GW_DELAY, GWQMN, ALPHA_BF, and RCHRG_DP parameters, which control the recharge, contribution and recession of baseflow due to shallow aquifer processes, and loss of groundwater to the deep aquifer.

Water that moves past the lowest depth of the soil profile by percolation or bypass flow enters and flows through the vadose zone before becoming shallow aquifer recharge. The lag between the time that water exits the soil profile and enters the shallow aquifer will depend on the depth to the water table and the hydraulic properties of the geologic formations in the vadose and groundwater zones. The GW_DELAY parameter

controls this through an exponential decay function for situation where the recharge from the soil zone to the aquifer is not instantaneous, i.e. 1 day or less (Neitsch et al., 2002).

The shallow aquifer contributes baseflow to the main channel within the subbasin. Baseflow is allowed to enter the channel only if the amount of water stored in the shallow aquifer exceeds a threshold value specified by the user, with the GWQMN parameter. Estimating an appropriate amount of baseflow was one of the most problematic aspects of streamflow calibration in this system. To ensure that sufficient quantities of water were available for this hydrograph component, the GWQMN parameter was set to 0. This enabled the model to allow baseflow contribution whenever any quantity of water was present in the shallow aquifer. No calibration was attempted beyond this setting. Recession of baseflow is controlled by the ALPHA_BF, and this has been consistently shown to be an important groundwater calibration parameter. It is a direct index of groundwater flow response to changes in recharge. The digital filter used to estimate the baseflow fraction was also used to estimate the base flow recession constant, which is referred to in SWAT as the base flow alpha factor (ALPHA_BF). ALPHA_BF is a direct index of groundwater flow response to changes in recharge. In forested watersheds, where base flow is important, the alpha factor can be an influential calibration parameter (Mangurerra and Engel, 1998). The range for this index is from 0 to 1, where groundwater flow response to recharge increases as the values approach 1 (Neitsch et al., 2002). ALPHA_BF cannot be directly measured, so the value estimated from the filter program was used as a starting point for groundwater parameter calibration. Using observed daily streamflow spanning 1995-2002, the filter suggested an ALPHA_BF value of 0.03 for the Tenderfoot Creek watershed, indicating slow recession. This seems appropriate because after the snowmelt period and spring rainy season, streamflow persists throughout the year, despite the fact that groundwater recharge is negligible.

A fraction of the total daily recharge can be routed to the deep aquifer. Percolation to the deep aquifer is allowed to occur only if the amount of water stored in the shallow aquifer exceeds a threshold value specified by the user with the RCHRG_DP parameter. This parameter controls the fraction of percolation from the root zone which is diverted to the deep aquifer and lost to the system. No adjustment was attempted after setting this parameter to 0.15 in calibration of Tenderfoot Creek.

MODEL PERFORMANCE DECOMPOSITION

Calibration of the snow parameter set had the greatest effect on model performance in the Tenderfoot Creek research watershed. In decreasing order of influence, snow parameters were followed by the surface lag coefficient (SURLAG*)*, and the groundwater, soil, and curve number parameter sets (Table 2).

Table 2. *Relative influence of factors affecting model calibration. Model performance was evaluated for daily streamflow in representative year, 1999 through analysis of the model efficiency statistic (NS_d).Changes in performance due to parameter set decomposition are described in relative terms. Results of simulations where all parameters in a group have been decomposed are shown in bold face. Results from variation of individual parameters within a composite are italicized. Only values for the primary layer are given for the groundwater and soil parameter sets.*

			NS_d	NS_d Change (%)
CALIBRATED MODEL PERFORMANCE			**0.92**	
Composite Snow	**Default Value**	**Calibrated Value**	**-0.06**	**106**
Timp	*1.0*	*0.06*	*0.52*	*43*
Smtmp	*0.5*	*1*	*0.71*	*23*
Snocov50	*0.5*	*0.1*	*0.73*	*20*
Smfmx	*4.5*	*3*	*0.89*	*3*
Snocovmx	*1.0*	*200*	*0.93*	*-2*
Smfmn	*4.5*	*2.9*	*0.91*	*1*
Composite SURLAG	**4.0**	**0.05**	**0.19**	**79**
Composite Groundwater			**0.80**	**13**
Alpha_BF	*0.05*	*0.01*	*0.81*	*12*
GW_Delay	*31*	*1*	*0.85*	*7*
Composite Soil			**0.88**	**4**
Sol_K	*23*	*75*	*0.88*	*4*
Sol_awc	*0.09*	*0.18*	*0.91*	*1*
Composite CN2			**0.89**	**3**
Lodgepole pine	*55*	*58*	*0.90*	*2*
Disturbed forest	*55*	*69*	*0.91*	*1*
Shrubland	*61*	*65*	*0.92*	*0*
Grassland	*69*	*70*	*0.92*	*0*
Spruce-fir	*55*	*55*	*0.92*	*0*

COMPOSITE SNOW PARAMETERS

Setting the snow parameters to their default values reduced the NS efficiency from 0.92 to -0.06. With the default snow values the snowmelt driven runoff peak occurred 75-80 days earlier than the calibrated and observed peaks, and the recession limb was extended by a similar number of days longer (Figure 9). The snow parameter with the greatest impact on model calibration was the snow pack temperature lag factor (TIMP), followed by the snow melt temperature (SMTMP), and the snow cover depletion curve (SNCOV50). Use of the default values for the maximum and minimum snowmelt rate factors (SMFMX and SMFMN) had only a minimal effect on model performance, while setting the snow covered area parameter back to the default value of 1 improved the model efficiency by 1%.

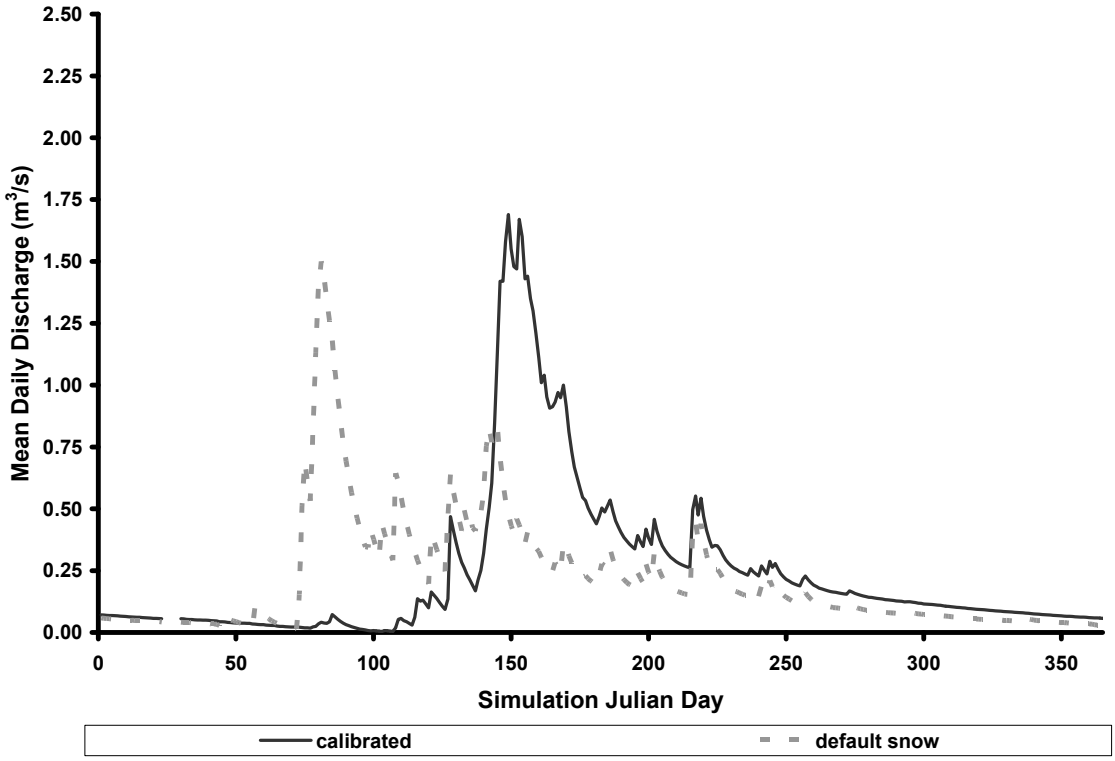

Figure 1. *Impact of the snow parameter set decomposition on the calibrated daily streamflow hydrograph simulated in 1999.*

Individual Snow Parameters

SMTMP - snowmelt temperature

Adjustment of the maximum snowmelt temperature is parameter affects the timing and magnitude of spring runoff, particularly the rising limb of the annual peak. If snowmelt temperature is too low then snowmelt will occur too soon. When snow is melted prematurely, not enough snow is available later on and there will be insufficient melt water to match the actual spring runoff.

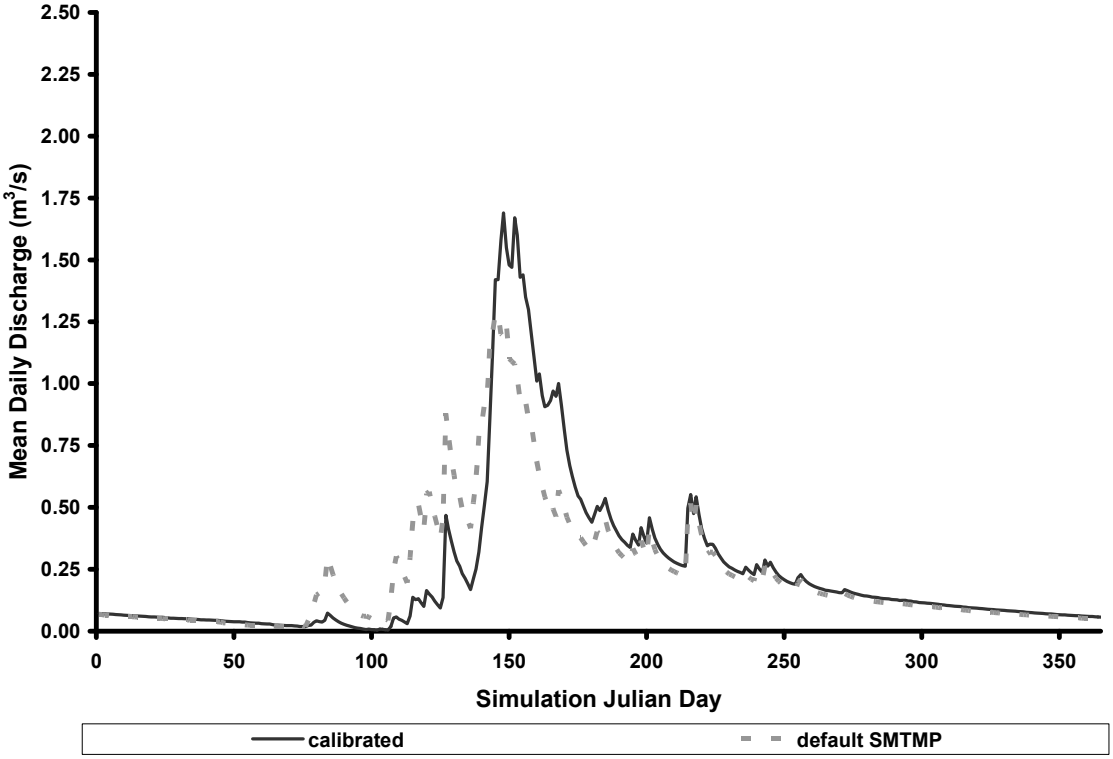

Figure 2. *Impact of snowmelt temperature (SMTMP) adjustment on the calibrated daily streamflow hydrograph simulated in 1999.*

SMFMX – maximum snowmelt rate

If maximum (MX) and minimum (MN) snowmelt rates are set to the same value (i.e. 3°C) then the melt rate for any given day is calculated as that single value. Similarly, is MX=3 and MN=0, then the melt rate will be that of MX, moderated by the day of year. That is, as the year progresses toward June 21 the melt rate increases from 0 to 3°C. With the current calibration, SMFMX was decreased from 4.5 to 3.0°C, causing a 3% improvement in NS_d. To match the largest annual peaks more closely, a value closer to 5.0°C may be a better choice, but this will also increase early runoff peaks.

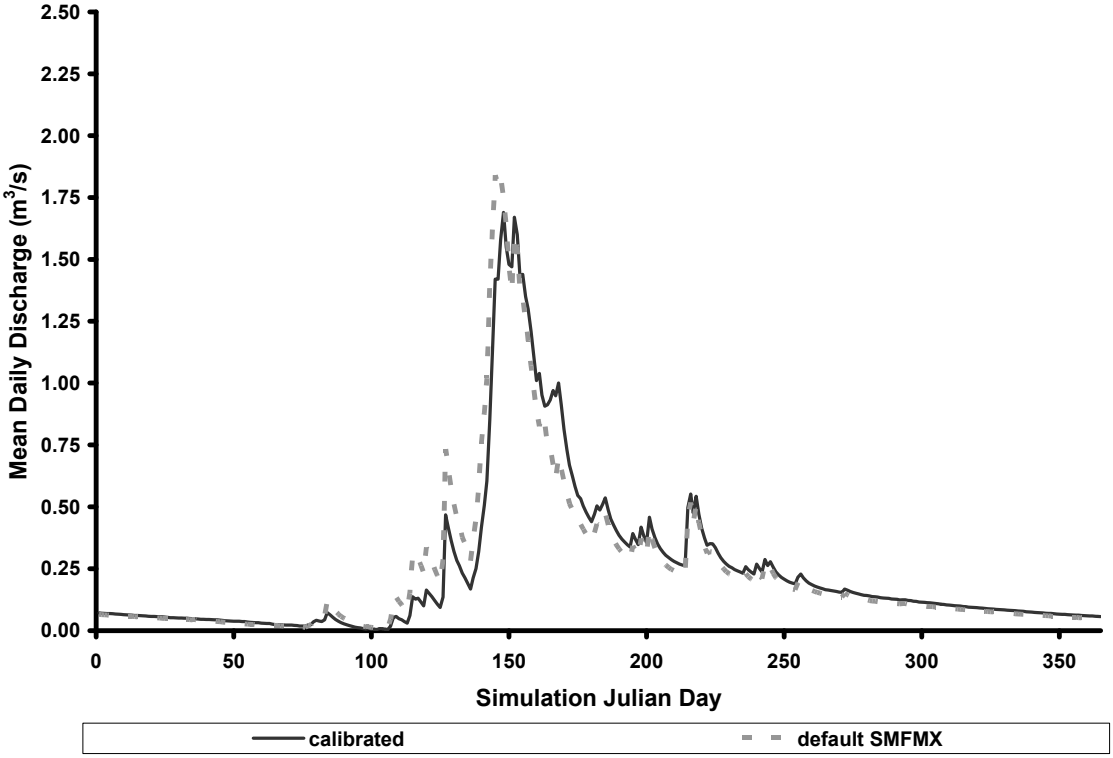

Figure 3. *Impact of the maximum snowmelt rate (SMFMX) adjustment on the calibrated daily streamflow hydrograph simulated in 1999.*

SMFMN – minimum snowmelt rate

Adjustment of the minimum snowmelt rate had little impact on the calibration. The only observable changes imparted to the hydrograph shape affected the magnitude of early snowmelt events.

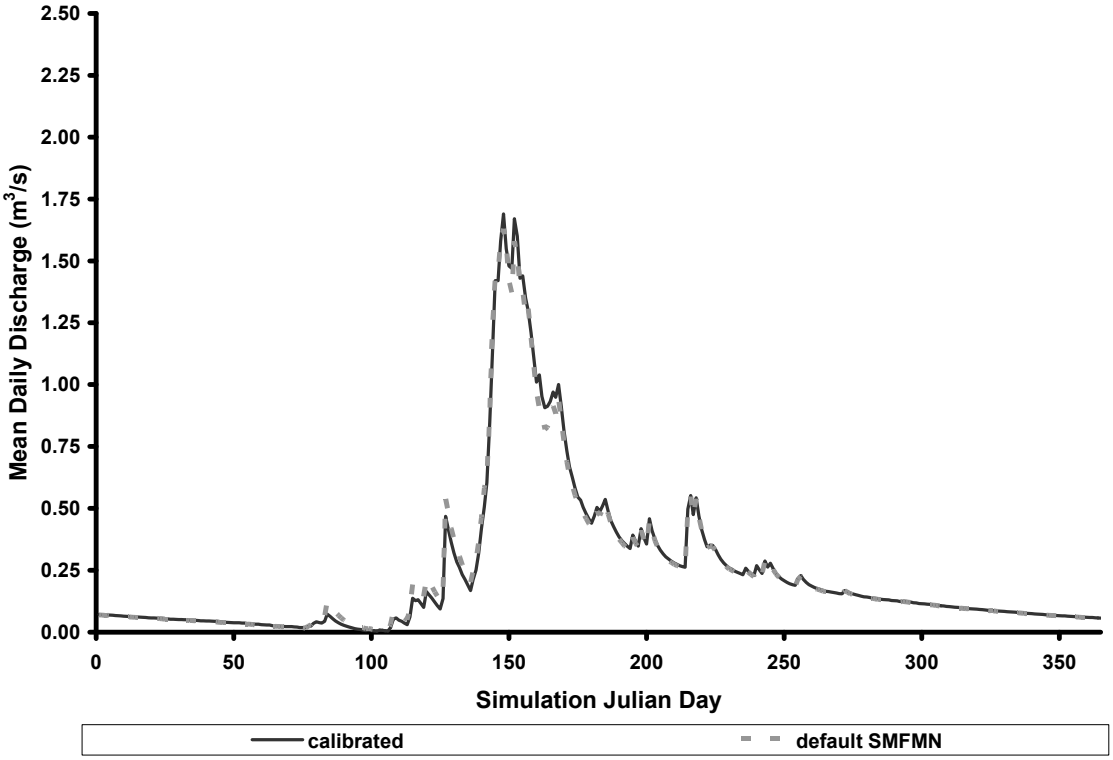

Figure 4. *Impact of minimum snowmelt rate (SMFMN) adjustment on the calibrated daily streamflow hydrograph simulated in 1999.*

TIMP – snowpack temperature lag factor

High snowpack temperature lag factor (TIMP) values cause current day temperature to melt snow. Therefore, when a single warm winter day occurs, the model melts snow and creates runoff. This does not actually happen. The snow has to ripen before it melts, and this takes many days of mean daily temperatures that are above the snowmelt temperature threshold. For this reason, it makes sense that TIMP has to be a small number; forcing the model to weight the temperature of pervious days more strongly. That is why snow does not melt early in the year even when single days can be above the snowmelt temperature threshold.

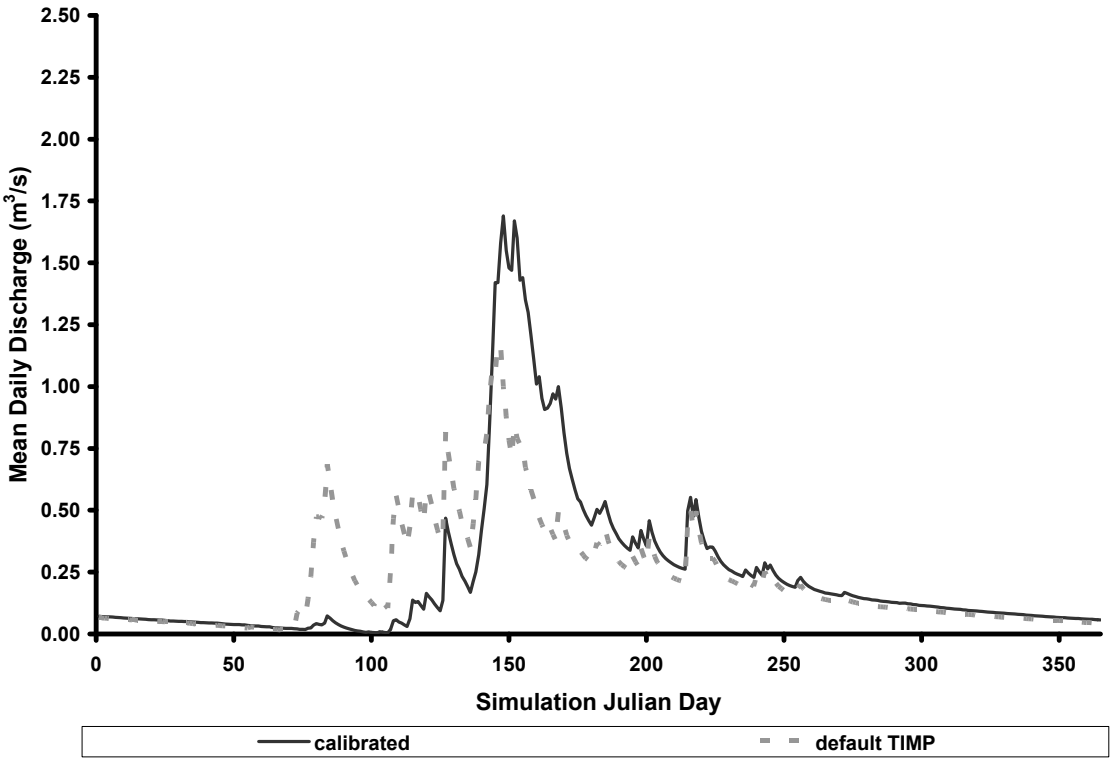

Figure 5. *Impact of snowpack temperature lag factor (TIMP) adjustment on the calibrated daily streamflow hydrograph simulated in 1999.*

SNOCOVMX – minimum snow water content that corresponds to 100% snow cover

Threshold depth of snow above which there is 100% snow coverage is defined by the SNOCOVMX parameter. The actual depth of snow that entirely blankets TCEF is unknown because of high spatial variability within forested mountain watersheds, but to be safe SNOCOVMX was set to 200 mm in the current TCSWAT calibration. This may have been too high, but the true value is essentially immeasurable. The default for this parameter is 1.0 mm, suggesting that very little snow is required to create full coverage. More importantly, though, is the notion that by lowering the threshold depth of snow, the influence of the depletion curve (SNOCOV50) is reduced. This is because once the snow depth exceeds the threshold depth, snow cover is assumed to be uniform.

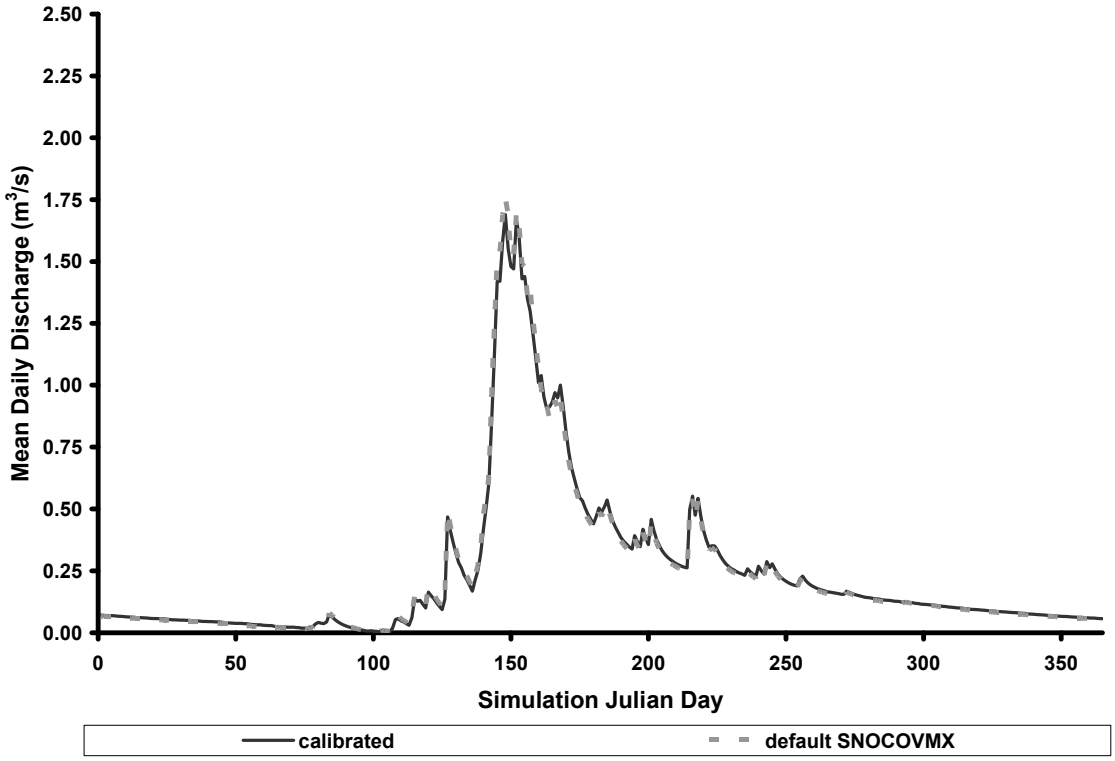

Figure 6. *Impact of the threshold depth of snow above which there is 100% snow coverage snowmelt temperature (SNOCOVMX) adjustment on the calibrated daily streamflow hydrograph simulated in 1999.*

SNOCOV50 – fraction of snow volume (SNOCOVMX) that corresponds to 50% cover

The snowmelt depletion curve affects snowmelt when the snow depth is between 0 and the threshold. If the threshold parameter (SNOCOV50) is low the depletion curve only takes affect when depth goes below the threshold. As threshold increases, the influence of the depletion curve will assume more importance in snowmelt processes. In the current calibration, threshold depth for full snow coverage in the watershed was set to a relatively large value of 200 mm to account for spatial variability across the watersheds. With a large value like this, the depletion curve had a large influence, affected snowmelt whenever the snowpack SNOCOV50 is set to 0.1, and the calibration may benefit from making this value even smaller – i.e. < 0.1. Also, the threshold may be too high, so changing it to 175 mm maybe worth attempting.

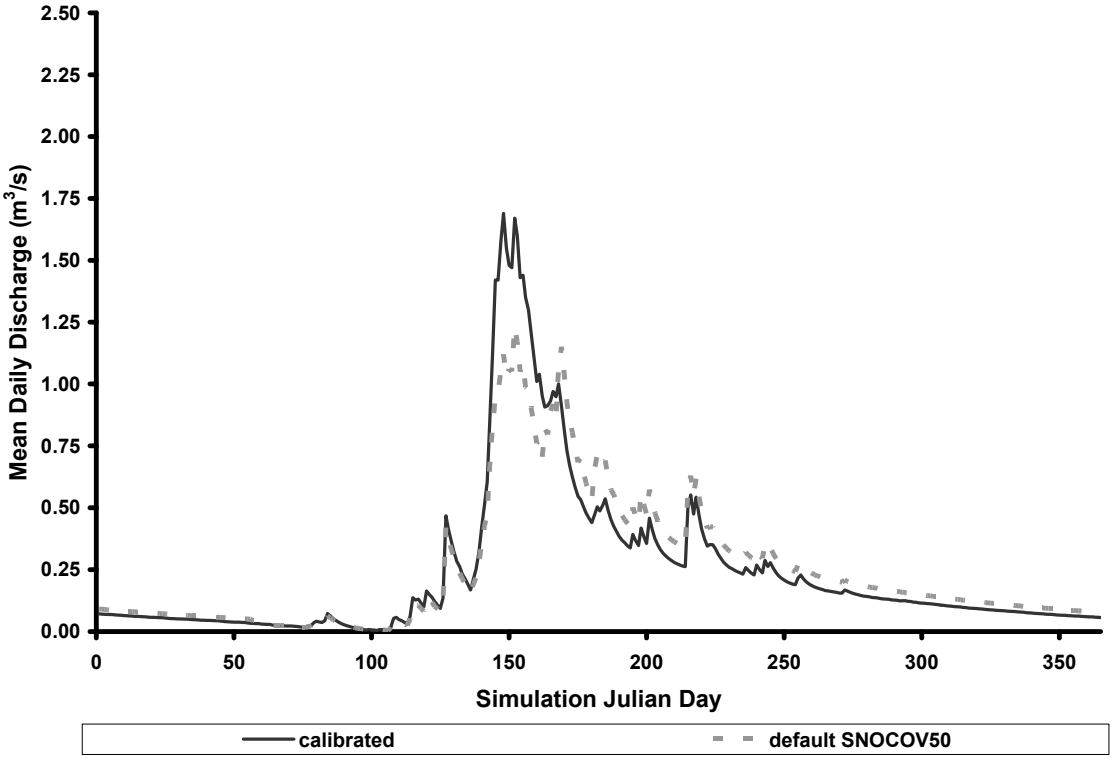

Figure 7. *Impact of snowmelt depletion curve (SNOCOV50) adjustment on the calibrated daily streamflow hydrograph simulated in 1999.*

SURFACE RUNOFF LAG

Re-setting the surface runoff lag factor coefficient (SURLAG) from the calibrated value of 0.05 to the default value of 4.0 reduced the model efficiency from 0.92 to 0.19, nearly 80%. The default value made the hydrograph too flashy during runoff. Discharge needs to be lagged and that is why the calibrated SURLAG is such a small number. In fact, this number is much smaller than what is reported by most calibration studies. It makes sense though. Most studies have been in watersheds with less topography than TCEF, and also do not have snowmelt hydrology. The combination of steep slopes, frozen soil, and rapid water inputs due to snowmelt and lack of infiltration create a situation where too much runoff can be predicted unless corrective adjustments are made. In the case here, parameters may have to be adjusted beyond physically based limits because the model was designed for this type of system.

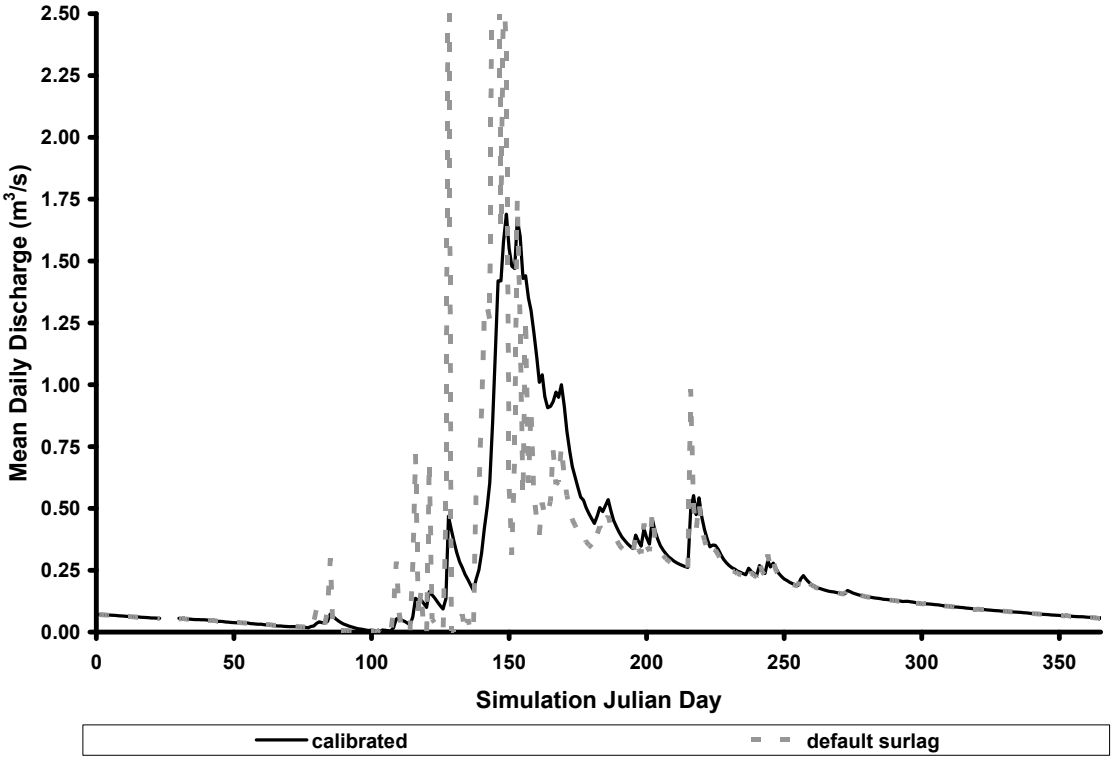

Figure 8. *Impact of surface runoff lag coefficient (SURLAG) adjustment on the calibrated daily streamflow hydrograph simulated in 1999.*

COMPOSITE GROUNDWATER PARAMETERS

When compared with snow and surface runoff parameters, re-setting the groundwater parameters to their default values had relatively little effect on model performance. The model efficiency with the default parameters was only 12% lower than with the calibrated parameter set (Table 2). However, calibration of the groundwater parameter set improved the model fit during the streamflow recession period, and made more water available for baseflow (Figure 9).

Individual Groundwater Parameters

Of the calibrated groundwater parameters, adjustment of the ALPHA_BF parameter yielded the greatest improvement in model performance. Reducing ALPHA_BF from the default value of 0.048 to 0.01 slowed the shallow aquifer response to recharge, causing a reduction in the annual runoff peak during snowmelt and making more water available for streamflow later in the year. Reducing the value of GW_DELAY from the default of 31 days to 1 day affected both the width of the peak discharge and the quantity of water available for baseflow. To improve the current calibration slight increases in both ALPHA_BF and GW_DELAY parameters may make the runoff peak narrower and taller, while maintaining baseflow late in the year.

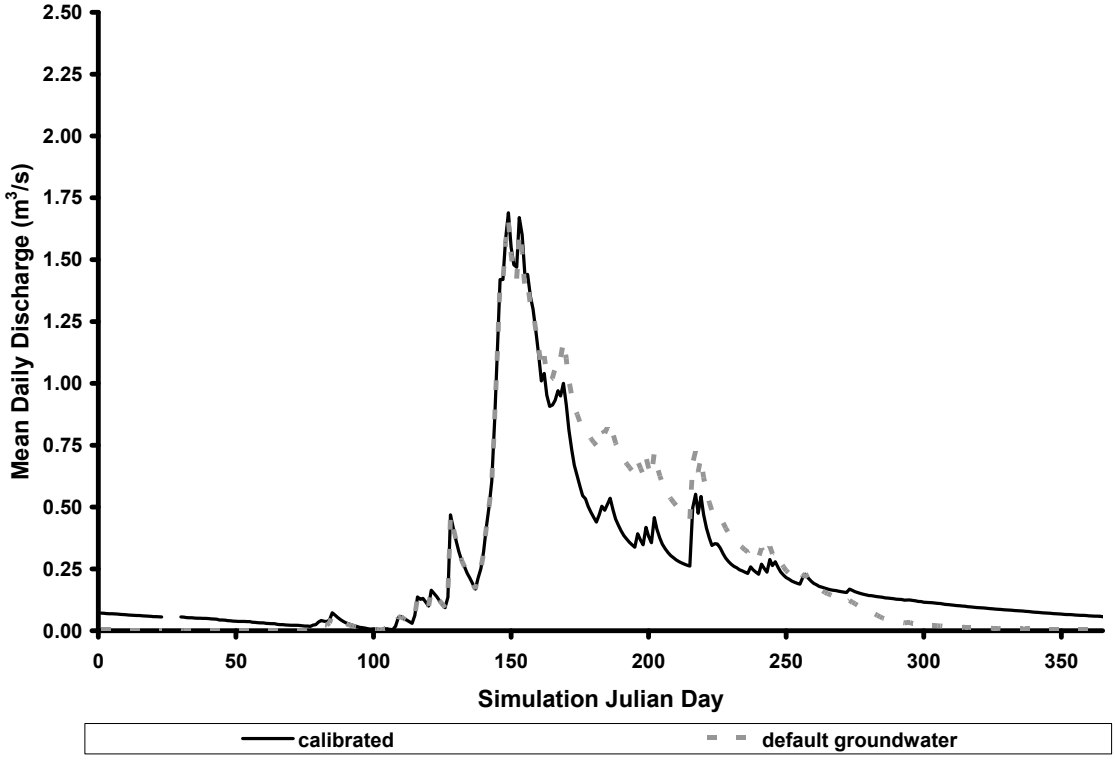

Figure 9. *Impact of the groundwater parameter set decomposition on the calibrated daily streamflow hydrograph simulated in 1999.*

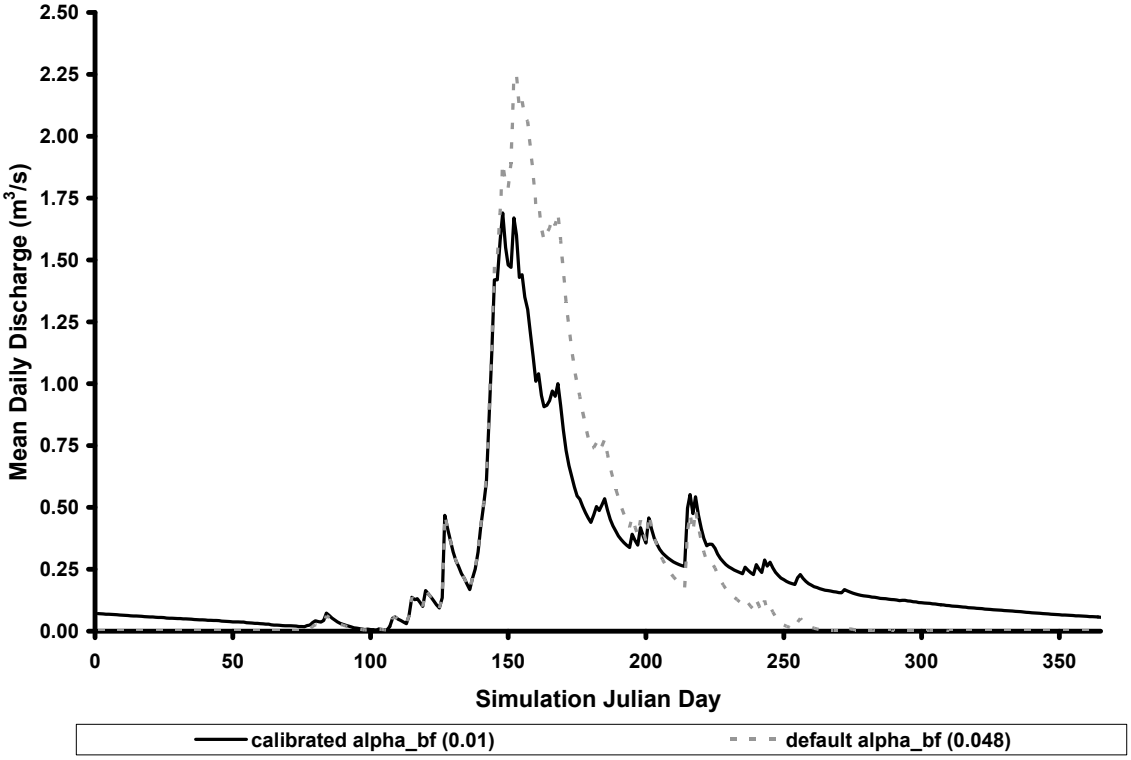

Figure 10. *Impact of ALPPH_BF adjustment on the calibrated 1999 daily hydrograph.*

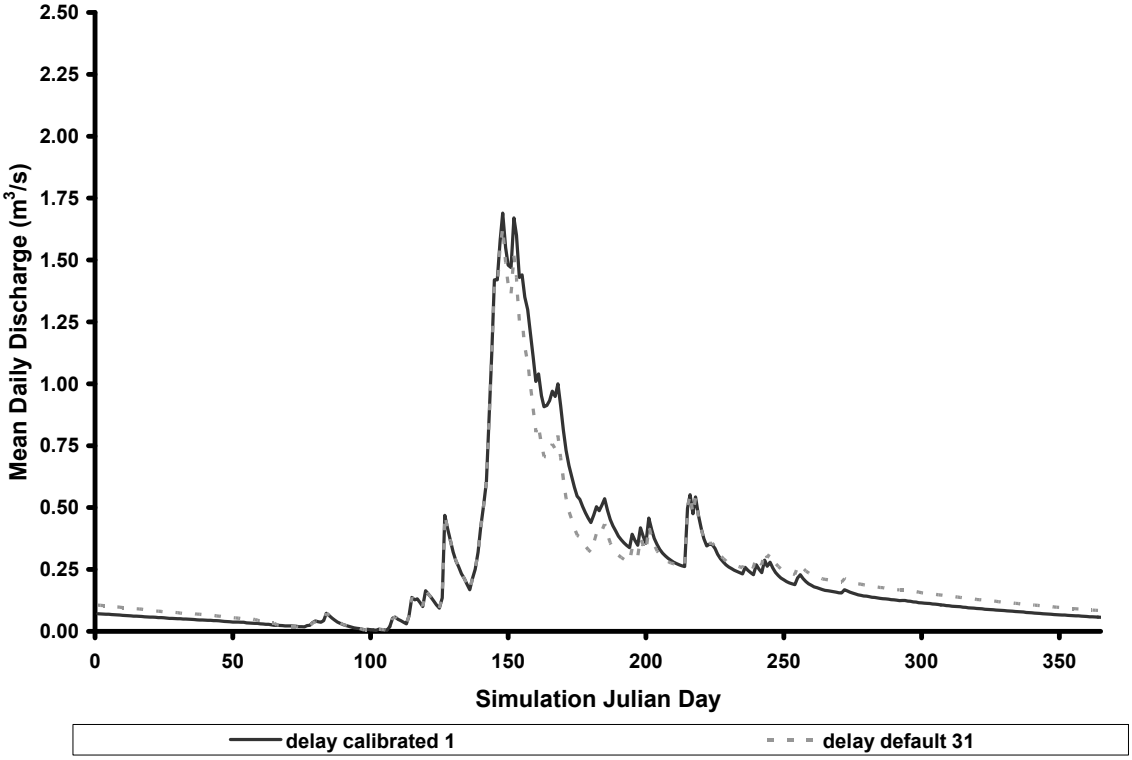

Figure 11. *Impact of GW_DELAY adjustment on the calibrated 1999 daily hydrograph.*

Use of the default soil parameters reduced the overall model efficiency by just 4% (Table 2). Calibration of the soil parameters primarily improved model fit to the observed daily streamflow on the recession limb of the hydrograph (Figure 12).

Individual Soil Parameters

Of the two soil parameters adjusted, the soil hydraulic conductivity (SOL_K) had the greatest influence on model fit. Increasing SOL_K from the default value of 23 to the calibrated value of 75 increased the modeled peak flows during the snowmelt season. Increasing the available water holding capacity (SOL_AWC) made more water available for streamflow in the baseflow period, but improvement in model efficiency was < 1%.

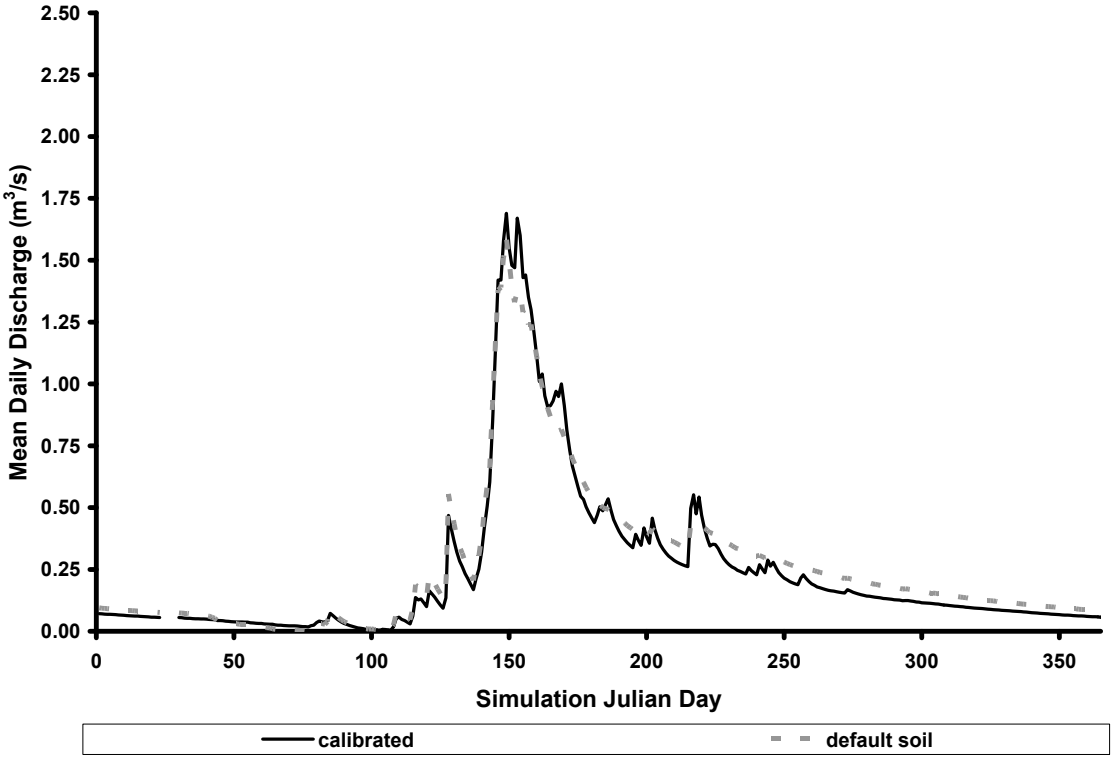

Figure 12. *Impact of the soil parameter set decomposition on the calibrated daily streamflow hydrograph simulated in 1999.*

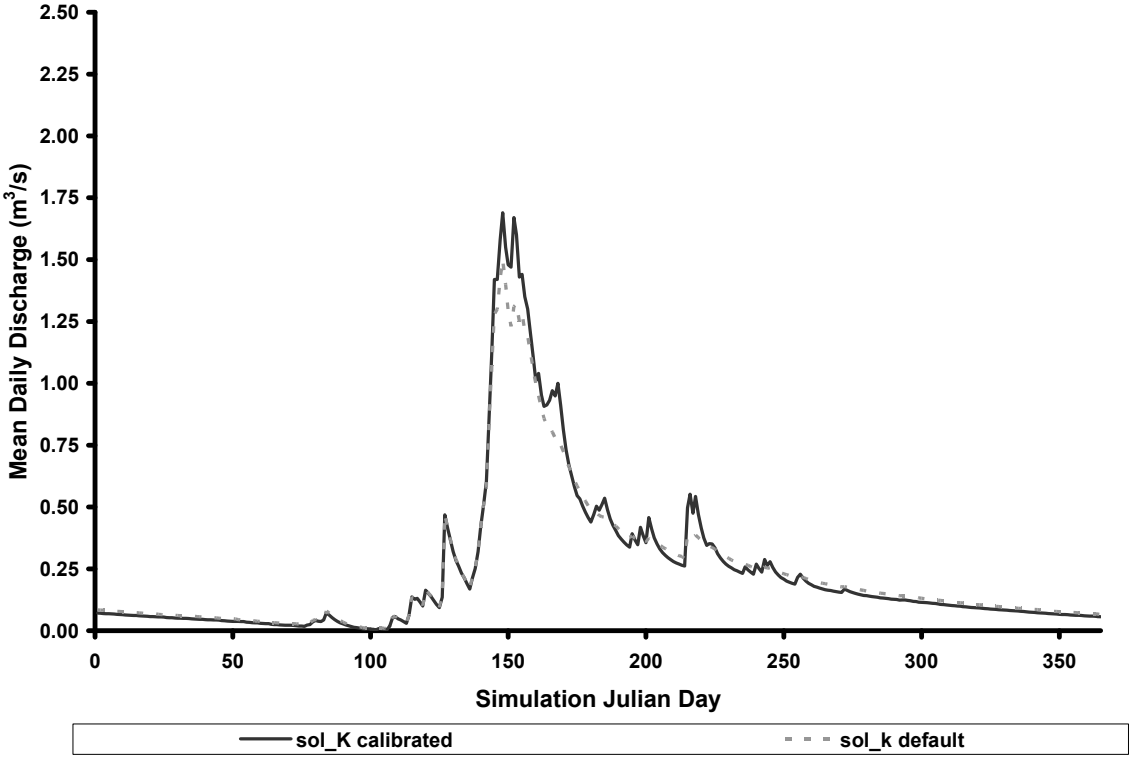

Figure 13. *Impact of SOL_K adjustment on the calibrated 1999 hydrograph.*

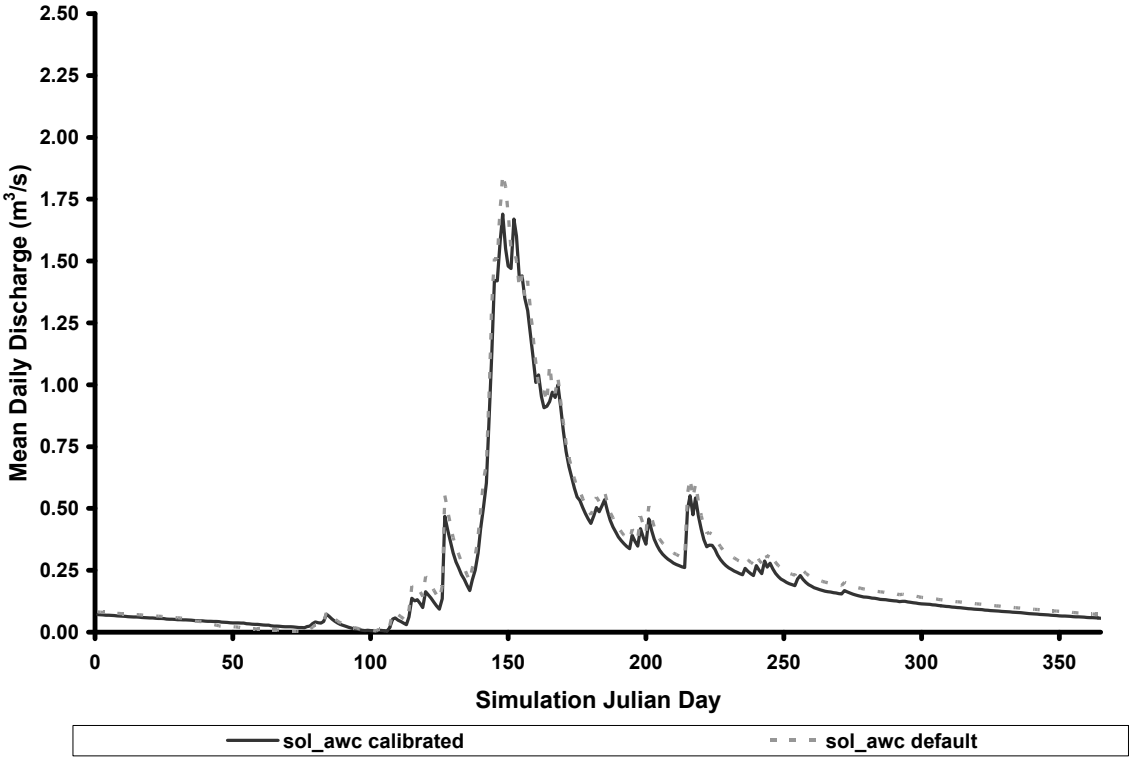

Figure 14. *Impact of SOL_AWC adjustment on the calibrated 1999 hydrograph.*

COMPOSITE SCS CURVE NUMBERS (CN)

SWAT model performance can be sensitive to the selection of appropriate SCS Curve Numbers, and this was the primary reason why a more detailed forest landcover dataset was used in the analysis, with each forest type attributed with unique curve number values. However, of all the parameter sets evaluated, CN, moisture condition 2, in soil class B (CN2B, referred to as CN) had the least effect on model efficiency (Table 2). When CN for all represented landcover types were set to their default values, the decrease in model efficiency was just 2.5%. The only detectable effect on model fit was a reduction in the early runoff peaks (Figure 15).

Individual landcover SCS Curve Numbers

Lodgepole pine forest covers the majority of the watershed, and changing the default curve number from 55 to 58 yielded the greatest increase in simulation efficiency (Table 2, Figure 19). Following lodgepole pine, introduction of the disturbed forest landcover produced the second largest improvement in efficiency (Table 2). While this landcover type occupies only 10% of the watershed, the change in curve number from 55 to 69 had a noticeable effect on the model fit to observed values (Figure 20).

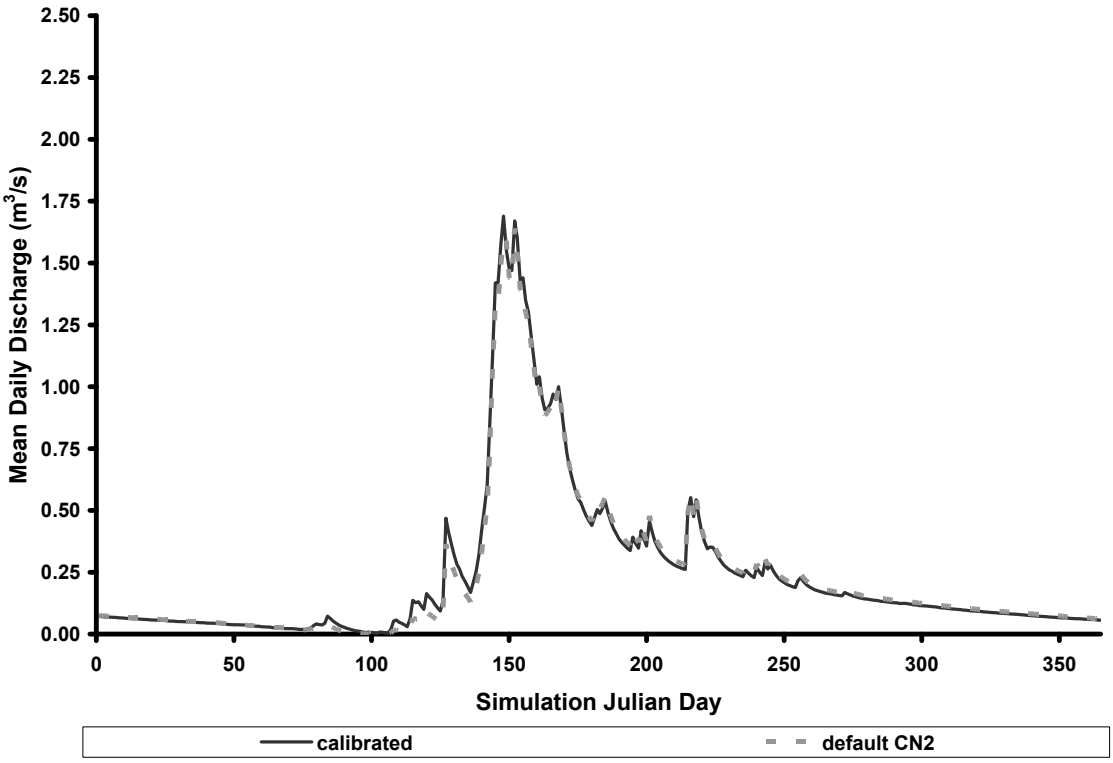

Figure 15. *Impact of the SCS Curve Number set (CN) decomposition on the calibrated daily streamflow hydrograph simulated in 1999.*

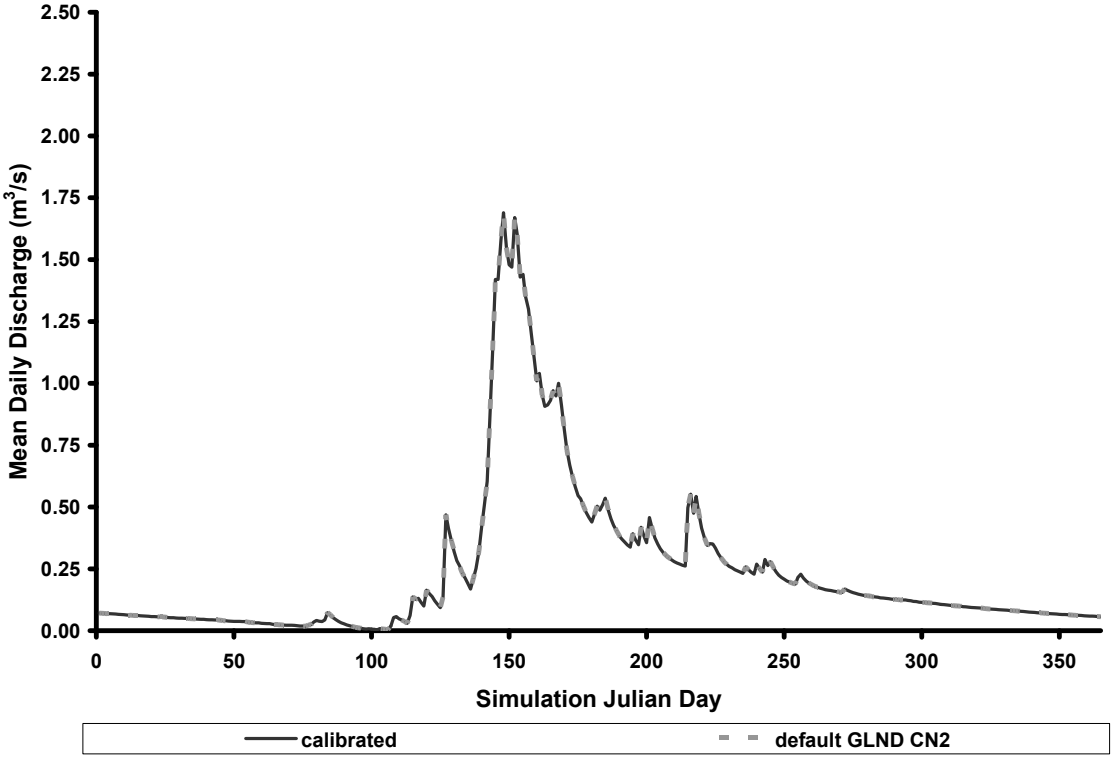

Figure 16. *Impact of GLND CN adjustment on the calibrated 1999 hydrograph.*

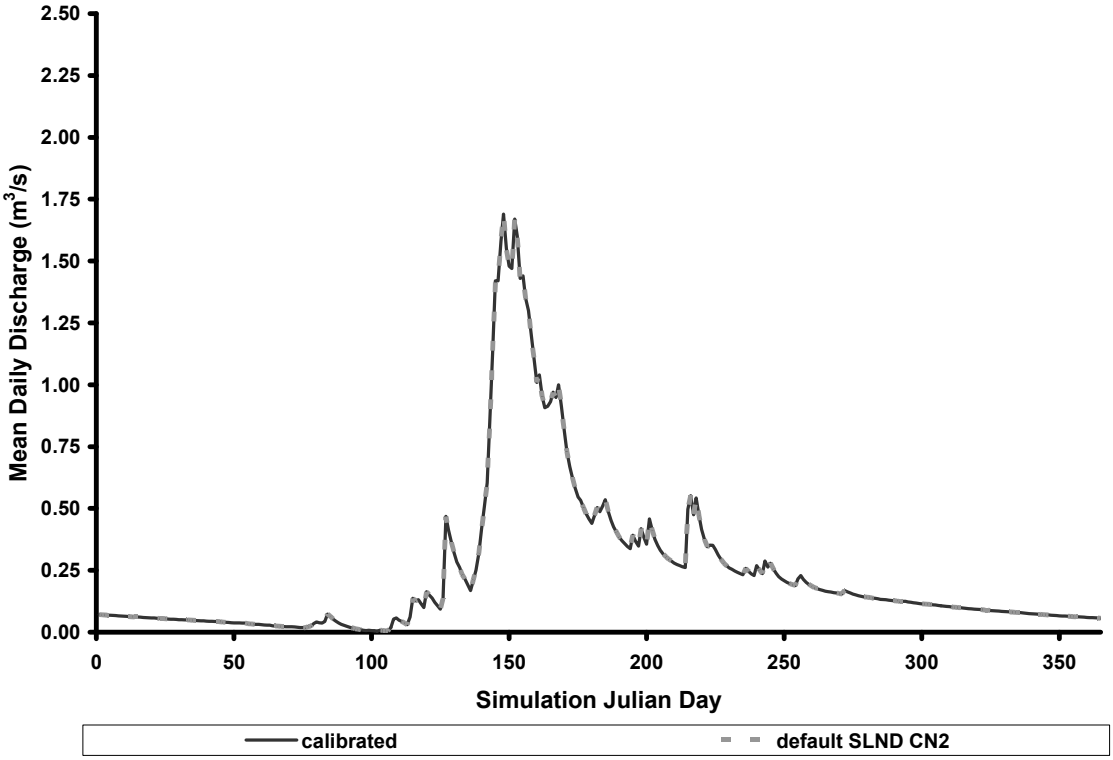

Figure 17. *Impact of SLND CN adjustment on the calibrated 1999 hydrograph.*

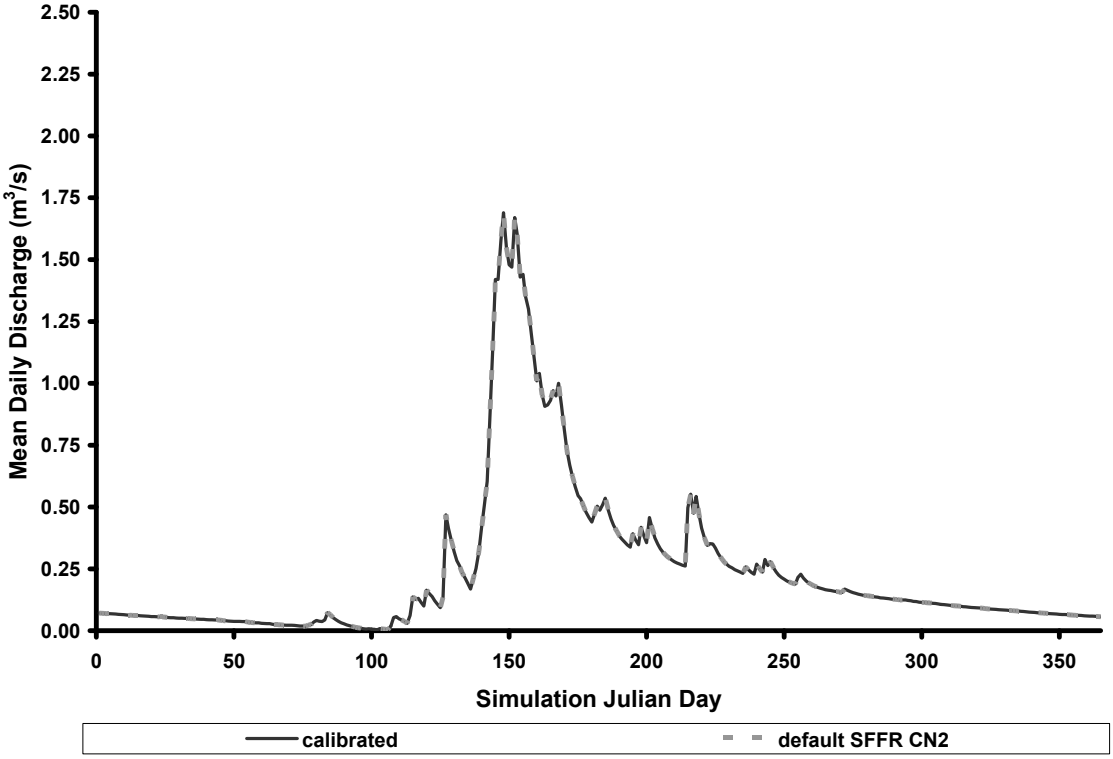

Figure 18. *Impact of SFFR CN adjustment on the calibrated 1999 hydrograph.*

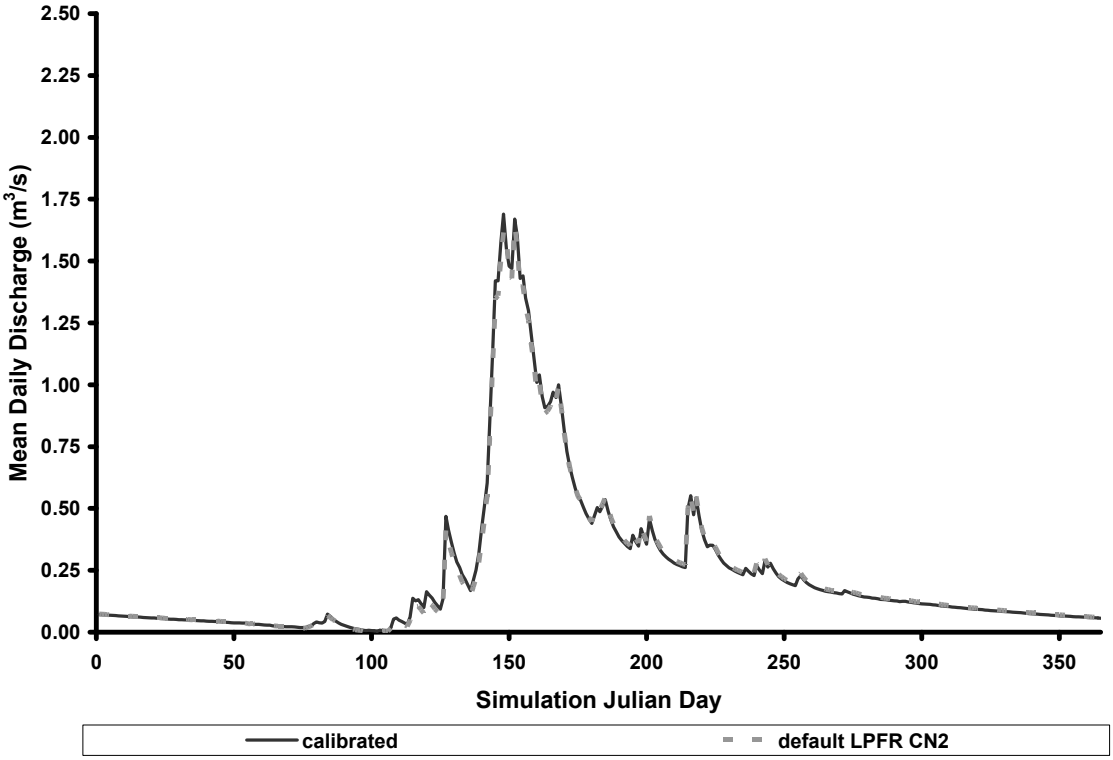

Figure 19. *Impact LPFR CN adjustment on the calibrated 1999 hydrograph.*

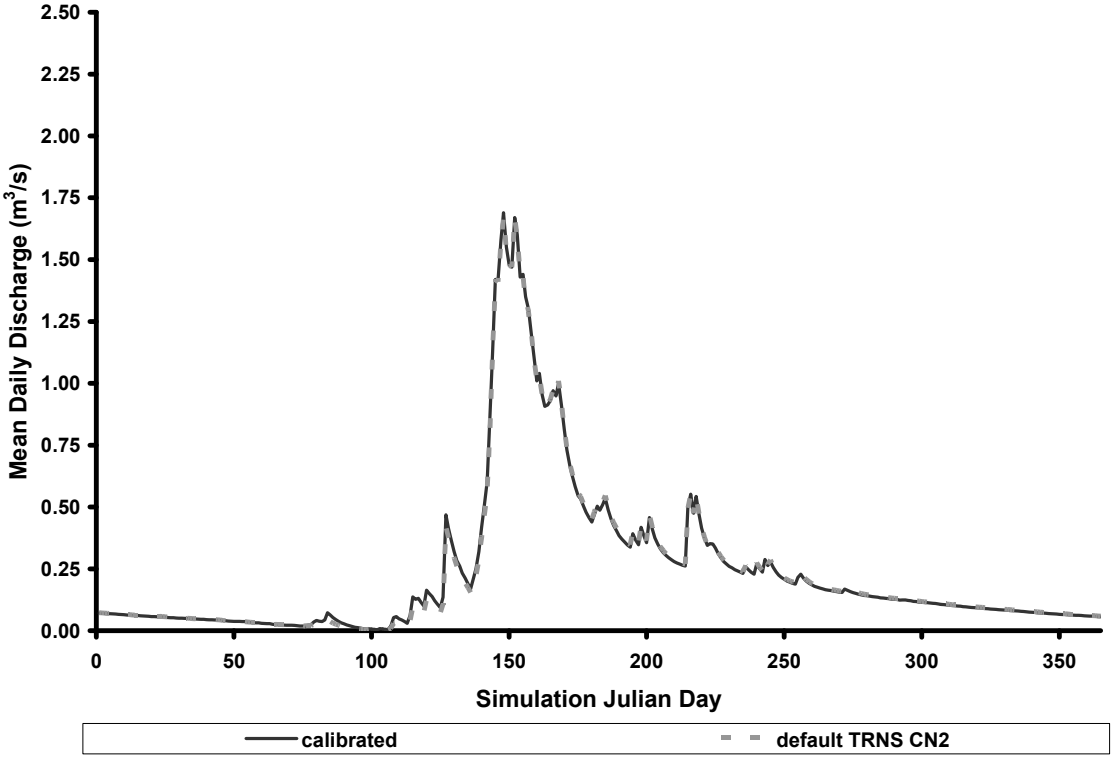

Figure 20. *Impact of TRNS CN adjustment on the calibrated 1999 hydrograph.*

LITERATURE CITED

Anderson, E.A. 1976. A point energy and mass balance model of snow cover. NOAA Technical Report NWS 19, U.S. Department of Commerce, National Weather Service.

Arnold, J.G. and P.M. Allen. 1999. Automated methods for estimating baseflow and groundwater recharge from streamflow records. Journal of the American Water Resources Association 35(2):411-424.

Arnold, J.G.; P.M. Allen, R. Muttia and G. Bernhardt. 1995. Automated base flow separation and recession analysis techniques. Ground Water 33(6):1010-1018.

Sloto, R.A. and M.Y. Crouse. 1996. HYSEP: A Computer Program for Streamflow Separation and Analysis. U.S. Geological Survey – Water Resources Investigations Report 96-4040.

Mangurerra, H.B. and B.A. Engel. 1998. Hydrologic Parameterization of Watersheds for Runoff Prediction Using SWAT. Journal of the American Water Resources Association 34(5): 1149-1162.

Neitsch, S.L., J.G Arnold, J.R Kiniry, J.R Williams, and K.W. King. 2002. Soil and Water Assessment Tool Theoretical Documentation, Version 2000. Texas Water Resources Institute, College Station, Texas, TWRI Report TR-191, GSWRL Report 02-01, BRC Report 02-05.

Wang, X. and A.M Melesse. 2005. Evaluation of the SWAT Model's Snowmelt Hydrology in a Northwestern Minnesota Watershed. Transactions of the ASAE 48(4): 1359-1376

APPENDIX C

TCSWAT Landcover Sensitivity Analysis

The Soil and Water Assessment Tool (SWAT) was calibrated for streamflow prediction in the headwaters of the Tenderfoot Creek watershed. The research area was located in the Little Belt Mountains of central Montana, USA, and calibration was based on current biophysical watershed conditions. The model was configured with 30 m resolution topographic data, extracted from the U.S. Geological Survey - National Elevation Dataset (USGS-NED), Montana STATSGO soils data (NRCS), a custom landcover map, and continuous daily climate and streamflow records spanning the 1993-2000 time period.

While they are distinct, the terms *landuse* and *landcover* are often used interchangeably. In essence, *landuse* implies some form of land management, whereas *landcover* refers to a land classification category. Because no management was specified, the mapped distribution of vegetation, rock, and barren ground is referred herein as landcover.

Changes in landcover patterns have to potential to alter hydrologic processes, but limitations in time, space, and resources make it difficult to experimentally quantify the relationship between landcover and streamflow at the watershed scale. Because direct manipulation and monitoring are generally not possible, modeling is one way to evaluate the impact of landcover change on watershed processes.

The calibrated SWAT model of Tenderfoot Creek (TCSWAT) was used to assess hydrologic responses associated with each landcover category in the watershed. The model was calibrated to current landcover patterns, which include a mixture of barren, non-forest, and forest cover types (Table 1.).

Table 1. *Current TCSWAT watershed landcover distribution.*

Landcover Category	Area (Ha)	Relative Watershed Area (%)
Barren (BRRN)	40	~ 2
Grassland (GLND)	5	< 1
Shrubland (SLND)	8	< 1
Lodgepole pine forest (LPFR)	1,493	67
Spruce-fir forest (SFFR)	465	21
Transitional Forest (TRNS)	240	11
	2,251	100

After calibration to current mixed landcover composition, the model was reconfigured and run so that the whole watershed was entirely covered by each type of landcover. As such, distinct models representing the Tenderfoot Creek watershed composed of entirely barren, grassland, shrubland, quaking aspen, lodgepole pine, Douglas fir, spruce-fir, and transitional forest landcover types were created. For each model, calibrated landcover and basin-wide parameters were set, and SWAT was run from 1993-2000. The time from October1, 1993 to December 31, 1996 was used to equilibrate the model, and the years 1997-2000 represented the time period over for which SWAT was originally calibrated, and Table 2 illustrates hydrologic estimates of basin wide parameters from that model. Results from 1997-2000, describe the hydrologic patterns associated with each independently simulated landcover category.

Table 2. *Calibrated basin estimates (based on 1997-2000 simulation period).*

Year	PCP (mm)	ET (mm)	Yield (mm)	Peak (m^3/s)	Runoff (%)	SWQ (%)	LWQ (%)	GWQ (%)
1997	812	417	563	3.45	69	48	10	42
1998	791	430	376	1.25	48	23	17	60
1999	719	434	338	1.69	47	39	12	49
2000	676	363	375	1.49	55	35	12	53
mean	750	411	413	1.97	55	36	13	51
stdev	63	33	102	1.00	10	10	3	7
sterr	32	16	51	0.50	5	5	1	4

For each type of landcover, average annual basin estimates for evapotranspiration (ET), total water yield, precipitation-runoff ratio, peak discharge rate, and surface, lateral, and groundwater flow proportions were tabulated, and are given below in Table 3.

Table 3. *Average annual basin estimates (based on calibration period 1997-2000).*

Landcover	PCP (mm)	ET (mm)	Yield (mm)	Peak (m^3/s)	Runoff (%)	SWQ (%)	LWQ (%)	GWQ (%)
Calibrated	750	411	413	1.97	55	38	12	50
UTRN	750	231	522	2.39	70	83	4	13
GLND	750	355	397	2.10	53	62	10	29
SLND	750	372	382	1.95	51	51	11	38
QAFR	750	380	403	1.97	54	50	11	39
LPFR	750	416	414	1.92	55	36	13	51
DFFR	750	424	407	1.88	54	36	13	51
SFFR	750	428	409	1.84	55	31	13	56
TRNS	750	341	435	2.14	58	57	10	33

Tables 4 – 10 provide annual summaries of ET, total water yield, precipitation-runoff ratio, peak discharge rate, and surface, lateral, and groundwater flow proportions for every relevant landcover category, for the 1997-2000 simulation period. Information given in the tables is shown graphically in Figures 1 – 7.

The year 1999 represented standard hydrologic conditions, and comparison of daily streamflow predictions between the calibrated model with mixed landcover and those from models representing the watershed with unique landcover types were used to assess the influence each had on hydrograph characteristics. Over the 1999 period, relative difference in water yield, Nash-Sutcliffe model efficiency, and mean paired deviations were described, and presented in Table 10 and Figures 8 – 15.

Table 4. *Annual evapotranspiration (ET), as mm.*

Year	Calibrated	BRRN	GLND	SLND	QAFR	LPFR	DFFR	SFFR	TRNS
1997	417	231	352	369	380	422	430	436	342
1998	430	260	373	389	400	435	443	447	357
1999	434	228	386	401	406	439	447	451	366
2000	363	205	310	329	334	368	374	379	299
mean	411	231	355	372	380	416	424	428	341
stdev	33	22	33	32	33	33	34	34	29
sterr	16	11	17	16	16	16	17	17	15

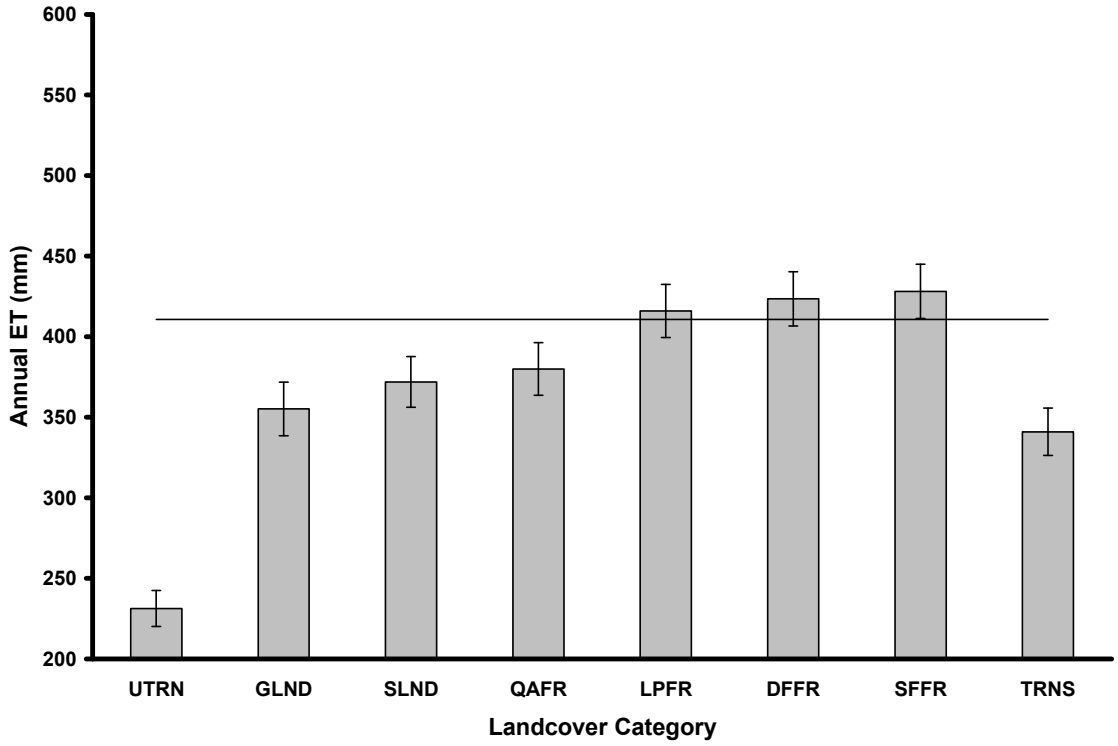

Figure 1. *Estimated average annual evapotranspiration (ET) for each simulated landcover category, based on the 1997-2000 model calibration period. The horizontal line represents the average annual ET predicted by the calibrated model with mixed landcover. Whiskers surrounding mean landcover ET show the standard error of estimate.*

Table 5. *Annual water yield, as mm.*

Year	Calibrated	BRRN	GLND	SLND	QAFR	LPFR	DFFR	SFFR	TRNS
1997	563	686	552	534	559	565	557	557	595
1998	376	455	341	333	349	377	370	378	378
1999	338	468	320	307	330	339	331	333	365
2000	375	478	373	356	374	374	369	368	403
mean	413	522	397	382	403	414	407	409	435
stdev	102	110	106	103	106	102	102	100	108
sterr	51	55	53	52	53	51	51	50	54

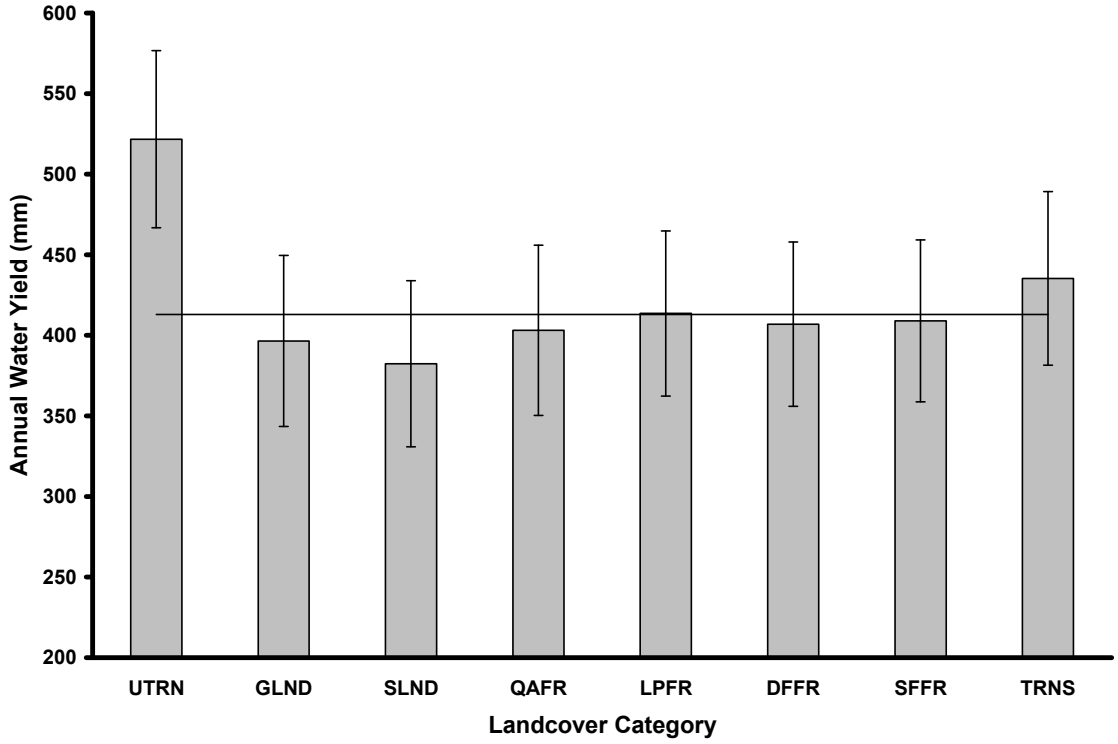

Figure 2. *Estimated average annual water yield for each simulated landcover category, based on the 1997-2000 model calibration period. The horizontal line represents the average annual volume predicted by the calibrated model with mixed landcover. Whiskers surrounding mean landcover volume show the standard error of estimate.*

Table 6. *Peak flow rate (m^3/s).*

Year	Calibrated	BRRN	GLND	SLND	QAFR	LPFR	DFFR	SFFR	TRNS
1997	3.5	4.1	3.8	3.6	3.5	3.3	3.3	3.2	3.8
1998	1.3	1.8	1.3	1.2	1.2	1.2	1.2	1.2	1.3
1999	1.7	2.0	1.8	1.7	1.7	1.6	1.6	1.6	1.8
2000	1.5	1.7	1.5	1.4	1.5	1.5	1.4	1.4	1.6
mean	2.0	2.4	2.1	2.0	2.0	1.9	1.9	1.8	2.1
stdev	1.0	1.2	1.2	1.1	1.1	1.0	1.0	0.9	1.2
sterr	0.5	0.6	0.6	0.5	0.5	0.5	0.5	0.4	0.6

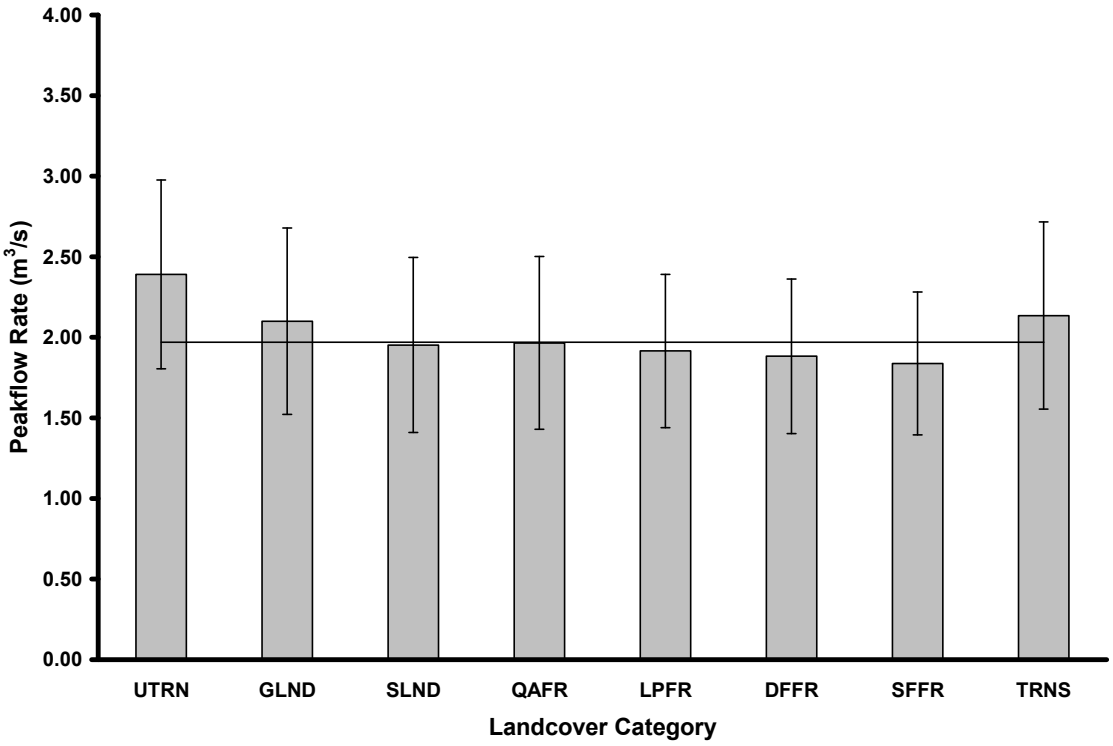

Figure 3. *Estimated average annual peak flow rate (m3/s) for each simulated landcover category, based on the 1997-2000 model calibration period. The horizontal line represents the average annual peak flow rate predicted by the calibrated model with mixed landcover. Whiskers surrounding mean landcover rates show the standard error of estimate.*

Table 7. *Surface water proportion (%).*

Year	Calibrated	BRRN	GLND	SLND	QAFR	LPFR	DFFR	SFFR	TRNS
1997	47.9	84.5	70.0	60.9	59.9	47.5	47.4	42.3	66.2
1998	23.3	84.0	45.8	34.7	32.9	21.3	21.1	16.9	41.0
1999	38.6	82.9	64.2	52.7	51.5	36.8	36.8	31.7	57.6
2000	35.1	80.8	61.7	49.7	49.3	33.1	32.9	26.9	57.3
mean	36.2	83.1	60.4	49.5	48.4	34.7	34.6	29.4	55.5
stdev	10.2	1.7	10.3	10.9	11.3	10.8	10.8	10.6	10.6
sterr	5.1	0.8	5.2	5.5	5.6	5.4	5.4	5.3	5.3

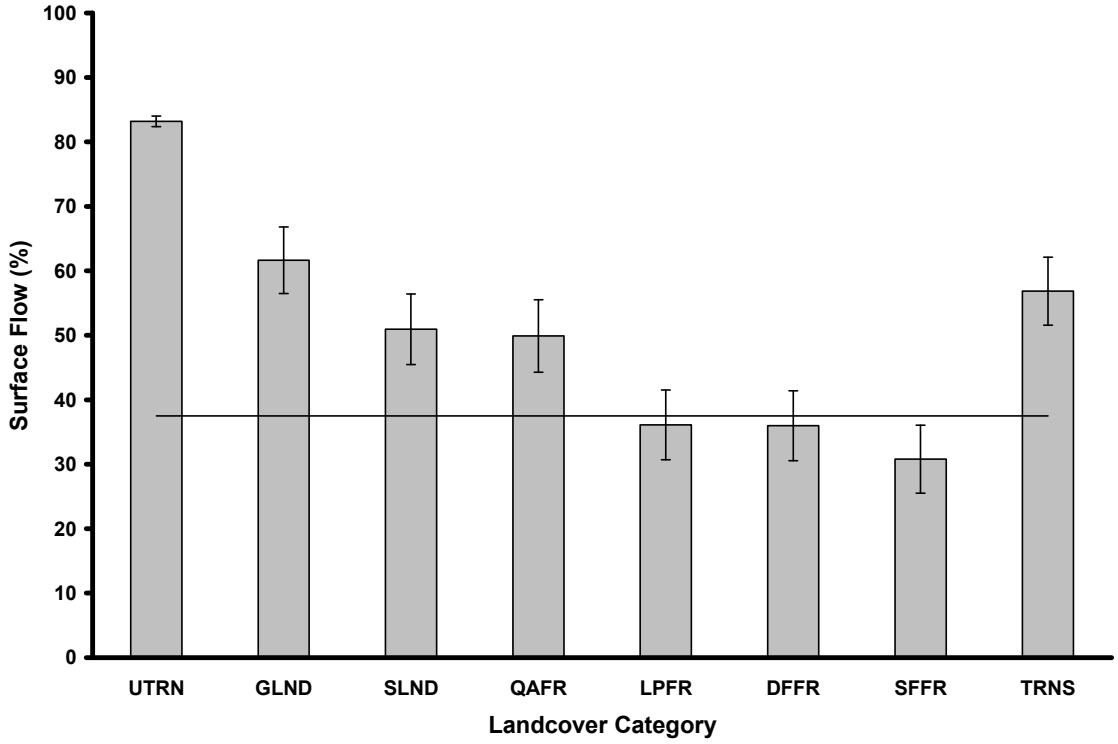

Figure 4. *Estimated average annual proportion of runoff that comes from surface flow for each simulated landcover category, based on the 1997-2000 model calibration period. The horizontal line represents the average annual surface flow predicted by the calibrated model with mixed landcover. Whiskers surrounding mean landcover flow show the standard error of estimate.*

Table 8. *Lateral flow proportion (%)*.

Year	Calibrated	BRRN	GLND	SLND	QAFR	LPFR	DFFR	SFFR	TRNS
1997	10.0	3.3	7.4	8.6	8.8	10.2	10.2	10.8	7.7
1998	16.9	4.4	14.8	16.4	16.6	17.3	17.5	17.7	14.8
1999	12.3	3.9	9.6	11.1	11.2	12.6	12.7	13.3	9.8
2000	11.7	4.0	8.6	10.2	10.3	12.1	12.2	12.9	8.8
mean	12.7	3.9	10.1	11.6	11.7	13.0	13.1	13.7	10.3
stdev	2.9	0.4	3.2	3.4	3.4	3.0	3.1	2.9	3.1
sterr	1.5	0.2	1.6	1.7	1.7	1.5	1.5	1.5	1.6

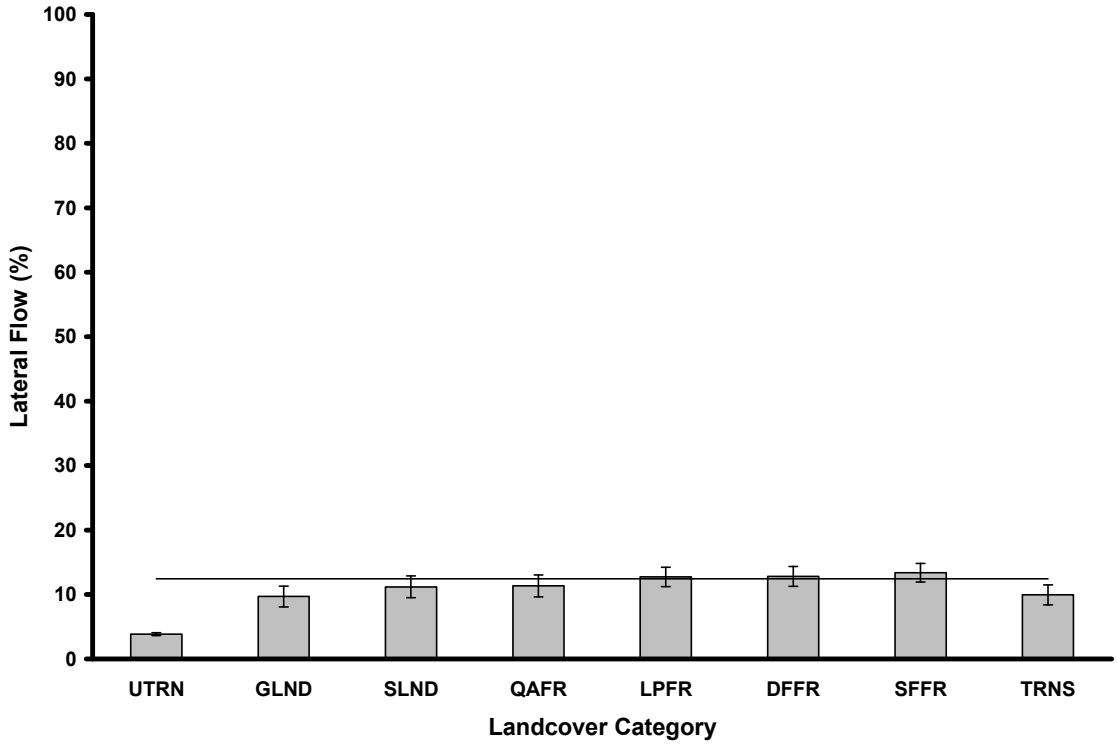

Figure 5. *Estimated average annual proportion of runoff that is lateral flow for each simulated landcover category, based on the 1997-2000 model calibration period. The horizontal line represents the average annual lateral flow predicted by the calibrated model with mixed landcover. Whiskers surrounding mean landcover flow show the standard error of estimate.*

Table 9. *Groundwater proportion (%).*

Year	Calibrated	BRRN	GLND	SLND	QAFR	LPFR	DFFR	SFFR	TRNS
1997	42.2	12.3	22.8	30.6	31.5	42.4	42.5	47.0	26.2
1998	59.9	11.7	39.6	49.1	50.6	61.5	61.6	65.5	44.5
1999	49.2	13.4	26.5	36.4	37.5	50.8	50.7	55.2	32.8
2000	53.4	15.4	30.0	40.3	40.5	55.0	55.1	60.4	34.1
mean	51.2	13.2	29.7	39.1	40.0	52.4	52.5	57.0	34.4
stdev	7.5	1.6	7.2	7.8	8.0	8.0	8.0	7.9	7.5
sterr	3.7	0.8	3.6	3.9	4.0	4.0	4.0	4.0	3.8

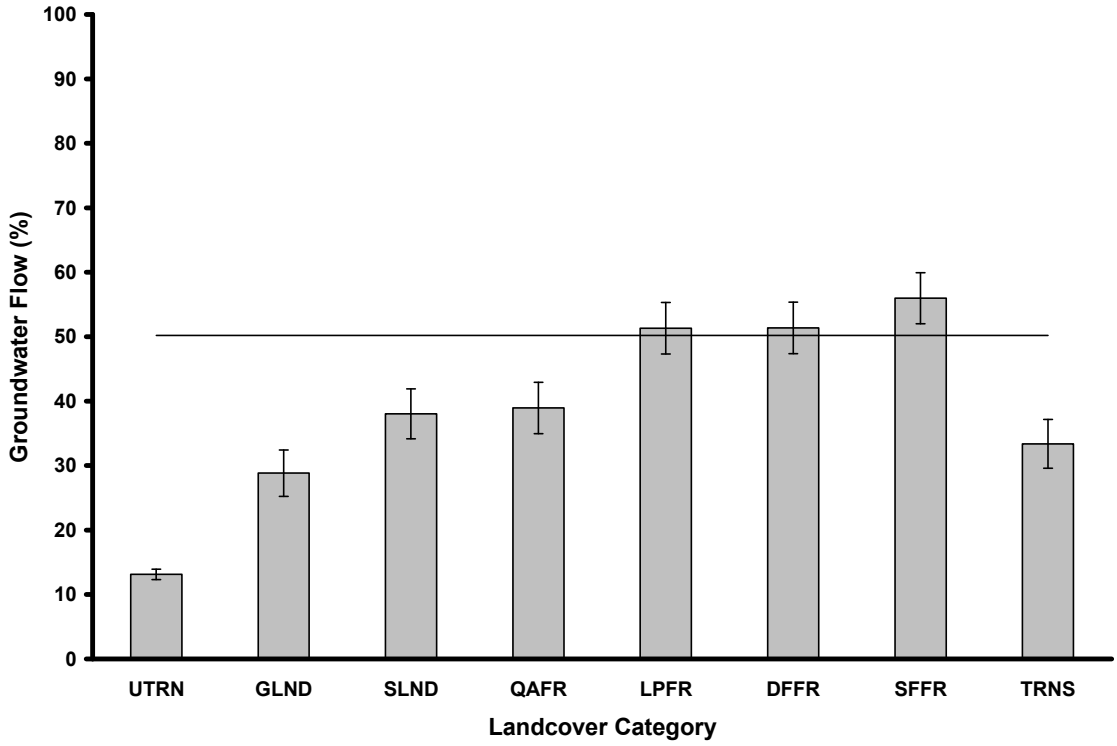

Figure 6. *Estimated average annual proportion of runoff that is groundwater flow for each simulated landcover category, based on the 1997-2000 model calibration period. The horizontal line represents the average annual groundwater flow predicted by the calibrated model with mixed landcover. Whiskers surrounding mean landcover flow show the standard error of estimate.*

Table 10. *Runoff as a proportion of precipitation (%).*

Year	Calibrated	BRRN	GLND	SLND	QAFR	LPFR	DFFR	SFFR	TRNS
1997	69.4	84.5	68.0	65.8	68.9	69.6	68.7	68.6	73.3
1998	47.5	57.5	43.1	42.1	44.1	47.6	46.8	47.8	47.8
1999	47.0	65.1	44.4	42.7	45.9	47.1	46.0	46.3	50.8
2000	55.4	70.7	55.2	52.6	55.4	55.3	54.6	54.5	59.7
mean	54.8	69.5	52.7	50.8	53.6	54.9	54.0	54.3	57.9
stdev	10.4	11.4	11.6	11.1	11.3	10.5	10.5	10.2	11.5
sterr	5.2	5.7	5.8	5.6	5.7	5.2	5.2	5.1	5.7

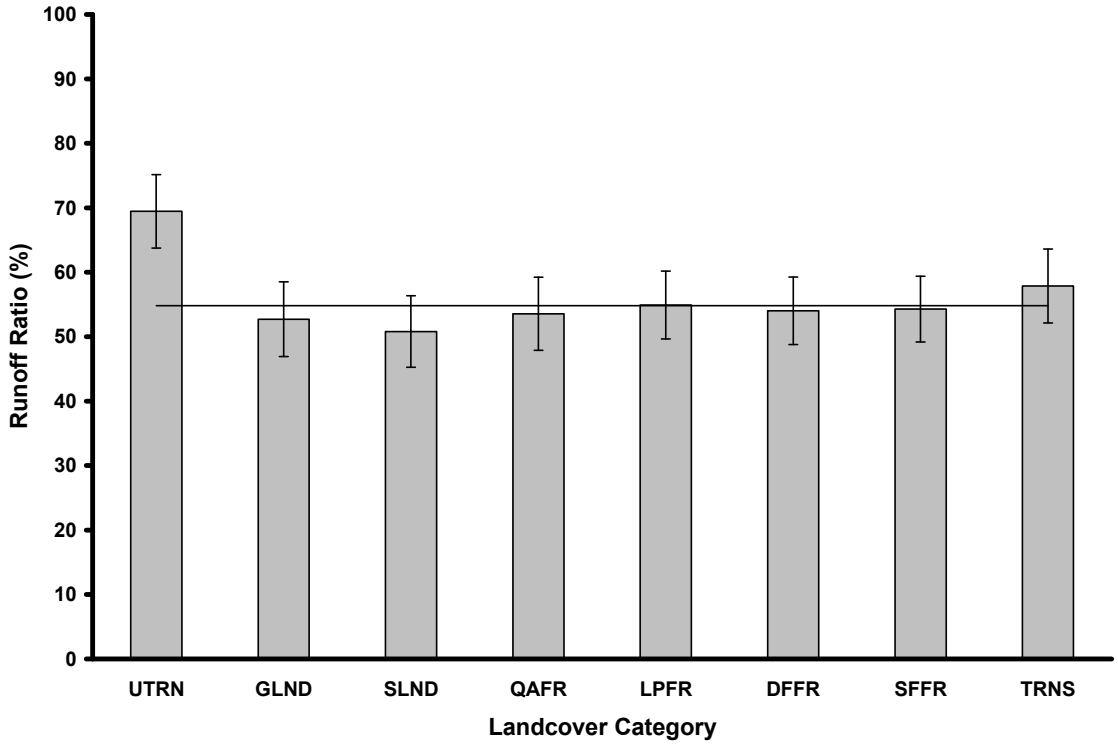

Figure 7. *Estimated average annual proportion of precipitation that is converted into runoff for each simulated landcover category, based on the 1997-2000 model calibration period. The horizontal line represents the average annual runoff ratio predicted by the calibrated model with mixed landcover. Whiskers surrounding mean ratios show the standard error of estimate.*

Table 11. *Streamflow simulation performance statistics for the year 1999. Signed RE values indicate whether the simulated landcover produced more (positive) or less (negative) water than the calibrated model with mixed landcover.*

Landcover	Water Yield RE	DV	NS
Barren (BRRN)	38.6	54.20	0.69
Grassland (GLND)	-5.4	29.17	0.96
Shrubland (SLND)	-9.2	17.01	0.99
Quaking Aspen (QAFR)	-2.3	14.96	0.99
Lodgepole pine (LPFR)	0.2	7.60	0.99
Douglas fir (DFFR)	-2.0	6.97	0.99
Spruce-fir (SFFR)	-1.5	12.21	0.98
Transitional (TRNS)	8.0	21.63	0.96

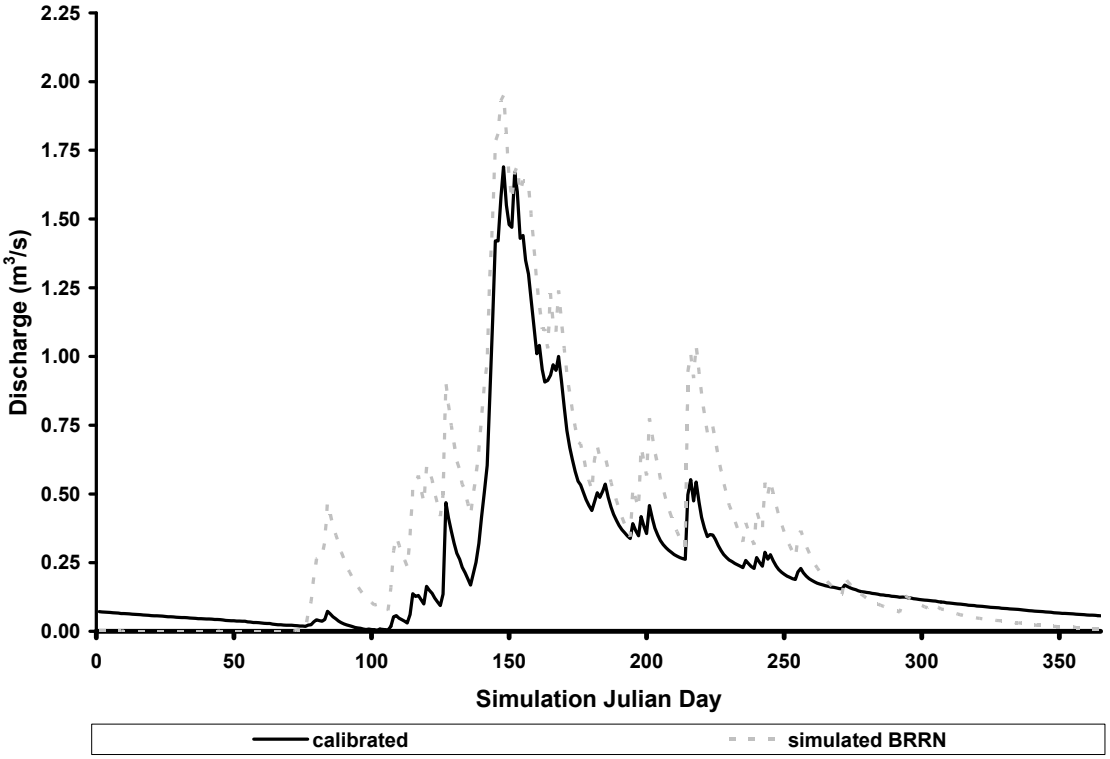

Figure 8. *1999 daily streamflow hydrographs for BRRN vs. calibrated landcover.*

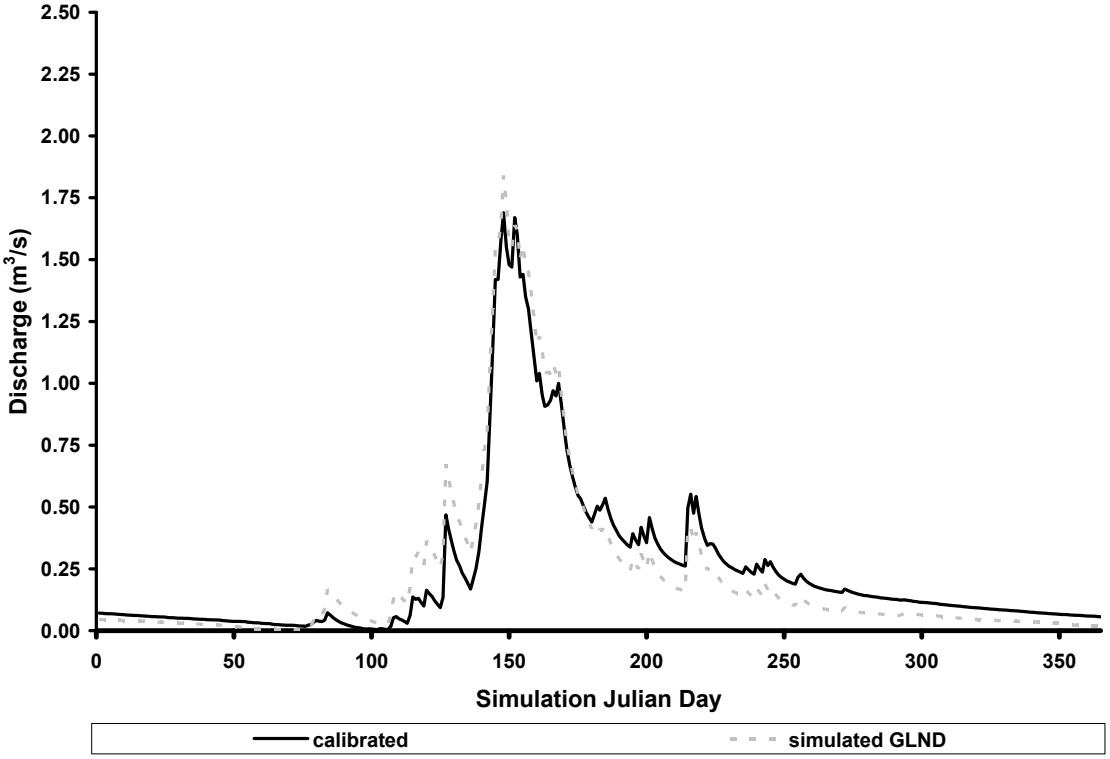

Figure 9. *1999 daily streamflow hydrographs for GLND vs. calibrated landcover.*

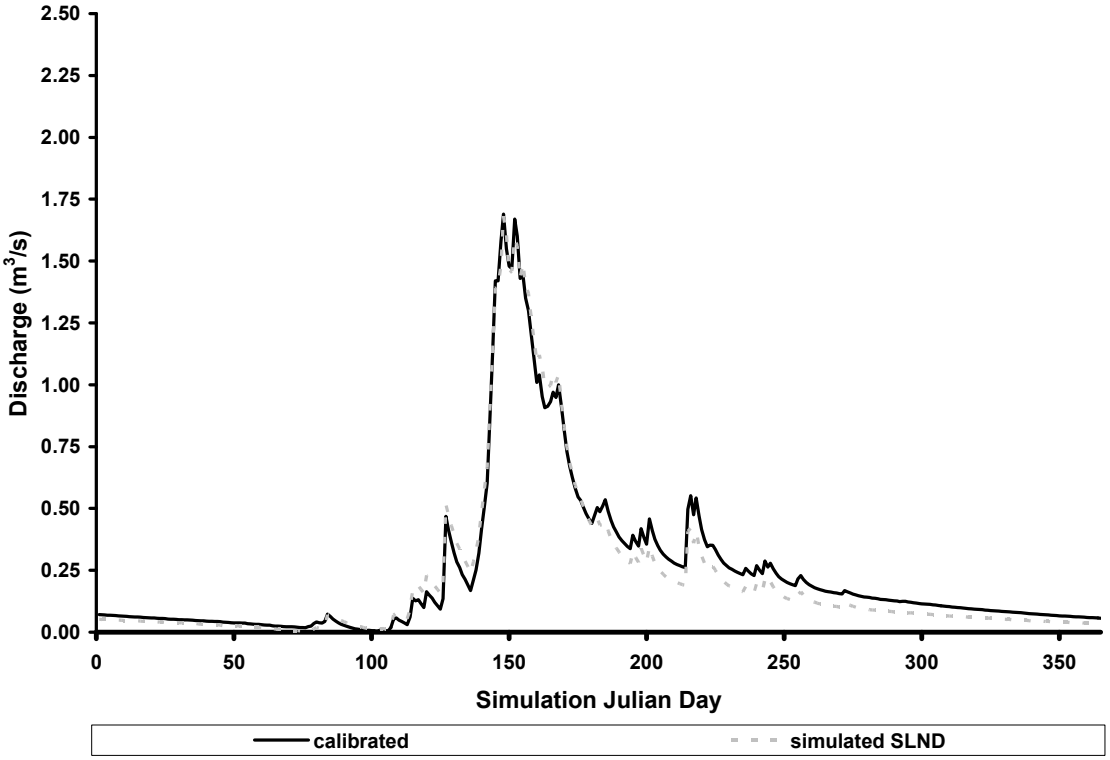

Figure 10. *1999 daily streamflow hydrographs for SLND vs. calibrated landcover.*

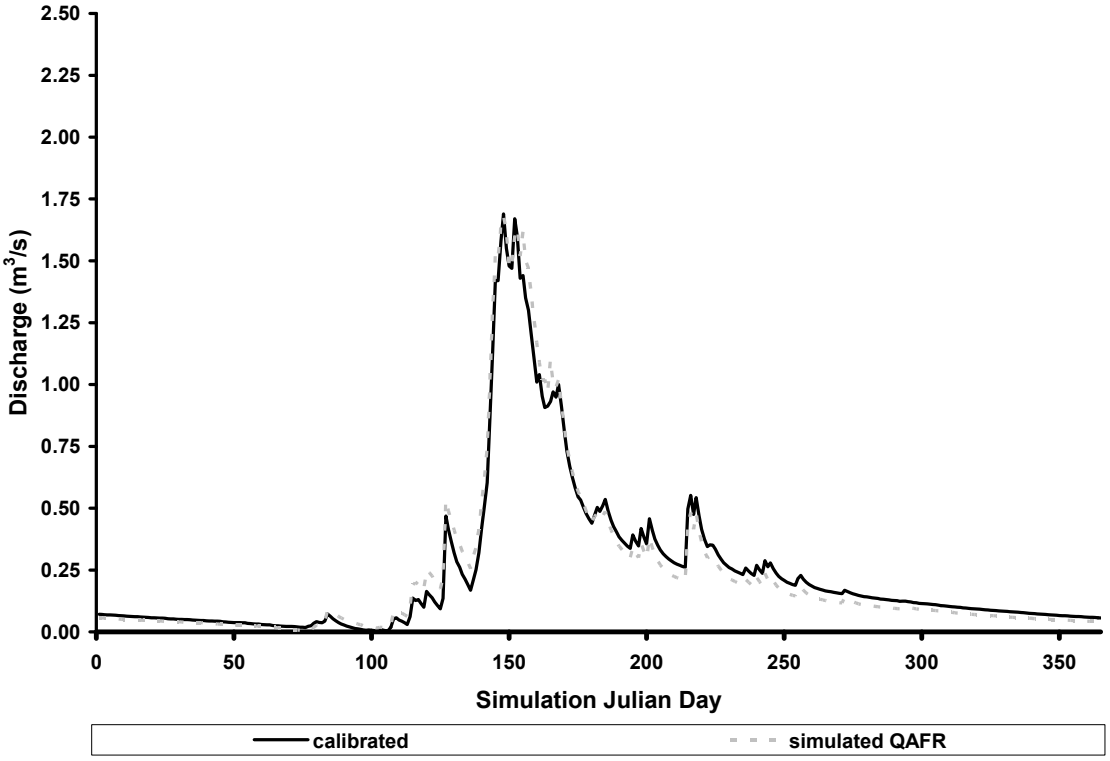

Figure 11. *1999 daily streamflow hydrographs for QAFR vs. calibrated landcover.*

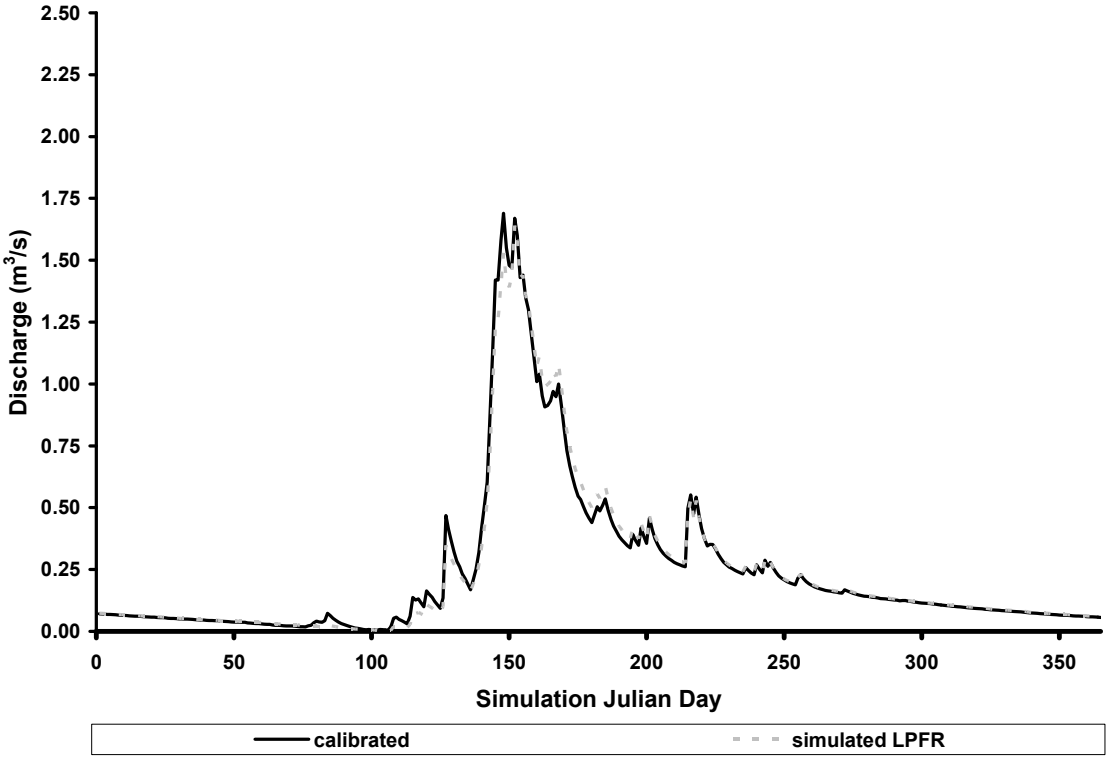

Figure 12. *1999 daily streamflow hydrographs for LPFR vs. calibrated landcover.*

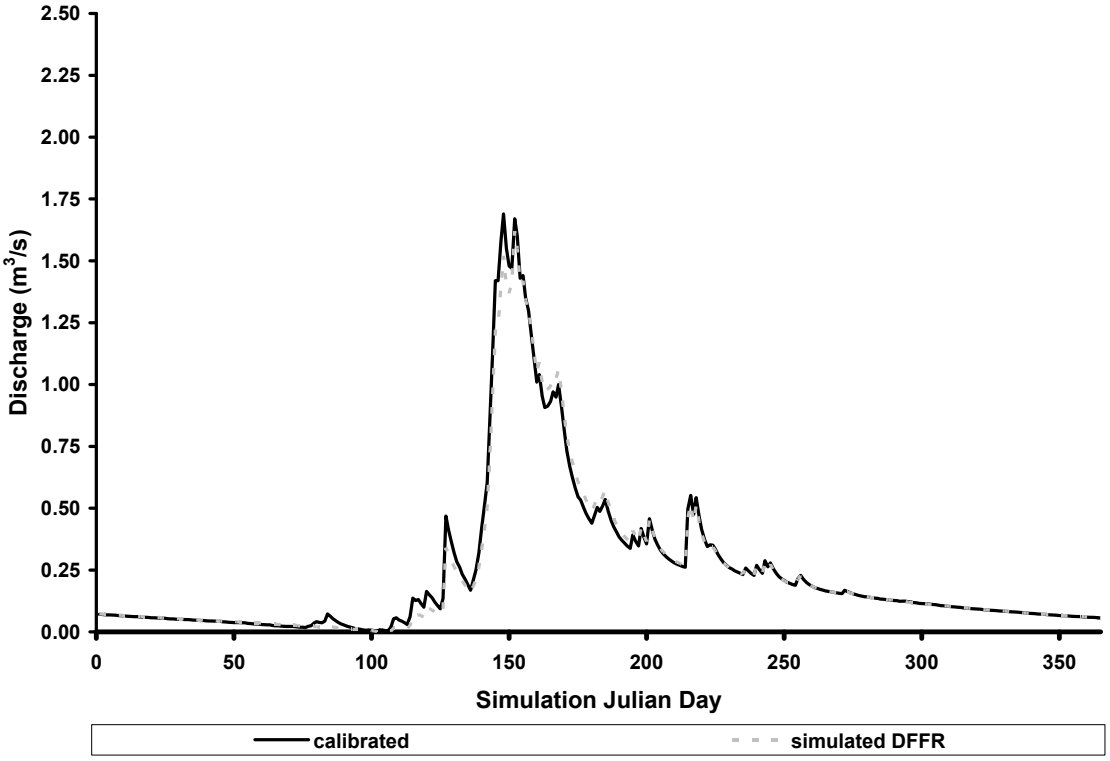

Figure 13. *1999 daily streamflow hydrographs for DFFR vs. calibrated landcover.*

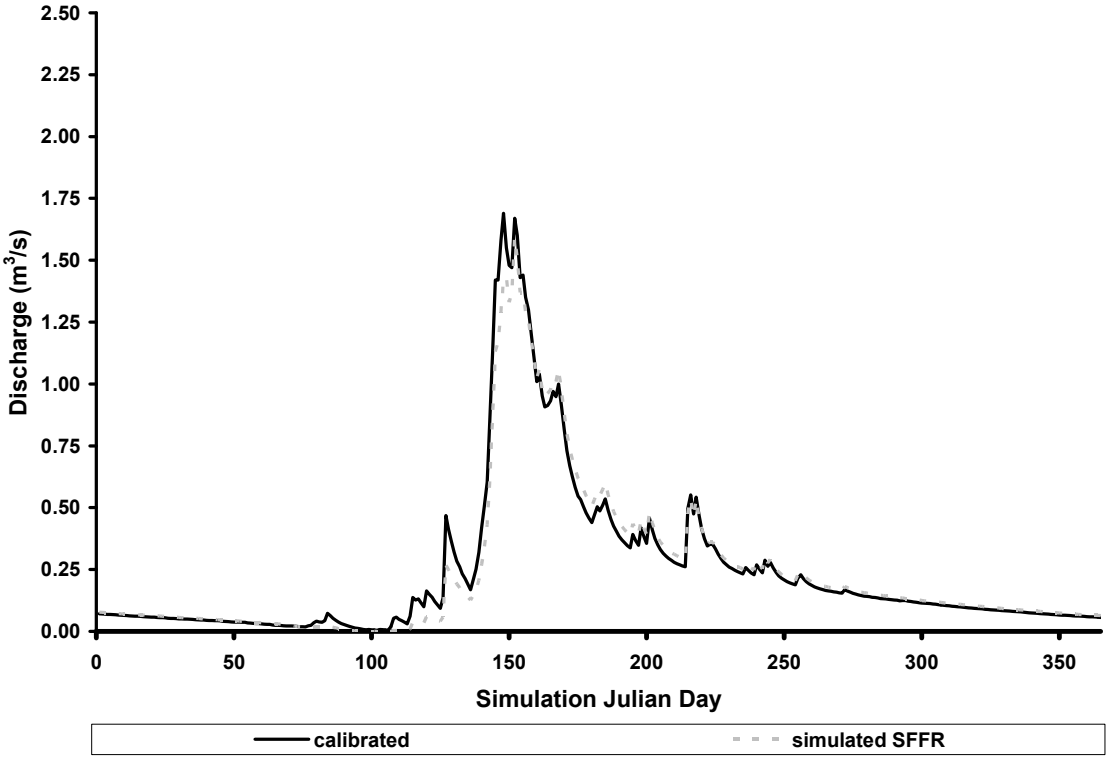

Figure 14. *1999 daily streamflow hydrographs for SFFR vs. calibrated landcover.*

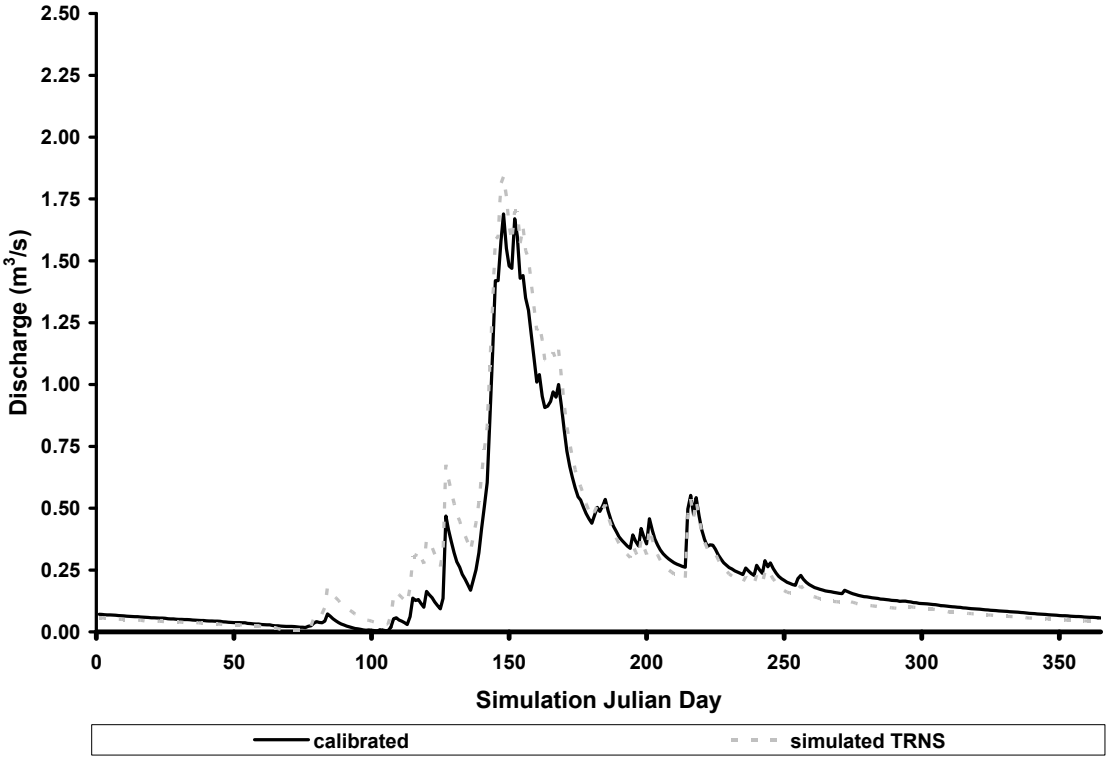

Figure 15. *1999 daily streamflow hydrographs for TRNS vs. calibrated landcover.*

APPENDIX D

Regression-Based Model Invalidation

MODEL INVALIDATION CONCEPT

Calibration procedures established the set of final parameter values, and analysis of the validation time period provides an independent check on the robustness of those parameter estimates. With this concept, the relationship between streamflow estimated by SWAT during the validation and measured streamflow for corresponding periods is evaluated. A simple linear regression model is developed where simulated values (x), derived from a model developed from another independent dataset, predict the actual values (y) from the validation dataset for each time frame being tested. When modeled and measured values are closely matched, the y-intercept, b_0, of the above relationship should be close to zero and the slope, b_1, near 1. To test for differences in magnitude and variation between data pairs, a joint set of null hypotheses is constructed of the form:

$$H_0: \beta_0 = 0 \text{ and } \beta_1 = 1 \text{ versus } H_1: \text{not } H_0 \qquad \text{at a specified } \alpha \text{ level}$$

Next the following test statistic, **Q**, is computed:

$$\mathbf{Q} = (\beta - b)' \, X'X \, (\beta - b) \sim p \, S^2 \, F_{p, v, 1-\alpha} \qquad \text{(Eqn. 1)}$$

Where:

β =	hypothesized values for y-intercept and slope, i.e. 0 and 1
b =	vector of actual regression coefficients
X'X =	matrix term in independent variables (predicted y's)
S^2 =	residual mean square
p =	number of regression coefficients – 1
v = n – p =	residual degrees of freedom (DF)
α =	significance level

For meaningful interpretation of this parametric test, the assumptions of normality and independence must be considered within the datasets. In analyses with appropriate datasets, failure to reject the above joint null hypothesis indicates that there is no detectable discrepancy between observed and predicted data.

MONTHLY VOLUME INVALIDATION EXAMPLE

In the following example, the validity of monthly water yield (mm) estimates generated by the calibrated SWAT model is tested. Streamflow estimates from the 48 month validation period are first paired with actual monthly volumes, and a simple linear regression line is then fit through the data pairs with an equation of the form:

$$\text{Observed Monthly Volume} = b_0 + b_1 * (\text{Monthly SWAT Volume}) \qquad \text{(Eqn. 2)}$$

Regression statistics were then generated:

Table 1. *Regression summary.*

R	R^2	Adjusted R^2	Std. Error	Durbin Watson
0.95	0.91	0.91	16.97	1.34

Table 2. *Regression ANOVA.*

	Sum of Squares	DF	Mean Square	F	Sig.
Regression	130,875	1	130,875	454	0.0001
Residual	13,254	46	288		
Total	144,129	47			

Table 3. *Regression coefficients.*

	Unstandardized Coefficients			
	b	Std. Error	t	Sig.
Y-intercept (b_0)	-1.76	2.97	-0.59	0.56
Slope (b_1)	1.10	0.05	21.31	0.0001

Computing the test statistic, **Q**, according to equation 1 and using matrix algebra yields:

$$\mathbf{Q} = \begin{bmatrix}(0-\left[-1.76\right]) & (1-1.10)\end{bmatrix}\begin{bmatrix}48 & 1{,}564\\ 1{,}564 & 159{,}831\end{bmatrix}\begin{bmatrix}(0-\left[-1.76\right])\\ (1-1.10)\end{bmatrix} = \mathbf{1{,}119}$$

Lastly, $\mathbf{F = Q / pS^2}$ = 1,119 / 288 = **3.88** with DF = 1, 46. Based on the distribution of the **F** statistic, a value of **3.88** is associated with a **P**-value of **0.06**. At the **0.05** significance level, the joint null hypothesis cannot be rejected. Monthly predictions by the SWAT model, therefore, cannot be invalidated.